An Investigation into the Underlying Mechanisms of Hyphal Branching in Filamentous Microorganisms

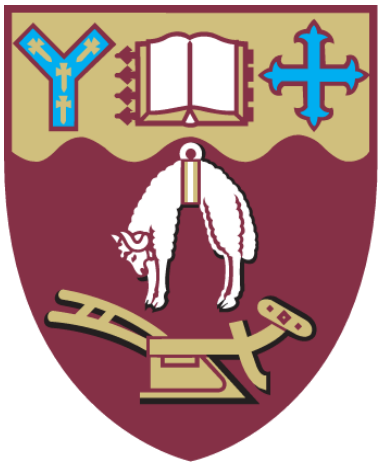

A thesis
submitted in partial fulfilment
of the requirements for the Degree of

Master of Science in Biochemistry

in the
School of Biological Sciences
University of Canterbury
New Zealand

Emma Swadel
2013

i. Contents

ii. List of Figures

iii. List of Tables

iv. Acknowledgements

I am very thankful for all the help and support my supervisor Dr. Ashley Garrill has provided me throughout my thesis. I would also like to thank my associate supervisor Dr. David Collings for all his advice. I am grateful for all the technical advice and support Manfred Ingerfeld, Kenny Chitcholtan, Craig Galilee and Alan Woods have provided me over this time. I am extremely thankful for the support that my friends and family have given me whilst completing this degree, especially Sitara, Patrick and Aliaa from the lab and my flatmates Lucie and Emma who have been there for me through the ups and downs.

v. Abstract

Understanding how hyphal organisms grow and develop is essential in order to manipulate mycelial colonies for purposes such as disease prevention and food production. One aspect of hyphal development that is not well understood is hyphal branching. Hyphal organisms branch as a way of creating new hyphal tips required for the search for nutrients, the acquisition of these nutrients and for hyphal fusion events that facilitate communication of signals within a mycelial colony. This investigation focused on the branching process occurring in the fungus *N. crassa* and in the oomycete *A. bisexualis*. An induction technique was developed to study branching in *N. crassa* involving local application of amino acids towards hyphae. This induced a branch to form along the hypha within the field of view. The use of this technique will enable the study of underlying events occurring internally prior to the visible branching stages. The role of Ca^{2+} hyphal branching was investigated in *N. crassa* suggesting Ca^{2+} is involved in apical dominance of the hyphal tip. This is based on a dose dependent response of increased branch frequency, decreased colony radius and decreased distance between the hyphal tip and the first branch, to the Ca^{2+} channel inhibitor verapamil. The stretch-activated Ca^{2+} channel inhibitors also had an effect on mycelial morphology. Gd^{3+} resulted in an increased branch frequency and a decreased colony radius and La^{3+} resulted in a decreased colony radius. The local application of verapamil towards *N. crassa* showed an increase in the number of multiple branches forming. Cytoplasmic Ca^{2+} was imaged in hyphae of *A. bisexualis* and *N. crassa* showing a tip-high Ca^{2+} gradient in *A. bisexualis* and Ca^{2+} sequestered into organelles in *N. crassa*. The role of F-actin in the process of hyphal branching was investigated using Lifeact *N. crassa* where F-actin could dynamically be seen at the site of both growing and non-growing hyphal branches. The involvement of F-actin at sites of septa development and associated with suspected vesicles was also observed.

vi. Abbreviations

ABP	Actin Binding Protein
AM	Acetoxymethyl
BAPTA	1,2-bis(ortho-aminophenoxy)ethane-N,N,N',N'-tetrapotassium acetate
Ca^{2+}	Calcium ion
CRIB	Cdc42/Rac Interactive Binding
CTC	Chlorotetracyline
DMA	Defined Media Agar
ER	Endoplasmic Reticulum
EZ	Extension Zone
FH	Formin Homology
Gd^{3+}	Gadolinium ion
GM	Genetically Modified
IP_3	Inositol 1,4,5-triphosphate
La^{3+}	Lanthanum ion
LMP	Low Melting Point
MES	2-(N-morpholino)ethanesulfonic acid
MP	Micropipette
PAK	p21-activated kinase
PGZ	Peripheral Growth Zone
PLC	Phospholipase C
PYG	Peptone Yeast Glucose
SA	Stretch-activated
SD	Standard Deviation
SEM	Standard Error of the Mean
TBS-T	Tris-Buffered Saline and Tween 20
WASP	Wiscott Aldrich Syndrome Protein
w/v	Weight/Volume
v/v	Volume/Volume

Chapter 1
Introduction

1.1 Overview

Branching is a morphogenic process which is used as a way of increasing the surface area of hyphal organisms through the growth of new tips. Hyphal branching is an important feature in the growth of mycelial colonies of both fungi and oomycetes. Due to the importance of branching in the growth of a colony, it is critical to understand the mechanisms that underlie branching in these filamentous microorganisms.

1.2 Filamentous Microorganisms

Filamentous microorganisms are made up of cylindrical cells with a rounded or tapered tip. These cells are known as hyphae which branch to form a colony called a mycelium. A colony is formed from a single spore that has germinated when conditions are favourable for growth (Bezzi and Ciliberto, 2004). Mycelial growth occurs through the interplay of two processes; tip growth, which enables the search for new sources of nutrients and branching, which creates new hyphal tips and therefore more surface area for nutrient acquisition (Morris et al., 2011). The growth rate of a mycelium is determined by the rate at which the hyphal tips are growing and the branch frequency (Bezzi and Ciliberto, 2004).

The growth of mycelia is exponential after the germination of a spore. This is a direct result of the exponential increase in new tips. The growth rate of the colony then slows down to a constant rate as the colony matures and the mycelium covers a greater surface area (Trinci, 1974). There are a number of mechanisms involved in the development of a hyphal colony. Highly polarised growth at hyphal tips enables rapid elongation of hyphae. This high velocity growth at the tip is supported by a long span of the hypha known as the peripheral growth zone (PGZ). This zone provides the material required for tip growth at the very apex

of the hypha, an area known as the extension zone (EZ). Another mechanism involved in the formation of a mycelial colony is the regulation of branch formation and the distribution of these branches within the colony (Prosser and Trinci, 1979). In order to be successful in colonising different substrates, hyphae within the mycelia need to be able to communicate with one another. The mechanism by which this communication is achieved is through hyphal fusion, enabling the neighbouring hyphae to exchange signals and nutrients with each other (Harris, 2008).

In fungal colonies there are two different types of mycelia produced when growing on solid media. The first is a vegetative mycelium and it is responsible for the uptake of nutrients from the surrounding environment. This type of mycelium is able to grow in two different ways in order to acquire nutrients. The first way is via invasive growth and this is where the hyphae penetrate and grow through solid substrates. Force is needed in order to grow invasively through substrates, therefore a relationship between turgor pressure, yielding of the cell wall and cytoskeleton dynamics is needed (Geitmann and Emons, 2000). Through invasive growth, hyphae have the ability to grow through living tissues of plants and animals (Sietsma and Wessels, 2006). The second way a vegetative mycelium is able to grow is through non-invasive growth where hyphae grow on top of solid substances or in liquid media. The ability for hyphal organisms to grow in such diverse ways in varying environments contributes to their evolutionary success (Geitmann and Emons, 2000). The second type of mycelium that fungal colonies produce is an aerial mycelium which is produced from a vegetative mycelium. This type of mycelium is responsible for the development and release of spores into the air (Bezzi and Ciliberto, 2004).

Through the main structure of fungal colonies, vegetative hyphae, fungi are able to occupy varying terrestrial ecosystems with great success (Harris, 2008). They have the ability to colonise substrates ranging from those that are nutrient rich to those that are nutrient poor. This is because they are able to utilise the available resources which they are exposed to, however, the colony morphology is different at these two extremes. These colonies can cover the same distance however there is a difference in the total biomass produced. There are fewer tips produced in nutrient poor conditions enabling the colony to put the available resources into forming a greater PGZ that elongates with a high extension rate through nutrient poor media. Alternatively when the substrate is nutrient rich, the colony produces more tips via branching in order to acquire the nutrients available. As a result of the increased number of tips that must be maintained, there is a smaller PGZ (Bezzi and Ciliberto, 2004).

1.3 Tip Growth

The growth of a hypha occurs at the tip of the cell in a process called tip growth (Castle, 1958). This occurs in the area with the rounded cell wall in the apical region of the hypha. Tip growth results in hyphal cells growing forward at one edge, producing an elongated cell with a cylindrical shape (Geitmann and Emons, 2000). This mechanism of growth enables the hypha to extend forward whilst at the same time being able to sense the immediate environment it is in. With the information about the surrounding environment, hyphae are capable of changing their orientation towards a more favourable area for growth whilst tip extension is maintained (Brand and Gow, 2009). Tip growing cells include oomycete and fungal hyphae as well as pollen tubes, algal rhizoids and root hairs (Yu et al., 2004).

A common feature that is shared by all tip growing hyphal organisms is the presence of a cell wall. This structure aids in the protection of the cell from the external environment and maintains the characteristic shape of the hypha as a result of the internal turgor pressure pressing against the cell wall (Sietsma and Wessels, 2006). The main components of the cell wall are polysaccharides and manno-proteins that form a lattice around the outside of the hypha (Sietsma and Wessels, 2006). The greatest synthesis of cell wall material occurs in the very first 1 μm of the hyphal tip supporting the idea that hyphal growth is confined to this area (Bartnicki-Garcia and Lippman, 1969; Gooday, 1971). The hyphal wall is dynamic and malleable and these features enable the modification of the morphology of the hypha to enable hyphal branching, fusion and developmental processes (Riquelme et al., 2011).

Although the cell wall provides protective and structural support to the hypha, it also acts as a physical barrier to the uptake of nutrients from the external environment. Therefore hyphae require a way in which the movement of nutrients can occur between the external and internal environments. Hyphae release proteins into their immediate surroundings mainly at the growing tips. Among these proteins are lytic enzymes which are capable of digesting polymers present in the environment they are growing in. The digested substrates can then be taken up as a source of nutrients and by breaking down materials in the immediate vicinity it effectively clears the areas for forward growth of the hyphal tips (Sietsma and Wessels, 2006). It is thought that after nutrients are taken up at the tips of hyphae they are moved to internal sites of the mycelium where they are then used to maintain growth and development (Semighini and Harris, 2008).

The cells of filamentous fungi are arranged linearly and are partitioned from each other by barriers called septa (Bezzi and Ciliberto, 2004) whereas oomycetes are filamentous microorganisms composed of a multinucleated cell which is not divided by any internal barriers (Bhattacharya et al., 1991). In filamentous fungi the elongation of hyphae via tip growth results in the development of apical and subapical regions which are divided by septa. The apical region is where growth of the hypha is localised and is responsible for obtaining nutrients from the surrounding environment as well as sensing the immediate environment the hypha is growing in. The subapical region is responsible for manufacturing the material needed for tip growth as well as forming lateral branches to increase surface area (Bezzi and Ciliberto, 2004; Harris, 2008). These regions contain different structures and distributions of organelles. In fungal hyphae, the first region is the area at the very tip covering the first 1-5 μm. This area contains the Spitzenkorper (German for apical body) which is an accumulation of vesicles and cytoskeletal elements required for tip growth. This region also contains a few mitochondria and sometimes smooth endoplasmic reticulum (ER) and Woronin bodies. The next region is 2-20 μm back from the tip. The main components of this region are mitochondria and some ER. This area is deficient in nuclei and other key organelles. The third region covers the area to the first septum and contains all types of organelles. The fourth region is the oldest and contains all the organelles however, the quantity and arrangement can be different to the region before the septum (Riquelme et al., 2011) (Figure 1.1). In oomycetes, vesicles are abundant within the first 5 μm of the hyphal tip along with cytoskeletal elements. The next region is 5 μm to 10 μm back from the hyphal tip. This area is abundant in mitochondria and ER. Golgi bodies are not present in the first 5 μm from the hyphal tip but are found in areas back from this region. In the region 10 μm-15 μm back from the hyphal tip is where the nuclei are first found (Heath and Kaminskyj, 1989; Jackson and Heath, 1990) (Figure 1.1).

An initial growth site is founded at the hyphal tip which then is maintained enabling tip growth to continue forward in the EZ (Steinberg, 2007). A build-up of vesicles at the very apex of the hypha is required for tip growth. These vesicles contain the necessary components for extending the tip wall forward such as cell wall precursors and enzymes (Fiddy and Trinci, 1976). The two contributing factors to the shape and length of the hyphal EZ and the width of the hypha are firstly, the rate at which the vesicles containing cell wall and membrane precursors are delivered to the apex and secondly, the rate at which these precursors are fixed in the cell wall at the tip after integration (Steele and Trinci, 1975). In

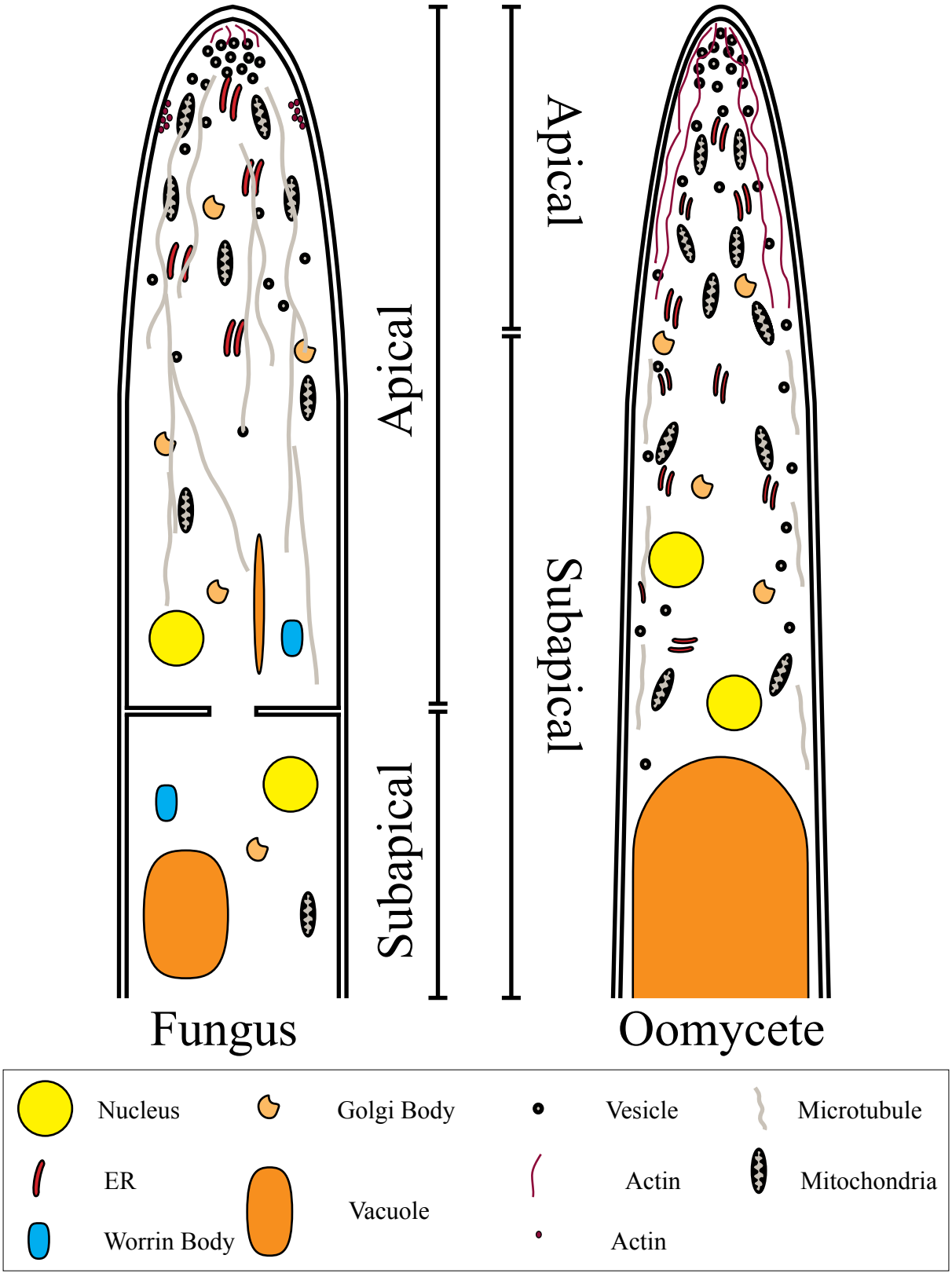

Figure 1.1 - Organelle distribution within fungal and oomycete hyphae. Apical and subapical regions are indicated. Modified from Riquelme et al. (2011) and Heath and Kaminskyj (1989).

order to facilitate tip growth, the cell wall at the apex of the hypha can be thinner resulting in the structure being softer and more malleable (Harold, 1997). The rate at which the EZ extends is directly related to the temperature it is growing in as this determines precursor supply rate to the tip and wall ridification rate at the tip (Steele and Trinci, 1975). The growth rate of some filamentous fungi can reach up to 1 µm/s (Seiler and Plamann, 2003).

Research has focused heavily on the mechanisms underlying tip growth in filamentous microorganisms as well as in other tip growing cells including pollen tubes, root hairs and algal zygotes. Although these all grow by tip growth, it is unknown if the same mechanisms are used by all (Harold, 1997). Even though theories of aspects of tip growth have been suggested, none have been universally accepted (Grinberg and Heath, 1997). Current models of tip growth which are common to all these cell types are firstly, that the movement of vesicles to the tip via cytoskeleton-based polar exocytosis results in tip growth due to cellular expansion pushing the cytoplasm against the cell wall at the apex. This model is based partly on the phenotypic similarities fungi share with plant cells. The second theory of tip growth is that fungal cells display amoeboid movement which is based on the fact that the slime mutants of *Neurospora* are able to generate protrusions of protoplasm in the absence of a cell wall. Also, the similarities in rRNA and conserved proteins shared between animals and fungi, suggest fungi are closer relatives of animals (Steinberg, 2007).

1.4 Hyphal Branching

The morphological process of hyphal branching is an important feature in the growth of mycelial colonies for both filamentous fungi and oomycetes as it enables the generation of new hyphal tips in order to search for new sources of nutrients and to increase the surface area which aids in the assimilation of these nutrients. Branching also appears to be important in sharing nutrients and signals between hyphae of a single colony through hyphal fusion. The mechanisms underlying the branching process in fungi and oomycetes is thought to be similar despite the fact that oomycetes do not contain septa, which have been implicated in the determination of branching sites in some fungi (Harris, 2008). Understanding the mechanisms that underlie branching in filamentous hyphal organisms is of upmost importance because of the role it plays in mycelial dynamics.

1.4.1 Hyphal Branching and Mycelium Dynamics

The foraging strategy of filamentous hyphal organisms lies in the morphology of the colony that can be attributed to the where and when branches form (Reissig and Kinney, 1983). The degree of branching a colony displays is a result of interplay of both exploratory and exploitative growth (Thomas and Paul, 1996). The mechanism by which hyphal cells grow through an interplay of tip growth and branching is very advantageous as it enables a single organisms to grow over a large area in search of new sources of nutrients when the current area is nutrient deficient (Dynesen and Nielsen, 2003; Sietsma and Wessels, 2006).

The environmental conditions fungi and oomycetes are exposed to directly affect the mycelial colony morphology. As the external conditions change so does the frequency and the pattern of branching events (Dynesen and Nielsen, 2003). The process of hyphal branching is sensitive to changes in temperature, light, physical disruption, surrounding hyphae and alterations to the source of nutrients (Riquelme et al., 2011). As mentioned earlier, nutrient availability is a key factor in determining colony morphology as it regulates the development of branches. Medium that is high in nutrient availability supports branching events, unlike low nutrient environments (Bezzi and Ciliberto, 2004).

Within hyphal colonies it is apparent that they are able to directly regulate the relationship between growth at the hyphal tip and the formation of new tips through branching. This relationship has been expressed by the hyphal growth unit model. This model describes the mean length of hypha which is required for the growth of a single tip (Trinci, 1973).

$$\boldsymbol{Hyphal\ growth\ unit}\ (\boldsymbol{h}, \mu\boldsymbol{m}) = \frac{\boldsymbol{Total\ hyphal\ length}\ (\boldsymbol{l}, \mu\boldsymbol{m})}{\boldsymbol{Number\ of\ hyphal\ tips}\ (\boldsymbol{t})}$$

The development of branches is suggested to be regulated by cytoplasmic volume changes (Trinci, 1974). The concentration of nuclei and vesicles in the cytoplasm controls the length of the hypha, along with branching and septation events (Prosser and Trinci, 1979). A contributing factor to the formation of a new branch in a filamentous hyphal organism is when a threshold level of vesicles that are required for tip growth is surpassed. As a result of this, more surface area must be created to accommodate the excess of vesicles and cytoplasm which is accomplished by forming a new branch which develops into its own mature, tip

growing hypha (Trinci, 1974). When a branch forms it uses up excess vesicles, decreasing the concentration of free vesicles present at the two tips. The time it takes for a branching event to occur can be regulated by the time it takes for vesicles to build-up again (Katz et al., 1972).

1.4.2 Types of Branches

There are two types of branches that hyphal organisms produce. These are apical and lateral branches which can be seen in Figure 1.2. The developmental mechanisms that underlie the formation of these two types of branches are different (Riquelme and Bartnicki-Garcia, 2004).

Apical branching events occur through the splitting of the hyphal tip into two growing tips and this type of branching changes the dynamics of hyphal tip growth. This occurs through alterations to hyphal tip physiology and morphology. The growth rate of the primary hypha rapidly decreases as apical branching occurs. The development of apical branches begins with a contraction of the cytoplasm. The Spitzenkörper then undergoes a retraction and disappears resulting in a reduction of the growth rate. The tip then begins to swell as the hypha enters into a stage of isotropic growth. Two or more new points of growth which contain their own Spitzenkörper are then formed (Riquelme and Bartnicki-Garcia, 2004). The cause of apical branching events could possibly be that an irregular amount of vesicle build-up at the tip of the hypha as a result of the growth rate slowing down but with no effect on transport of vesicles to the tip. This accumulation of vesicles in the apical region then results in the formation of multiple new branches at the hyphal tip. A wide range of fungi have been shown to form apical branches (Harris, 2008).

Lateral branches are new tips that form along the trunk of a growing hypha (Geitmann and Emons, 2000). Lateral branching has no effect of the dynamics of the main growing tip as the same materials are not required for the two processes. Sites of lateral branch emergence require the development of a new Spitzenkörper, akin to what is present at the tip of a growing hypha. The area undergoes weakening of the cell wall which succumbs to the effects of turgor pressure inside the cell as well as forming a new hub for growth development (Riquelme and Bartnicki-Garcia, 2004). Enzymes that are able to modify the cell wall are necessary at the sites where lateral branches form (Riquelme et al., 2011). The occurrence of lateral branches and the location of septa are thought to be linked, with the discovery that branches in *Geotrichum candidum* generally formed behind septa. This is

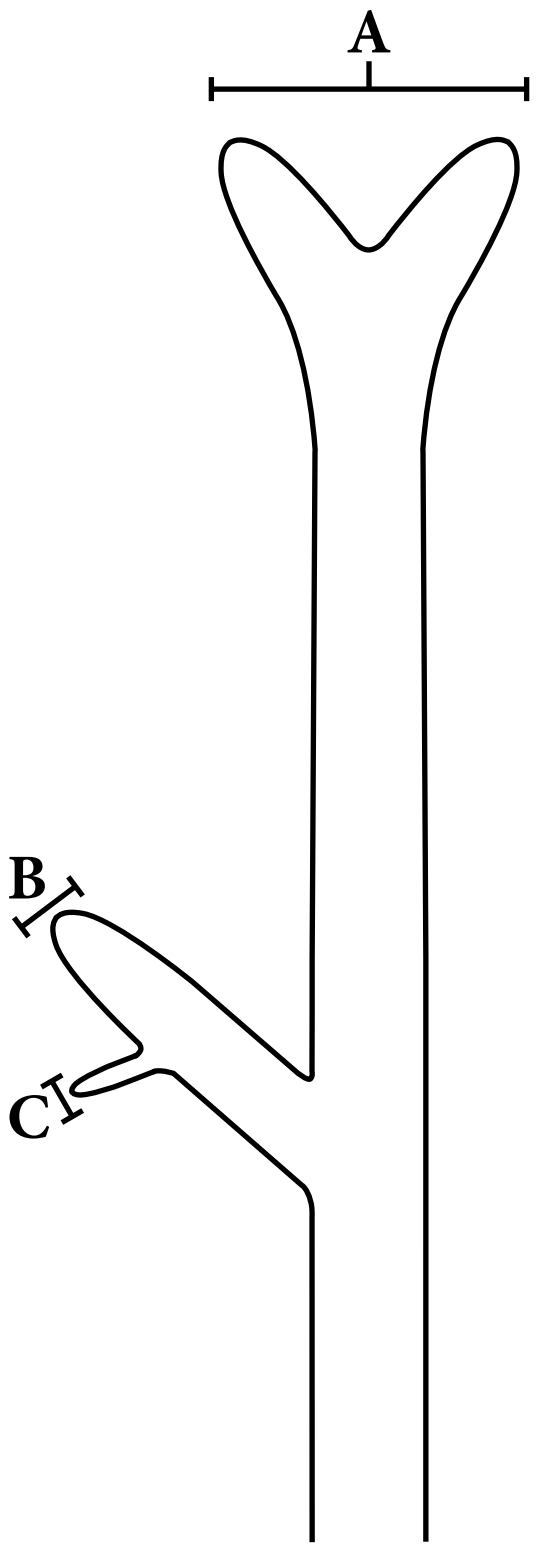

Figure 1.2 - Types of branches in hyphal organisms. A shows apical branching present at the hyphal tip, B shows primary lateral branching occuring along the trunk of the hypha and C shows secondary lateral branching occuring along the trunk of the primary branch.

thought to be caused by vesicles building up behind the septa. These are used to form new branches once the supply of vesicles to the growing tip reaches a threshold required for maximal tip extension (Fiddy and Trinci, 1976). However there is a difference in the dynamic relationship between the process of hyphal branching, growth and septa formation for different species of fungi as branches can form close to, or far away from septa (Bezzi and Ciliberto, 2004). Even when branches do not form near septa, it is thought that septa still could play a role in the development of lateral branches by regulating the timing of the branching event (Harris, 2008).

1.5 Branch Induction

In hyphal organisms, it is very difficult to accurately predict where a lateral branch will form. To investigate underlying mechanisms that precede and occur during the development of lateral branches in *N. crassa*, there needs to be a way of knowing where and when a branch will form along the hyphal trunk. To solve this problem there have been two branch techniques developed to date that reliably induce branches, although these have been used in oomycetes rather than in fungi.

One of these techniques was developed by Schreurs et al. (1989) using the oomycete *A. bisexualis* and enabled the accurate determination of the site in which a lateral branch will form along the trunk of a hypha. The basis of this technique was that *A. bisexualis* will develop lateral branches in response to an amino acid supply. Using this knowledge, Schreurs et al. (1989) filled micropipettes with solutions containing individual amino acids of varying concentrations and applied the solutions towards growing hyphae. It was found that phenylalanine and methionine had the strongest effect on branch development. When branches formed as a result of this amino acid gradient generated, they developed near the location where the micropipette was positioned. This technique was then further modified by Morris et al. (2011) using a solution of phenylalanine added to a media solution. The other technique to induce branches that has been developed was by Grinberg and Heath (1997) using *Saprolegnia ferax*. This involved the irradiation of the hypha with UV microbeams which resulted in the development of one or more branches along the hyphal trunk.

In this study, I will develop a technique for inducing branch formation in the fungus *N. cras*sa, modelling it on the technique used with *A. bisexualis* that was modified by Morris et al. (2011) involving micropipettes filled with the amino acid phenylalanine in a media

solution. This technique will enable the comparison of branch formation between *A. bisexualis*, an oomycete, and *N. crassa*, a true fungus. This is a relatively non-disruptive technique to use for investigating the underlying mechanisms of branch formation in comparison with the use of UV microbeams as the UV microbeams may cause a stress response by the hyphae and alter the internal mechanisms.

1.6 Cytoplasmic Ca^{2+} and Hyphal Dynamics

1.6.1 Ca^{2+} Regulation in Cells

Calcium ions play an essential role in physiological process within cells, functioning as a signalling ion. Due to its important role, the level of Ca^{2+} present inside cells is closely and carefully regulated. Most cells maintain the level of Ca^{2+} in the cytosol at ~0.1 µM. Although Ca^{2+} is frequently higher than this in the external environment cells are exposed to, they sequester Ca^{2+} into certain organelles as a storage mechanism because it plays such an important role (Bowman et al., 2009). As a secondary messenger, Ca^{2+} is involved in a number of signalling events. The characteristic response of Ca^{2+} acting in signal transduction pathways is for the level of free Ca^{2+} to increase within the cell (Mouriño-Pérez et al., 2006). Tip-high Ca^{2+} gradients have been characteristically found within cells that carry out polarised growth; these include hyphae of filamentous fungi and oomycetes (Torralba and Heath, 2001) along with higher plant root hairs, pollen tubes and fucoid algae (Silverman-Gavrila and Lew, 2001). This tip-high Ca^{2+} gradient is thought to play a role in the fusion of vesicles with the plasma membrane at the hyphal tip (Silverman-Gavrila and Lew, 2000).

1.6.2 Ca^{2+} in Hyphal Organisms

Ca^{2+} from external sources is required for the growth and morphogenesis of the fungus *N. crassa* (Takeuchi et al., 1988) and the oomycete *S. ferax* (Jackson and Heath, 1989). This requirement of Ca^{2+} from external sources may be necessary to sustain an internal concentration needed for growth (Silverman-Gavrila and Lew, 2000). The minimum external concentrations of Ca^{2+} required for growth of *N. crassa* (Schmid and Harold, 1988) and the oomycete *S. ferax* (Jackson and Heath, 1989) is between 10 and 100 nM. Below this

concentration there are abnormalities in the morphology of hyphae, including irregular hyphal width and bulbous, spherical tips (Silverman-Gavrila and Lew, 2003).

Ca^{2+} may play a role in determining the pattern of vesicle exocytosis and cell wall deposition at the hyphal tip during tip growth. There is a working hypothesis to explain the involvement of Ca^{2+} in tip growth. Vesicles containing Ca^{2+} channels are transported to the tip possibly moving in a directional manner along actin cables. Vesicle exocytosis occurs as they reach the hyphal tip. As a result of this, Ca^{2+} channels are incorporated into the plasma membrane where they regulate the influx of Ca^{2+} which aids in vesicle fusion with the plasma membrane, polymerisation of actin and the local deposition of cell wall. As these channels have a short lifespan, they stop working as new apical membrane is created and new Ca^{2+} channels are inserted. This would explain the maintenance of a tip-high Ca^{2+} gradient (Harold, 1997; Jaffe, 1981).

Ca^{2+} appears to play a role in the process of tip growth however in the ascomycete *N. crassa*, the movement of ions across the plasma membrane is not thought to be involved. It is proposed that the tip-high Ca^{2+} gradient is created by the release of Ca^{2+} from intracellular stores (Silverman-Gavrila and Lew, 2000). In *N. crassa*, the tip-high Ca^{2+} gradient has been visualised using fluorescent Ca^{2+} probes. In growing hyphae, the gradient was discovered in the first 10 µm back from the tip. This gradient was not present in non-growing hyphae, adding to the idea that there is an obligatory role of Ca^{2+} in tip growth. After the addition of a Ca^{2+} chelator, 1,2-bis(ortho-aminophenoxy)ethane-N,N,N',N'-tetrapotassium acetate (BAPTA), the tip-high Ca^{2+} gradient dissipated and caused hyphal growth to stop. This suggests that the mechanism by which Ca^{2+} directs polarised growth was disturbed. As growth resumed, the Ca^{2+} gradient reappeared therefore supporting the requirement of Ca^{2+} in tip growth (Silverman-Gavrila and Lew, 2000). The fact that Ca^{2+} gradients are found in growing hyphae but not in non-growing hyphae suggests that Ca^{2+} has an important role in tip growth (Levina et al., 1995).

In order to see the distribution of Ca^{2+} within cells, there needs to be a way of visualising it. The original dyes that were used to image Ca^{2+} in living hyphae were salt and dextran forms. However these were sequestered rapidly into organelles after microinjection of the dye into the hyphae therefore did not enable cytoplasmic Ca^{2+} imaging (Knight et al., 1993). The use of microinjection of Ca^{2+} dyes has the possibility of damaging hyphae so is not a preferred method for Ca^{2+} imaging (Silverman-Gavrila and Lew, 2003). Acetoxymethyl (AM) esters have been used as a non-invasive way for living hyphae to take up dyes which are biologically inert and non-toxic. The carboxylate groups of the dyes are attached to AM

esters making them non-polar, non-fluorescent and cell-permeable. After the AM-dye enters the cell, esterases which are present internally hydrolyse the AM group removing it from the probe. Without the AM group, the dye is not able to pass back across the plasma membrane, therefore it remains inside the cell where it binds to free Ca^{2+} (Nair et al., 2011). The most promising way of imaging Ca^{2+} is through the use of the protein aequorin inside modified fungal cells. Aequorin is a 22 kDa protein expressed in *Aequorea victoria* that has a high affinity for free Ca^{2+}. When Ca^{2+} is bound to this protein, it undergoes a conformational change and as a result, blue light is emitted at a wavelength of 469nm. The emission at this wavelength increases in intensity as the free Ca^{2+} concentration increases. Fungal colonies of *N. crassa*, *Aspergillus niger* and *Aspergillus awamori* have successfully been modified to express the aequorin gene and have the ability to express high levels of aequorin (Nelson et al., 2004).

The role of Ca^{2+} in the branching process is still not clear. The current hypotheses relating to Ca^{2+} and branching contradict one another. One states that Ca^{2+} is involved in the establishment of apical dominance acting to prevent branches forming near the tip of the growing hypha while the other states that the presence of Ca^{2+} promotes the formation of branches. These hypotheses are discussed further below. Clearly additional studies are required to identify the role Ca^{2+} plays in branch formation.

1.6.3 Hypothesis 1: Ca^{2+} Promotes Apical Dominance of Hyphal Tips

Hyphae have quite a distinct morphology where there are no branches present in the immediate area of the growing tip, with the exception of apical branching events. This pattern of branch formation gives the mycelia its characteristic organisation. This characteristic pattern means that hyphae could, through some mechanism be inhibiting the formation of new tips in the form of lateral branches in the region of the growing tip (Rayner, 1991).

The theory of apical dominance in hyphal cells suggests that there is suppression of a secondary axis of polarity within the immediate area of the growing tip. Apical dominance enables the sole delivery of vesicles containing the necessary materials for cell wall growth to the growing tip, without the expense of vesicles being delivered to new areas of growth. When the distance is great enough from the growing tip, a new site of growth will be activated (Semighini and Harris, 2008). Without control on the pattern of hyphal branching

through apical dominance, it would likely result in a colony with a disordered pattern of growth.

Ca^{2+} may play an important role in regulating apical dominance in filamentous fungi (Jackson and Heath, 1993). When the tip-high Ca^{2+} gradient is dissipated using the Ca^{2+} ionophore A23187 in *N. crassa*, branches form closer to the hyphal tip. The addition of this ionophore resulted in the loss of up to half of the internal cytoplasmic Ca^{2+} however there was no significant effect on hyphal growth. This suggests that the Ca^{2+} gradient has no effect on polarised hyphal extension; instead it is required for the dominance of the apical region of the hypha (Schmid and Harold, 1988). The development of apical branches in the presence of this Ca^{2+} gradient would occur when there is a disruption to apical dominance, allowing the hypha to carry on growing through creating tip new tips via a branching event (Harris, 2008). An increase in the Ca^{2+} concentration in the external environment can result in hyperbranching suppression, therefore linking Ca^{2+} influx and hyperbranching in *N. crassa* (Watters, 2013).

In *A. bisexualis* this tip-high Ca^{2+} gradient is generated through the influx of Ca^{2+} through Ca^{2+} channels present in the plasma membrane. This is thought to result in apical dominance of the main growing tip. When Ca^{2+} channels are blocked with inhibitors, it prevents the influx of Ca^{2+} into the hypha. With exposure of these hyphae to the Ca^{2+} channel inhibitor verapamil, there was an increase in the frequency of branches, a decrease in the colony radius and a decrease in the distance from the tip of the hyphae to the first branch as the concentration of the inhibitor increased. This result suggests the tip-high Ca^{2+} gradient was diminished to some extent allowing branches to form closer to the tip. This supports the idea of the involvement of Ca^{2+} in maintaining apical dominance. An increase in the Ca^{2+} channel inhibitors Gd^{3+} and La^{3+} in the growth media also increased the branch frequency however; the response was not as strong compared with the verapamil treatment (Morris et al., 2011). The local application of Ca^{2+} channel inhibitors towards hyphae of *A. bisexualis* resulted in multiple branch formation, however, in some cases it inhibited bump to branch transition. The reason behind the different effects of verapamil on branch formation is unclear (Morris et al., 2011).

1.6.4 Hypothesis 2: Ca^{2+} Promotes Branch Formation

Alternatively it has been hypothesised that Ca^{2+} may be involved in the promotion of branch formation in oomycetes. This may be attributed to the ability of Ca^{2+} to promote the local accumulation of materials which are involved in branch formation to a new site of growth. The use of UV microbeams to induce branch formation in *S. ferax* resulted in a local increase in cytoplasmic Ca^{2+} level prior to branch formation. Following this increase in cytoplasmic Ca^{2+}, one or more branches formed from the main hyphal trunk. This branch formation occurred around 4 minutes after exposure to the UV microbeams. This suggests that Ca^{2+} is required for recruitment of branch initiation factors to the site of the future branch. When irradiations were focused in the apical region, 10 µm from the tip of the hypha, it was more successful in producing branches than when they were focused in the subapical region 50 µm from the tip. This success in the apical region can be correlated with a greater number of structures that store Ca^{2+} in the apical region. In *S. ferax*, mitochondria are known stores of Ca^{2+} of which there are a greater number within the first 10 µm back from the tip. There is a possibility that there is also a higher concentration of ER in this area. The ability for UV microbeams to produce branches closer to the tip suggests that there is no required length of hypha to support a growing tip however new branches that form in the same area must compete against one another for materials required for tip growth such as vesicles that contain membrane and wall materials as well as mitochondria, which provide cellular energy (Grinberg and Heath, 1997).

The way in which the increase in Ca^{2+} may result in the formation of a branch has not been clarified. UV microbeams have been shown to produce cytoplasmic contractions and the release of Ca^{2+} from internal stores of hyphae (Jackson and Heath, 1992; McKerracher and Heath, 1986). Even though contractions were not seen when Grinberg and Heath (1997) exposed *S. ferax* to UV microbeams, there could be partial activation the contractile system within the hyphae, providing a way to transport materials to the branch site and result in the accumulation of branch initiation factors at the new branch site in the vicinity of the irradiations. There are a number of different cellular structures that could be acting as branch initiation factors. These include Ca^{2+}-transmitting channels, organelles that play a role in the homeostasis of Ca^{2+} and wall vesicles that are involved in the process of tip growth.

The induction of branches using UV microbeams and the conclusions that can be made from this induction method should be approached with caution. This is because the

exposure of hyphae to UV microbeams could be causing a stress response within the hyphae. This stress response may manifest itself as a change in the Ca^{2+} dynamics, releasing Ca^{2+} into the cytoplasm. The subsequent production of branches may be a result of the stress caused by the UV irradiations as stress can result in the development of branches (Jackson, 1995).

A change to the external Ca^{2+} concentration has the ability to alter branching patterns of colonies of *A. bisexualis* and *N. crassa*. In both of these organisms, the addition of Ca^{2+} ionophores has resulted in the development of branches which is suggested to be a result of Ca^{2+} release into the cytoplasm from Ca^{2+} stores (Harold and Harold, 1986; Reissig and Kinney, 1983).

1.7 Actin and Hyphal Dynamics

1.7.1 Cell cytoskeleton

The actin cytoskeleton is an important feature of eukaryotic cells. Actin is a highly conserved protein that has a diverse range of roles within cells. The monomeric form of actin is 42kDa and is referred to as globular actin or G-actin. This form is capable of assembling by polymerisation into microfilaments which are called filamentous actin or F-actin. This assembly takes place with the aid of actin-binding proteins (ABPs). There are a number of ABPs, each with their own role and effect on the state of the structure of actin assembly (Berepiki et al., 2010).

The cytoskeleton in fungal cells is dynamic and its roles include maintaining the shape of hyphae, organisation of the elements within the cytoplasm, providing structures by which vesicles and organelles can use for transportation within the cell and in cell division (Riquelme et al., 2011). Tip growing cells are used a model systems for studying the role of the cytoskeleton in polarised cell growth (Geitmann and Emons, 2000).

1.7.2 Actin Structure

The actin monomer contains two domains; large and small and within these are four subdomains. There are particular features of these proteins that influence the dynamics of microfilaments. G-actin has a binding site for a nucleotide and a cation in the central cleft.

The nucleotide binding site can bind ATP or ADP and the cation binding site typically binds Mg^{2+} or Ca^{2+}. When the nucleotide is hydrolysed it changes the dynamics of F-actin. Another feature that changes the dynamics of F-actin is that the different ends of G-actin have different biochemical properties. As G-actin forms F-actin, one end of the monomer promotes the association of actin monomers. This end is known as the "plus" end or "barbed" end. The other end of G-actin promotes the disassociation of actin monomers. This end is known as the "minus" end or the "pointed" end. The overall effect of the biochemical nature of actin monomers gives F-actin an intrinsic polarity, with G-actin tending to assemble at one end and disassembling at the other (Walker and Garrill, 2006).

The polymerisation of actin can be characterised in four steps. The first step is the activation of G-actin which undergoes salt-binding and conformational changes. The second step is nucleation where oligomers of actin monomers are formed which are more likely to form into filaments than dissociate from one another. This is the rate limiting step of actin polymerisation as it is a very unfavourable reaction. The stability of dimers and trimers is greater in the presence of Mg^{2+} than Ca^{2+} as Mg^{2+} causes a conformational change. The third step is the elongation of the oligomers by polymerisation in both directions. The fourth step involves annealing of the ends of two filaments. The process of polymerisation is reversible at every stage (Pollard and Cooper, 1986). The two polymers that make up an actin filament have a left handed helical pattern with a diameter of ~7nm (Geitmann and Emons, 2000). F-actin has a flexible structure (Pollard and Cooper, 1986) and filaments are capable of joining with other microfilaments and form both fine and thick bundles (Geitmann and Emons, 2000).

1.7.3 Actin and Hyphal Tip Growth

F-actin is thought to be critically involved in the process of tip growth, facilitating vesicle delivery to the tip and controlling tip yielding in both fungi and oomycetes (Heath, 1990; Suei and Garrill, 2008). The distribution of actin at the tips of fungi and oomycete hyphae differ. This suggests that convergent evolution of these hyphal organisms is likely to have occurred with different F-actin distributions (Walker and Garrill, 2006).

One theory of how the establishment of polarity occurs in hyphal tips involves firstly, marking the growth site with cortical markers or intrinsic/external polarity cues. The signal is amplified involving mainly small Rho and Ras GTPases. The cytoskeleton and secretory

apparatus is then organised in the apical region of the cell. This restricts the area in which vesicles fuse with the plasma membrane. Another theory is that polarity is established internally by a shift in the Spitzenkörper, which acts at the vesicle supply centre (Riquelme et al., 2011). When the actin cytoskeleton is disturbed in *N. crassa*, along with other filamentous fungi, the tips swell. This indicates that actin plays a key role in determining the site of vesicle exocytosis (Heath et al., 2000; Knechtle et al., 2006; Torralba et al., 1998).

Actin is unlikely to function alone. Any such rearrangement at the tip is likely to occur through rapid modification of actin via ABPs, based on the requirements of the cell (Walker and Garrill, 2006). ABPs can be categorised into the following groups; monomer-binding proteins, nucleating proteins, capping proteins, severing proteins and proteins involved in the organisation/stabilisation of arrays/bundles (Asakura et al., 1998).

1.7.4 The Involvement of Actin in Branch and Septa Development

As new lateral branches form, tip growth of the parent hypha continues forwards. The new branch requires the establishment of its own polarity and then maintenance of this polarity as it establishes itself as a mature growing tip (Momany, 2002). The role of actin in generating polarity in new lateral branches is of great importance as this is thought to be an underlying factor involved in branching events. Relatively little is known about the role of actin in this event therefore, is an area of possible interest for research.

F-actin plays an important role in the formation of septa which, as mentioned earlier, are thought to be involved in the branching process. Septa are cross walls in filamentous fungi that are formed by cytokinesis (Harris et al., 1994). Septa are composed of glucans, chitin and other extracellular polysaccharides (Riquelme et al., 2011). Chitin is a key component of septa in the fungus *N. crassa* (Hunsley and Gooday, 1974). Septa function to compartmentalise hyphae into different zones. Septa do not separate the hyphal zones completely, as septal pores allow the movement of nuclei and organelles to different areas of the hypha. Another role of septa is that, when the hypha is damaged Woronin bodies (septal plugs) can use actin as a scaffold to move along in order to block off damaged areas of the colony (Rasmussen and Glass, 2005). As septa are formed, a band of microfilaments contract towards the location where wall material is being deposited (Harris et al., 1994). The ABPs that are thought to be involved in developing actin bands are formin and myosin. Formin aids

in the generation of the actin ring and myosin is involved in the ability of the F-actin ring to contract. The septal band pulls the plasma membrane inwards as the band contracts (Walker and Garrill, 2006).

1.7.5 Rho GTPases and Hyphal Dynamics

In response to external signals/nutrients, the actin cytoskeleton may need to be rapidly rearranged. The ability for this to occur is most likely based on signal transduction machinery targeting ABPs. The Rho family of GTPases are key signalling proteins involved in cytoskeleton organisation (Li et al., 1995) and these are generally found attached to the plasma membrane by their C-terminal farnesyl tail (Raudaskoski et al., 2001). The activity of these proteins is determined by the presence of GTP or GDP where GTP activates the protein turning it on and when GTP is hydrolysed the protein is turned off (Bourne et al., 1991). These are important proteins in the processes of cell polarisation, control of cell division and rearranging elements of the cytoskeleton (Rasmussen and Glass, 2005). Subfamilies within the Rho GTPase family include Rho, Rac and cdc42 (Takaishi et al., 1997).

1.8 Aims of Thesis

Clearly there is a need to better understand the branching process in hyphal organisms. In this study I will investigate some of the underlying mechanisms of hyphal branching process in the filamentous microorganisms *N. crassa* and A. *bisexualis.* In order to study branching events from the stages prior to the visible morphological changes, it is necessary to have the ability to predict where a branch will form. Therefore, in this study I will attempt to develop a branch induction technique for use on *N. crassa* which was initially developed in previous studies on oomycetes. Using this technique I will investigate the involvement of Ca^{2+} and F-actin on branch formation. Ca^{2+} channel inhibitors will be used to see if Ca^{2+} in *N. crassa* promotes or inhibits branching. This will be studied through the addition of various Ca^{2+} channel inhibitors to the growth media and the local application of the inhibitor verapamil towards hyphae using the branch induction technique. Cytoplasmic Ca^{2+} levels will be imaged using non-invasive dyes to see if there is Ca^{2+} present at sites of branch formation in both *A. bisexualis* and *N. crassa*. The involvement of F-actin in branching events will be imaged in live cells using a GM strain of *N. crassa*, Lifeact. This will enable the visualisation

of F-actin dynamics in real time and the spatial organisation of F-actin within the hyphae. The role of the Rho-GTPase family of signalling proteins in the branching process will be determined to see if there is an increase in protein expression when there is an increase in branch formation.

1.8.1 Hypotheses

1. Ca^{2+} inhibits hyphal branching in *N. crassa* and *A. bisexualis.*
2. Actin filaments are required at sites of hyphal branching in *N. crassa.*
3. Rho GTPase levels increase as branch frequency increases in *N. crassa* and *A. bisexualis.*

1.8.2 Model Organisms

In this study, two model filamentous hyphal organisms were used, the fungus *N. crassa* and the oomycete *A. bisexualis*. Even though these organisms are very different phylogenetically, they have a few key similarities including the morphology of tips and the rates at which they grow. These similarities are thought to be a result of convergent evolution (Lew et al., 2004).

N. crassa is an ascomycete belonging to the fungal kingdom, which inhabits terrestrial ecosystems (Lew et al., 1990). It is often found in areas of burned vegetation and in humid tropical and subtropical areas (Turner et al., 2001). It has a number of key attributes that make it an attractive candidate for modelling the fungal growth system. These features include a fast growth rate, an easily managed culture and an abundance of genetic knowledge about the species (Hickey et al., 2002). It has been used extensively in the field of eukaryotic biochemistry and genetics as a model organism.

A. bisexualis is an oomycete belonging to the Protoctista kingdom (Lew et al., 1990). The habitats of oomycetes include soil and freshwater and marine ecosystems. They have the ability to live parasitically on living material such as higher plants as well as on dead material of both plant and animal origin (Bhattacharya et al., 1991). Historically *A. bisexualis* and *S. ferax* have been used as model organisms for experiments on hyphal tip growth; this is in spite of their phylogenetic distance to the fungi. Of course studies on oomycetes are pertinent given that *Phytophthora* belongs to this group and is an organism of great economic, socioeconomic and ecological relevance.

Chapter 2

Materials and Methods

2.1 Materials

2.1.1 Reagents

Sucrose	Ajax Finechem Ltd, NZ
Na_3citrate.$2H_2O$	BDH Ltd, Poole, England
KNO_3	BDH Ltd, Poole, England
$(NH_4)H_2PO_4$	BDH Ltd, Poole, England
$MgSO_4.7H_2O$	BDH Ltd, Poole, England
$CaCl_2.2H_2O$	BDH Ltd, Poole, England
Biotin	Sigma, USA
Citric acid.$1H_2O$	J. T. Baker, Australia
$Fe(NH_4)_2(SO_4)_2.6H_2O$	BDH Ltd, Poole, England
H_3BO_3 (anhydrous)	Sigma, USA
PIPES	Sigma, USA
KH_2PO_4	BioLab (Aust) Ltd
K_2HPO_4	Fisher Scientific, Australia
$MgCl_2$	BDH Ltd, Poole England
$MnSO_4.1H_2O$	BDH Ltd, Poole England
$CoSO_4.7H_2O$	BDH Ltd, Poole, England
$NaMoO_4.2H_2O$	BDH Ltd, Poole, England
$ZnSO_4.7H_2O$	BDH Ltd, Poole, England
$CuSO_4.5H_2O$	Sigma-Aldrich, United Kingdom
Glutamic acid	Sigma, MO, USA

Methionine	Sigma, MO, USA
Isoleucine	Sigma, MO, USA
Leucine	Sigma, MO, USA
Threonine	Sigma, MO, USA
Valine	Sigma, MO, USA
Lysine	Sigma, MO, USA
Glycine	Sigma, MO, USA
Arginine	Sigma, MO, USA
Phenylalanine	Sigma, MO, USA
Tyrosine	Sigma, MO, USA
Serine	Sigma, MO, USA
Histidine	Sigma, MO, USA
Tryptophan	Sigma, MO, USA
KOH	BioLab (Aust) Ltd
Tris-HCl	Invitrogen, CA, USA
NaCl	Ajax Finechem Pty Ltd, NZ
EDTA	BDH Ltd, Poole, England
NP-40	Sigma, NZ
SDS	BioRad Laboratories, CA, USA
Na_3VO_4	BDH Ltd, Poole, England
Glycerol	BDH Ltd, Poole, England
Protease Inhibitor Cocktail Tablet	Complete, Germany
Bacteriological Peptone	Oxoid, Hampshire, England
Glucose	Merek, Darmstadt, Germany
Yeast extract	Oxoid, Hampshire, England
Agar Bacteriological, Agar No. 1	Oxoid, Hampshire, England
Fluo-3, AM cell permeable	Invitrogen, Molecular Probes USA
Fura red, AM cell permeable	Invitrogen, Molecular Probes USA
30% Acrylamide	BioRad Laboratories, CA, USA
$(NH_4)S_2O_8$	BioRad Laboratories, CA, USA
TEMED	BioRad Laboratories, CA, USA
Tris	Invitrogen, CA, USA

Methanol	Ajax Finechem Pty Ltd, NZ
Skim milk	Pam's, Australia
BSA	Gibco, Life Technologies,
Tween-20	BioRad, CA, USA
Verapamil-hydrochloride	Sigma, China
Gadolinium (III) chloride hexahydrate	Sigma, USA
Lanthanum (III) chloride heptahydrate	Sigma-Aldrich, USA
UltraPure L.M.P. Agarose	Invitrogen, Spain
DMSO	BDH Ltd, Poole, England
Ethanol	Technical grade
Coomassie Blue	Sigma, NZ
Glacial acetic acid	Ajax Finechem Pty Ltd, NZ
Na_2HPO_4	BioLab (Aust) Ltd

2.1.2 Antibodies

Primary	Type	Concentration	Blocking Solution	Company
Actin	Mouse	1/500	BSA	Santa Cruz, USA
Cdc42	Rabbit	1/1000	Skim Milk	Cell Signalling Technology, USA
Phospho-Rac1/cdc42	Rabbit	1/1000	Skim Milk	Cell Signalling Technology, USA
Rac1/2/3	Rabbit	1/1000	Skim Milk	Cell Signalling Technology, USA
RhoA	Rabbit	1/1000	Skim Milk	Cell Signalling Technology, USA
RhoB	Rabbit	1/1000	Skim Milk	Cell Signalling Technology, USA
RhoC	Rabbit	1/1000	Skim Milk	Cell Signalling Technology, USA

Secondary	Type	Concentration	Blocking Solution	Company
Mouse	Donkey	1/10000	BSA	Santa Cruz, USA
Rabbit	Goat	1/5000	Skim Milk	Cell Signalling Technology, USA

2.1.3 General Solutions, Buffers and Media

2.1.3.1 Vogel's Media

Vogel's medium was made up containing the following; 43.82 mM sucrose, 8.84 mM Na_3citrate.$2H_2O$, 25 mM KNO_3, 25 mM $(NH_4)H_2PO_4$, 11.76 mM KH_2PO_4, 0.81 mM $MgSO_4.7H_2O$, 0.68 mM $CaCl_2.2H_2O$, 1.19 mM Citric acid.$1H_2O$, 0.87 mM $ZnSO_4.7H_2O$, 0.13 mM $Fe(NH_4)_2(SO_4)_2.6H_2O$, 50.06 μM $CuSO_4.5H_2O$, 14.79 μM $MnSO_4.1H_2O$, 40.43 μM H_3BO_3, 10.33 μM $Na_2MoO_4.2H_2O$ and 0.41 M biotin (in 50% v/v ethanol) in d.H_2O.

2.1.3.2 Peptone Yeast Glucose (PYG) Media

PYG medium was made up containing the following; Peptone 0.125% w/v, yeast extract 0.125% w/v and glucose 0.3% w/v in d.H_2O.

2.1.3.3 $DMA_{3.2}$ Media

$DMA_{3.2}$ medium was made up containing the following; 1 mM KPIPES, 0.5 mM KH_2PO_4, 0.5 mM K_2HPO_4, 1 mM $MgCl_2$, 0.5 mM $CaCl_2$, 11 μM H_3BO_3, 1.8 μM $MnSO_4$, 0.7 mM $CoSO_4.7H_2O$, 0.4 mM $NaMoO_4.2H_2O$, 0.4 mM $ZnSO_4.7H2O$, 0.3 μM $CuSO_4.5H_2O$, 1.36 mM glutamic acid, 0.22 mM methionine, 0.2 mM isoleucine, 0.2 mM leucine, 0.2 mM threonine, 0.2 mM valine, 0.2 mM lysine, 0.1 mM glycine, 0.1 mM arginine, 0.1 mM phenylalanine, 0.1 mM tyrosine, 0.1 mM serine, 0.05 mM histidine, 0.02 mM tryptophan and 10 mM glucose in d.H_2O. pH to 6.5 with KOH.

2.1.3.4 Inhibitor Solutions

The inhibitors verapamil, Gd^{3+} and La^{3+} were dissolved in d.H_2O containing 0.01% DMSO.

2.1.3.5 Phosphate Buffer Solution (PBS)

PBS was made up containing the following, 131 mM NaCl, 5.1 mM Na_2HPO_4 and 1.56 mM KH_2PO_4 in d.H_2O.

2.1.3.6 RIPA Lysis Buffer

RIPA lysis buffer was made up containing the following, 50 mM Tris-HCl pH7.4, 100 mM NaCl, 5 mM EDTA, 1% v/v NP-40, 0.1% w/v SDS, 1 mM Na_3VO_4, 10% v/v and a protease inhibitor cocktail tablet in d.H_2O.

2.1.3.7 5X Sample Buffer

5X sample buffer was made up containing the following, 6% v/v 1M Tris-HCl pH 6.8, 50% v/v 50% glycerol, 20% v/v 10% SDS, 5% v/v 2-mercaptoethanol and 10% v/v 1% bromophenol blue in d.H_2O.

2.1.3.8 SDS Gels

2.1.3.8.1 12% Acrylamide Separating Gel

12% acrylamide separating gel was made up containing the following; 40% v/v Solution A: 30% acrylamide; 25% v/v Solution B: 75% v/v 2 M Tris-HCl (pH 8.8) and 4% v/v 10% v/v SDS; 0.007% v/v 10% $(NH_4)S_2O_8$; and 0.0005% v/v TEMED in d.H_2O.

2.1.3.8.2 7% Acrylamide Stacking Gel

7% acrylamide stacking gel was made up containing the following, 25% v/v Solution A: 30% acrylamide; 25% v/v Solution C: 50% v/v 1 M Tris-HCl (pH 6.8) and 4% v/v 10% SDS in water; 0.01% v/v 10% $(NH_4)S_2O_8$; and 0.001% TEMED in d.H_2O.

2.1.3.9 MES Running Buffer

MES running buffer was made up containing the following, 20x Bolt MES running buffer (lot 1172017) (CA, USA) diluted to 1x with nanopure H_2O.

2.1.3.10 SDS-PAGE Running Buffer

SDS-PAGE running buffer was made up containing the following, 24.76 mM Tris, 191.83 mM Glycine and 3.47 mM SDS in d.H_2O.

2.1.3.11 Coomassie Blue Gel Stain

Coomassie blue gel stain was made up containing the following, 1% w/v Coomassie blue, 45% v/v methanol and 10% v/v glacial acetic acid in d.H_2O.

2.1.3.12 Coomassie Gel Destain

Coomassie gel destain was made up containing the following, 10% v/v methanol and 10% v/v glacial acetic acid in d.H_2O.

2.1.3.13 Transfer Buffer

Transfer buffer was made up containing the following, 1.93% w/v Tris, 9% w/v of Glycine and 10% methanol in d.H_2O.

2.1.3.14 TBS-T

TBS-T was made up containing the following, 1% v/v 2M Tris-HCl pH 7.5, 0.8.18% w/v NaCl and 0.1% v/v Tween-20 in d.H_2O.

2.1.3.15 Blocking Solutions

Blocking solutions were made up containing the following, either 5% w/v skim milk or 4% w/v BSA in TBS-T.

2.1.3.16 Antibody Solutions

Antibody solutions were made up containing the following, either 2.5% w/v skim milk or 1% w/v BSA diluted in TBS-T.

2.2 Methods

2.2.1 Cultures

2.2.1.1 *Neurospora crassa*

Neurospora crassa (Shear and Dodge, 1927) mating type A was obtained from the University of Canterbury culture collection (C213). The culture was maintained on Vogel's media with 2% agar. A 6mm diameter cork borer was used to excise a plug of agar from the growing edge of the culture. When subculturing, this would be used as an inoculum for a fresh stock plate. Stock cultures were maintained at 20-26°C.

2.2.1.2 Lifeact *Neurospora crassa*

Lifeact strains were obtained from the Fungal Genetics Stock Collection (Kansas, USA). Two Lifeact strains were used; FGSC#10598 pAL12-Lifeact [Ptef-1::Lifeact-TagRFP-T::nat1] and FGSC#10599 pAL12-Lifeact [Ptef-1::Lifeact-TagRFP-T::nat1]. Plasmids used

in these strains were pAL12-Lifeact, promoter P*tef-1*, reporter peptide Lifeact (GGVADLIKKFESISKEE), fluorescent protein TagRFP-T, terminator T*trpC*, and selection gene/marker *nat1*/nourseothricin. Full details of the construction of Lifeact-RFP expression plasmids can be found on the fungal genetics stock centre website http://www.fgsc.net/FGR/FGR57/Lichius/FGR57_Lichius.htm. These strains were cultured on 2% Vogel's agar using a 6mm cork borer to excise a section from the growing edge of the culture. This was used as an inoculum when subculturing. Stock cultures were maintained at 20-26°C.

2.2.1.3 *Achlya bisexualis*

Achlya bisexualis (Coker), female strain, was obtained from the University of Canterbury culture collection. This strain was originally isolated in New Zealand from *Xenopus laevis* dung. The culture was maintained on 2% PYG agar using a 6mm cork borer to excise a section from the growing edge of the culture which was used as an inoculum when subculturing. Stock cultures were maintained at 20-26°C.

2.2.2 Experimental Cultures

2.2.2.1 *N. crassa* Cellophane Plates

Circles with a diameter of 8cm were cut out of cellophane (Artworx). These circles were boiled in distilled water while stirring for 30 minutes. The water was changed a total of 3 times during the 30 minutes. This was to ensure that any chemicals used in the manufacture of the cellophane were removed. The cellophane circles were autoclaved and stored in jars containing d.H_2O. The sterile circles were placed on top of Vogel's agar in 84 mm petri dishes. A 6 mm plug of agar was cut from the growing edge of a mycelium growing on Vogel's agar and placed in the middle of the cellophane overlaying the agar. The mycelia grew flat on the cellophane and were not in direct contact with the agar. This system was used so *N. crassa* could be more easily manipulated and lain flat in the experimental chambers. The experimental cultures were maintained at 26°C.

2.2.2.2 *A. bisexualis* Cellophane Plates

Sterile cellophane circles were made as describe above. The sterile circles were placed on top of PYG agar in 84 mm petri dishes. From the growing edge of the *A. bisexualis* mycelium (growing on PYG agar) a 6 mm plug of agar with hyphae growing on it was removed and placed in the middle of the cellophane overlaying the agar. This ensured the mycelia grew flat on the cellophane without coming in direct contact with the agar enabling easy manipulation for experimental purposes. The experimental cultures were kept at 26°C.

2.2.3 Branch Induction

2.2.3.1 Experimental chambers

Sixteen millimetre holes were drilled through plastic microscope slides. A 22 mm by 22 mm coverslip was attached the bottom of the slide with vaseline so that it covered the hole, creating a small chamber that mycelia could grow in. After the first 20 inductions, the welled slides were replaced with tissue culture dishes with coverslip bottoms, FluoroDish (World Precision Instruments, Inc.) which enabled an easier experimental setup.

Sections were cut from the leading edge of the mycelia that had grown on the cellophane plates. The piece of cellophane with the section of mycelium attached was placed on the prepared microscope slide/culture dish so the cellophane touched the coverslip and the hyphae were on top. Molten 2% low melting point (LMP) Vogel's agar, which had been cooled, was pipetted on top of the hyphal mat to cover it with a thin, even coat of agar. The agar was then left to solidify for 5 minutes after which liquid Vogel's media was applied to the top of the agar to prevent the agar drying out. Hyphae were left to recover and resume their normal growth rate at 26°C for at least one hour before experiments were conducted.

2.2.3.2 Micropipettes

Micropipettes were pulled from borosilicate glass capillaries with an outer diameter of 1.0 mm, inner diameter of 0.58 mm and inner filament (Harvard Apparatus Ltd GC100F-10, Kent) using a Narishge PC-10 (Japan) micropipette puller. The aperture of the micropipette tip needed to be the same for each induction in order to be consistent between experiments

therefore the size of the micropipette tip was always checked. This was to ensure that the amount of liquid media applied to the hypha was as consistent as possible from trial to trial. The size of the aperture of the micropipette tip was checked by connecting the micropipette to a rubber tube which was attached to a 60 ml syringe. The micropipette tip was placed into a beaker of methanol. The syringe was then compressed until bubbles emerged from the tip of the micropipette. The volume of compressed air in the syringe when bubbles first begin emerge from the tip of the pipette indicated the amount of pressure required to push air out of the tip which was dependent on the aperture of the tip. This is referred to as the bubble number. A bubble number between 38 and 42 was always used for induction experiments.

2.2.3.3 Water Filled Pressure Microinjector

Initially a microinjector that was manually controlled (Narishige, Japan) was used for the inductions. After the first 20 inductions, the water-filled pressure probe was modified by adding a motor to ensure a more consistent flow of induction media towards the hypha. Motorised inductions did not differ in terms of the percentage of successful inductions compared to inductions with the non-motorised water-filled pressure probe so for data analysis all of the trials were added together.

2.2.3.4 Induction assays

Micropipettes were filled with the induction solution which contained 1 mM phenylalanine dissolved in liquid Vogel's media. This induction solution was used in all induction trials. To ensure the hypha from which a branch was being induced was growing, it was monitored for 5 minutes before the pipette was positioned and the induction started. The micropipette was placed into a water-filled pressure microinjector which was used to apply moderate pressure to the solution in the micropipette. The micropipette was positioned on average 6 μm away from the hypha perpendicular to the long axis of the hypha and 34 μm away back the growing tip. Once the micropipette was positioned, a timer was started and pressure was applied to the induction solution. Images were captured with a Nikon Coolpix 5400 digital camera (New York, USA) using the time lapse function where an image was captured every 30 seconds. Vogel's media alone and water alone were used as controls to see

if it was the phenylalanine solution or mechanical disturbance of the pipette that resulted in branch formation.

2.2.3.5 Microscope

Specimens were examined with a Zeiss IM35 microscope (Germany) using an x40 objective (numerical aperture 0.75).

2.2.3.6 Hyphal measurements

Using the time lapse images obtained from the inductions, a number of measurements were made. The start time of the inductions was the point where the micropipette was positioned next to the hypha and pressure was applied. The time taken for bump formation to occur was taken from the start of the trial and was the point at which the wall of the hypha began to curve out. The time taken for a bud to form was the time to transition from the bump stage to the point where the shape of the bump changes to a protrusion. The time taken for a branch to form was the time to transition from the bud stage to the point where the bud grew outward and formed the shape of a branch. The hyphal width was measured 50 μm back from the tip when the induction began. The growth rates for both the hypha and the branch were measured from the tips based on distance covered over time. The distance from the micropipette to the hyphal trunk was measured from the tip of the micropipette to the closet point on the hyphal trunk. The distance of the micropipette to the hyphal tip was measured from the micropipette tip to the very apex of the hypha. The distance from the micropipette to the hyphal branch was measured from the micropipette tip to the site on the hyphal trunk where the branch grows out of. Branches which were apical to the position of the micropipette were given as positive distances and branches that were subapical the measurements were given negative distances.

2.2.4 Whole Plate Ca^{2+} Channel Inhibitor Experiments

2.2.4.1 Experimental Set Up

Three Ca^{2+} channel inhibitors were used in these experiments; Verapamil, Gd^{3+} and La^{3+}. All inhibitors were made up as stock solutions by dissolving individually in 0.01% v/v DMSO in d.H_2O. Plates set up as in 2.2.2.1 but with inhibitors in the Vogel's media with 2% agar containing the following concentrations of each inhibitor; 5 μM – 1000 μM and 1000 μM with 10 mM $CaCl_2$. Controls were 5 mM $CaCl_2$, 10 mM $CaCl_2$ and 0.1% v/v DMSO.

2.2.4.2 Microscope

Specimens were examined with a BH2 Olympus microscope (Japan) using an x4 objective (numerical aperture 0.1). Images were taken with a Leica DM5000B microscope (Wetzlar, Germany) using an x2.5 objective (numerical aperture 0.07). Whole plates were scanned using an Epson Perfection V700 scanner (Suwa, Nagano, Japan).

2.2.5 Effect of Verapamil on Branch Inductions

2.2.5.1 Experimental Set Up

Branch inductions were carried out as described in 2.2.3 except that verapamil was added to the Vogel's media containing 1mM phenylalanine at concentrations of 50 μM, 500 μM or 1000 μM.

2.2.6 Live Ca^{2+} Imaging

2.2.6.1 Ca^{2+} Fluorescent Probes

Fluo-3, AM cell permeable and fura red, AM cell permeable were used to image the cytoplasmic Ca^{2+} levels within the hyphae, these dyes enable ratio imaging. Dyes were

visualised individually to gauge the appropriate concentration of each and to determine emission wavelengths to avoid bleed through of light between channels. This revealed 10 μM fluo-3 AM and 20 μM fura red AM were adequate to give good fluorescence. Dyes were prepared in DMSO.

2.2.6.2 Experimental Chambers

N. crassa cells were cultured on cellophane plates (2.2.2.1) for 18 hours at 26°C. *A. bisexualis* cells were cultured on cellophane plates (2.2.2.2) for 48 hours at 26°C. A 1cm x 1cm square was cut from the growing edge of the mycelium and placed on a microscope slide. The dyes were diluted in PBS solution for *A. bisexualis* or d.H_2O for *N. crassa* and applied on top of the mycelia. The slides were left at 20°C for 1 hour for the hyphae to take up the dye. PBS alone or water alone was used to wash away the excess dye that had not been taken up by the cells. Hyphae were washed 3 times. A cover slip was then lowered on top of the hyphae and the cells were then imaged.

2.2.6.3 Confocal Microscopy

Cells were imaged using a Leica confocal microscope (Wetzlar, Germany). The x20 (numerical aperture 0.7) and x63 (numerical aperture 1.3) glycerol objectives were used. Both dyes were excited by the 488nm argon laser (20% intensity). Fluo-3 emitted light in the range of λ 500-600 nm. Fura Red emitted light in the range of λ 600-750 nm. Emitted fluorescence was detected simultaneously using different channels to collect the emitted light.

2.2.6.4 Autofluorescence

N. crassa and *A. bisexualis* were imaged on the confocal using the same settings as were used for the dyes to detect any autofluorescence. *N. crassa* had a weak, even level of fluorescence throughout the colony. *A. bisexualis* had fluorescence in the tip region however this fluorescence was weaker than the fluorescence emitted when the dye present.

2.2.7 Live Actin Imaging

2.2.7.1 Experimental Chambers

Lifeact expressing strains of *N. crassa* were cultured on a thin sheet of 2% Vogel's agar at 26°C for 10-14 hours. The inverted block method was used to image the two strains on the confocal microscope in which a block of agar is removed from the growing edge of the mycelia and placed into the experimental chambers (FluoroDish, World Precision Instruments, Inc.). The mycelia growing on top of the agar were inverted so they came in direct contact with the coverslip on the base of the culture dish.

2.2.7.2 Confocal Imaging

The cells were imaged using a Leica confocal microscope (Wetzlar, Germany) using the x63 glycerol immersion objective (numerical aperture 1.3). Excitation of the hyphae was conducted using the 561 nm laser at 20% laser intensity. Fluorescence was emitted in the range of λ 580 nm – 670 nm.

2.2.7.3 Autofluorescence

Wild type *N. crassa* cells were imaged on the confocal using the same settings as were used for the Lifeact strains to detect any autofluorescence. *N. crassa* had a weak, even level of fluorescence throughout the colony.

2.2.8 Western Blotting

2.2.8.1 Protein Extraction *N. crassa*

Cultures were grown on Vogel's agar for 24 hours. A 6mm cork borer was used to remove plugs from the growing edge of the culture. Verapamil was added to 2% Vogel's agar at concentrations ranging from 5 μM-200 μM. Cellophane was placed on the verapamil plates as described above. Six plates of each concentration were cultured at 26°C for 18 hours. The

mycelia at the growing edge of each plate was scraped off the cellophane and placed in a mortar with RIPA lysis buffer. Liquid nitrogen was added and the cells were ground into a powder using a pestle. Extracts were centrifuged at 13680 g at 4°C for 10 minutes. The supernatant was removed and stored for analysis. This was repeated 4 times on separate days.

2.2.8.2 Protein Extraction *A. bisexualis*

Verapamil was added to $DMA_{3.2}$ agar at concentrations of between 5 μM and 200 μM. Cultures were grown on $DMA_{3.2}$ agar for 48 hours. A 6 mm cork borer was used to remove plugs from the growing edge of the culture. Cellophane was placed on the verapamil plates as described above. Six plates of each concentration were cultured at 26°C for 18 hours. The growing 1 cm of hyphae from the mycelial edge of each plate was scraped off the cellophane and placed in a mortar with RIPA lysis buffer. Liquid nitrogen was used to freeze the cells and they were then ground into a powder. Extracts were centrifuged at 13680 g at 4°C for 10 minutes. The supernatant was removed and stored for analysis.

2.2.8.3 BCA Protein Assay

A BCA protein assay was carried out using an assay kit (Thermo Scientific, Illinois, USA) to determine the total protein in the samples. This was conducted to normalise the protein concentrations in each sample for Western Blotting. 25 μl of each unknown sample was added to a microplate well. To each well 200 μl of the working reagent (50:1, Reagent A:B) was added. The plate was mixed well and incubated at 37°C for 30 minutes. Absorbance was measured at λ 562 nm on a Molecular Devices SpectraMax M5 plate reader (USA). Analysis of the absorbance values was carried out with SoftMax Pro 5.4.1.

2.2.8.4 Protein Sample Preparation *N. crassa* and *A. bisexualis*

In order to normalise the protein concentrations the *N. crassa* and *A. bisexualis* samples they were diluted in 95% ethanol. The protein was left to precipitate at 4°C for 60 minutes. The samples were centrifuged at 18620 g at 4°C for 30 minutes. The ethanol was evaporated and 15 μl of 5X sample buffer was added. The samples were heated to 95°C for 10 minutes.

2.2.8.5 SDS-PAGE

Proteins were separated on Novex Bolt 4-12% Bis-Tris Plus gels (Life Technologies, USA). Gels were run using MES running buffer for 40 minutes and then incubated with Coomassie Blue Stain for 2 hours at room temperature with gentle shaking. Gels were the incubated with Coomassie Blue Destain overnight until bands were clear. The gels were then imaged using Chemi Genius^2 Bioimaging system.

2.2.8.6 Western Blotting

Gels were prepared with the 12% acrylamide separating gel and 7% stacking gel. Gels were run for 2 hours in SDS-PAGE running buffer. The proteins were transferred to a nitrocellulose membrane (BioRad, Germany) using transfer buffer at 100V for 1 hour. Membranes were put in the appropriate blocking solution (see 2.1.2 for antibodies and blocking solutions) for 60 minutes. The diluted primary antibody was added and incubated overnight at 4°C. The membranes were washed with TBS-T and incubated with diluted secondary antibody for 90 minutes at room temperature. The membranes were washed with TBS-T and developed using Western Blotting Luminol Reagent SC-2048 (Santa Cruz Biotechnology Inc., Santa Cruz, USA). The membranes were imaged using Chemi Genius^2 Bioimaging system with 60 second exposure time.

2.9 Image Processing

Images were processed using LAS AF Lite 2.6.0 (Germany) and Adobe Photoshop CS6 (Ireland).

2.10 Statistical Analysis

Statistical analysis was carried out using GraphPad Prism 6.0 software (California, USA). When variances were not significantly different between samples, a parametric test was conducted. When variances were significantly different between samples, a non-parametric test was conducted. Significance was denoted as $p \leq 0.05$ - *, $p \leq 0.01$ - **, $p \leq 0.001$ - ***, $p \leq 0.0001$ - ****.

Chapter 3

Branch Induction of *Neurospora crassa*

3.1 Introduction

In order to study branch formation, the ability to predict where branches will form in fungal hyphae will enable investigations aiming to determine the underlying mechanisms of hyphal branching. In this chapter a branch induction technique involving the local application of the amino acid phenylalanine was used to determine the response in fungal hyphae. This technique has previously been used to induce hyphae to produce branches in oomycetes (Morris et al., 2011; Schreurs et al., 1989). To date there has not been a technique developed to induce branches in fungal hyphae, however oomycetes and fungi are morphologically similar so may show a similar response to this technique.

3.1.1 Branch Induction Techniques

As discussed earlier, there have been two techniques developed to date that induce the formation of branches in oomycetes. The first involved using UV microbeams to induce branches in *Saprolegnia ferax* (Grinberg and Heath, 1997) and the second technique used the local application of amino acids to induce branches in *A. bisexualis* (Schreurs et al., 1989). Induction techniques like the ones above appear to be capable of overriding factors governing the hyphal growth unit and produce branches in a certain area (Jackson et al., 2001).

The technique used by Schreurs et al. (1989) was modified by Morris et al. (2011) in an attempt to reduce the variability in the time taken for the formation of branches. The modifications were; the hyphae were covered with LMP agar in order to immobilise them, the micropipettes were fabricated so that they all had a similar tip diameter and hyphae that were picked for induction had a relatively constant width of 20-25 µm. The amino acid phenylalanine was added to liquid media and this solution was locally applied to the hyphae

using a micropipette. This technique resulted in branches forming in 28 of 36 hyphae (a success rate of 78%). When the liquid media alone was used, branching occurred in only two of 10 hyphae, a success rate of 20%. The growth rate of the hyphal tip did not change as the induction was occurring. These branches were thought to be forming as a result of amino acids binding to certain receptor proteins on the surface of the hypha which influence where exocytosis of vesicles will occur and thus determines where a branch will form (Schreurs et al., 1989).

The branch induction technique developed by Grinberg and Heath (1997) on *S. ferax* produced branches 84% of the time. Branches were formed up to 170 µm away from the site where the irradiations occurred and within 10 minutes of the beginning of the irradiation. With respect to the number of branches produced, 70% of the branches resulted in a single branch forming with the remainders forming two or occasionally three. A majority of the branches (92% of branches formed) formed at, or subapical to the location where the irradiation occurred. The UV microbeams that were used had wavelengths of 300-380 nm and 385-450 nm. There is however a possibility that the microbeams might result in a stress response from the hyphae. Therefore the health of the hyphae being induced may not reflect the natural state of growth which would be required for further investigation into the underlying mechanisms of hyphal branching.

Both of these induction techniques have resulted in disruption of tip growth of the hyphae being induced to some degree. With the local application of amino acids towards the hyphae, the tip growth was reoriented as it showed a chemotropic response towards the source of the amino acids (Schreurs et al., 1989). Alternatively, with the use of UV microbeams, the growing tip of the hyphae ceased to grow after being irradiated (Grinberg and Heath, 1997). The local application of amino acids is thought to cause less disruption to the normal growth of the hyphae compared with the use of UV microbeams. Therefore it was decided that local application of amino acids would be used in this study on *N. crassa*. This will also allow for comparisons of factors involved in branch formation between oomycetes and fungi.

3.1.2 Branch Development Steps

There are two models that attempt to explain the process of branch initiation. The first of these suggests that the factors involved in the branching process are recruited to the new

site of growth from somewhere within the growing colony (Zalokar, 1959). Branches will form when the elongation capacity of the existing hyphal tip is surpassed (Katz et al., 1972), and the accumulation of vesicles is thought to precede the generation of the new branch (Trinci, 1974). A shift in the vesicle supply centre present at the tip may be involved in the branch determination process. The shift may be generated by a hyphal-based pushing mechanism where the cytoskeleton acts as a scaffold for the VSC to move forward (Bartnicki-Garcia et al., 1989). The second group branch initiation models fall into is based on events that are independently controlled at the tip. The VSC may be displaced by a tip-based pulling mechanism potentially involving microfilaments, integrin and spectrin-like proteins (Bartnicki-Garcia et al., 1989).

The development of branches has been proposed to be a four stage event with "discrete and genetically separable steps" (Seiler and Plamann, 2003). The first step involves the selection of a future branch site through internal signalling pathways. The second step is when the branch site broadens forming a bulge in the cell wall. These first stages involve the delivery of materials required for the development of a new branch to the future branch site such as the cytoskeletal elements and vesicles containing cell wall materials etc. The third step is the production of a small protrusion from the bump which involves the establishment of polarity in the branch. The fourth and final step is the maturation of the new branch into a mature growing hyphal tip. In the final stage, polarity in the new branch is stabilised at which point it will reach its highest growth rate (Harris, 2008; Seiler and Plamann, 2003). After a branch has been formed it must grow using the same mechanism employed by the original growing tip that produced it (Watters et al., 2000). These stages of branch formation are shown in Figure 3.1.

The steps involved in the process of branch formation were evident in *A. bisexualis* after the local application of amino acids to induce branches. Once the induction media was applied locally towards the hypha, a bump in the hyphal wall began to form with a width of between 15 and 25 µm. Within this bump along the cell wall of the hypha, another bump formed in the middle with a width of about 8 µm. This occurred approximately 8 minutes after the induction began. This second bump formed into the branch and therefore the new growing tip. The time it took for a bump to form was not consistent ranging from 8-52 minutes (n=18) with an average of 22.7 ± 13.2 minutes (mean ± SD) from the start of the induction. The time to branch was also variable taking an average of 27.3 ± 14.1 minutes ranging from 11-56 minutes (n=18). Hyphae with a width between 20-25 µm had less variability in these times therefore they were picked for further inductions. The positioning of

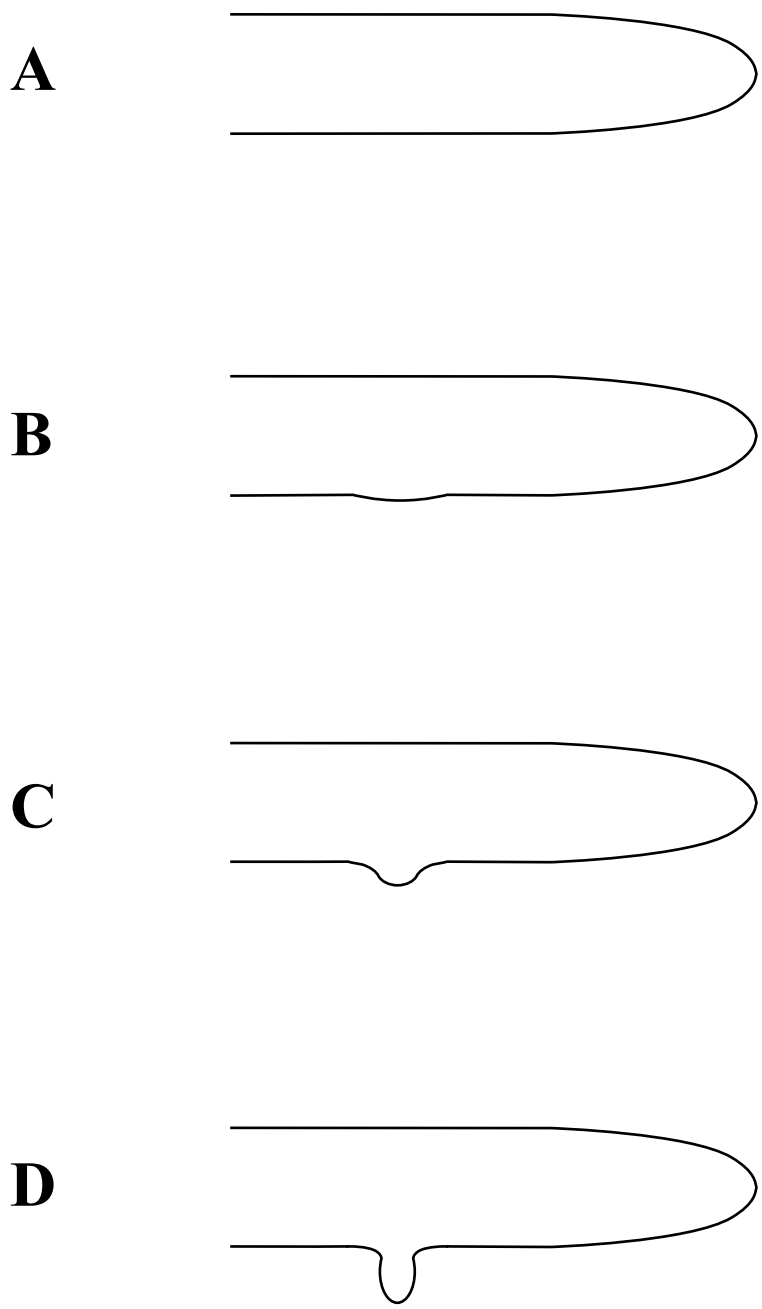

Figure 3.1 - Branch formation steps in a filamentous hyphae. A shows the hypha pre visable stages of branch formation. B shows the bump stage. C shows the formation of a bud from the hypha. D shows the branch stage which is the final stage of the branching process. This branch then matures and becomes a new growing tip which will branch.

the micropipette was also keep consistent relative to the hypha. It was kept between 40-60 µm back from the tip and 15 µm from the side of the hypha (Morris et al., 2011).

The mechanism underlying branch formation is of great interest for the study of tip growth as a branch is the development of a new growing hyphal tip and therefore a new axis of polarity. Branch formation in fungi and oomycetes can be triggered by either intrinsic factors or external factors. These factors initiate a single signal cascade or multiple signal cascades which converge forming a single signalling pathway. When there is no other branch formation factors present, the hyphal growth unit could be acting as an intrinsic factor for branch formation. The possible stages of branch formation start with a signal that is perceived then results in signal transduction within the hypha. This signal then provides a directional cue for the location of a new branch and the development of a polarised domain at the branch site. This stage is potentially the first point in which the new branch can be seen. The structure of the components involved in branch formation become ordered in the way seen at the tip as polarity increases and feedback loops are in place to continue outgrowth of the new branch (Jackson et al., 2001).

3.1.3 Chemotropism of Tip Growing Hyphae

Chemotropism is a change in the direction of growth of the hyphal tip (Schreurs et al., 1989). Through the sensing of the immediate environment, hyphae are able to reorient their growth providing information for the whole colony. This enables a variety of tissues to be exploited by the colony and determination of when to form mating structures (Brand and Gow, 2009). The ability for hyphae to alter their direction of growth is a key feature of hyphal growth. Prior to work conducted by Schreurs et al. (1989), the processes of branching and chemotropism appeared to be governed by different processes. Chemotropism was thought to be involved in the acquisition of nitrogen whereas branching was thought to occur as a result of an adequate supply of nitrogen. However, after further investigation these processes appear to be alternative responses to nutrient signals that are mediated by receptors on the cell surface which are closely related (Schreurs et al., 1989).

Oomycetes have displayed a chemotropic response when amino acids were used to induce branching bending towards the tip of the micropipette. The chemotropic response was measured by the degree at which the hyphae changed its direction of growth. The average angle tip growth changed by was 42.3 ± 60º ranging from -2.1º away from the micropipette to

73.8º towards the micropipette. When hyphae bent less than 6º they did not branch, therefore these events may be linked (Morris et al., 2011).

In order to change the direction of growth, it has been suggested that the location of exocytosis of vesicles is shifted towards the gradient of amino acids present in the media (Schreurs et al., 1989). The possible reason that amino acid gradients result in branching formation is that receptors which amino acids bind to are relocated to the area exposed to the gradient and when the response reaches a threshold level, vesicles undergo exocytosis in this area. The receptors that detect phenylalanine and methionine in *A. bisexualis* are thought to be different and distributed uniformly over the surface of the cell. When receptors that are found in the apical region of the cell are activated by the presence of these amino acids, it can alter the direction of the tip's growth, thus resulting in a chemotropic response. When receptors that are found in the subapical region of the hypha are activated by the presence of these amino acids, it triggers the formation of a new branch (Schreurs et al., 1989).

3.1.4 Aims of Chapter 3

In this chapter I will use the technique for inducing branch formation that involves the local application of the amino acid phenylalanine to see what effect it has on the fungus *N. crassa*. This will enable the determination of mechanisms that occur before, during and after the formation of branches in this filamentous fungus. It will also allow the comparison of branching events between fungi and oomycetes in order to see if they involve similar mechanisms.

3.2 Materials and Methods

See Chapter 2 for full Methods and Materials.

3.3 Results

3.3.1 Branch Induction in *N. crassa*

Hyphae that were growing invasively (i.e. through the agar rather than on top of it) were chosen for inductions as they will stay in position during the induction and the solution, when applied will disperse in a more direct manner towards the hypha. To enable this, LMP agar was used to cover growing hyphae that were transferred to the experimental chamber on cellophane. This approach to branch induction required the technically difficult movement of the glass micropipette through the agar to the invasively growing hypha selected. The hypha of interest was observed before the positioning of the micropipette containing the induction solution to ensure that it was growing. There was a significant reduction in the average hyphal growth rate before and after the induction ($p>0.05$ see Appendix 1). The average hyphal growth rate before the induction was 13 ± 7 μm/minute (n=29 hyphae) and after the induction the growth rate slowed to 10 ± 6 μm/minute (n=29 hyphae) (Figure 3.2). For an induction to be included in the results, the micropipette had to be positioned close to the hypha without it being broken or blocked. Due to the technically difficult procedure of moving the micropipette through agar, on some occasions agar would block the tip of the micropipette or the tip was broken as it was being positioned. In such instances the induction was discounted.

Branches were reliably induced in *N. crassa* with a success rate of 83% (24 out of 29 hyphae). For a trial to be considered successful, at least one branch had to form along the hypha in the field of view (Figure 3.3). Two separate controls were used to analyse the effects of phenylalanine on branch formation. The first control involved using water rather than the induction media. No branches were formed with this treatment however a bump formed in 1 trial (n=4 hyphae). Vogel's liquid media alone was also used as a control. This resulted in a branch success rate of 50% (n=4 hyphae).

During some induction trials with 1 mM phenylalanine in Vogel's media, the growth and/or morphology of the hypha changed. In 3 out of 29 hyphae (10%) the tip stopped growing and bulged then resumed growing normally. In 2 out of 29 hyphae (7%) the tip stopped growing and bulged then resumed growing with normal tip morphology as a new branch formed. In 3 out of 29 hyphae (10%) the tip stopped growing and bulged as a branch formed but did not resume growth. In 1 out of 29 hyphae (3%) the cytoplasm became blebby

and stopped growing. The control trials with water did have an effect on tip growth as in 1 out of 4 hyphae (25%) the hyphal tip stopped growing initially then continued (n=4 hyphae).

3.3.2 Stages of Branching

Like in *A. bisexualis*, branches formed in a three stage process. The first stage was the formation of a bump along the hyphal wall at the future branch site. A bump was defined as a slight curvature of the hyphal wall towards the outside of the cell. The average time taken for a bump to form in the induction trials was 4.8 ± 4.5 minutes (n=24 hyphae) (Table 3.1). The second stage of branching was the development of a bud. The newly forming branch was considered a bud when the curvature of the hyphal wall protruded further outwards than that of a bump. The average time for the transition from the bump stage to the bud stage was 0.7 ± 0.3 minutes (n=24 hyphae) (Table 3.1). The third and final stage was the formation of the branch. The outgrowth was considered a branch when the hyphal wall had protruded to form a tubular structure with a parabolic shaped tip. The average time to transition from the bud stage to the branch stage was 1.2 ± 1.8 minutes (n=24 hyphae) (Table 3.1). The average growth rate of a new branch was 4 ± 3 μm/minute (n=24 hyphae) (Table 3.1).

3.3.3 Micropipette Positioning and Branch Induction Reliability

During the induction, the positioning of the micropipette relative to the hypha was kept consistent with respect to the distance from the tip of the micropipette to the trunk of the hypha and the distance from the tip of the micropipette to the tip of the hypha. The positioning of the micropipette and the distances measured are shown in Figure 3.4. The average distance from the micropipette tip to the hyphal trunk was 6 ± 3 μm (n=29 hyphae) (Table 3.1). The average distance from the micropipette tip to the hyphal tip was 38 ± 13 μm (n=29 hyphae) (Table 3.1). Despite this consistency, the average distance from the micropipette tip to the hyphal branch, when one formed was quite variable with the average distance measured laterally along the hypha being 30 ± 27 μm (n=24 hyphae) (Table 3.1).

To see if there was any relationship between the position of the micropipette and branch formation, the correlation values were analysed and are detailed below. There was a slight negative correlation between the time to bump and the distance of the micropipette to

the hyphal tip, r=-0.129 (Figure 3.5). The time taken to form a bump decreased as the distance of the micropipette to the hyphal tip increased. This shows that the closer the micropipette was to the tip of the hypha, the longer it took for a bump to form. All correlation values can be seen in Table 3.2.

There was a negative correlation between the distance from the micropipette tip to the hyphal tip and time it took for a branch to form, r=-0.626 (Figure 3.6). The time to branch decreased as the distance of the micropipette to the hyphal tip increased. The closer the micropipette was to the tip of the hypha, the longer the hypha took to branch. When the micropipette was 30 μm or further back from the tip it took the same amount of time to branch.

There was a slight positive correlation between the distance from the micropipette tip to the hyphal tip and the branch growth rate, r=0.228 (Figure 3.7). The branch growth rate increased as the distance of the micropipette to the hyphal tip increased. The closer the micropipette was to the hyphal tip, the slower the growth rate of the new branch.

A positive correlation was obtained between the distance from the micropipette tip to the hyphal tip and the distance from the micropipette tip and the hyphal branch, r=0.513 (Figure 3.8). The distance of the micropipette to the new branch increased as the distance of the micropipette to the hyphal tip increased. The closer the micropipette was to the hyphal tip, the closer the new branch was to the micropipette.

A slightly negative correlation was identified between the micropipette to the hyphal trunk distance and time it took for a bump to form, r=-0.107 (Figure 3.9). The time it took for a bump to form decreased as the distance of the micropipette to the hyphal trunk increased. The further away the micropipette is to the trunk of the hypha, the less time it takes for a bump to form.

There was also a negative correlation with the distance between the micropipette to the hyphal trunk and the time it took for a branch to form, r=-0.503 (Figure 3.10). The time to branch decreased as the distance between the micropipette and the hyphal trunk increased. The further away the micropipette was from the hyphal trunk, the less time it took for a branch to form.

There was a slight positive correlation between the distance from the micropipette tip to the hyphal trunk and the branch growth rate, r=0.373 (Figure 3.11). The branch growth rate increased as the distance of the micropipette to the hyphal trunk increased. The further away the micropipette was from the hyphal trunk, the faster the growth rate of the new branch was.

Finally there was a slight positive correlation between the distance from the micropipette tip to the hyphal trunk and the hyphal branch, r=0.319 (Figure 3.12). The distance of the micropipette to the new branch increased as the distance of the micropipette to the hyphal trunk increased. The closer the micropipette was to the hyphal trunk, the closer the branch was to the micropipette.

3.3.4 Correlation with Time to Bump

Correlation values were analysed to determine if there was any relationship between the time taken for the hypha to form a bump and the various factors involved in the induction process. There was a positive correlation between the time to bump with the time taken to bud (r=0.459) (see Figure 3.13). This suggests that as the time to bump increases so does the time to bud (i.e. hyphae that are slow to form a bump are also slow to form a bud). There was no correlation between the time to bud and the time to branch (r=0.027) (see Figure 3.14). There was a slight negative correlation between the time taken for a bump to form and the hyphal width (r=-0.316) (see Figure 3.15). This suggests that the wider the hypha is before the induction begins, the less time it takes for a bump to form (it takes longer for hyphae with smaller widths to form a bump). A slight negative correlation was also observed between the time taken to bump and the hyphal growth rate before the start of the induction (r=-0.288) (see Figure 3.16). The faster the hypha is growing pre-induction, the less time it takes for it to form a bump. There was a negative correlation between the time taken to bump and the hyphal growth rate one minute after the induction began (r=-0.589) (see Figure 3.17). The time taken for a bump to form increased as the hyphal growth rate decreased. The faster the growth rate of the hypha was after the induction began, the less time it took for a bump to form. There was a negative correlation between the time taken to bump and the branch growth rate (r=-0.645) (see Figure 3.18). The branch growth rate decreased as the time taken for a bump to form increased. The less time it takes for a bump to form, the quicker the branch growth rate is. Conversely, there was a slight positive correlation between the time taken for a bump to form and the chemotropic response of the growing tip (r=0.146) (see Figure 3.19). As the chemotropic response of the tip increased with a greater angle of bending towards the micropipette, the time taken for the bump to form increased. The greater the response of the tip bending towards the micropipette, the longer it took for a bump to form.

3.3.5 Multiple Branch Formation

Multiple branches formed in some of the induction trials. In 4 out of 24 hyphae (16.7%) in which branches formed, two or more branches formed off the main hyphal trunk (Figure 3.20). In 1 out of 24 hyphae (4.2%) one branch formed off the hyphal trunk from which another branch formed and another branch formed off this branch (Figure 3.21). There were no multiple branches formed in the control trial with water in the micropipette however in 1 out of 2 hyphae (50%) that formed branches with Vogel's media in the micropipette resulted in multiple branches forming.

3.3.6 Chemotropism

Hyphal tips showed a chemotropic response to the induction solution, either bending towards or away from the micropipette tip. The growing hyphal tip bent towards the micropipette tip in 16 out of 29 inductions (55%) and away from the micropipette in 3 out of 29 inductions (10%). The average chemotropic response was a bend of 23 ± 59˚ with a range of -157-150˚ (n=29). A typical chemotropic response is shown in Figure 3.22. Chemotropism towards the micropipette was displayed using Vogel's media in all of the hyphae (n=4). The average chemotropic response was a bend of 103 ± 151˚ with a range of 20-330˚ (n=4). When the micropipette was filled with water, 1 out of 4 hyphae (25%) bent towards the micropipette tip and 1 out of 4 hyphae (25%) bent away from the micropipette tip. The average chemotropic response was a bend of 7 ± 20˚ with a range of -9-35˚ (n=4).

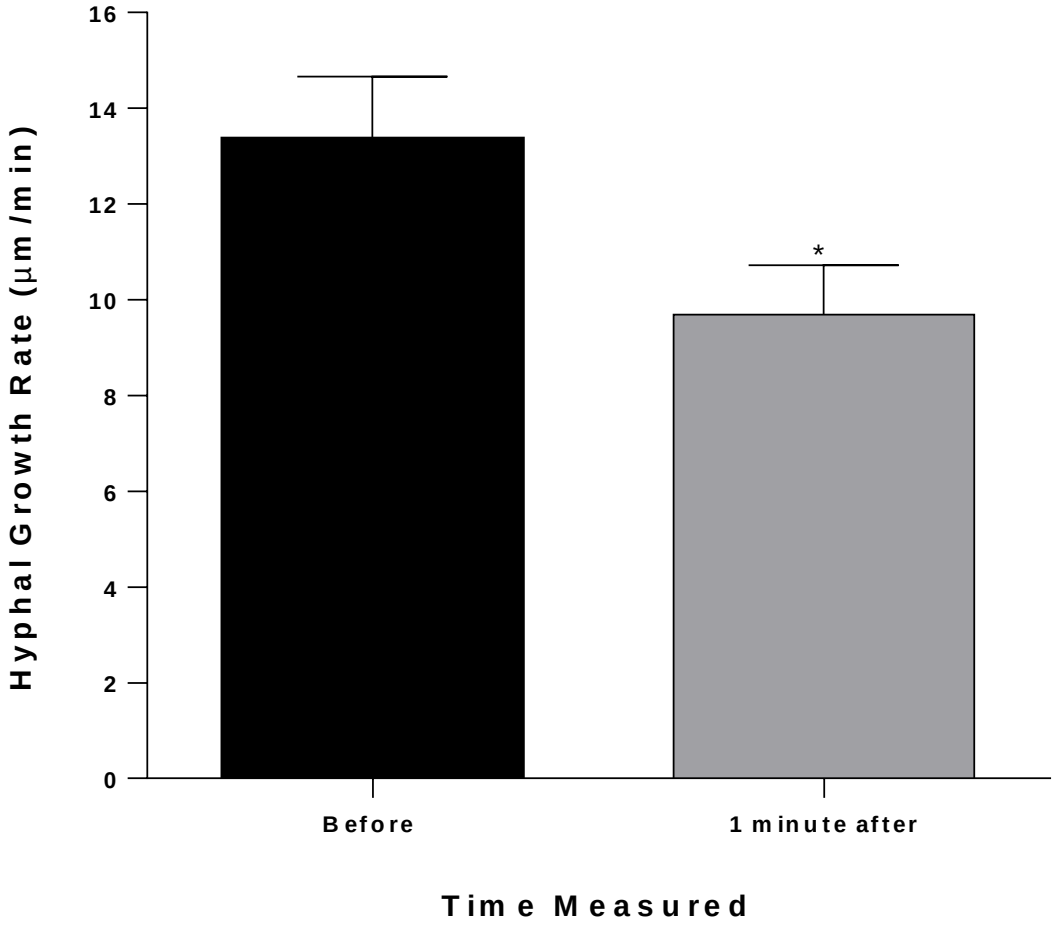

Figure 3.2 – Average hyphal growth rates before and 1 minute after the induction started (n=29). There was a significant reduction in hyphal growth rate 1 minute after the induction began (see Appendix 1 for statistics).

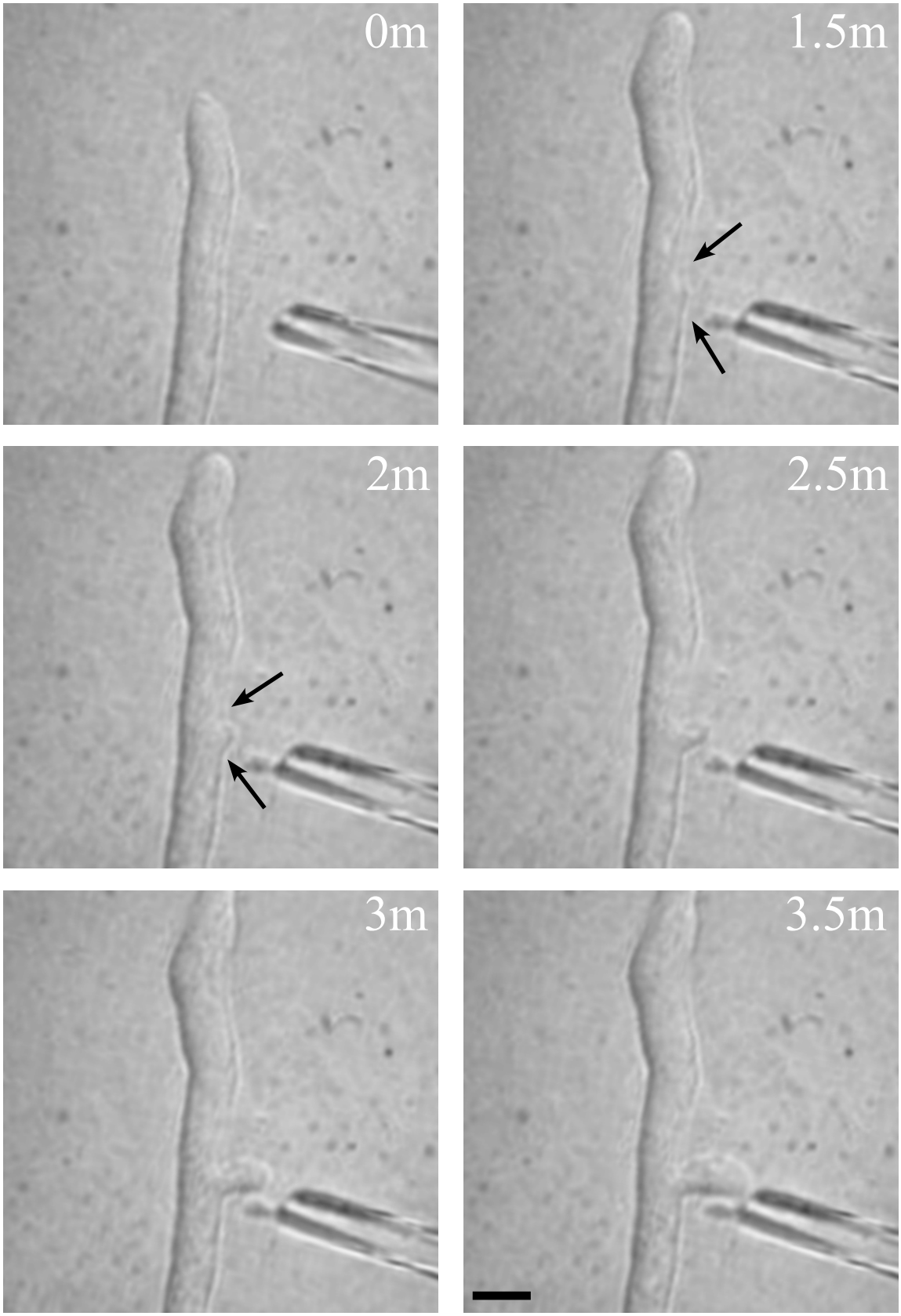

Figure 3.3 – A hypha of *N. crassa* being induced to branch using Vogel's media and 1 mM phenylalanine. The glass micropipette was positioned next to the hypha 40 µm from the hyphal tip and 9 µm to the side of the hyphal trunk. The future branch site is indicated with arrows. The bump forms at 1.5 minutes, the bud forms at 2 minutes and the branch forms at 2.5 minutes. Bar = 10 µm. Time in minutes (m).

	Average	SD	Range
Hyphal Width (µm)	7	2	4.2-14.3
Time to Bump (minutes)	4.8	4.5	0.5-19
Time to Bud (minutes)	0.7	0.3	0.5-1.5
Time to Branch (minutes)	1.2	1.8	0.5-9
Hyphal Growth Rate Before Induction (µm/minute)	13	7	2.5-29.1
Hyphal Growth Rate After Induction (µm/minute)	10	6	1.5-24.1
Branch Growth Rate (µm/minute)	4	3	0.8-10
Distance from Micropipette Tip to Hyphal Trunk (µm)	6	3	0.9-12
Distance from Micropipette Tip to Hyphal Tip (µm)	38	13	13.6-64
Distance from Micropipette Tip to Hyphal Branch (µm)	30	27	-17.3-75.5
Chemotropism of the Hyphal Tip (˚)	22	59	-157-150

Table 3.1 – Summary of the various parameters measured during the branch induction experiments.

	Bump (min)	Bud (min)	Branch (min)	Hyphal Growth Rate Before Induction (µm/min)	Hyphal Growth Rate 1min After Induction (µm/min)	Branch Growth Rate (µm/min)	MP Tip to Hyphal Trunk (µm)	MP Tip to Hyphal Tip (µm)	MP Tip to Hyphal Branch (µm)	Chemotropism (˚)	Hyphal Width (µm)
Bump (min)		0.459	0.151	-0.288	-0.589	-0.645	-0.107	-0.129	0.232	0.146	-0.316
Bud (min)	0.459		0.027	-0.387	-0.389	-0.528	-0.130	-0.194	-0.013	0.345	-0.146
Branch (min)	0.151	0.027		-0.310	-0.058	-0.132	-0.502	-0.626	-0.030	-0.045	0.084
Hyphal Growth Rate Before Induction (µm/min)	-0.288	-0.387	-0.310		0.572	0.653	0.477	0.551	0.163	-0.122	0.5783
Hyphal Growth Rate 1min After Induction (µm/min)	-0.589	-0.389	-0.0580	0.572		0.529	0.306	0.256	-0.049	-0.182	0.613
Branch Growth Rate (µm/min)	-0.645	-0.528	-0.132	0.653	0.529		0.373	0.228	0.045	-0.200	0.438
MP Tip to Hyphal Trunk (µm)	-0.107	-0.130	-0.503	0.477	0.306	0.373		0.612	0.319	-0.022	0.158
MP Tip to Hyphal Tip (µm)	-0.129	-0.194	-0.626	0.551	0.256	0.228	0.612		0.513	0.104	0.058
MP Tip to Hyphal Branch (µm)	0.232	-0.013	-0.030	0.163	-0.049	0.045	0.319	0.513		-0.168	-0.092
Chemotropism (˚)	0.146	0.345	-0.045	-0.122	-0.182	-0.200	-0.022	0.104	-0.168		-0.182
Hyphal Width (µm)	-0.316	-0.146	0.084	0.578	0.613	0.438	0.158	0.058	-0.092	-0.182	

Table 3.2 – Summary table of correlation values for the various factors involved in the branch induction technique.

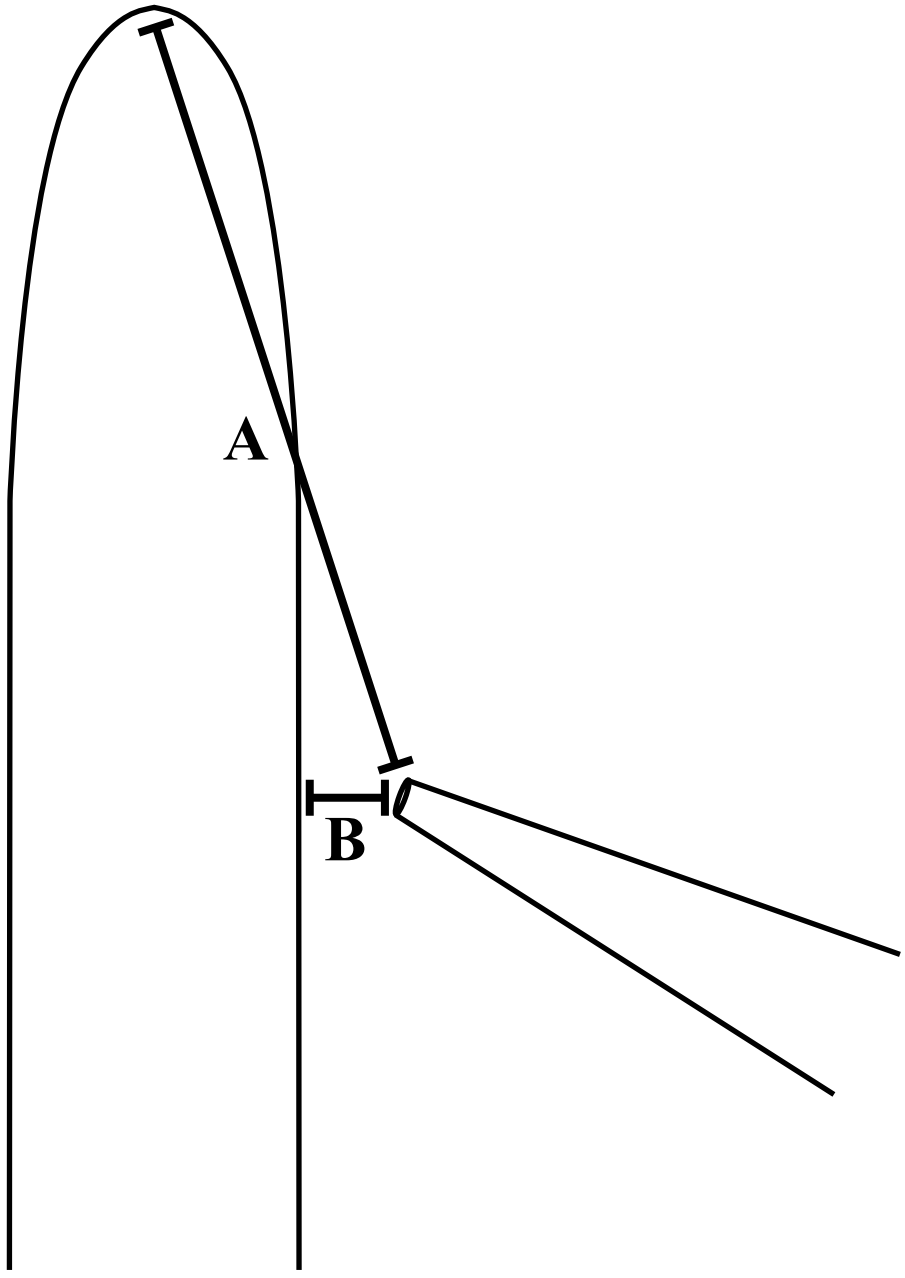

Figure 3.4 - The positioning of the micropipette relative to the hypha. A shows the distance between the tip of the hypha to the tip of the micropipette. B shows the distance between the trunk of the hypha to the tip of the micropipette.

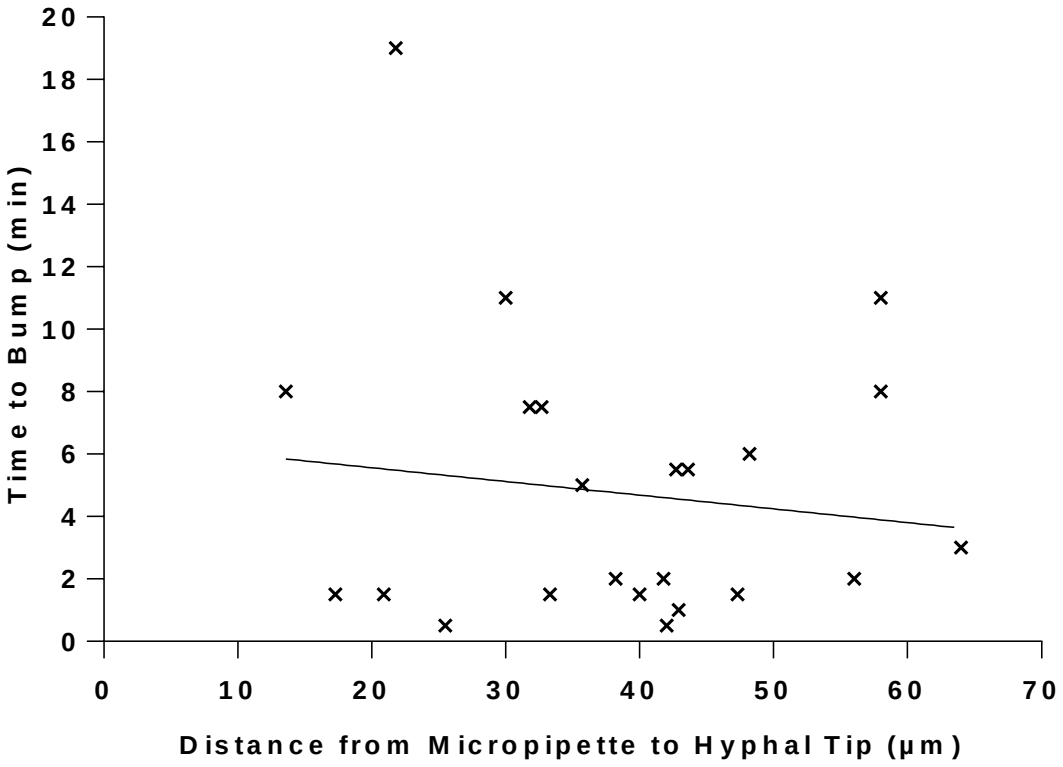

Figure 3.5 – Scatter graph showing the slight negative correlation between the distance of the micropipette relative to the hyphal tip and the time it took for the hypha to bump in the successful inductions (n=24, r=-0.129).

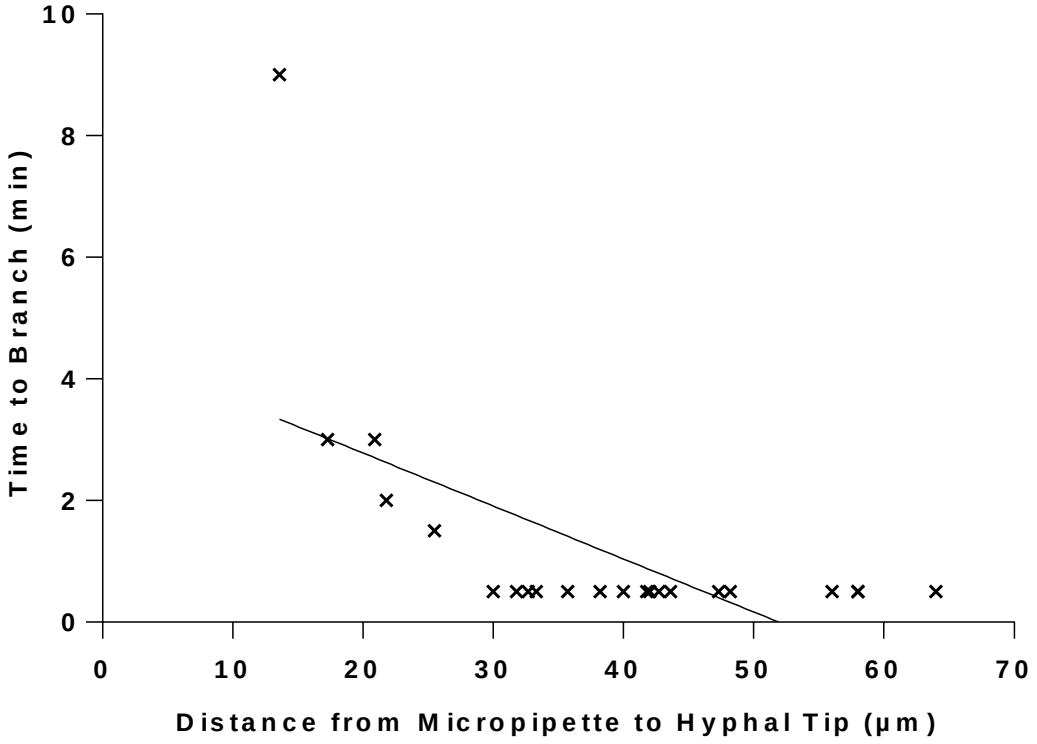

Figure 3.6 – Scatter graph showing a negative correlation between the distance of the micropipette relative to the hyphal tip and the time it took for the hypha to branch in the successful inductions (n=24, r=-0.626).

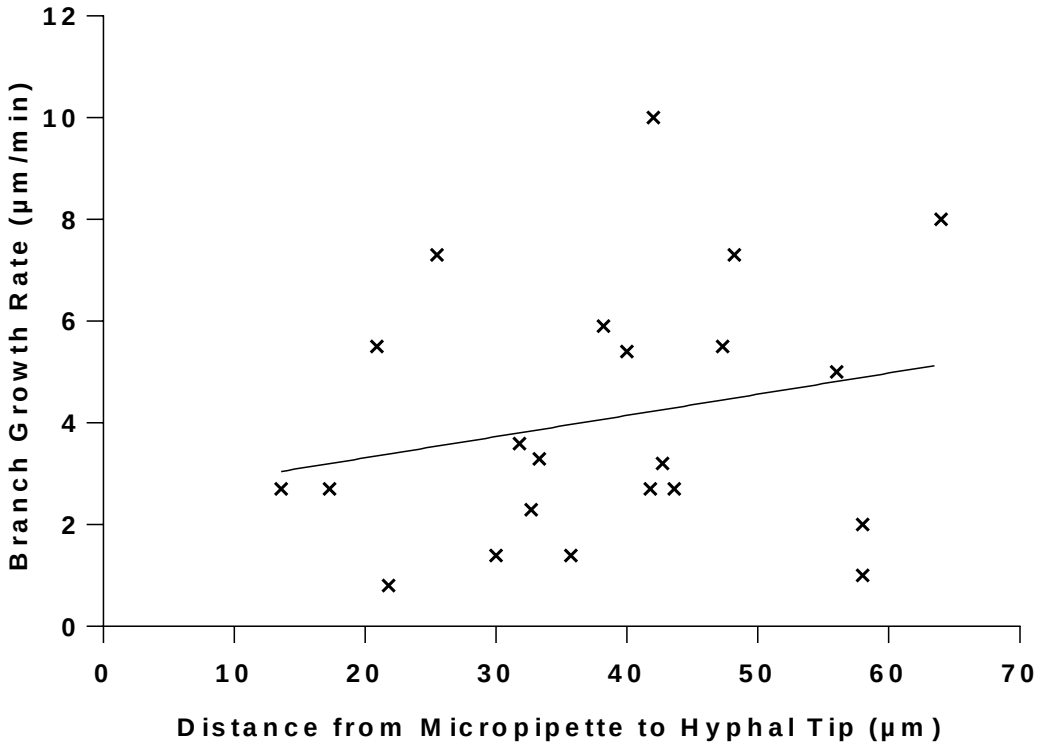

Figure 3.7 - Scatter graph showing the slight positive correlation between the distance of the micropipette relative to the hyphal tip and the growth rate of the branches for the successful inductions (n=24, r=0.228).

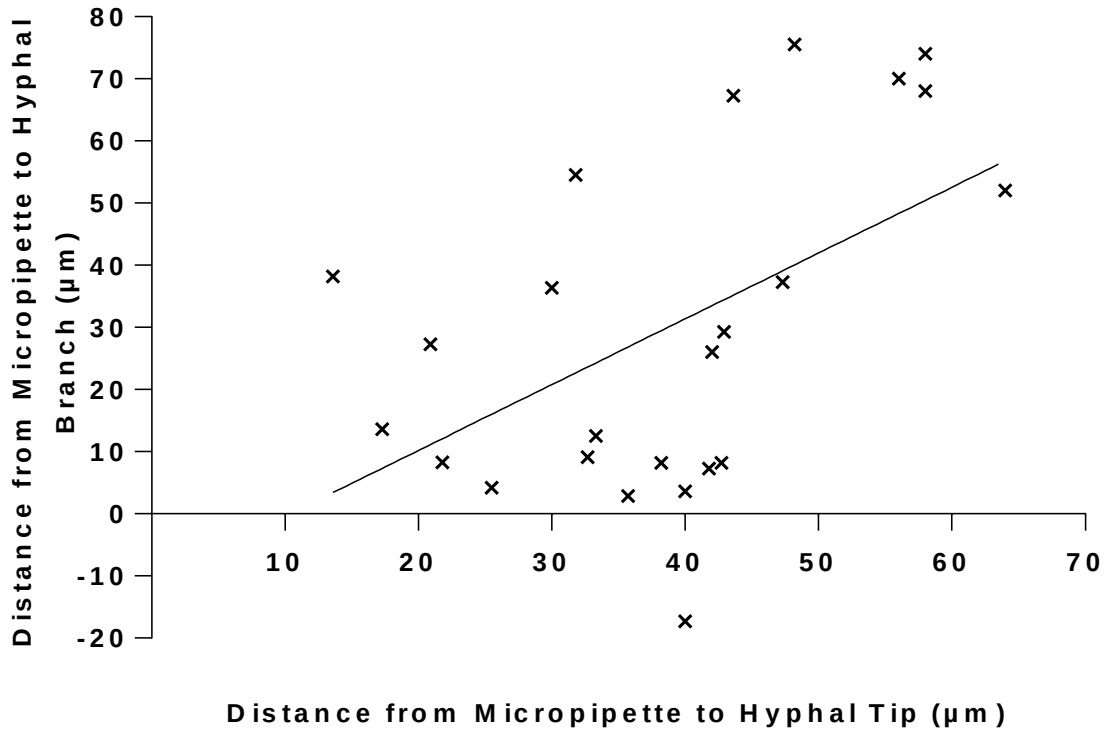

Figure 3.8 - Scatter graph showing a positive correlation between the distance of the micropipette relative to the hyphal tip and the distance of the micropipette relative to the branch for the successful inductions (n=24, r=0.513).

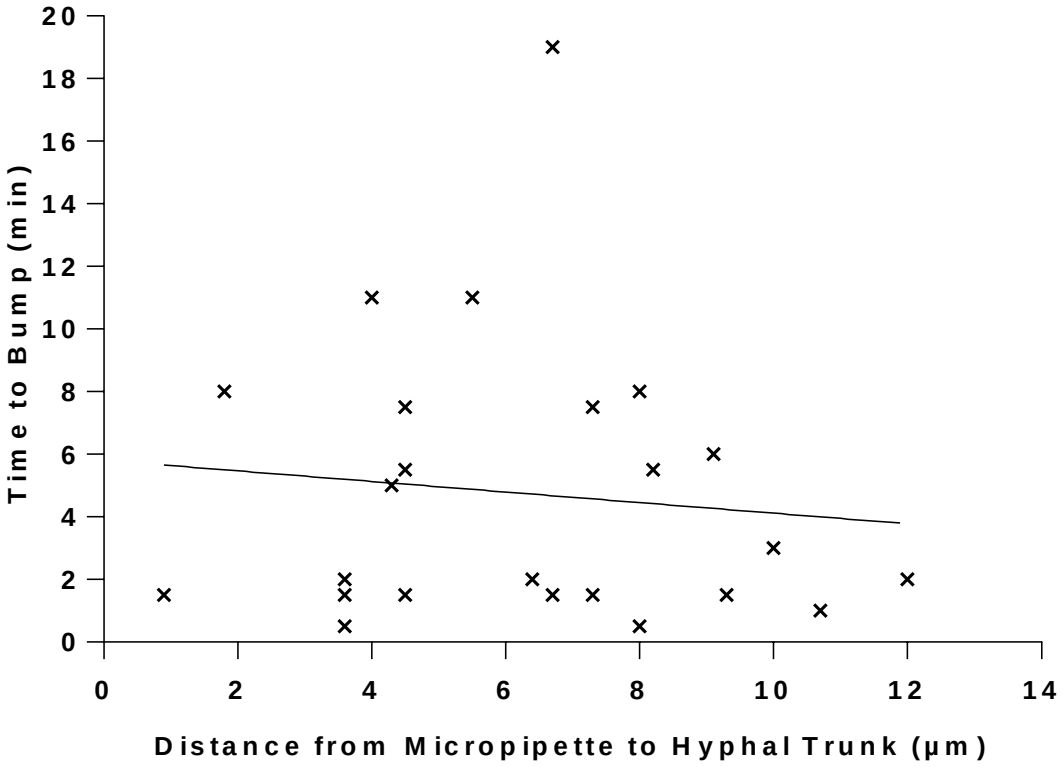

Figure 3.9 - Scatter graph showing a slight negative correlation between the distance of the micropipette relative to the hyphal trunk and the time it took for a bump to form for successful inductions (n=24, r=-0.107).

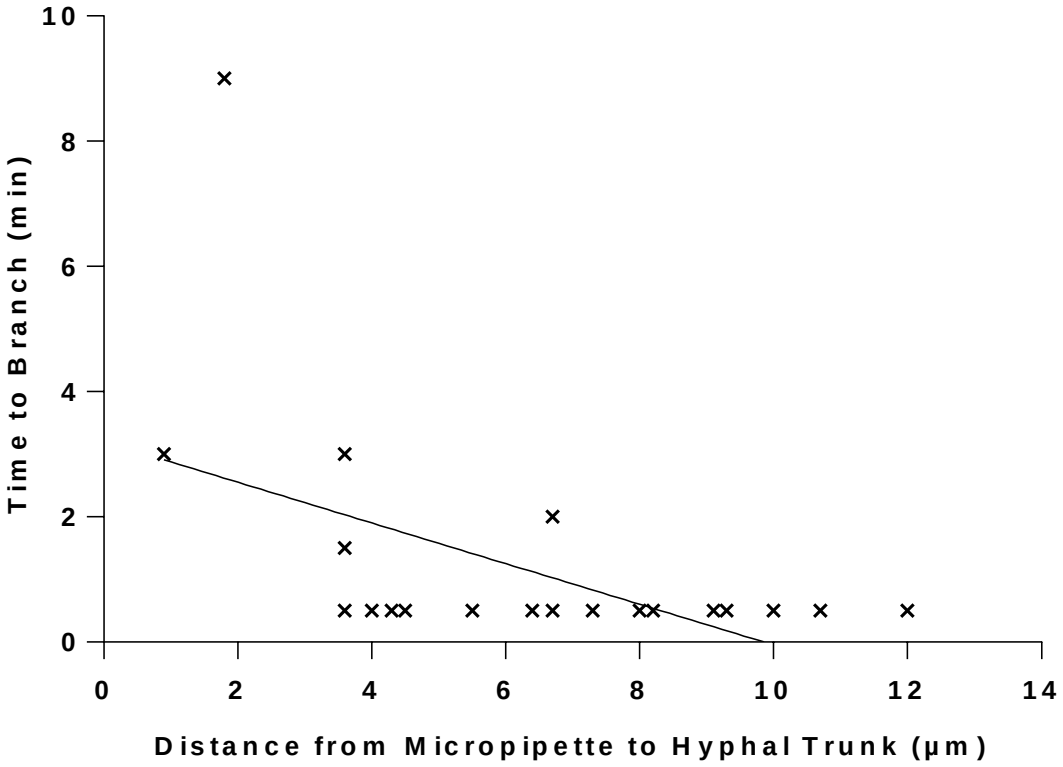

Figure 3.10 - Scatter graph showing the negative correlation between the distance of the micropipette relative to the hyphal trunk and the time it took for a branch to form for successful inductions (n=24, r=-0.503).

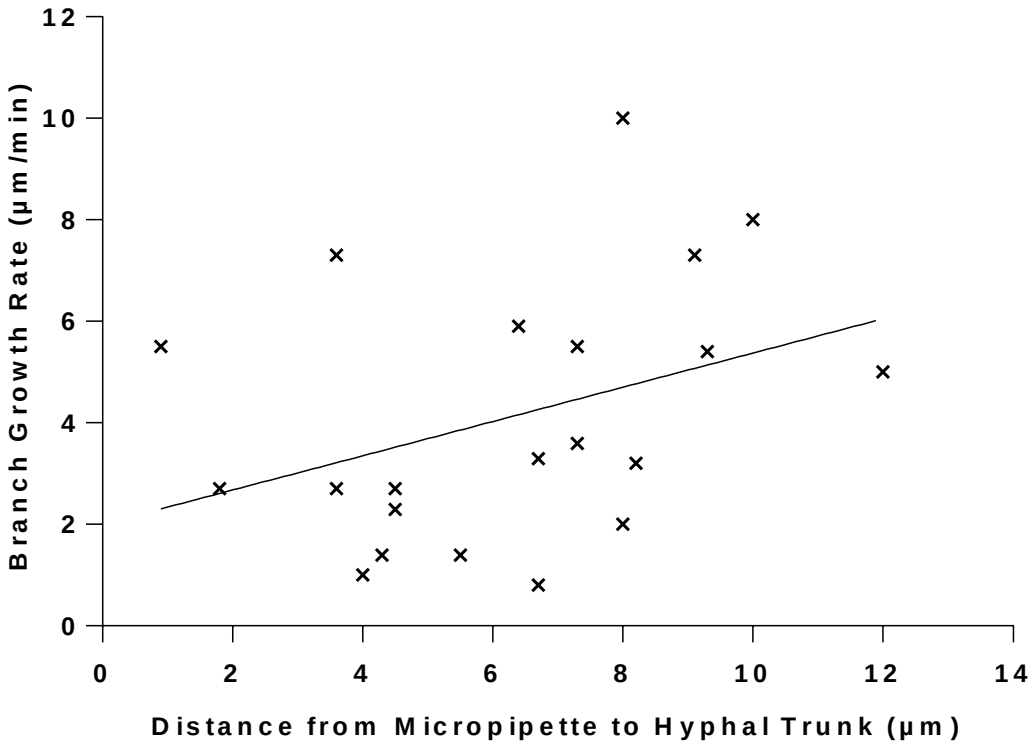

Figure 3.11 - Scatter graph showing the slight positive correlation between the distance of the micropipette relative to the hyphal trunk and the branch growth rate for successful inductions (n=24, r=0.373).

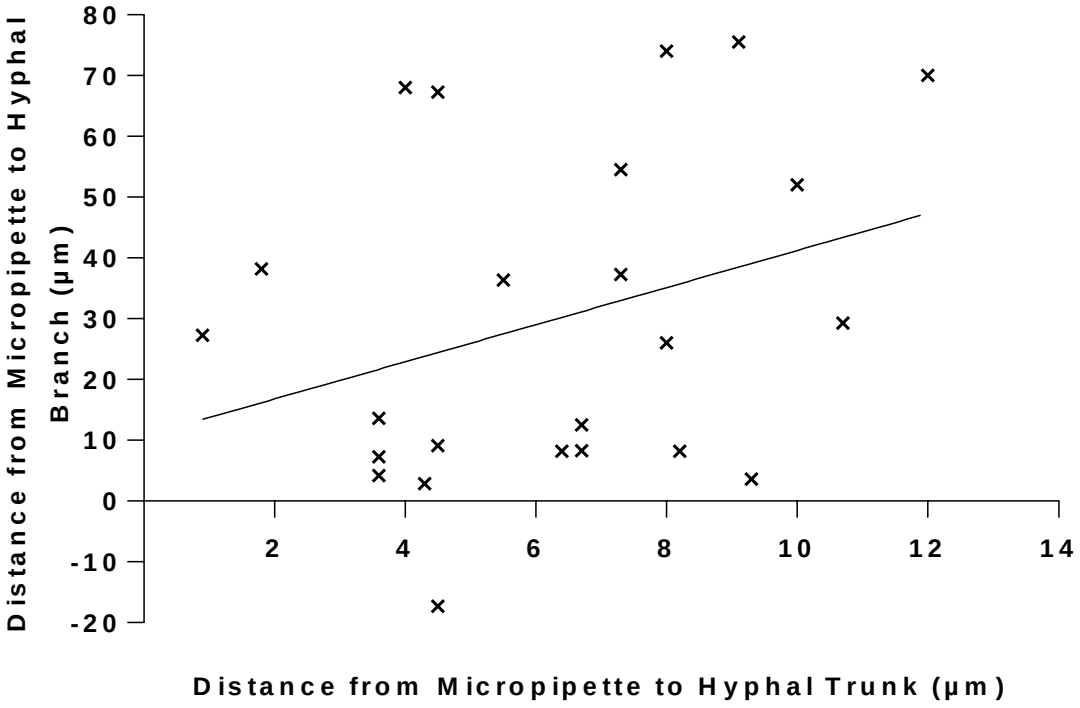

Figure 3.12 - Scatter graph showing the slight positive correlation between the distance of the micropipette relative to the hyphal trunk and the distance from the micropipette tip to the hyphal branch for successful inductions (n=24, r=0.319).

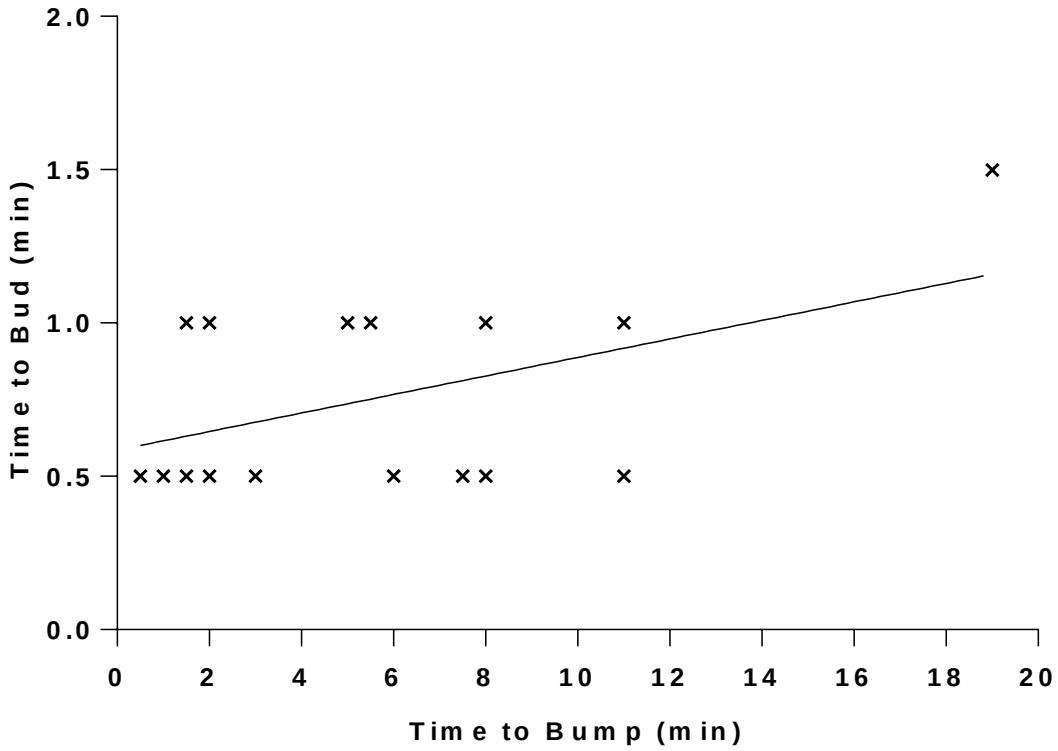

Figure 3.13 - Scatter graph showing a positive correlation between the time for the hypha to bump and the time for the hypha to bud for successful inductions (n=24, r=0.459).

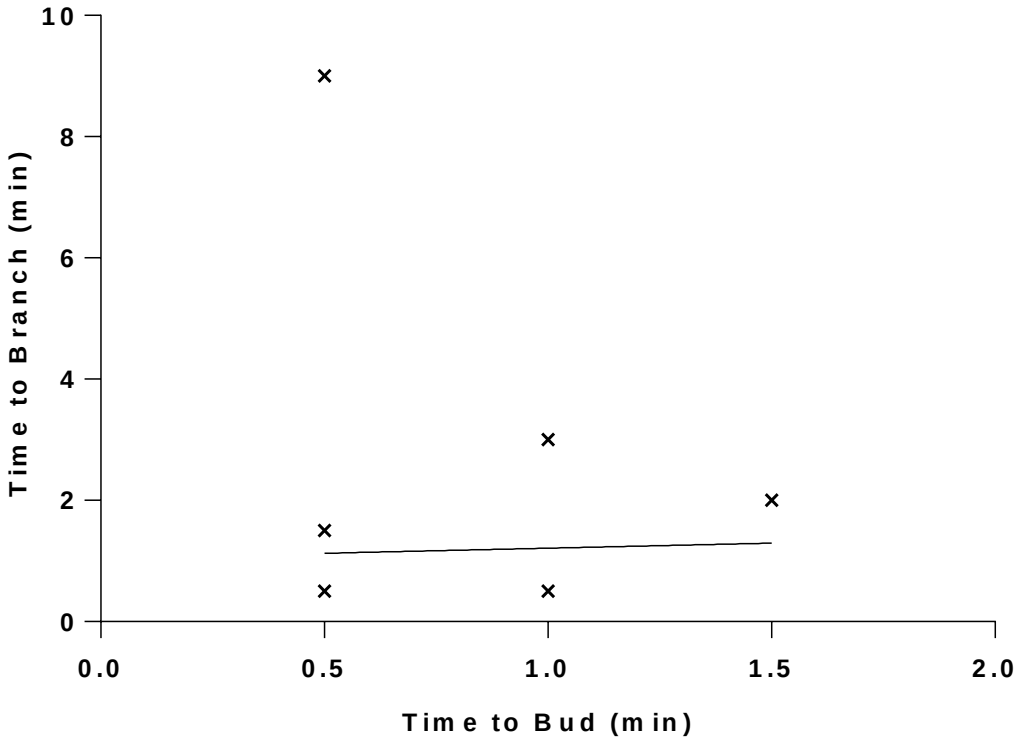

Figure 3.14 - Scatter graph showing that there was no correlation between the time taken for the hypha to form a bud and the time taken to form a branch for successful inductions (n=24, r=0.027).

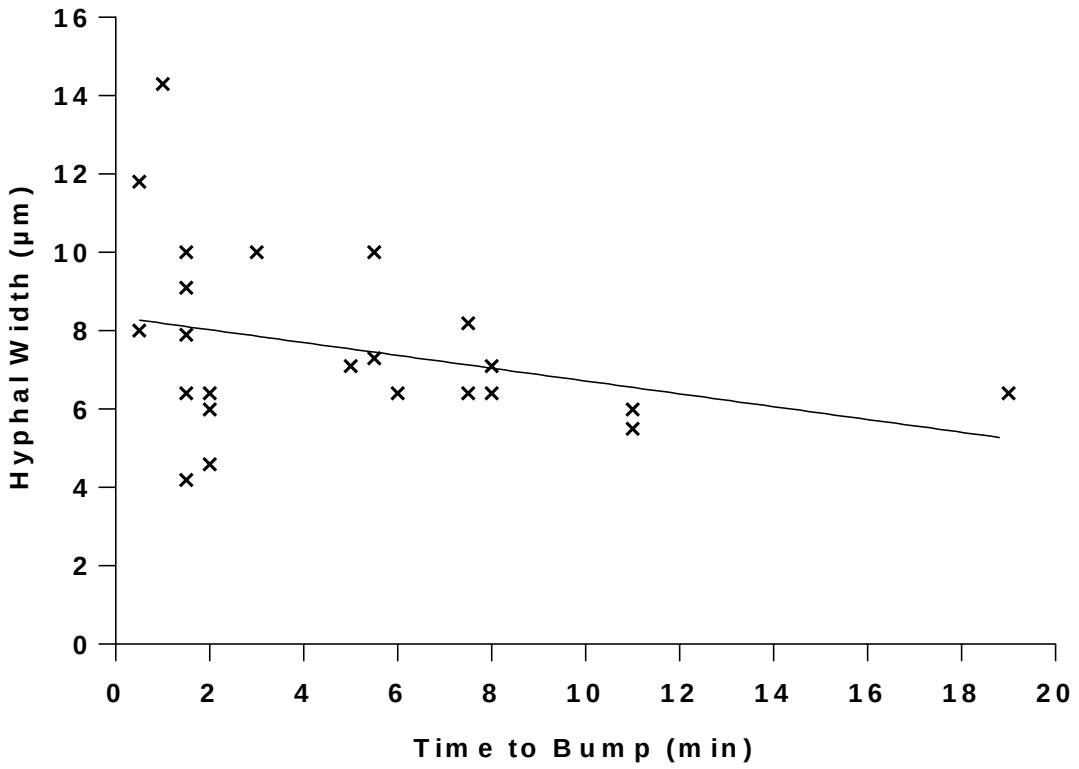

Figure 3.15 - Scatter graph showing a slight negative correlation between the time for the hypha to bump and hyphal width for successful inductions (n=24, r=0.316).

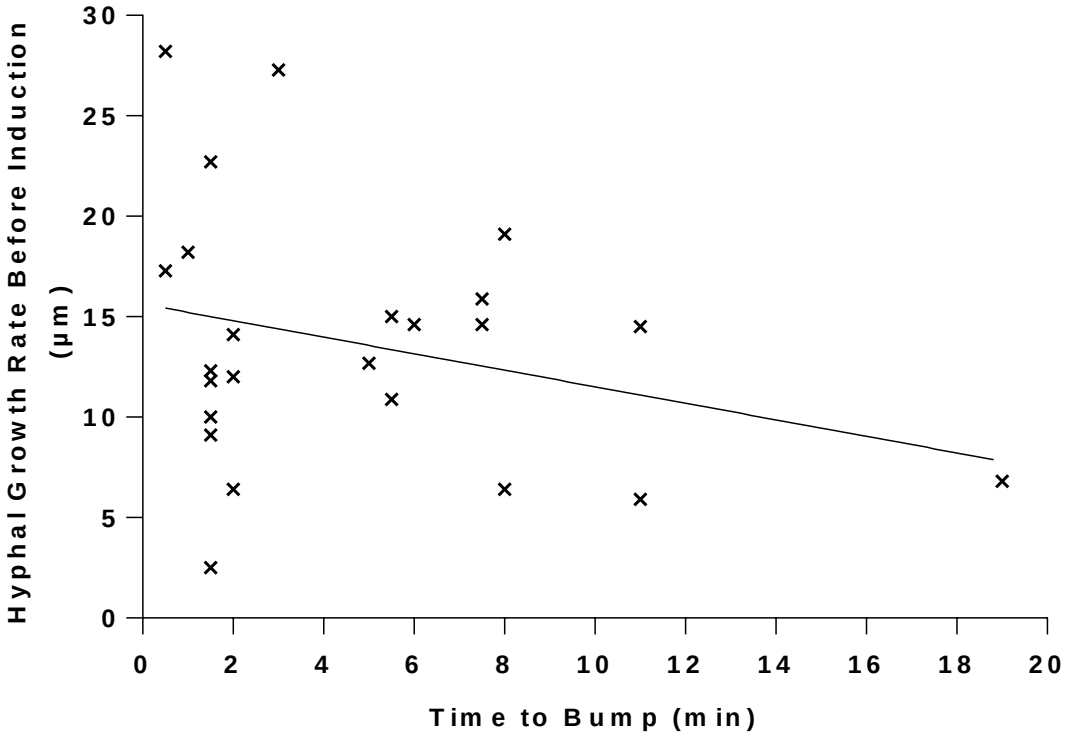

Figure 3.16 - Scatter graph showing the slight negative correlation between the time for the hypha to bump and the hyphal growth rate before the induction began for successful inductions (n=24, r=-0.288).

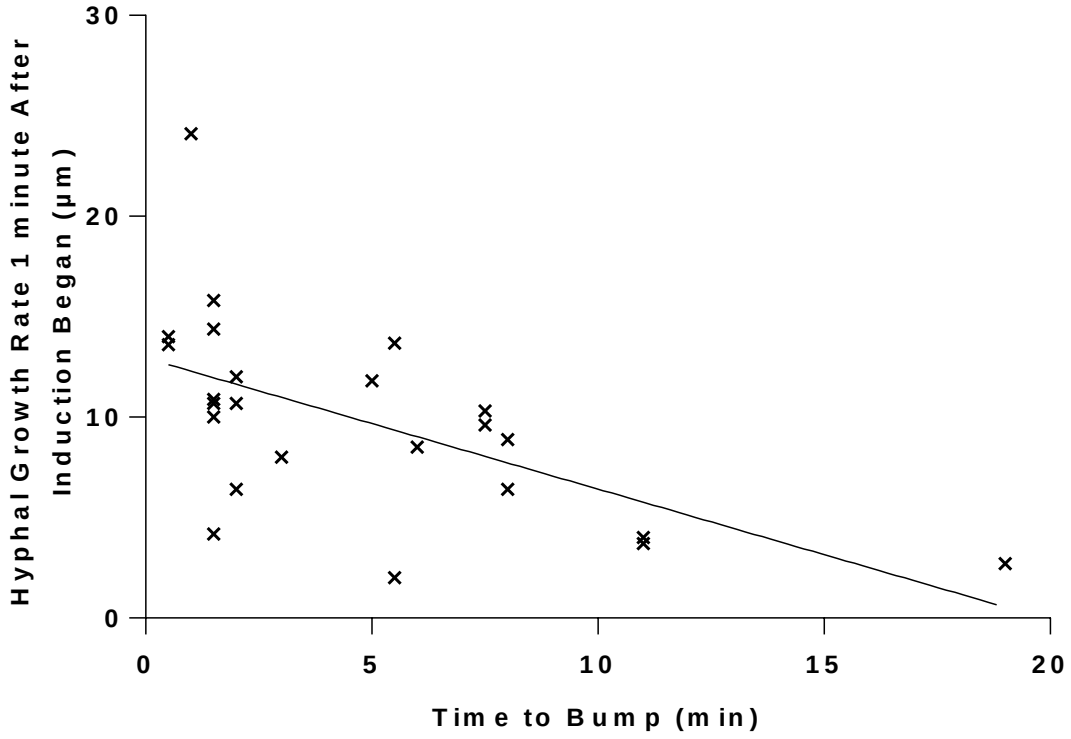

Figure 3.17 - Scatter graph showing the negative correlation between the time for the hypha to bump and the hyphal growth rate 1 minute after the induction began for successful inductions (n=24, r= -0.589).

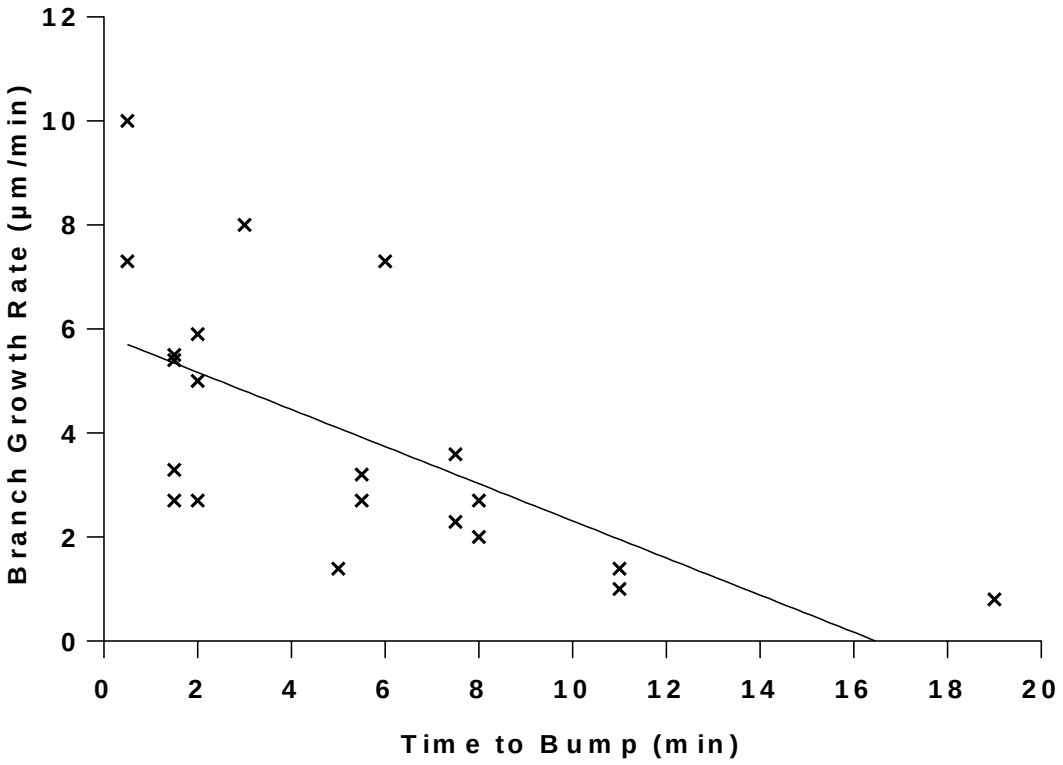

Figure 3.18 - Scatter graph showing the negative correlation between the time for the hypha to bump and the branch growth rate for successful inductions (n=24, r=-0.645).

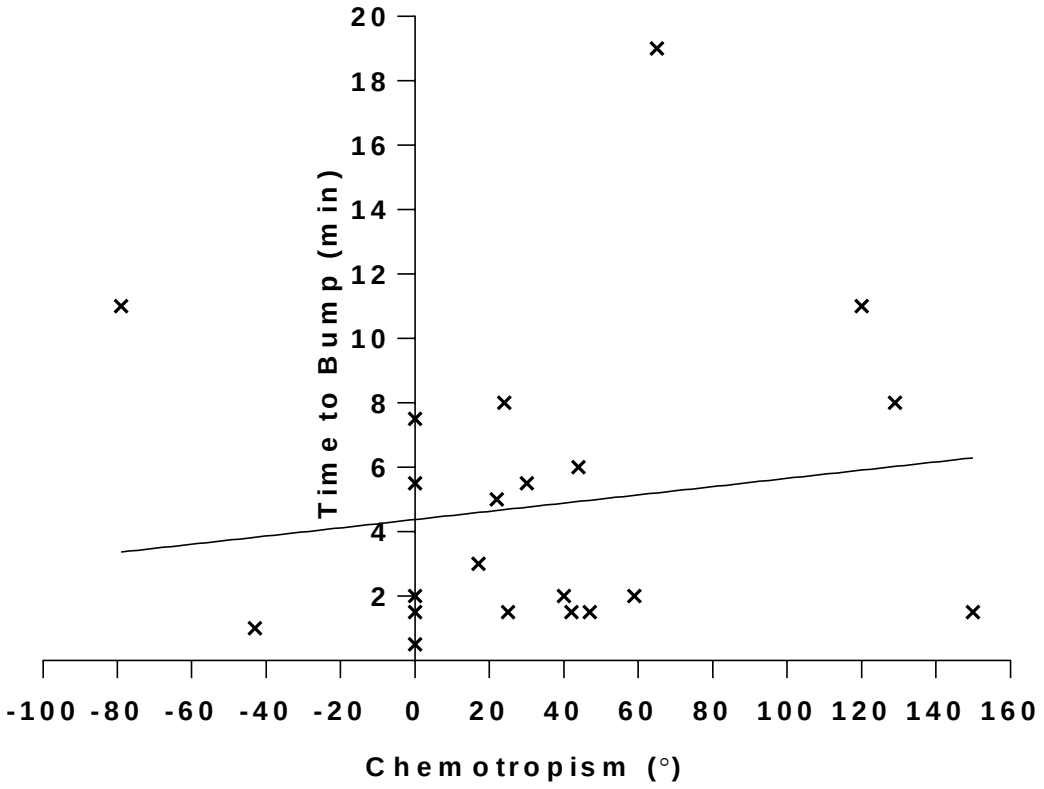

Figure 3.19 – Scatter graph showing a slightly positive correlation between the chemotropism of the tip and the time it took for a bump to form (n=24, r=0.146).

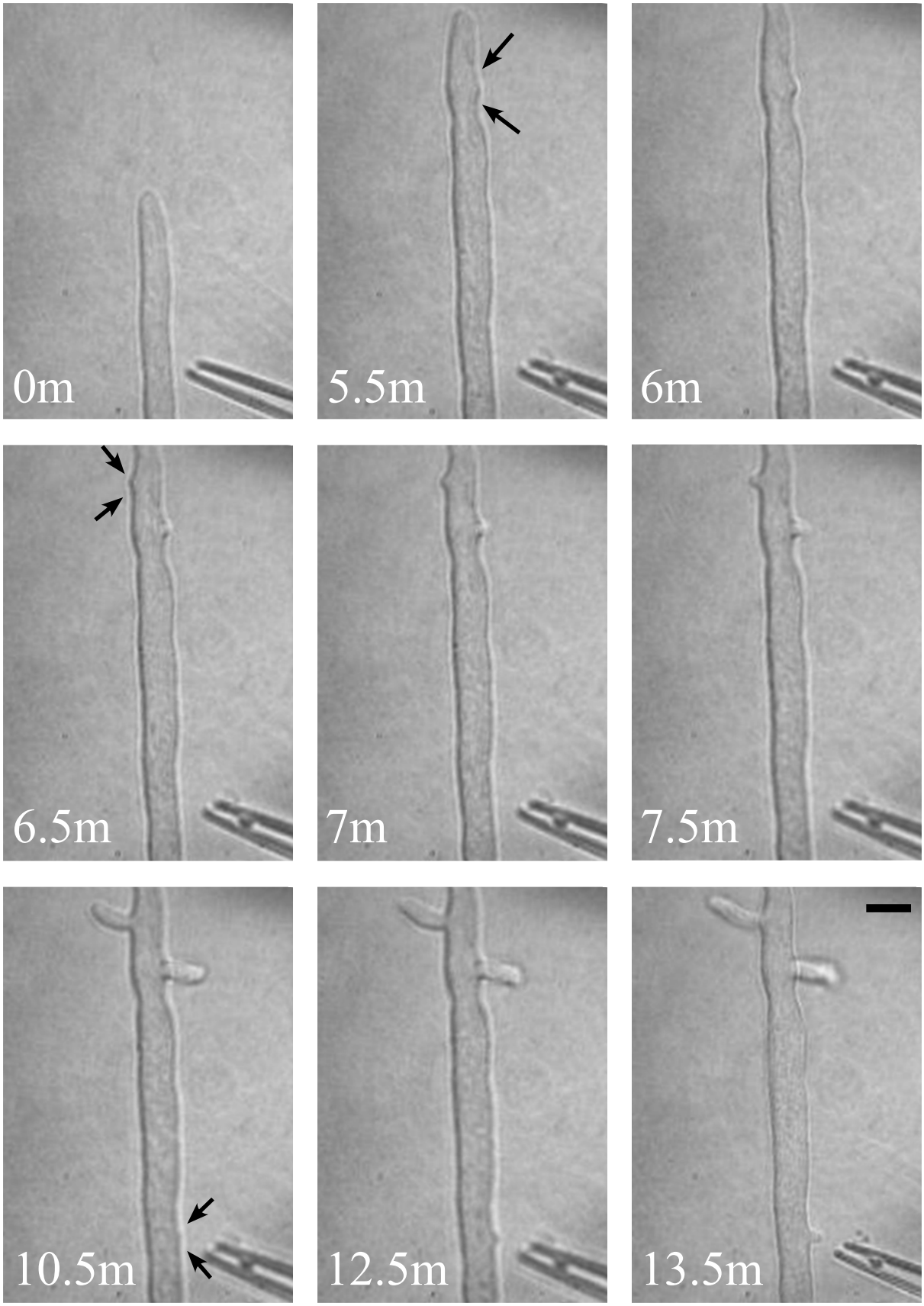

Figure 3.20 – Multiple branches forming on a single hypha of *N. crassa* being induced to branch using Vogel's media and 1 mM phenylalanine. The glass micropipette is positioned next to the hypha 44 μm below the tip and 5 μm to the side of the hyphal trunk. Future branch sites are indicated with arrows. Bar = 10 μm. Time in minutes (m).

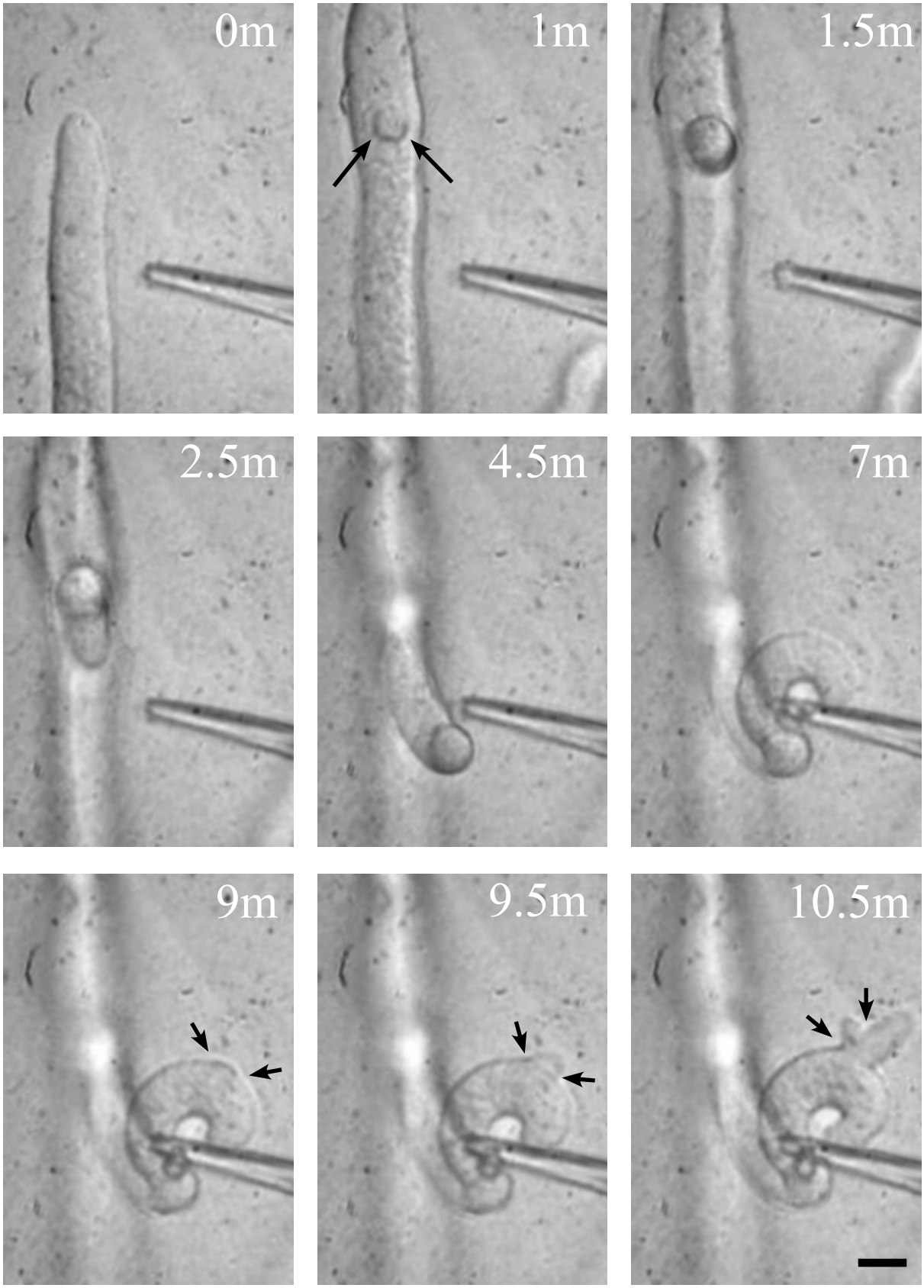

Figure 3.21 – Multiple branches forming from a single branch on a *N. crassa* hypha being induced to branch using Vogel's media and 1 mM phenylalanine. The glass micropipette is positioned next to the hypha 43 μm below the tip and 11 μm to the side of the hyphal trunk. Future branch sites are indicated with arrows. Bar = 10 μm. Time in minutes (m).

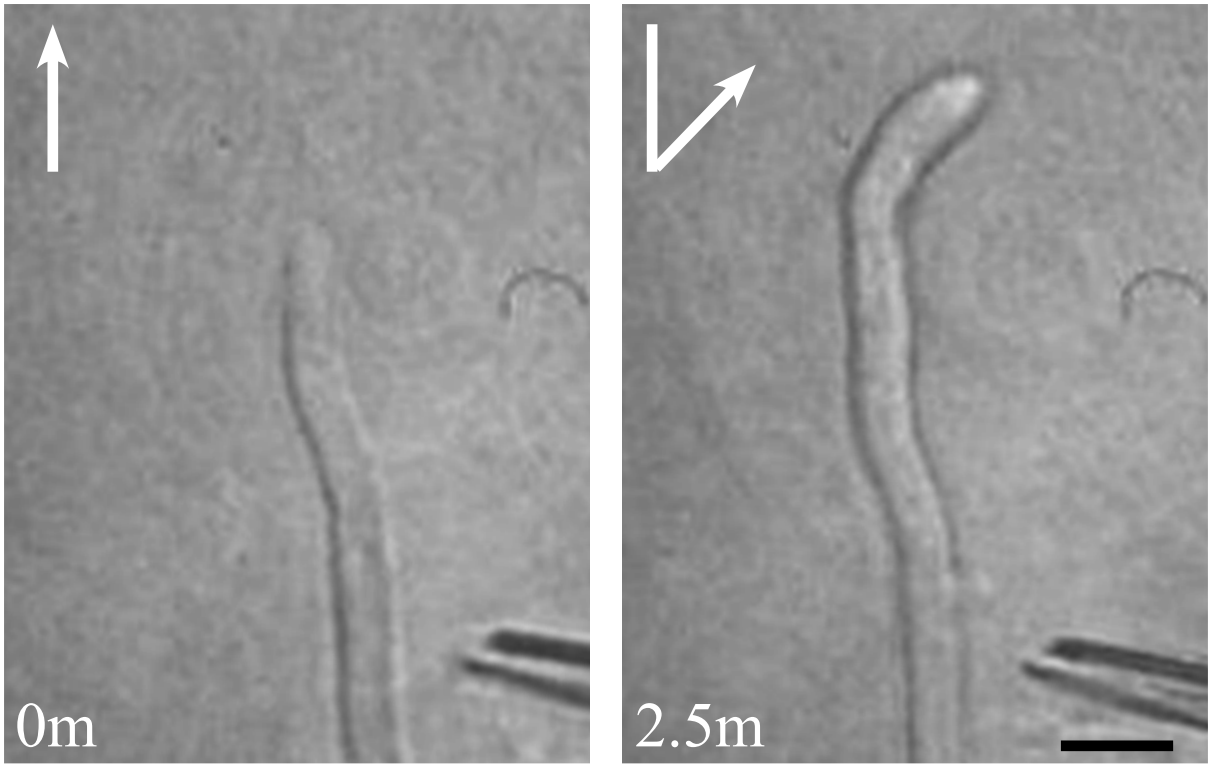

Figure 3.22 – Chemotropic response of the growing tip. Arrows show direction of growth at time 0 minutes and time 2.5 minutes. Angle 44°. Bar = 10 μm. Time in minutes (m).

3.4 Discussion

The ability to predict where branches form in filamentous fungi will enable investigations into the various underlying molecular mechanisms of branch formation. In this study, the local application of 1 mM phenylalanine in Vogel's media resulted in the formation of branches in 83% (n=29) of trials using *N. crassa*. A similar result was seen when the same induction technique was used on *A. bisexualis* with a branch formation success rate of 78% (n=36) (Morris et al., 2011). Comparisons between the mechanisms used by these two types of filamentous microorganisms in the branching process can be made using this technique.

Using the induction technique morphological changes in the cell wall as a branch formed were observed and appeared to have three main morphological stages. Firstly, a bump in the cell wall formed. This occurred on average 4.8 ± 4.5 minutes after the micropipette was positioned and the solution applied to the hypha. The second stage was the outgrowth of this bump into a bud. This stage took on average 0.7 ± 0.3 minutes after the formation of the bump. These early stages involved the establishment of polarity at the extension site. The third stage involved the maturation of the bud into what looks like a branch. This stage took on average 1.2 ± 1.8 minutes. These stages occurred much faster in *N. crassa* than in *A. bisexualis* which corresponds to the faster growth rate of *N. crassa*.

Symporters that carry amino acids with protons across the plasma membrane are possible sensors of the induction media and may function in branch formation and chemotropism. Transport through these channels can result in the development of an inward current of ions which is thought to occur at sites of new growth (Gow, 1984; Kropf, 1986; Kropf et al., 1983; Schreurs and Harold, 1988). The movement of ions into the cell at the site of new growth is thought to be involved in the localisation of future growth as a signal. The inward flow of H^+ at the hyphal tip and a future branch sites may result in a more acidic cytoplasmic pH which then affects the cytoskeleton assembly and therefore has an effect on developmental processes. When H^+ moves in at the site of new growth, it may provide information for the development of a new branch (Kropf et al., 1983). Another hypothesis for the underlying mechanism of amino acids interacting with receptors inducing branch formation and chemotropism is that these receptors may be interacting with the cytoskeleton, resulting in a disruption to the cytoskeletal dynamics and therefore enabling a change in the site of vesicle exocytosis (Schreurs et al., 1989). It could be involved in the movement of

vesicles containing materials required for new growth to the site of the new branch (Kropf et al., 1983)

These amino acid receptors are thought to be mobile within the plasma membrane and possibly accumulate in the area where the gradient of the amino acid is high (Hewitt, 1978). It is thought that the amino acid receptors cause the localised exocytosis of vesicles in the same area as the receptors. For chemotropism to occur it is thought that the location of vesicle exocytosis only needs to shift towards the side of the hypha that is exposed to the high concentration of the amino acid, as a result of the shift of these receptors. Normal tip growth does not require these receptors to be activated. Therefore a change in their distribution via activation in the presence of amino acids could result in chemotropism. Branches are formed along the trunk of the hypha when a threshold of vesicles builds-up in the area, causing localised exocytosis (Schreurs et al., 1989).

In *A. bisexualis*, a proton gradient is present internally. This gradient is generated through protons which enter through the apical region of the hypha via amino acid symporters and then exit subapically via a proton-translocating ATPase (Kropf et al., 1984). Like oomycetes, fungi have receptors that bind amino acids which could be involved in determining where exocytosis of wall materials will occur therefore resulting in the production of branches in areas of high amino acid concentrations (Schreurs et al., 1989). This is one possibility that could explain the higher frequency of branch production compared with the control inductions. It is possible that there are receptors along the surface of the hyphae that, when activated, result in the production of a branch along the trunk of the hypha, a hypothesis generated by Schreurs et al. (1989) for *A. bisexualis*. It is possible that the receptor proteins involved in chemotropism and branching are separate but they have "similar specificities (Schreurs et al., 1989). These receptors are capable of sensing gradients of amino acids. The receptors present at the tip of a growing hypha could sense this gradient and reorient the direction of growth on a time scale towards the source of the gradient, whereas the receptors present along the hyphal trunk are unable to change the direction of growth in a suitable time scale and therefore put out a new growing tip in the form of a branch towards the source of the gradient (Schreurs et al., 1989).

The formation of branches in response to the local application of amino acids cannot be solely attributed to the phenylalanine as the presence of Vogel's medium alone also resulted in the production of branches, albeit less frequently. Furthermore, the hyphal tip still responded chemotropically to the micropipette in all the trials (n=4). However, when the micropipette was filled with water it resulted in no branches forming but the hypha may be

responding in some way to the micropipette as a bump did form on the opposite side to the micropipette in one of the inductions and the hyphal tip did respond chemotropically to the micropipette in half of the trials (n=4). The ability for branches to form in the absence of a nutrient gradient suggests that the locally application of solution towards the hypha could be having a mechanical effect on the hyphal wall. This force of the solution acting upon the hyphal wall could be affecting mechanosensitive channels and because of this, a branch is being formed. The sample sizes for the control experiments were small with an n value of 4 for each the water alone and the Vogel's alone therefore it is possible that with a larger sample size for each of these inductions, a higher percentage of branches would have formed as in the phenylalanine inductions. However, the presented data suggests that the presence of phenylalanine may make the response stronger in response to the local application of solution towards the hypha with a success rate of 83% compared with 50% for Vogel's alone. Another possibility for the difference between the responses seen between trials with Vogel's media and those with water is that there may be a difference in the nutrient composition between the Vogel's media agar that the hyphae are growing in and the liquid Vogel's media present in the micropipette. This cannot be discounted and may have occurred through possible human error in making the media. If the difference in nutrient composition between the two solutions was the case, a nutrient gradient may have been generated which the hyphae were responding to.

In this investigation, a change in the growth rate of the hyphal tip was observed immediately after the induction began with a significant reduction in hyphal growth rate from 13 ± 7 µm/minute before the induction to 10 ± 6 µm/minute one minute after the induction. The immediate reduction in growth rate could be the response of hyphae to the external stimulus of the amino acid gradient generated by the micropipette. This signal is possibly overruling the hyphal growth unit, resulting in a decrease in the rate of vesicle supply to the hyphal tip, with a portion of them instead building up in the area exposed to the high amino acid gradient. A reduction in the vesicle supply at the hyphal tip would correspond to a decrease in hyphal growth rate. This build-up of vesicles to the site where the hypha is exposed to the amino acid gradient would undergo exocytosis and develop a new branch growing in the direction of the source of the amino acid.

The positioning of the micropipette with respect to the hypha appears to have an influence on the timing of the branching event, the growth rate of the future branch and the location of the future branch. When the micropipette was positioned further back from the hyphal tip prior to the start of the induction, it took less time for a bud to transition into a

branch. However, from the position of the micropipette 30 μm back from the tip and onwards, it took the same amount of time to branch no matter where the micropipette was positioned. This suggests that there are some mechanisms preventing branching events occurring close to the hyphal tip because when the micropipette is initially positioned closer to the tip, the branches take longer to form. The hyphal tip will continue to grow in these inductions, therefore when the tip is the set distance away from the tip, a branch will form causing a longer bud to branch transition to occur. The branches that formed also grew faster the further back they were formed from the tips. The further back from the tip, the greater the PGZ is for the supply of vesicles to the tip therefore enables the supply of a portion of vesicles to be delivered to the new area of growth. The branch growth rate also increased as the micropipette was further from the hyphal trunk. This suggests that the response by the hypha is stronger when the amino acid gradient is generated further away.

The closer the micropipette was to the hyphal tip before the induction started resulted in branches forming closer to the micropipette. This suggests that the location of the signal may be perceived stronger when the micropipette is positioned closer to the tip. More H^+/amino acid symporters may be present in this area and therefore more could be recruited to the area, resulting in branch development near the micropipette tip. This would make predicting the positioning of the new branch easier for future use.

In some branch induction trials multiple branches were formed. In 16.7% (n=24) of the inductions, two or three branches formed from the trunk of the hypha being induced to branch. Multiple branches from a single branch induced occurred in 4.2% (n=24) of the trials. The development of more than one branch in response to the nutrient gradient could be caused by the signal perceived by the presence of amino acids being so strong that the hypha is triggered to produce more surface area in order to uptake the available source of nutrients and therefore it develop multiple tips.

When hyphae were being induced to branch the primary growing tip also displayed a chemotropic response with the tips bending on average $23 \pm 59^{\circ}$ towards the micropipette. There was no significantly obvious relationship between the time to bump and the degree that the growing tip bends, whereas in *A. bisexualis*, no branches were formed when the tip bent less than 6° (Morris et al., 2011).

It is suggested that this branch induction technique enables the stimulation of branch formation in a known location. Using this technique it will allow for further investigation into the underlying mechanisms of branch development in filamentous fungi. In the next two chapters I will use this induction technique on *N. crassa* to investigate the roles of Ca^{2+}

(Chapter 4), actin and the signalling Rho-GTPase proteins (Chapter 5) in the development of branches.

Chapter 4
The Role of Ca^{2+} in Determining Mycelial Morphology

4.1 Introduction

The interplay of hyphal tip growth and hyphal branching determines the morphology of mycelial colonies of filamentous microorganisms such as *N. crassa* and *A. bisexualis*. The ability for the colony to balance both exploratory growth in search of new sources of nutrients and exploitive growth in order to uptake the available nutrients in the immediate vicinity gives the colony its characteristic morphology. A hyphal colony typically consists of a growing edge region with very few branches and a highly branched region back from the growing edge. The sparsely branched growing edge enables the colony to invest its available resources into extending outwards without expending resources on developing a number of new growing tips. In contrast, a number of new branches are formed further back from the tip which are primarily involved in the uptake of nutrients which have already been covered by the growing hyphal tips. In order to have such a defined branching pattern there must be internal mechanisms in place that prevent branches forming close to the hyphal tips. If branches were to form close to the hyphal tips, the growth rate of the colony would slow down. This is because more resources are required to support a number of new tips therefore decreasing the area that can be covered in a period of time. This would hinder the ability of the colony to search for new sources of nutrients.

The regulation of physiological and structural components of tip-growing cells is required to enable tip growth. Ion transport is one of these key components involving ion transporters present in the plasma membrane, facilitating the movement of ions across the membrane. These ion transporters include ion channels, carriers and active pumps (Lew, 1999). Ion currents are important in the generation and maintenance of cellular polarity (Jaffe and Nuccitelli, 1977; Takeuchi et al., 1988). One ion that may play a role in forming this

current is Ca^{2+} (Takeuchi et al., 1988). It is proposed that an influx of Ca^{2+} in through the tip of tip-growing cells increases the concentration of Ca^{2+} at the tip of the cell. This results in vesicles exocytosis being localised to the very tip of the cell. Ca^{2+} sequestering organelles can be found behind the tip where they sequester cytoplasmic Ca^{2+} as a storage mechanism. A lower concentration of Ca^{2+} in the subapical regions results in the actin cytoskeleton relaxing (Ca^{2+} is involved in stabilising F-actin) thus allowing extension to only occur at the apex of the hypha (Picton and Steer, 1982). Tip-high Ca^{2+} gradients have been discovered in in growing hyphae of the *N. crassa* (Levina et al., 1995) and in the oomycete *S. ferax* (Garrill et al., 1992; Hyde and Heath, 1997) through the use of fluorescent Ca^{2+}-sensitive dyes.

The tip-high Ca^{2+} gradient in *N. crassa* is an important feature of its ability to undergo tip growth. The level of Ca^{2+} at the tip is required to be raised above basal level in order to grow forward. The difference between the concentration at the tip and the subapical region needs to be at least 30 nM. It is this difference, not the steepness of the gradient that is required for growth (Silverman-Gavrila and Lew, 2003). For the normal morphology to be established in *N. crassa*, hyphae must be exposed to a minimum of 1 µM of Ca^{2+} in the growth medium. For the hyphae to reach the maximal extension rate, the growth medium needs to contain 10 µM of Ca^{2+} (Takeuchi et al., 1988). Internal sources of Ca^{2+} in *N. crassa* are likely to be involved in creating and maintaining the Ca^{2+} gradient in hyphae. Storage structures such as vacuoles and mitochondria are likely to recycle internal Ca^{2+} (Levina et al., 1995). When the Ca^{2+} levels present in the external environment drop below the required level for *N. crassa*, the hyphal tips bulge which may be a direct result of the cell wall becoming more plastic and giving in to the internal pressure, causing in the tips to swell (Jackson and Heath, 1989)

External Ca^{2+} is also required by *S. ferax* to maintain normal morphology and maximal extension rate. The growth rate increases as the external Ca^{2+} concentration is increased to 5×10^{-2} M. However, levels above this concentration result in decreased growth rates. When Ca^{2+} was removed from the external media, depletion of the internal Ca^{2+} concentration occurred, allowing growth to continue for a short period of time using internal Ca^{2+} stores. Whereas, when high external concentrations of Ca^{2+} were present in the growth media it increased the internal Ca^{2+} concentration. This directly reflects the ability of external Ca^{2+} to influence the internal concentration. However, the range in which the external Ca^{2+} concentration changed resulted in a smaller range of internal change therefore suggesting

they have the ability to tightly regulate internal Ca^{2+} in response to a gradient of Ca^{2+} present (Jackson and Heath, 1989).

4.1.1 Ca^{2+} Channels

Stretch activated (SA) Ca^{2+} channels can be found in a range of hyphal organisms including *S. ferax* and *N. crassa* (Garrill et al., 1992; Gustin et al., 1988; Zhou et al., 1991; Zhou and Kung, 1992). Aspects of these channels have been investigated by Lew (1998) using patch clamping, analysis of channel self-clustering and the association occurring between channels of different types, exposing different mechanisms underlying the ion dynamics required for tip growth in these organisms. A stretch force at the tip of growing hyphae could activate the influx of Ca^{2+} through these channels. The Ca^{2+} levels within the hyphae are then possibly involved in the process of tip extension (Levina et al., 1995). The SA channels in *S. ferax* are suggested to be a growth sensor; however their role in *N. crassa* is unclear (Lew, 1998). There are similarities in the morphology of the tips, the rate of growth and the presence of a tip-high Ca^{2+} gradient in *N. crassa* and *A. bisexualis* however it is obvious that the mechanisms underlying the generation of this Ca^{2+} gradient are not the same between them (Lew, 1999).

4.1.1.1 Mechanism of tip-high Ca^{2+} gradient generation in *A. bisexualis*

In *S. ferax*, the influx of Ca^{2+} is regulated via SA channels which are concentrated at the hyphal tip (Garrill et al., 1993). These SA Ca^{2+} channels present at the tip are thought to act as a sensor for the growth of *S. ferax* as they are activated by the influence of internal pressure upon the plasma membrane and the cell wall, resulting in a stretch force. Therefore, an increase in the tension of the plasma membrane and cell wall would increase as the tip grows and expands, activating these channels (Silverman-Gavrila and Lew, 2003). Ca^{2+} influx across the plasma membrane occurs in the first 8 µm of the tip of the hypha (Lew, 1999). This localised influx through the SA Ca^{2+} channels is responsible for the generation and maintenance of the tip-high Ca^{2+} gradient (Garrill et al., 1993; Garrill et al., 1992; Levina et al., 1994). When these channels are blocked with Gd^{3+}, a known inhibitor of SA Ca^{2+} channels, there is no influx of Ca^{2+} (Garrill et al., 1993; Lew, 1999). The result is the disappearance of the tip-high Ca^{2+} gradient and hyphal growth stops (Garrill et al., 1993).

One of the ways in which the actin cytoskeleton may play an important role in the polarised tip growth of hyphae is through the maintenance of the high gradient of SA Ca^{2+} channels at the tip in *S. ferax*. The presence and location of these SA channels is vital for tip growth to occur. When the actin inhibitor cytochalasin E is added to these hyphae it disrupts the actin cytoskeleton at the tip, changing the tip morphology and localisation of the SA Ca^{2+} channels at the tip. The mechanism by which the actin cytoskeleton could be maintaining the high gradient of SA Ca^{2+} channels at the tip is by forming tracks for the vesicles containing the SA channels to reach the hyphal tip or alternatively there could be a direct interaction between the channels and the actin cytoskeleton keeping them in place (Levina et al., 1994).

4.1.1.2 Mechanism of tip-high Ca^{2+} gradient generation in *N. crassa*

As discussed earlier, *N. crassa*, like other tip growing cells, has a tip-high Ca^{2+} gradient. Unlike *S. ferax*, there is no net influx of Ca^{2+} across the plasma membrane through SA Ca^{2+} channels at the tip and there is no tip-high gradient of these channels (Lew, 1998). Therefore, *N. crassa* must rely upon another mechanism to generate and maintain a tip-high Ca^{2+} gradient.

A self-referencing probe was used to show that there is no net flux of Ca^{2+} at the tip or along the trunk of the hypha whilst they are growing (Lew, 1999). Also, a change in the magnitude and direction of the transport of ions across the plasma membrane using voltage clamping had no effect on the tip's growth. This suggests that Ca^{2+} flux across the membrane is not involved in the process of tip growth (Silverman-Gavrila and Lew, 2000). When the inhibitor of some SA channels, Gd^{3+}, was added it only partially inhibited the activity briefly, decreasing the growth rate and having no effect on the morphology of the tip. The tip-high gradient of Ca^{2+} in growing hyphae does not dissipate when Gd^{3+} is present. This suggests that influx of Ca^{2+} through these channels is not responsible for Ca^{2+} gradients (Levina et al., 1995), and hence the generation of the tip-high Ca^{2+} gradient that is required for growth must be generated through some other mechanism (Silverman-Gavrila and Lew, 2000). *N. crassa* requires external Ca^{2+} in order to maintain growth and morphology therefore it is thought that there may be Gd^{3+}-insensitive Ca^{2+} permeable channels which are necessary for the movement of Ca^{2+} into the hyphae, however the number of these channels may be below the detection level (Levina et al., 1995).

The reliance on internal stores of Ca^{2+} could explain the generation and maintenance of a tip-high Ca^{2+} gradient irrespective of the changing environment the hypha is growing in. Ca^{2+} is believed to enter the cell behind the tip where it collects in vesicles. When these vesicles dock at the plasma membrane at the apex of the hypha, Ca^{2+} is released into the cytoplasm, prior to the fusion of vesicles with the plasma membrane, stimulating the process (Silverman-Gavrila and Lew, 2000). There are two Ca^{2+} transporters that regulate the internal levels of Ca^{2+} in *N. crassa*. These transport proteins are an inositol 1,4,5-triphosphate (IP_3)-activated Ca^{2+}channel and a Ca^{2+}-ATPase. These proteins are located in different areas within the hypha. The IP_3-activated Ca^{2+} channels are found in the vesicles at the very apex of the hypha and these channels are involved in the release Ca^{2+}into the cytoplasm, whereas the Ca^{2+}-ATPases are found in the plasma membrane of ER behind the apex of the hypha and are involved in the sequestration of Ca^{2+} into the ER (Silverman-Gavrila and Lew, 2003).

Vacuolar membranes in fungi contain Ca^{2+} channels which are activated by the presence of IP_3 therefore they were initially thought to be the required Ca^{2+} stores for maintaining the tip-high Ca^{2+} gradient, however they are not present within the first 60 µm behind the growing hyphal tip (Lew, 1999). Therefore, Chlorotetracyline (CTC) fluorescing structures (CTC binds to Ca^{2+}) that are thought to correspond with ER are likely to be the Ca^{2+} storage organelles required for the generation of the gradient (Schmid and Harold, 1988). The generation of the internal Ca^{2+} gradient in *N. crassa* occurs via the interplay between Ca^{2+} sequestration into the ER and, in response to the presence of IP_3, the release of Ca^{2+} from vesicles held in place at the tip by actin cytoskeleton (Silverman-Gavrila and Lew, 2001).

The mechanism underlying the generation of the tip-high Ca^{2+} gradient in *N. crassa* can be seen in Figure 4.1. It begins with the activation of SA-phospholipase C (PLC) channels which act as growth sensors in *N. crassa*. SA-PLC channels are localised to the tips of *N. crassa* hyphae. When SA-PLC is activated by a stretch force, it results in the production of IP_3 internally. The increased concentration of IP_3 within the cytoplasm then activates IP_3-activated Ca^{2+} channels associated with the plasma membranes of the Ca^{2+} stores which are heavily located near the tip (Silverman-Gavrila and Lew, 2002). As the vesicles dock with the apical region of the hypha, Ca^{2+} is released into the cytoplasm. This tip-high Ca^{2+} gradient aids in the localised fusion of vesicles at the tip. The cytoplasmic Ca^{2+} is then sequestered into organelles, most likely ER, which are heavily present subapical to the tip. This occurs through the aid of a Ca^{2+} ATPase. This Ca^{2+} will be recycled as these two systems of Ca^{2+}

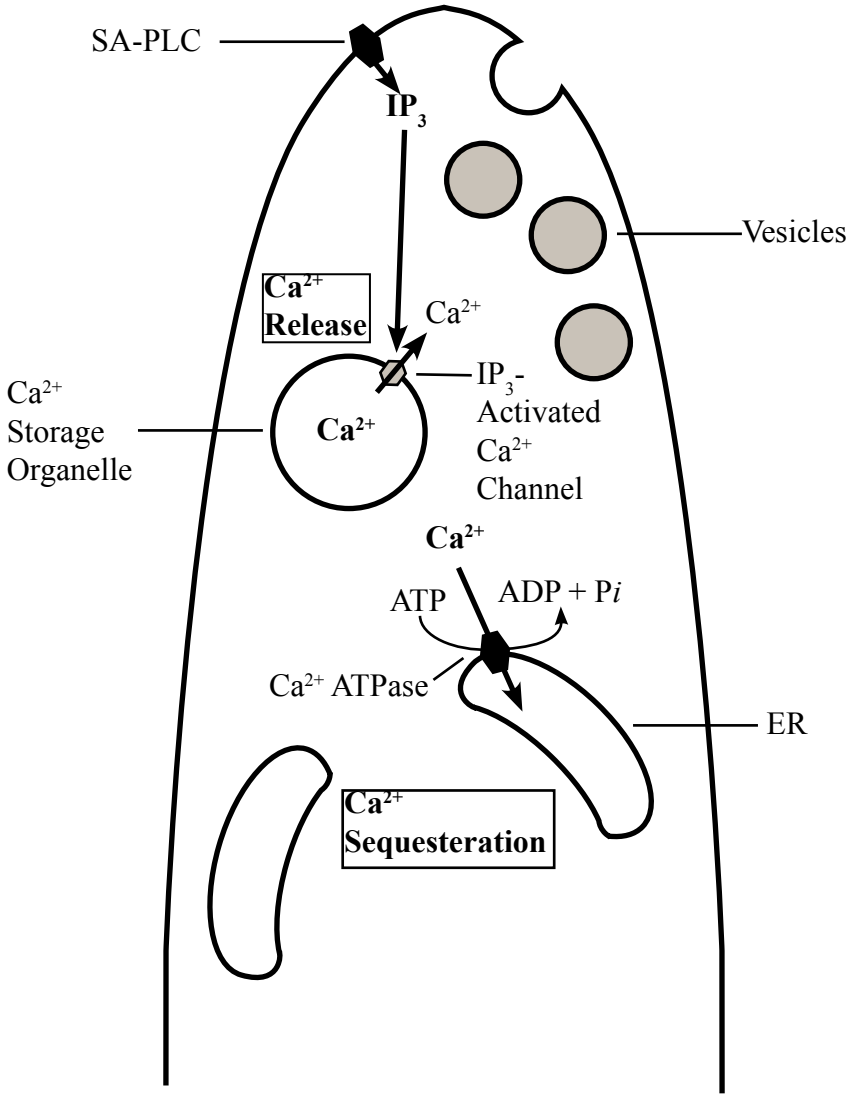

Figure 4.1 - Cytoplasmic Ca^{2+} regulation in *N. crassa*. IP_3-activated Ca^{2+} channels release Ca^{2+} from Ca^{2+} storage organelles after IP_3 is produced via SA-PLC, generating a tip-high Ca^{2+} gradient. Ca^{2+} is sequestered into ER further back from the tip removing free Ca^{2+} from the cytoplasm. Modified from Silverman-Gavrila and Lew (2002).

release and sequestration exist in a feedback mechanism with one another (Silverman-Gavrila and Lew, 2002).

When SA-PLC is inhibited, the release of Ca^{2+} from the Ca^{2+} stores can no longer occur due to the absence of IP_3 in the cytoplasm. This leads to hyphal growth ceasing and a diminished cytoplasmic tip-high Ca^{2+} gradient. When IP_3-activated Ca^{2+} channels were inhibited, it prevented the release of Ca^{2+} from vesicles. This resulted in fluorescence of Ca^{2+} in vesicles that were subapical to the tip. This was unexpected given the prediction that Ca^{2+} present within vesicles would be seen at the tip. The reasoning behind this subapical fluorescence in vesicles could be that they could not fuse with the tip as there was no cytoplasmic Ca^{2+} gradient and as a result they moved back to the subapical region. When the inhibitor was washed out, the vesicles moved to the tip and caused hyperbranching at the apex. When the ER- Ca^{2+} ATPase, responsible for sequestering Ca^{2+}, was inhibited there was no fluorescence in the vesicles however the cytoplasmic Ca^{2+} levels increased. This resulted in the cessation of tip growth (Silverman-Gavrila and Lew, 2002).

4.1.1.3 Reasons for Different Regulation of Ca^{2+} in Fungi and Oomycetes

There is a clear difference in the way the fungus *N. crassa* and the oomycete *S. ferax* generate and maintain the tip-high Ca^{2+} gradient. This difference may be a result of the environments they have adapted to live in; *N. crassa* inhabits terrestrial ecosystems whereas *S. ferax* inhabits aquatic ecosystems. When living in a terrestrial environment the external concentration of Ca^{2+} can change significantly therefore it would not be practical for them to rely upon this source for such a fundamental process as tip growth. However, in an aquatic environment there is likely to be a more reliable source of Ca^{2+} which can be used to maintain the Ca^{2+} gradient through influx at the tip (Levina et al., 1995). Another reason for a difference in the mechanism used to generate the Ca^{2+} gradient could be a difference in growth strategy between these two organisms. Oomycetes like *S. ferax* grow as a small zone of active cytoplasm found at the tip whereas fungi like *N. crassa* grow as a mycelium which has actively streaming cytoplasm found within a majority of the colony (Lew, 1999).

4.1.2 Ca^{2+} and Colony Morphology

There are several ways in which Ca^{2+} could be effecting the growth and morphology of filamentous microorganisms. These include the crosslinking of wall materials, acting as a signalling molecule, regulating the activity of some enzymes and regulating the cytoskeleton (Silverman-Gavrila and Lew, 2003). Ca^{2+} may also play a role in stimulating the fusion of vesicles with the hyphal membrane (Fischer, 2007). In this study, the role of Ca^{2+} in determining apical dominance or in signalling branch formation was the focus as mentioned earlier. This is important as it has implications on the development of the mycelial colony.

Previous investigations involving *A. bisexualis* show that Ca^{2+} channel inhibitors alter the branch frequency and the colony radius. It is thought that the addition of Ca^{2+} channel inhibitors diminishes the tip-high Ca^{2+} gradient, resulting in the development of more branches that are closer to the tip of the hypha and a smaller colony radius. When the Ca^{2+} channel inhibitor verapamil was added to mycelia of *A. bisexualis* it resulted in an increase in the number of branches produced per length of hypha as the concentration increased and also decreased the distance between the growing tips to the first branch. When hyphae were exposed to the SA channel inhibitors La^{3+} and Gd^{3+} it increased the branch frequency however this effect was not as profound as that with verapamil (Morris et al., 2011). With a diminished tip-high Ca^{2+} gradient, the mechanism by which apical dominance is maintained at the hyphal tip is removed and changes the colony morphology. Without a tip-high Ca^{2+} gradient, more resources are likely to be put towards forming branches than extending the colony radius. Oomycetes and fungi are morphologically similar however the mechanisms underlying hyphal branching could be different between the two groups.

Ca^{2+} channel inhibitors including La^{3+}, Gd^{3+} and verapamil should effect the growth and morphology of *N. crassa* hyphal tips if a Ca^{2+} gradient if required for growth. However when La^{3+} was added at 40 µM, Gd^{3+} at 40 µM and verapamil at 100 µM there was little to no effect on growth or morphology or on the Ca^{2+} gradient (Schmid and Harold, 1988). This agrees with the work by Takeuchi et al. (1988) where the addition of Gd^{3+} and La^{3+} showed no effect on the extension of the hyphae or the branching pattern. However, when Dicker and Turian (1990) conducted whole plate addition experiments exposing 1 mM verapamil to *N. crassa* the hyphal tips of these cultures had an increase in the number of branches formed forming a "fan-like" growth pattern. When 10 mM $CaCl_2$ was added along with the inhibitor to the growth media, the branch frequency is the same as the control branch frequency. The

addition of verapamil to the media and the effects this has on colony morphology can be attributed to a decrease in cytoplasmic Ca^{2+} levels as the rate of tip growth decreases as a result of the increased production of branches. This effect of verapamil is reverted back to control branch frequency and increases the tip growth rate, but not back to control rates, with the increase in external Ca^{2+} concentration (Dicker and Turian, 1990).

Work has also been conducted on another filamentous fungus, *Fusarium graminearum* that indicates that when treated with the Ca^{2+} channel blockers; cinnarizine, nifedipine, nicardipine and cobalt chloride, there was a decrease in the hyphal extension rate and a decrease in the hyphal growth unit length. It has therefore been suggested that Ca^{2+} plays a key role in both fungal tip growth and branching (Robson et al., 1991a). As the concentration Ca^{2+} increased within the growth medium of *F. graminearum*, the length of the hyphal growth unit increased to the concentration of 1.0×10^{-5} M where above this concentration there was no additional effect of Ca^{2+}. When the external concentration of Ca^{2+} was 1.4×10^{-8} M there was a high frequency of branches. These hyphae had irregular walls and in subapical regions there was swelling. This suggests that, by lowering the external Ca^{2+} concentration, there is a decrease in internal Ca^{2+} resulting in an increase in branch formation (Robson et al., 1991b).

4.1.3 Aims of Chapter 4

The aim of this chapter was to investigate the role of Ca^{2+} in the process of hyphal branching. The Ca^{2+} channel inhibitors verapamil, Gd^{3+} and La^{3+}were added to the growth media of *N. crassa* to determine whether these alter cytoplasmic Ca^{2+} levels and as a result of this, the mycelial morphology. The Ca^{2+} channel inhibitor verapamil was locally applied to hyphae of *N. crassa* using the branch induction technique described in Chapter 3 to see the direct effects it has on branch formation. Ca^{2+} dyes were used in order to see the internal levels of cytoplasmic Ca^{2+} in *N. crassa* and *A. bisexualis* at branching sites.

4.2 Materials and Methods

See Chapter 2 for full Methods and Materials.

4.3 Results

4.3.1 Ca^{2+} Channel Inhibitors have an Effect on *N. crassa* Mycelial Morphology in Whole Plate Cultures

Three different Ca^{2+} channel inhibitors were added at different concentrations to the medium *N. crassa* was cultured on. These inhibitors were verapamil, an organic phenylalkylamine which blocks L-type Ca^{2+} channels and the inorganic lanthanides, Gd^{3+} and La^{3+}, which block SA ion channels. Five aspects of colony morphology were measured in the whole plate experiments. These were colony radius, primary branch frequency, secondary branch frequency, distance from the tip to the first branch and the distance from the first branch to the second branch. The primary branch frequency was calculated from the number of branches that form from the main trunk hypha being analysed (Figure 1.2). The secondary branch frequency was calculated from the number of branches that form from the primary branches (Figure 1.2). The distance from the tip to the first branch was measured from the very apex of the hypha being measured to the first primary branch. The distance from the first branch to the second branch was the distance from the first primary branch to the second primary branch on the hypha measured. The colony radius was measured from the edge of the agar inoculum plug to the edge of the growing colony.

All of the inhibitors had an effect on the colony morphology with the most marked effect with verapamil. Figure 4.2 shows the effect of increasing verapamil concentration on colony morphology. The colony radius decreased as the verapamil concentration increased, resulting in the development of more branches that form closer together. The number of aerial hyphae increased as the concentration of verapamil increased. At a verapamil concentration of 1000 µM, most hyphae only grew a short distance out of the initial plug of agar and a number of aerial hypha grew out the top of the agar plug. Because of the large number of branches and how compacted the hyphae were relative to one another as the concentration of verapamil increased, a decision was made to stop counting the number of branches at concentrations above 250 µM. This is because above this concentration measurements would have been unreliable due to the difficulty in reliably counting branches (see for example the bottom plate of Figure 4.2). An increase in verapamil concentration significantly reduced the colony radius in a dose response manner at concentrations above 200 µM. The addition of 10mM $CaCl_2$ to 250 µM and 1000 µM verapamil led to the inhibitor

having no effect on the colony radius (Figure 4.3). The addition of Gd^{3+} significantly decreased the colony radius at the higher concentrations added (500 µM and 1000 µM). This decrease in the colony radius was again eliminated with the addition of 10 mM $CaCl_2$ to 1000 µM Gd^{3+} (Figure 4.3). La^{3+} generally significantly decreased the colony radius at concentrations above 5 µM; again the effect of the inhibitor on the colony radius was eliminated with the addition of 10 mM $CaCl_2$ to 1000 µM La^{3+}. (Figure 4.3) The addition of 5 mM and 10 mM $CaCl_2$ on their own to the media had no significant effect on the colony radius (Figure 4.3). The addition of DMSO at the highest concentration used in the experiments (0.1% v/v) had no significant effect on the colony radius (see Appendix 1 for full statistical analysis and sample sizes).

With verapamil, the primary branch frequency significantly increased at concentrations above 50 µM. This increase was not affected by the addition of 10 mM $CaCl_2$ to 250 µM of the inhibitor (Figure 4.4). The primary branch frequency generally increased at concentrations above 100 µM Gd^{3+}. This increase reverted back to the control level with the addition of 10 mM $CaCl_2$ along with 1000 µM of the inhibitor (Figure 4.5). When La^{3+} was added to the growth media there was an increase in the primary branch frequency at the higher concentrations used in the experiment. Primary branch frequency generally increased above concentrations above 400 µM with the addition of 10 mM $CaCl_2$ to 1000 µM still having a higher frequency of primary branches (Figure 4.6). The addition of $CaCl_2$ alone at concentrations of 5 mM and 10 mM had no significant effect on the primary branch frequency. The addition of DMSO at the highest concentration used in the experiments (0.1% v/v) also significantly increased the branch frequency. This may in part explain the increase in primary branch frequency seen with the inhibitors (see Appendix 1 for full statistical analysis and sample sizes).

The secondary branch frequency was significantly altered compared with the control with the addition of verapamil and Gd^{3+}. An increase in the concentration of verapamil increased the number of secondary branches in a dose response manner, with a significant increase in the frequency at concentrations above 50µM. The addition of 10mM $CaCl_2$ to 250 µM verapamil decreased the secondary branch frequency; however it was still significantly higher than the control (Figure 4.7). Gd^{3+} generally increased the secondary branch frequency at concentrations above 400 µM. The addition of 10 mM $CaCl_2$ to 1000 µM of the inhibitor decreased the secondary branch frequency back to control levels (Figure 4.8). La^{3+} had no significant effect on the secondary branch frequency of *N. crassa* (Figure 4.9). The addition of $CaCl_2$ alone at concentrations of 5 mM and 10 mM had no significant effect

on the secondary branch frequency. The addition of DMSO at the highest concentration used in the experiments (0.1% v/v) had no significant effect on the secondary branch frequency (see Appendix 1 for full statistical analysis and sample sizes).

The distance from the tip to the first branch was only sensitive to the addition of verapamil with no effect with the addition of Gd^{3+} or La^{3+} (Figure 4.10). The general trend when the concentration of verapamil increased was a decrease in the distance from the tip of the hypha to the first branch with a significant decrease at a concentration of 250 μM verapamil. The addition of 10 mM $CaCl_2$ to 250 μM verapamil still had a significantly shorter distance from the tip to the first branch. The addition at a concentration of 5 mM $CaCl_2$ to the media significantly decreased the distance from the tip to the first branch but 10 mM $CaCl_2$ had no significant effect. The addition of DMSO at the highest concentration used in the experiments (0.1% v/v) had no significant effect on the distance from the hyphal tip to the first branch (see Appendix 1 for full statistical analysis and sample sizes).

The distance from the first branch to the second branch was not affected significantly by the addition of any of the inhibitors (Figure 4.11). The addition of $CaCl_2$ alone to the media at concentrations of 5 mM and 10 mM also had no significant effect on this distance. The addition of DMSO at the highest concentration used in the experiments (0.1% v/v) had no significant effect on the distance from the first branch to the second branch (see Appendix 1 for full statistical analysis and sample sizes).

4.3.2 Local Application of Verapamil has an Effect on Tip Growth and Branching

In these experiments it was assumed that all the hyphae were exposed to the same concentration of inhibitor based on the positioning of the micropipette relative to the hypha and the aperture of the micropipette tip. For inductions with 50 μM verapamil, the micropipette was positioned on average 28 ± 4 μm away from the tip of the growing hypha and 9 ±1 μm away from the side of the hypha (n=6 hyphae) (Table 4.1 lists the full details of the inductions). For inductions with 500 μM verapamil, the micropipette was positioned on average 34 ±10 μm away from the tip of the growing hypha and 12 ±3 μm away from the side of the hypha (n=6 hyphae) (Table 4.2 lists the full details of the inductions). For inductions with 1000 μM verapamil, the micropipette was positioned on average 35 ± 7 μm away from

the tip of the growing hypha and 9 ± 3 μm away from the side of the hypha (n=7 hyphae) (Table 4.3 lists the full details of the inductions).

There was no significant difference in the average hyphal growth rate before and after the induction with 50 μM verapamil (n=6 hyphae, p>0.05) (see Appendix 1 for t test). The average hyphal growth rate before the induction was 14 ± 9 μm/minute and after the induction began was 25 ± 16 μm/minute (Figure 4.12). There was no significant difference in the average hyphal growth rate before and after the induction with 500 μM verapamil (n=6 hyphae, p>0.05) (see Appendix 1 for t test). The average hyphal growth rate before the induction was 27 ± 13 μm/minute and after the induction began was 22 ± 3 μm/minute (Figure 4.12). There was no significant difference in the average hyphal growth rate before and after the induction with 1000 μM verapamil (n=7 hyphae, p>0.05) (see Appendix 1 for t test). The average hyphal growth rate before the induction was 21 ± 11 μm/minute and after the induction began was 16 ± 13 μm/minute (Figure 14.12).

When 50 μM verapamil was added to the induction solution containing 1 mM phenylalanine in Vogel's liquid media, branches formed in 50% of induction trials (n=6 hyphae). In 1 out of 6 hyphae (17%) the tip immediately stopped growing and began to bulge before it continued growing (n=6 hyphae).

When 500 μM verapamil was added to the induction solution containing 1 mM phenylalanine in Vogel's liquid media, branches formed in 3 out of 6 hyphae (50%) (n=6 hyphae). In 1 out of 6 hyphae (17%) the tip continued to grow, however it briefly stopped and then started growing twice, bulging at the tip before resuming growth and forming a branch (n=6 hyphae) (Figure 4.13). In 1 out of 6 hyphae (17%) the tip continued to grow, however it briefly stopped and started growing, bulging at the tip when growth ceased then it formed a branch as the branch continued to grow (n=6 hyphae). In 2 out of 6 hyphae (33%) the tip continued to grow, however the cytoplasm became blebby (n=6 hyphae). In 1 out of 6 hyphae (17%) the tip continued to grow, however it briefly stopped and started growing twice, bulging at the tip when stopped, before it resumed growth (n=6 hyphae).

When 1000 μM verapamil was added to the induction solution containing 1 mM phenylalanine in Vogel's liquid media, branches formed in 5 out of 7 induction hyphae (71%) (n=7 hyphae). In 1 out of 7 hyphae (14%) the hyphal tip immediately stopped growing and the cytoplasm became blebby (n=7 hyphae). In 1 out of 7 hyphae (14%) the hyphal tip immediately stopped growing and began to bulge and became more rounded then continued to grow forming a new branch (n=7 hyphae). In 1 out of 7 hyphae (14%) the tips immediately

stopped growing and began to bulge and became more rounded then resumed growth as a new branch formed. The tip then stopped growing, becoming more rounded then continued to grow as a branch formed out of where the hyphal tip bulged (n=7 hyphae). In 1 out of 7 hyphae (14%) the hyphal tip stopped growing immediately and became more rounded then continued to grow. In 1 out of 7 hyphae (14%) growth continued and a branch formed however the cytoplasm then became blebby and the hyphal tip stopped growing (n=7 hyphae).

Correlation values were analysed to determine if there was a difference in the development of branches as a result of the local application of the inhibitor verapamil. There was no correlation between the time taken to form a bump and the time taken to form a bud when 50 μM verapamil was added to the induction solution (r=0, n=6 hyphae) (Figure 4.14). There was a strong negative correlation between the time taken to form a bump and the time taken to form a bud when 500 μM verapamil was added to the induction solution (r=-0.945, n=6 hyphae) (Figure 4.14). This suggests that as the time taken to form a bump increased, the time taken to form a bud decreased (i.e. hyphae that are fast to form a bump are slow to form a bud). There was a slight negative correlation between the time taken to form a bump and the time taken to form a bud when 1000 μM verapamil was added to the induction solution (r=-0.2374, n=7 hyphae) (Figure 4.14). This suggests that as the time taken to form a bump increased, the time taken to form a bud decreased (i.e. hyphae that are fast to form a bump are slow to form a bud).

When 500 μM verapamil was added to the induction solution there was no correlation between the time taken to form a bud and the time taken to form a branch (r=0, n=6 hyphae) (Figure 4.15). There was a strong positive correlation between the time taken to form a bud and the time taken to form a branch when 1000 μM verapamil was added in the induction solution (r=0.999, n=7 hyphae) (Figure 4.15). This suggests that as the time taken to form a bud increased ,so did the time taken to form a branch (i.e. hyphae that are fast to form a bud are fast to form a branch).

4.3.3 Effect of Verapamil on Multiple Branch Formation

When verapamil was not present in the induction solution, 4 out of 24 (17%) of the hyphae that formed branches formed multiple branches (n=24 hyphae). However when 50 μM (n=6 hyphae) and 500 μM (n=6 hyphae) verapamil were present in the induction

solution, none of the hyphae produced multiple branches. When the concentration of verapamil increased to 1000 μM, 2 out of 5 hyphae (40%) that formed branches formed multiple branches (n=5 hyphae) (Table 4.4) (Figure 4.16). This increase in the number of hyphae forming multiple branches from 0 μM to 1000 μM verapamil may be due to an effect verapamil is having on the underlying mechanisms of branch formation, however this effect may also possibly be a result of the small sample size acquired for the inhibitor inductions.

4.3.4 Chemotropic Response to the Local Application of Verapamil

Hyphal tips showed a chemotropic response to the induction media when inhibitors were added, either bending towards or away from the micropipette tip. The growing hyphal tip, when exposed to 50 μM verapamil, bent towards the micropipette tip in 4 out of 6 hyphae (67%). The average chemotropic response was a bend of 12 ± 12˚ with a range of 0-28˚. The growing hyphal tip, when exposed to 500 μM verapamil, bent towards the micropipette tip in 4 out of 6 hyphae (67%). The average chemotropic response was a bend of 15 ± 14˚ with a range of 0-30˚. The growing hyphal tip, when exposed to 1000 μM verapamil, bent towards the micropipette tip in 1 out of 7 hyphae (14%) and bent away from the micropipette tip in 3 out of 7 hyphae (43%). The average chemotropic response was a bend of -7 ± 15˚ with a range of -36-8˚.

4.3.5 Imaging Ca^{2+} in *N. crassa* and *A. bisexualis*

Ca^{2+} imaging dyes are typically made up in Ca^{2+}-free buffer solution. Therefore in the Ca^{2+} imaging experiments, the Ca^{2+}-free buffer PBS was first tested to identify any effect it has on *N. crassa* and *A. bisexualis* before the dyes were added to it. *A. bisexualis* was relatively healthy whereas *N. crassa* looked plasmolysed when exposed to PBS. Therefore d.H_2O was tested on *N. crassa* as a candidate solution for the dyes to be added to. In d.H_2O, *N. crassa* looked relatively healthy however *A. bisexualis* looked plasmolysed. Therefore dyes were added to PBS for *A. bisexualis* and d.H_2O for *N. crassa*. Within the colonies of both species, only a small number of hyphae took the dye up into the cell. Problems with Ca^{2+} dye loading into hyphae has been documented before with dye either not loading or

loading but not in growing hyphae using the following techniques; electroporation of *S. ferax*, microinjection of *Uromyces* germlings and cell-permeant dye loading of *Saprolegnia* and *Neurospora* (Jackson and Heath, 1993).

Ratio images were processed using ImageJ. A box was drawn along the centre of the hypha with a height of 2.54 μm. Within this area, fluorescence emitted by fluo 3 was divided by the fluorescence emitted by fura red. A tip-high Ca^{2+} gradient was seen in a hypha of *A. bisexualis*, in which the cytoplasm was moving but did not look healthy (Figure 4.17). A hypha of *N. crassa* showed no tip-high Ca^{2+} gradient, however the dye was concentrated within vesicles. To the best of observations made this hypha was not growing (Figures 4.18). A branch was seen in *N. crassa* in which the dye was sequestered into organelles and there was no tip-high Ca^{2+} gradient. To the best of observations made this branch was not growing (Figure 4.19). When 200 μM verapamil was added to *A. bisexualis* hyphae, dye was seen in the cytoplasm with a tip-high Ca^{2+} gradient in one hypha which was streaming but not clearly growing (Figure 4.20). With the loading of dye in relatively few hyphae of which were not growing, attempts to induce branching to visualise the dynamics of Ca^{2+} was not attempted in *N. crassa* or *A. bisexualis*. It is worth noting that fluorescence from both dyes was observed outside hyphae on some occasions in the same locations. This may be a result of esterases that have been secreted by the hyphae activating the dyes by cleaving off the AM group and then the dyes binding to Ca^{2+} associated with the hyphal cell wall. This is a possibility to explain the lack of fluorescence inside the cells as when the dye has been activated, it is no longer cell permeable.

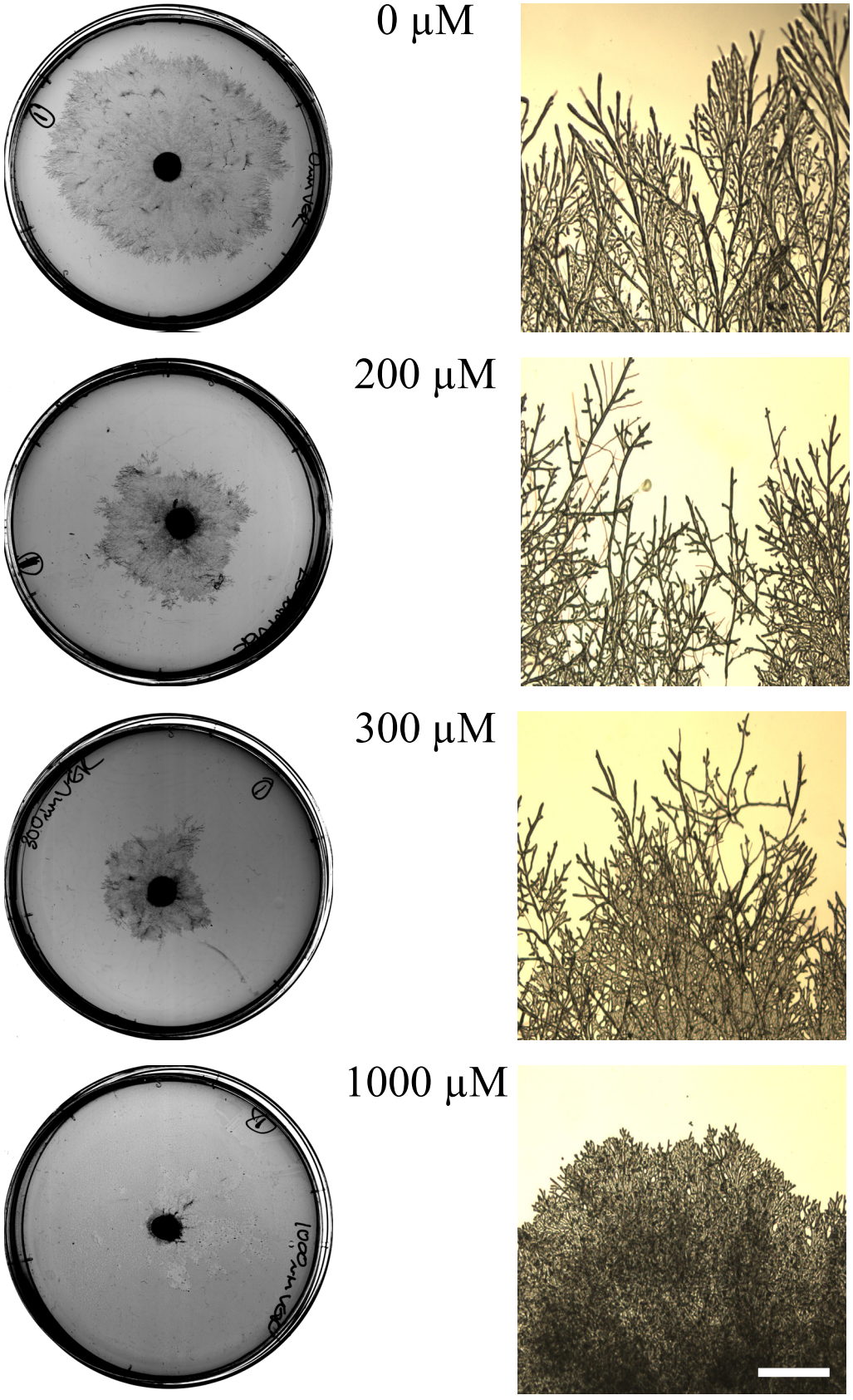

Figure 4.2 - Verapamil whole plate experiments showing the effect of verapamil on both the colony size and the branching pattern. The decision was made to stop counting the number of branches at concentrations above 250 µM as above this they could not be reliably counted. Bar = 1000 µm.

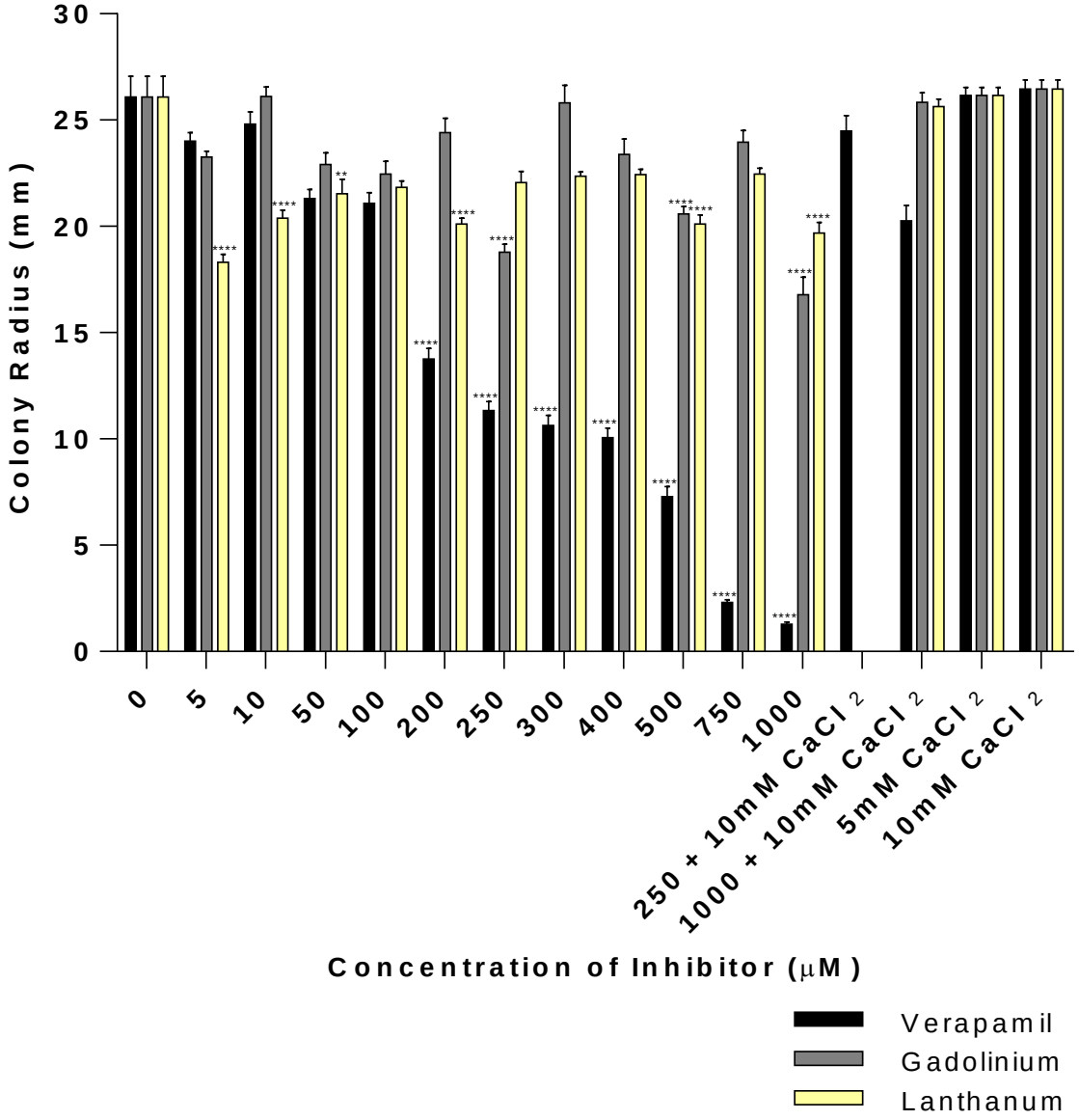

Figure 4.3 - Colony radius of *N. crassa* when treated with different concentrations of verapamil, Gd^{3+} and La^{3+}. Data are mean values ± SEM. Statistical significance was calculated compared to control values. Significance is indicated as follows; $p \leq 0.05$ - *, $p \leq 0.01$ - **, $p \leq 0.001$ - ***, $p \leq 0.0001$ - ****. See Appendix 1 for statistical analysis and sample sizes.

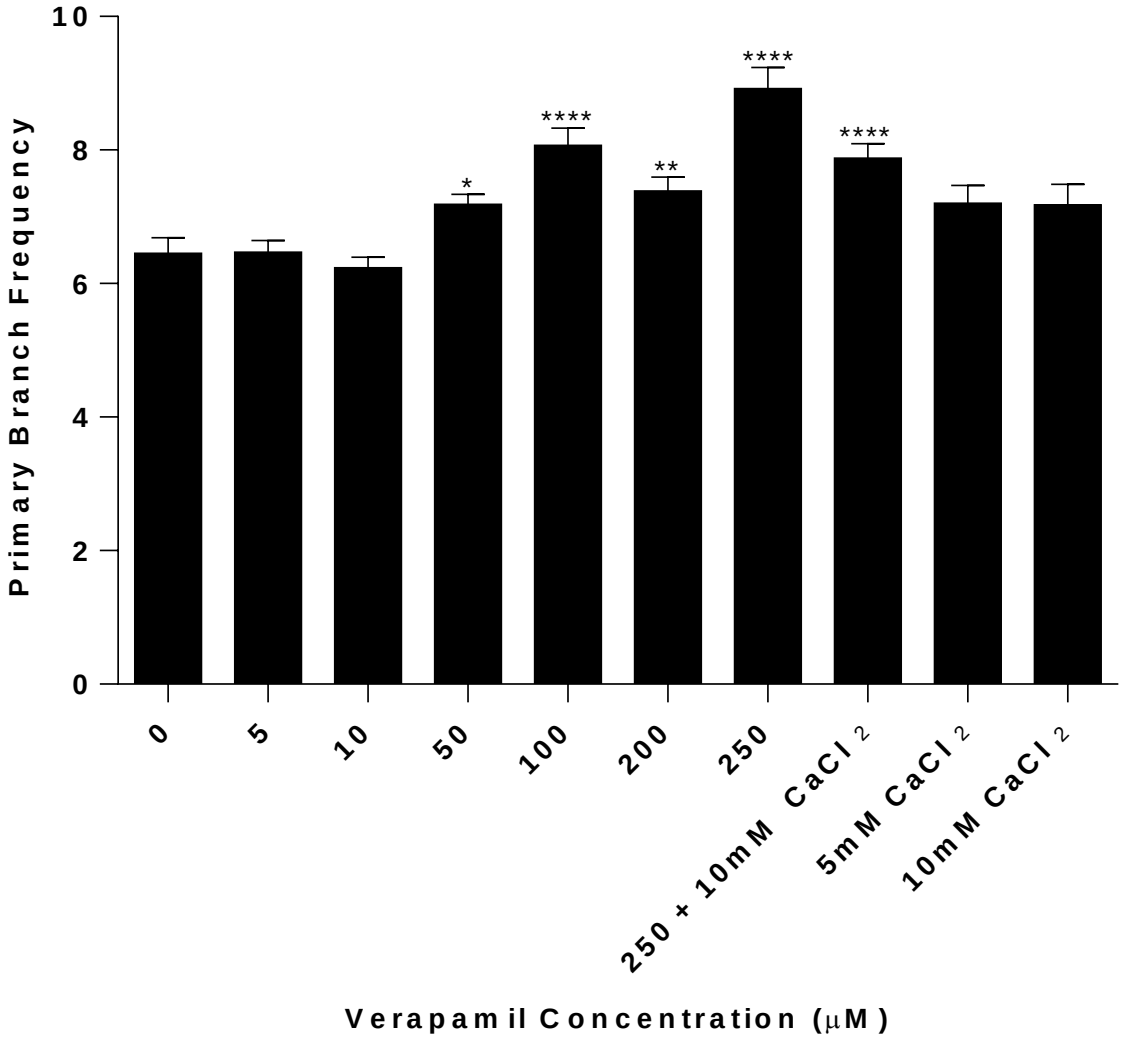

Figure 4.4 - Primary branch frequency of *N. crassa* generally increased when the concentration of verapamil increased. Data are mean values ± SEM. Statistical significance was calculated compared to control values. Significance is indicated as follows; $p \leq 0.05$ - *, $p \leq 0.01$ - **, $p \leq 0.001$ - ***, $p \leq 0.0001$ - ****. Statistical analysis revealed that concentrations of verapamil 0 µM ≠ 50 µM, 100 µM, 200 µM, 250 µM, 250 µM + 10mM $CaCl_2$; 5µM ≠ 50 µM, 100 µM, 200 µM, 250 µM; 250 µM + 10 mM $CaCl_2$; 10 µM ≠ 50 µM, 100 µM, 200 µM, 250 µM, 250 µM + 10 mM $CaCl_2$; 50 ≠ 250 µM; 200 ≠ 250 µM were significantly different ($p<0.05$). See Appendix 1 for statistical analysis and sample sizes.

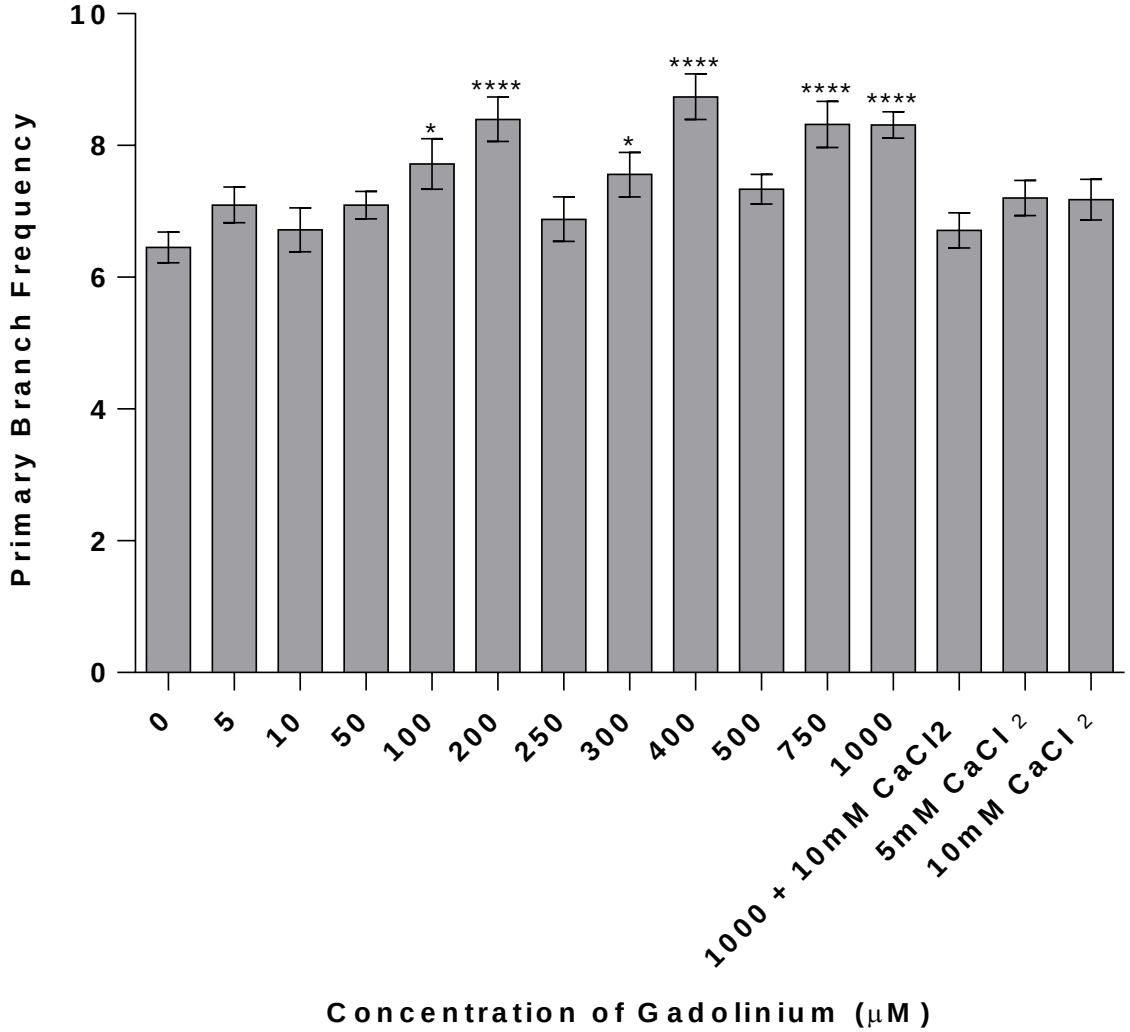

Figure 4.5 - Primary branch frequency of *N. crassa* generally increased when the concentration of Gd^{3+} increased. Data are mean values ± SEM. Statistical significance was calculated compared to control values. Significance is indicated as follows; $p \leq 0.05$ - *, $p \leq 0.01$ - **, $p \leq 0.001$ - ***, $p \leq 0.0001$ - ****. Statistical analysis revealed that concentrations of Gd^{3+} 0 µM ≠ 100 µM, 200 µM, 300 µM, 400 µM, 750 µM, 1000 µM; 5 µM ≠ 400 µM; 10 µM ≠ 200 µM, 400 µM, 1000 µM; 50 µM ≠ 200 µM, 400 µM, 1000 µM; 200 µM ≠ 1000 + 10 mM $CaCl_2$; 250 µM ≠ 400 µM; 400 µM ≠ 1000 µM + 10 mM $CaCl_2$; 750 µM ≠ 1000 µM + 10 mM $CaCl_2$; 1000 µM ≠ 1000 µM + 10 mM $CaCl_2$ were significantly different ($p<0.05$). See Appendix 1 for statistical analysis and sample sizes.

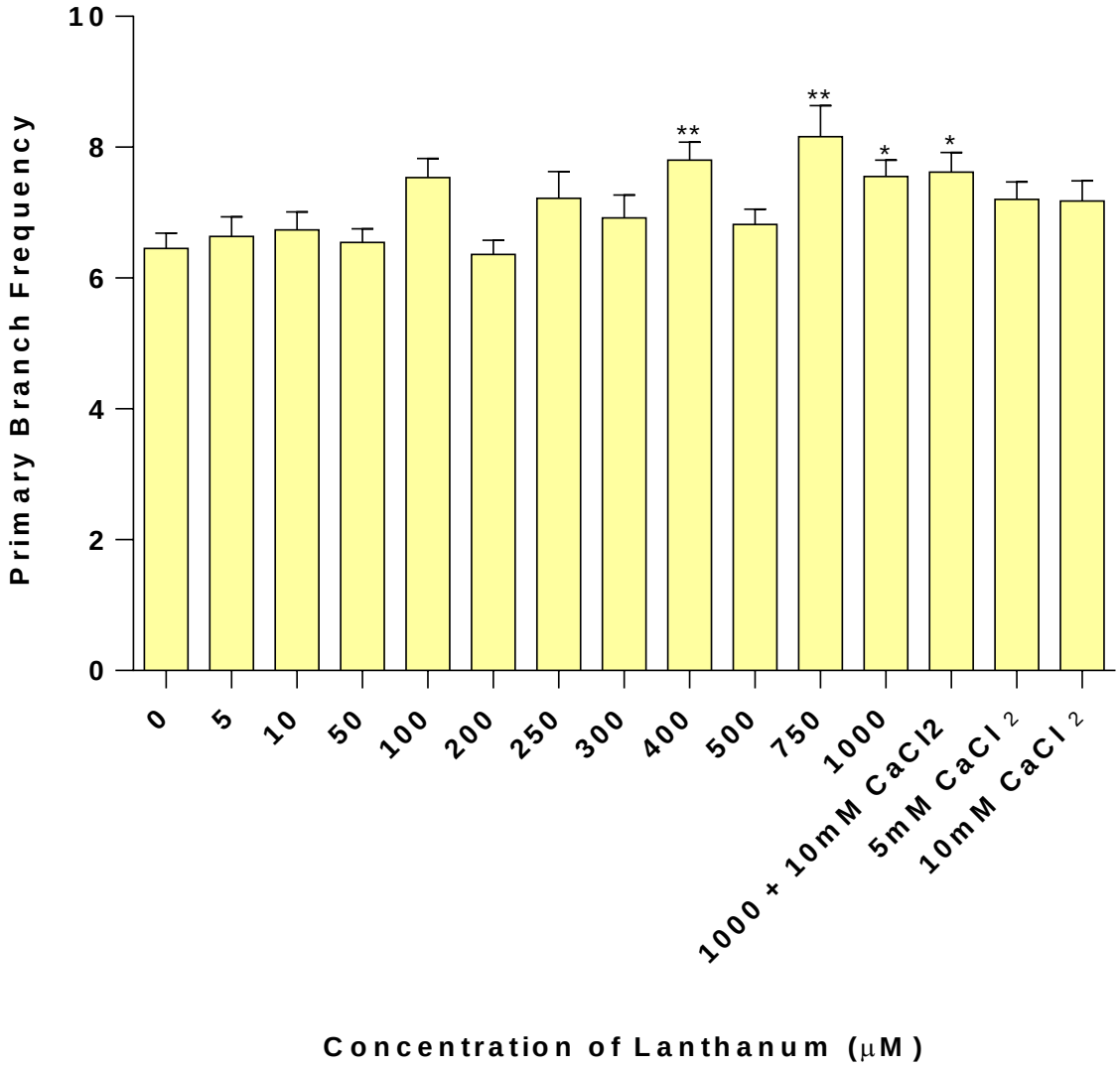

Figure 4.6 - Primary branch frequency of *N. crassa* increased at high concentrations of La^{3+}. Data are mean values ± SEM. Statistical significance was calculated compared to control values. Significance is indicated as follows; $p \leq 0.05$ - *, $p \leq 0.01$ - **, $p \leq 0.001$ - ***, $p \leq 0.0001$ - ****. Statistical analysis revealed that concentrations of La^{3+} 0 µM ≠ 400 µM, 750 µM, 1000 µM, 1000 µM + 10 mM $CaCl_2$ were significantly different ($p<0.05$). See Appendix 1 for statistical analysis and sample sizes.

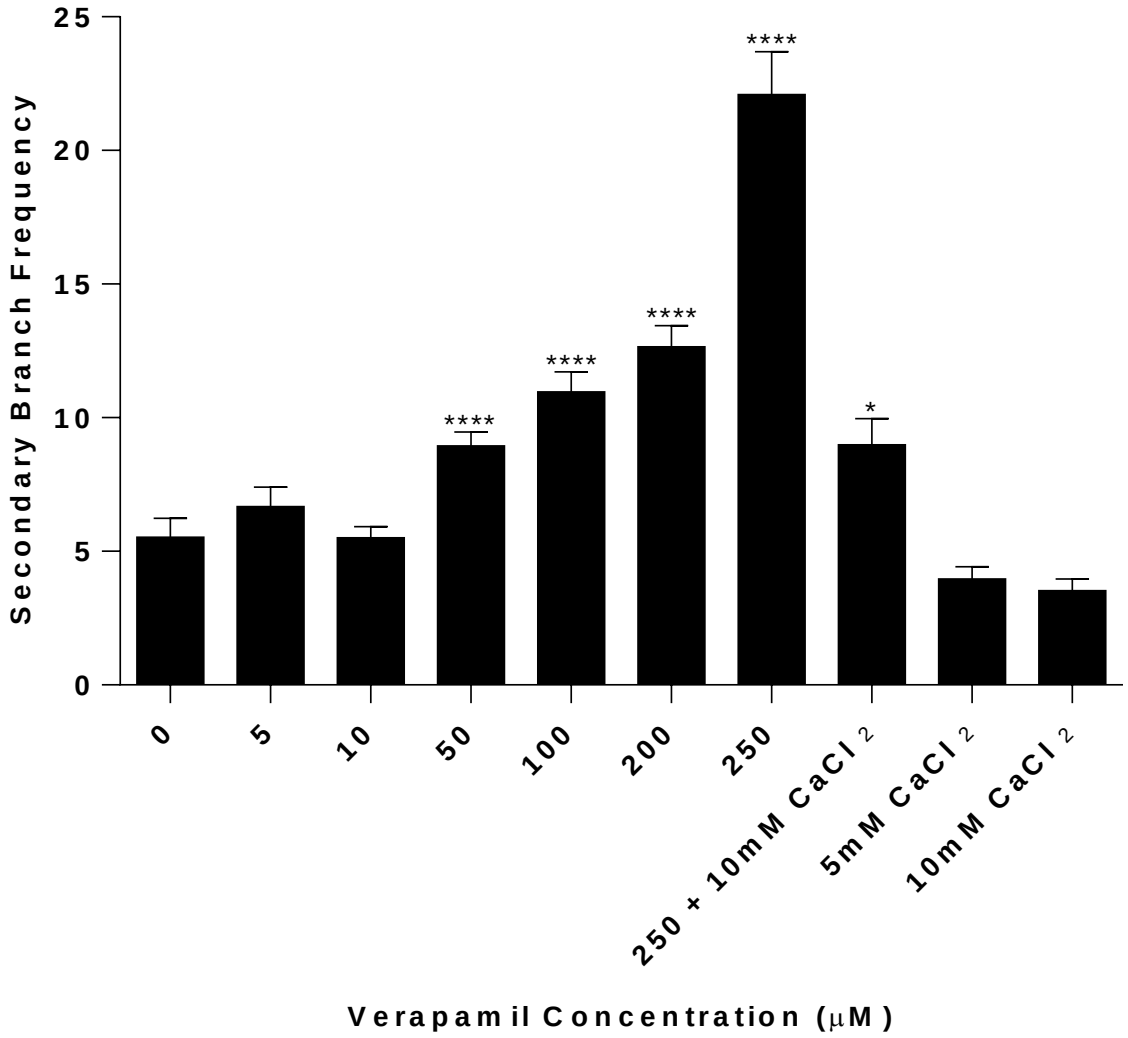

Figure 4.7 - Secondary branch frequency of *N. crassa* increased when the concentration of verapamil increased. Data are mean values ± SEM. Statistical significance was calculated compared to control values. Significance is indicated as follows; $p \leq 0.05$ - *, $p \leq 0.01$ - **, $p \leq 0.001$ - ***, $p \leq 0.0001$ - ****. Statistical analysis revealed that concentrations of verapamil 0 µM ≠ 50 µM, 100 µM, 200 µM, 250 µM, 250 µM + 10mM $CaCl_2$; 5µM ≠ 50 µM, 100 µM, 200 µM, 250 µM; 10 µM ≠ 50 µM, 100 µM, 200 µM, 250 µM; 50 µM ≠ 250 µM; 100 µM ≠ 250 µM; 200 µM ≠ 250 µM + 10 mM $CaCl_2$ and 250 µM ≠ 250 µM + 10 mM $CaCl_2$ were significantly different ($p<0.05$). See Appendix 1 for statistical analysis and sample sizes.

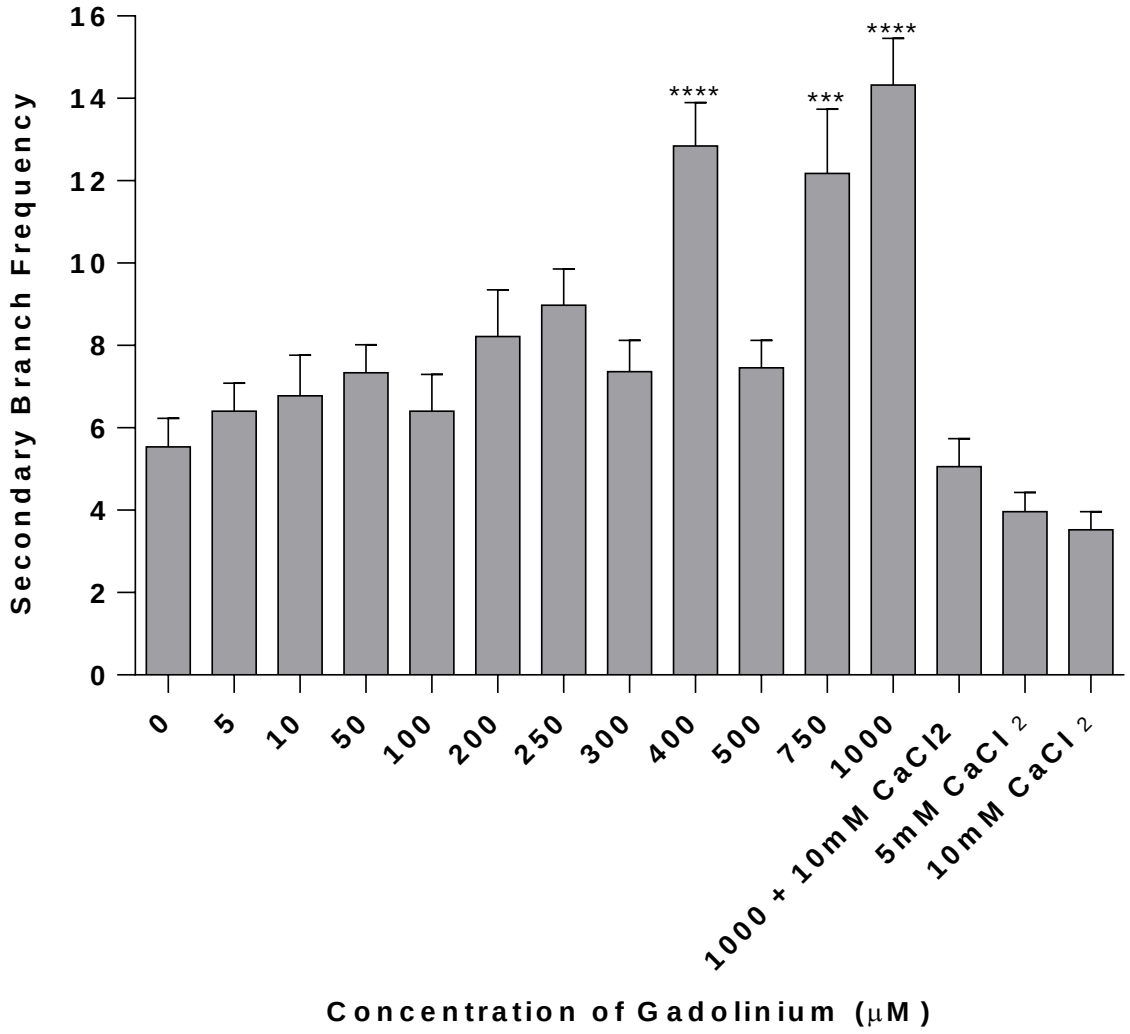

Figure 4.8 - Secondary branch frequency of *N. crassa* generally increased when the concentration of Gd^{3+} increased. Data are mean values ± SEM. Statistical significance was calculated compared to control values. Significance is indicated as follows; $p \leq 0.05$ - *, $p \leq 0.01$ - **, $p \leq 0.001$ - ***, $p \leq 0.0001$ - ****. Statistical analysis revealed that concentrations of Gd^{3+} 0 µM ≠ 250 µM, 400 µM, 750 µM, 1000 µM; 5 µM ≠ 400 µM, 1000 µM; 10 µM ≠ 400 µM, 1000 µM; 50 µM ≠ 400 µM, 1000 µM; 100 µM ≠ 400 µM, 1000 µM; 200 µM ≠ 1000 µM; 250 µM ≠ 1000 µM + 10 mM $CaCl_2$; 300 µM ≠ 1000 µM; 400 µM ≠ 500 µM, 1000 µM + 10 mM $CaCl_2$; 500 µM ≠ 1000 µM; 750 µM ≠ 1000 µM + 10 mM $CaCl_2$; 1000 µM ≠ 1000 µM + 10mM $CaCl_2$ were significantly different ($p<0.05$). See Appendix 1 for statistical analysis and sample sizes.

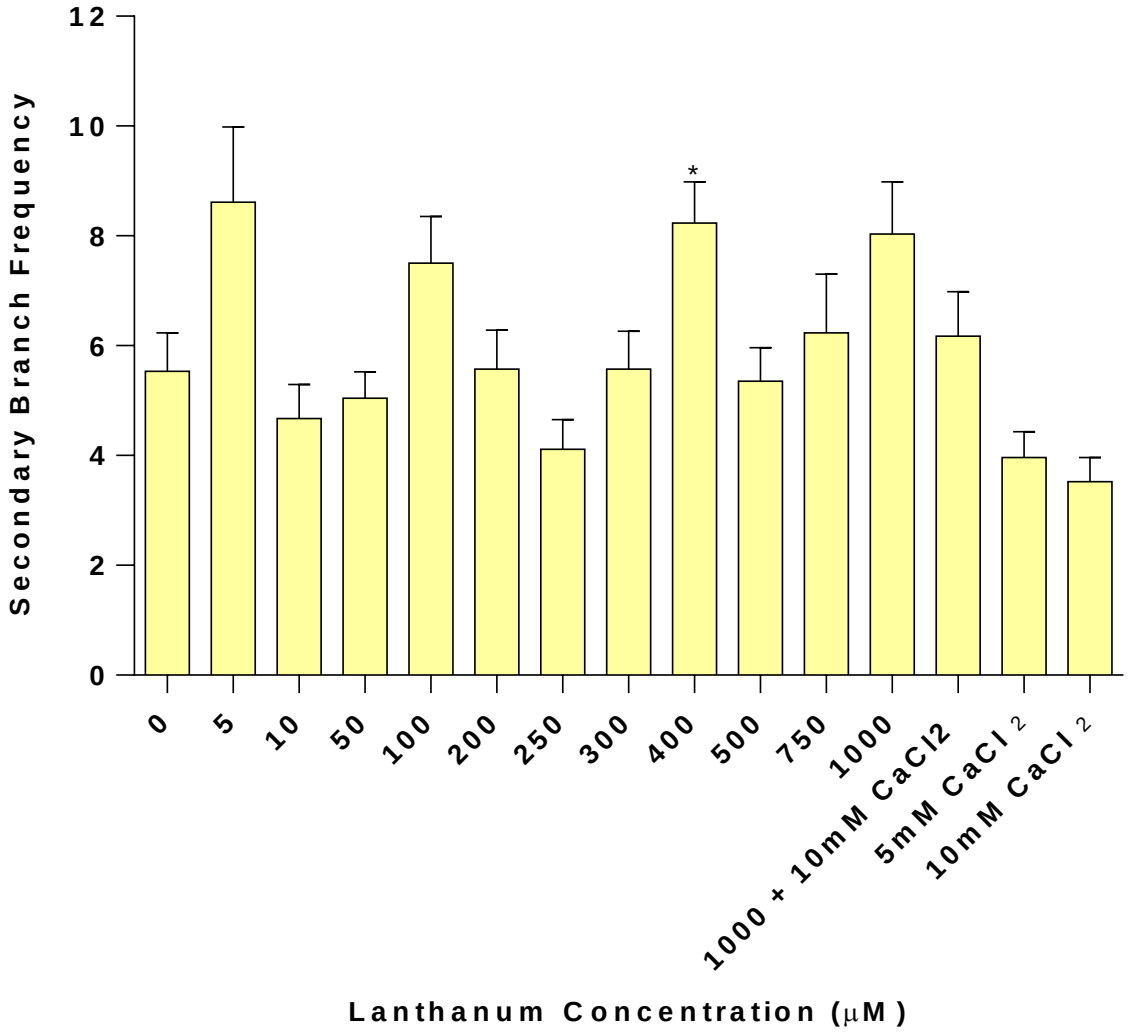

Figure 4.9 - Secondary branch frequency of *N. crassa* did not change when the concentration of La^{3+} increased. Data are mean values ± SEM. Statistical significance was calculated compared to control values. Significance is indicated as follows; $p \leq 0.05$ - *, $p \leq 0.01$ - **, $p \leq 0.001$ - ***, $p \leq 0.0001$ - ****. Statistical analysis revealed that concentrations of La^{3+} 0 µM ≠ 400 µM; 250 µM ≠ 400 µM were significantly different ($p<0.05$). See Appendix 1 for statistical analysis and sample sizes.

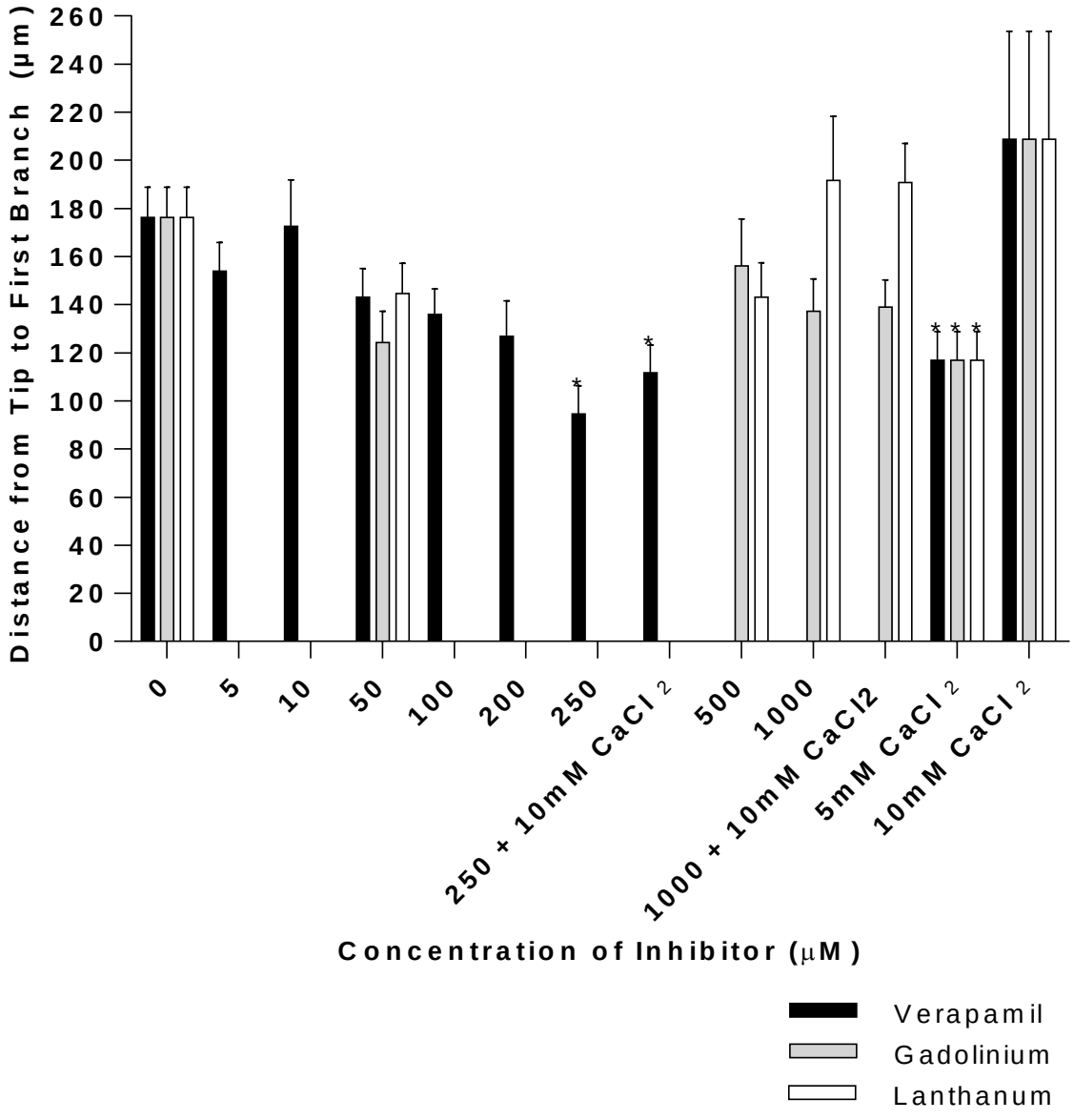

Figure 4.10 – The distance between the tips of hyphae to the first branch in *N. crassa* decreased when the concentration of verapamil increased. Data are mean values ± SEM. The distance did not change with the increase in Gd^{3+} and La^{3+}. Statistical significance was calculated compared to control values. Significance is indicated as follows; p≤0.05 - *, p≤0.01 - **, p≤0.001 - ***, p≤0.0001 - ****. Statistical analysis revealed that concentrations of verapamil 0 µM ≠ 250 µM, 250 µM + 10 mM $CaCl_2$ and the addition of Ca^{2+} 0 ≠ 5 mM $CaCl_2$ were significantly different ($p<0.05$). See Appendix 1 for statistical analysis and sample sizes.

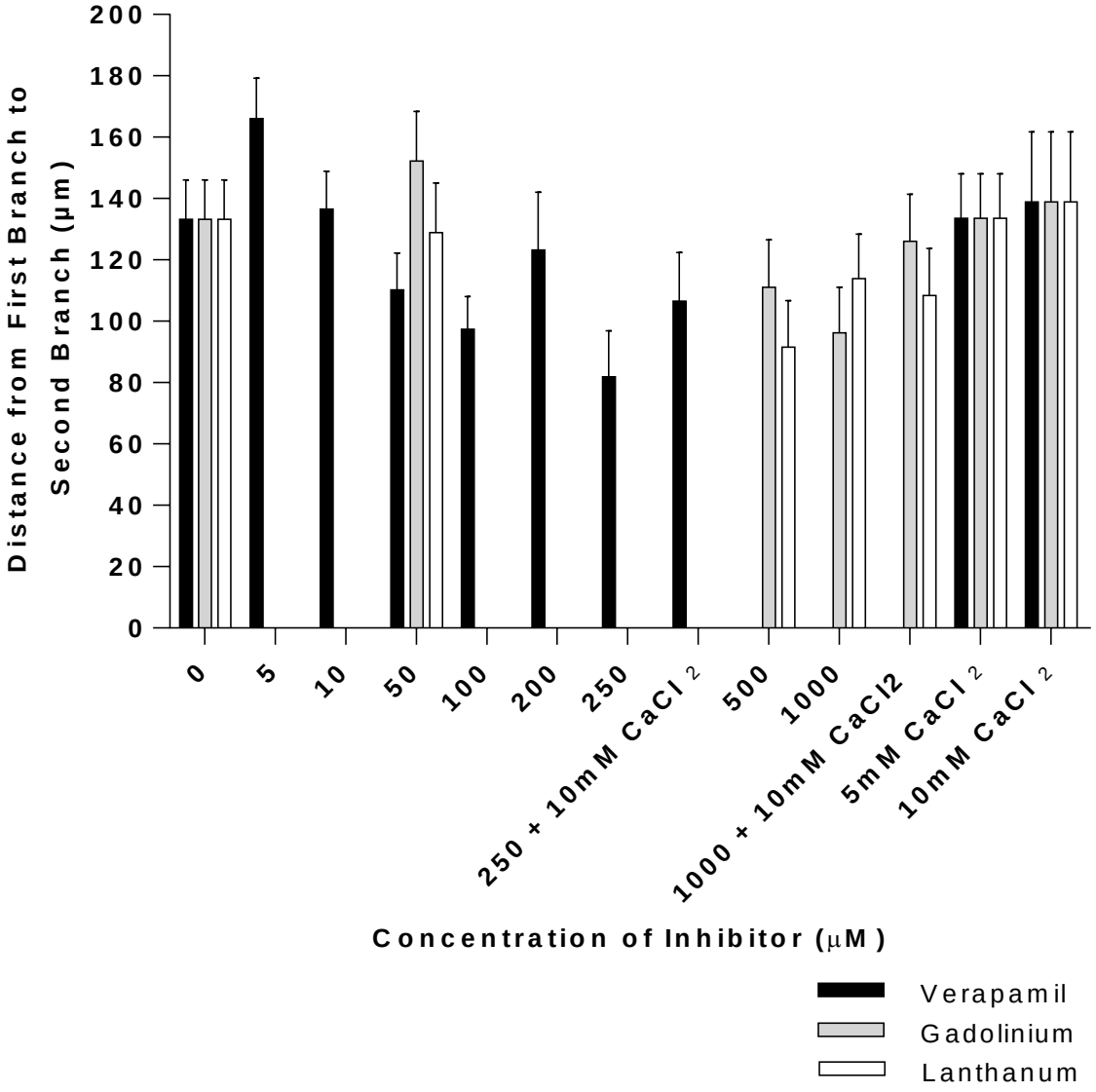

Figure 4.11 – The distance between the first branch and the second branch in *N. crassa* did not change when the concentration of all of the inhibitors increased. Data are mean values ± SEM. Statistical significance was calculated compared to control values. Significance is indicated as follows; $p \leq 0.05$ - *, $p \leq 0.01$ - **, $p \leq 0.001$ - ***, $p \leq 0.0001$ - ****. Statistical analysis revealed that concentrations of verapamil 5 µM ≠ 50 µM, 100 µM, 250 µM were significantly different ($p<0.05$). See Appendix 1 for statistical analysis and sample sizes.

	Average	SD	Range
Hyphal Width (µm)	9	2	6.4-11.8
Time to Bump (minutes)	2.5	1.3	1.5-4
Time to Bud (minutes)	3	1.3	2-4.5
Time to Branch (minutes)	3.5	1.3	2.5-5
Hyphal Growth Rate Before Induction (µm/minute)	14	9	13.6-40
Hyphal Growth Rate After Induction (µm/minute)	25	16	5.1-43.6
Branch Growth Rate (µm/minute)	11	3	9.1-13.6
Distance from Micropipette Tip to Hyphal Trunk (µm)	9	1	7.3-10.9
Distance from Micropipette Tip to Hyphal Tip (µm)	28	4	21.8-30.9
Distance from Micropipette Tip to Hyphal Branch (µm)	65	8	58.2-73.6
Chemotropism of the Hyphal Tip (°)	12	12	0-28

Table 4.1 – Summary of various parameters in the branch inductions on *N. crassa* using 50 µM verapamil present in 1 mM phenylalanine Vogel's solution.

	Average	SD	Range
Hyphal Width (µm)	11	2	9.1-13.6
Time to Bump (minutes)	3	1.3	2-4.5
Time to Bud (minutes)	4	0.9	3.5-5
Time to Branch (minutes)	4.7	0.8	4-5.5
Hyphal Growth Rate Before Induction (µm/minute)	27	13	17.3-50
Hyphal Growth Rate After Induction (µm/minute)	22	3	18.1-25.4
Branch Growth Rate (µm/minute)	8	2	5.5-9.1
Distance from Micropipette Tip to Hyphal Trunk (µm)	12	3	9.1-15.5
Distance from Micropipette Tip to Hyphal Tip (µm)	34	10	21.8-46.4
Distance from Micropipette Tip to Hyphal Branch (µm)	36	36	12.7-77.3
Chemotropism of the Hyphal Tip (˚)	15	14	0-30

Table 4.2 – Summary of various parameters in the branch inductions on *N. crassa* using 500 µM verapamil in 1 mM phenylalanine Vogel's solution.

	Average	SD	Range
Hyphal Width (µm)	10	2	7.1-14.5
Time to Bump (minutes)	2.6	2.8	1-7.5
Time to Bud (minutes)	4.3	3.2	1.5-8.5
Time to Branch (minutes)	6	5	2-13
Hyphal Growth Rate Before Induction (µm/minute)	21	11	10-44.5
Hyphal Growth Rate After Induction (µm/minute)	16	13	4-38.7
Branch Growth Rate (µm/minute)	3	2	0.9-4.5
Distance from Micropipette Tip to Hyphal Trunk (µm)	9	3	5.5-13.6
Distance from Micropipette Tip to Hyphal Tip (µm)	35	7	25.7-45.5
Distance from Micropipette Tip to Hyphal Branch (µm)	15	17	3.6-41.8
Chemotropism of the Hyphal Tip (˚)	-7	15	-36-8

Table 4.3 – Summary of various parameters in the branch inductions on *N. crassa* using 1000 µM Verapamil present in 1 mM phenylalanine Vogel's solution.

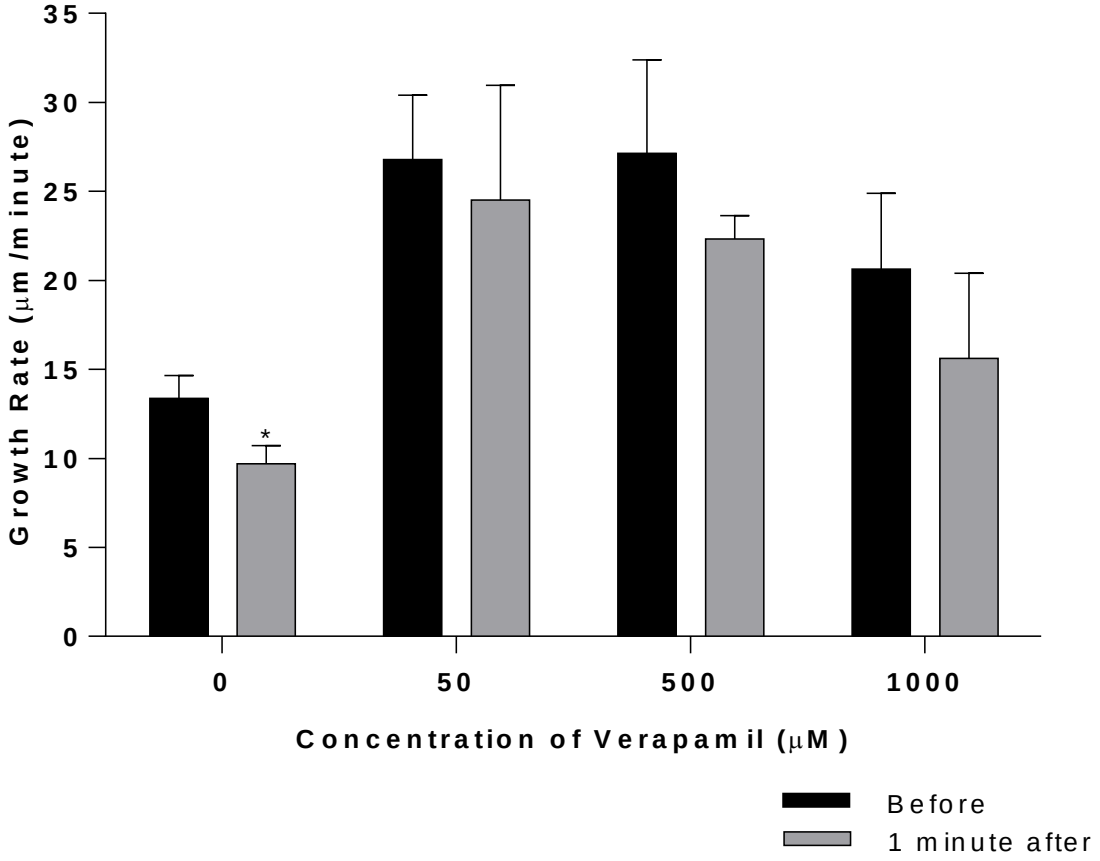

Figure 4.12 - Hyphal growth rates before and after the induction started for verapamil treatments. There was no significant difference between growth rates before and 1 minute after the induction began (see Appendix 1 for t tests).

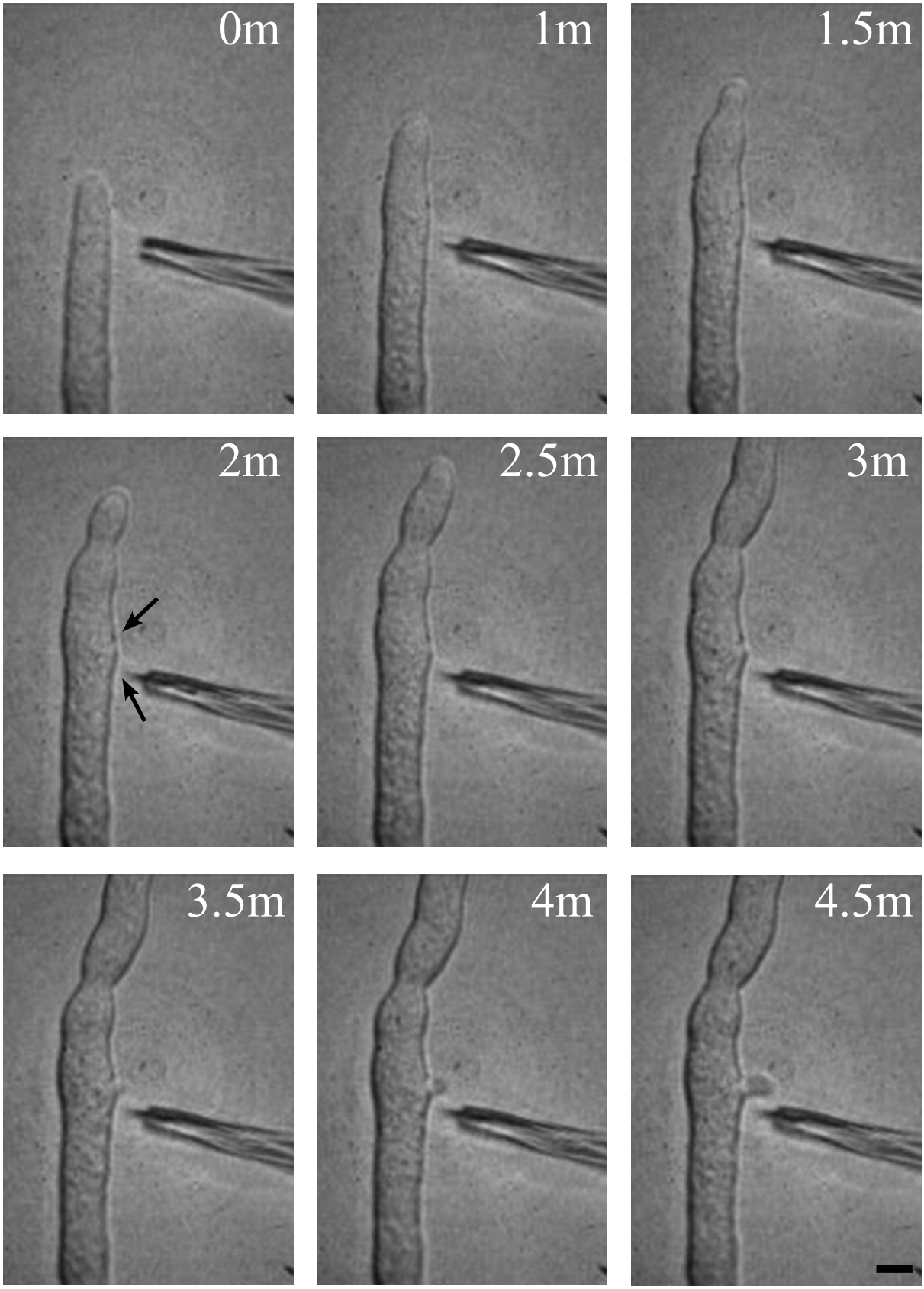

Figure 4.13 – Branch induction in the presence of 500 μM verapamil in Vogel's media with 1mM phenylalanine. The micropipette was positioned next to the hypha 26 μm back from the thyphal tip and 9 μm to the side of the hyphal trunk. The tip initially bulges twice before forming a branch next to the pipette tip. Future branch site is indicated with arrows. Bar=10 μm. Time measured in minutes (m).

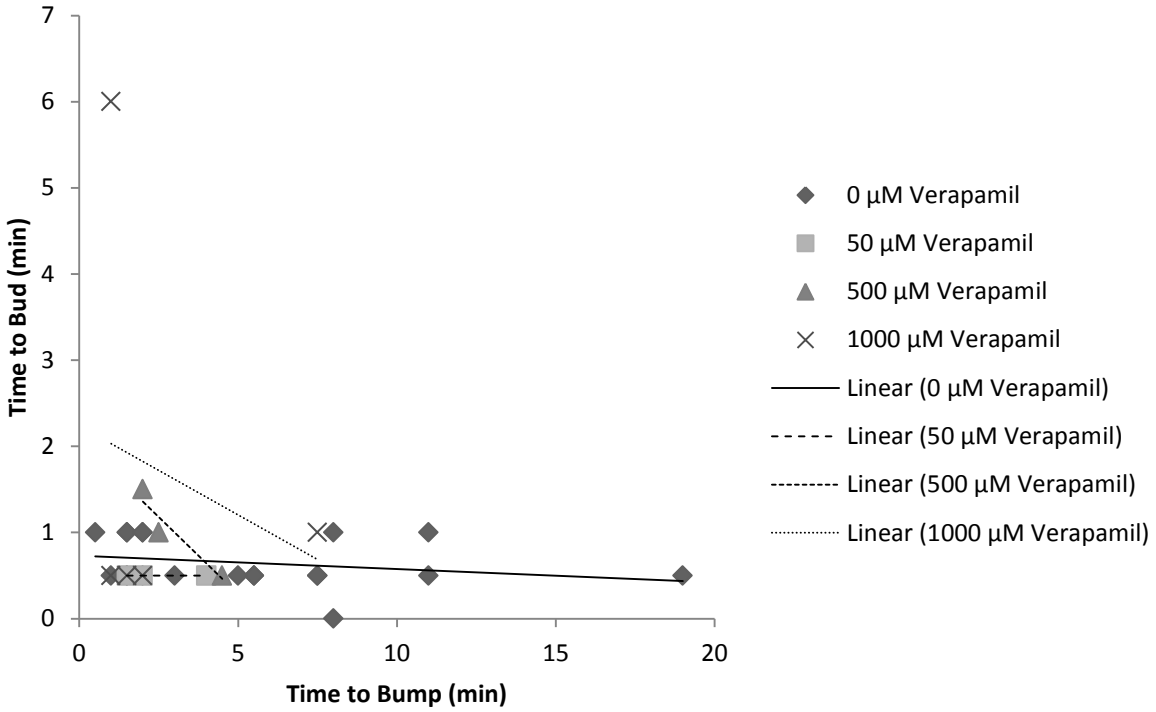

Figure 4.14 – Scatter graph showing the relationship between the time taken for a bump to form and the time taken to form a bud for the successful verapamil inductions (0 µM verapamil n=29 hyphae, r=0.459; 50 µM verapamil n=6 hyphae, r=0; 500 µM verapamil n=6 hyphae, r=-0.945; 1000 µM verapamil n=7 hyphae, r=-0.237).

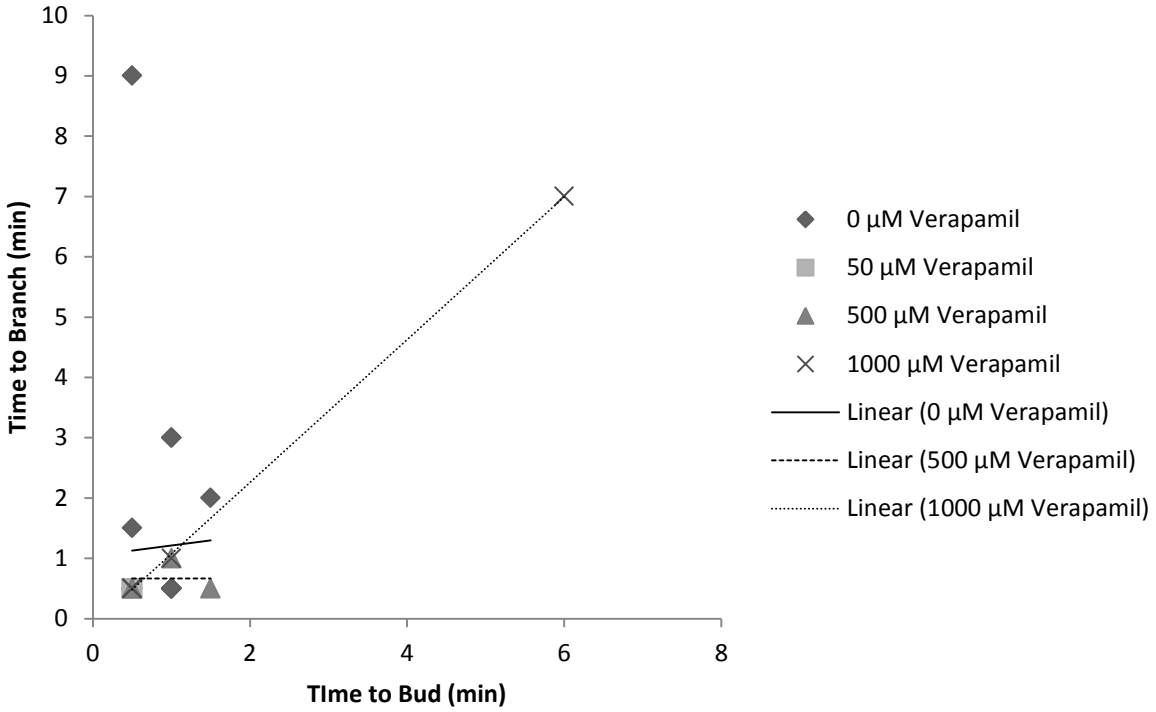

Figure 4.15 – Scatter graph showing the relationship between the time taken to form a bud and the time taken to form a branch for the successful verapamil inductions (0 µM verapamil n=29 hyphae, r=0.027; 50 µM verapamil n=6 hyphae, r=vertical line; 500 µM verapamil n=6 hyphae, r=0; 1000 µM verapamil n=7 hyphae, r=0.999).

Verapamil (μM)	% Branching	% Multiple Branches
0	83	17
50	50	0
500	50	0
1000	71	40

Table 4.4 – The effect of increasing concentration of verapamil in the induction media on branch frequency and multiple branch formation in *N. crassa*. Concentrations of verapamil 0 μM (n=29 hyphae), 50 μM (n=6 hyphae), 500 μM (n=6 hyphae) and 1000 μM (n=7 hyphae).

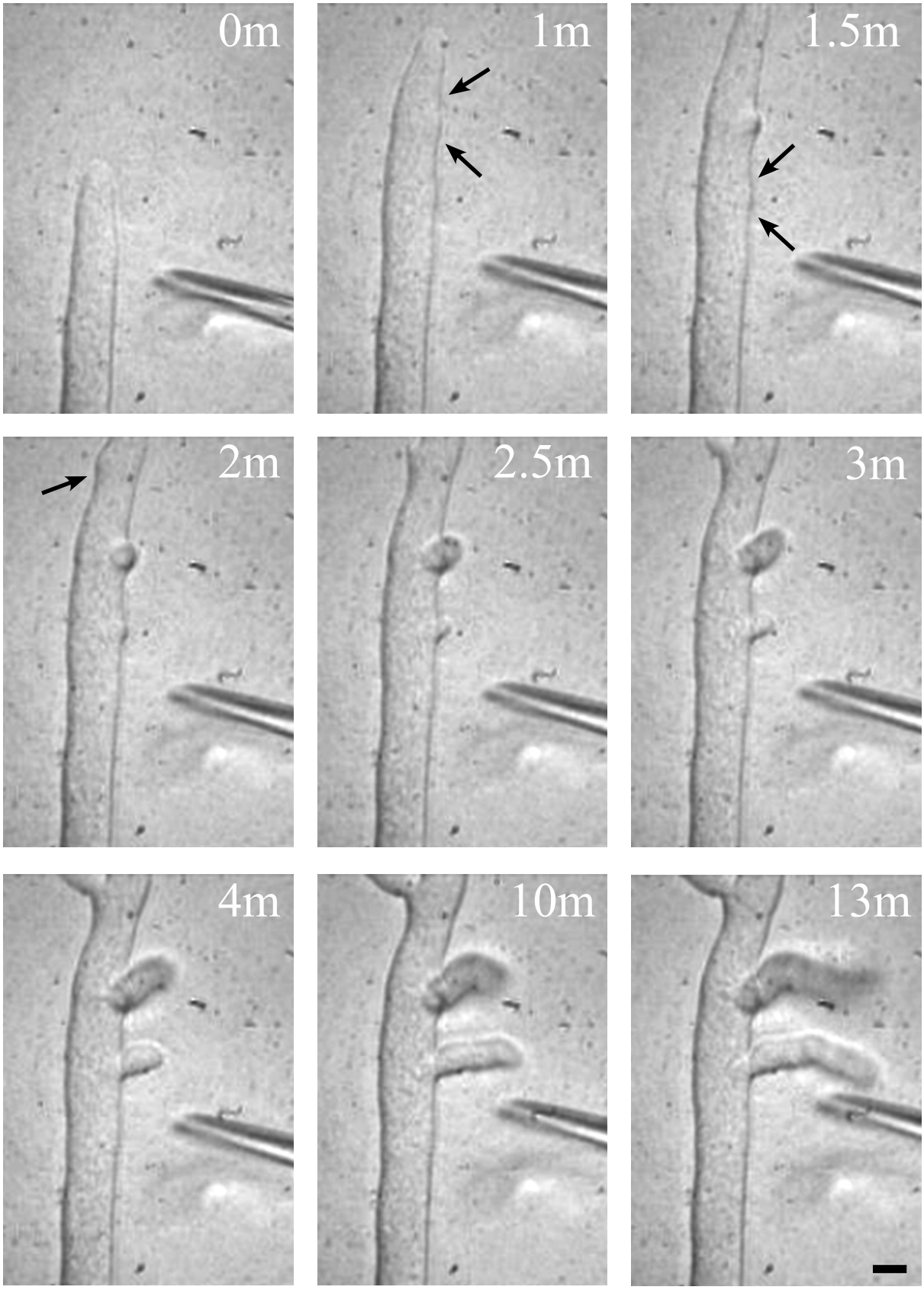

Figure 4.16 – Branch induction in the presence of 1000 μM verapamil in Vogel's media with 1mM phenylalanine. The micropipette was positioned next to the hypha 39 μm back from the hyphal tip and 14 μm to the side of the hyphal trunk. Three branches develop out of the hypha exposed to the inhibitor. Future branch sites are indicated with arrows. Bar = 10 μm. Time measured in minutes (m).

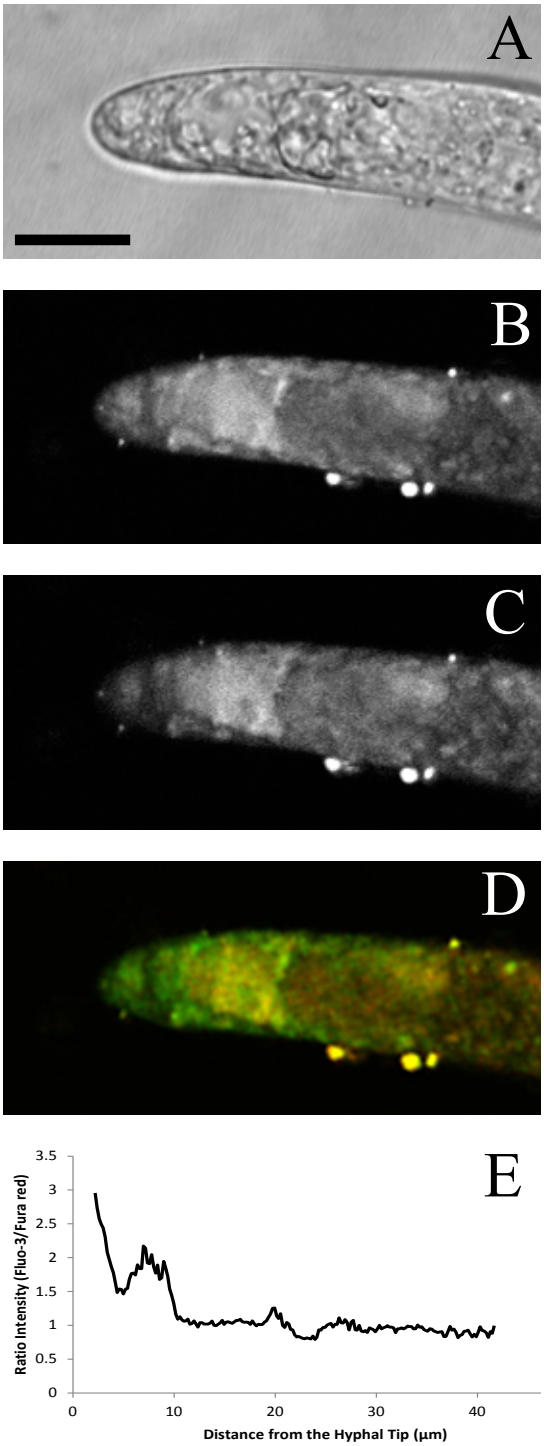

Figure 4.17 - Ca^{2+} levels in a streaming but non-growing hypha of the oomycete *A. bisexualis*. A shows the transmitted light image of the hypha, B shows the fluo-3 fluorescent image of the hypha, C shows the fura red fluorescent image of the hypha, D shows the merged fluorescent image of fluo-3 and fura red, E shows the ratio light intensity of the two dyes showing a tip-high Ca^{2+} gradient. Bar = 10 µm.

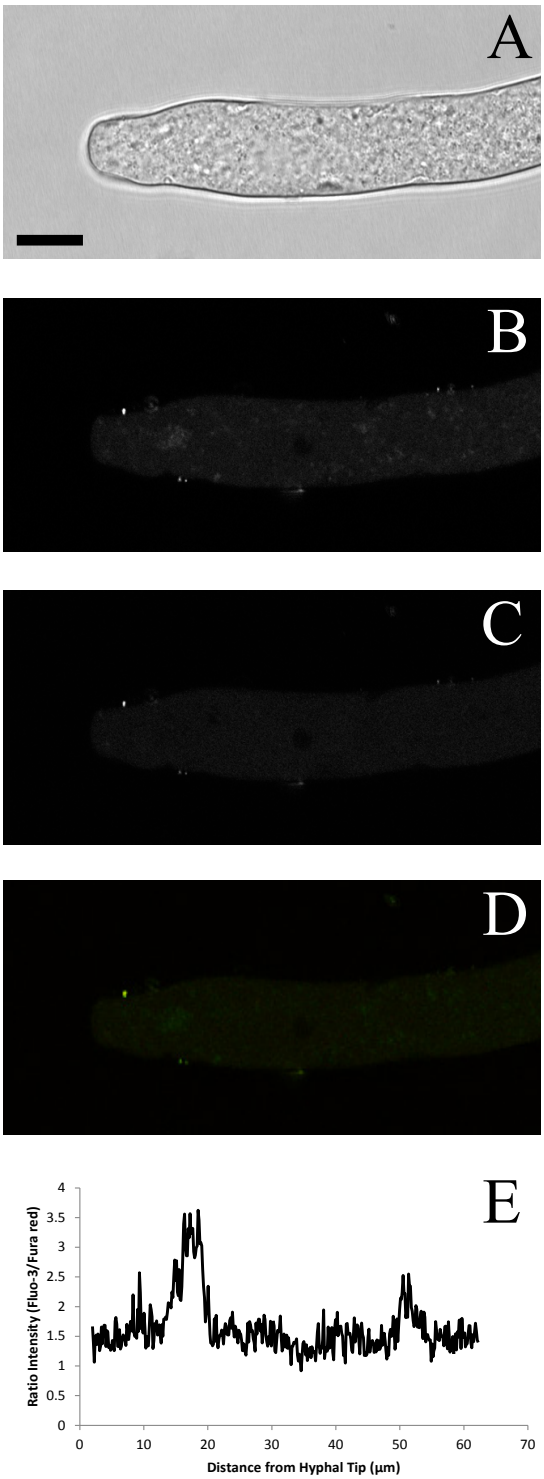

Figure 4.18 - Ca^{2+} levels in a *N. crassa* hypha. A shows the transmitted light image of the hypha, B shows the fluo-3 fluorescent image of the hypha, C shows the fura red fluorescent image of the hypha, D shows the merged fluorescent image of fluo-3 and fura red, E shows the ratio light intensity of the two dyes showing a no tip-high Ca^{2+} gradient. Bar = 10 µm.

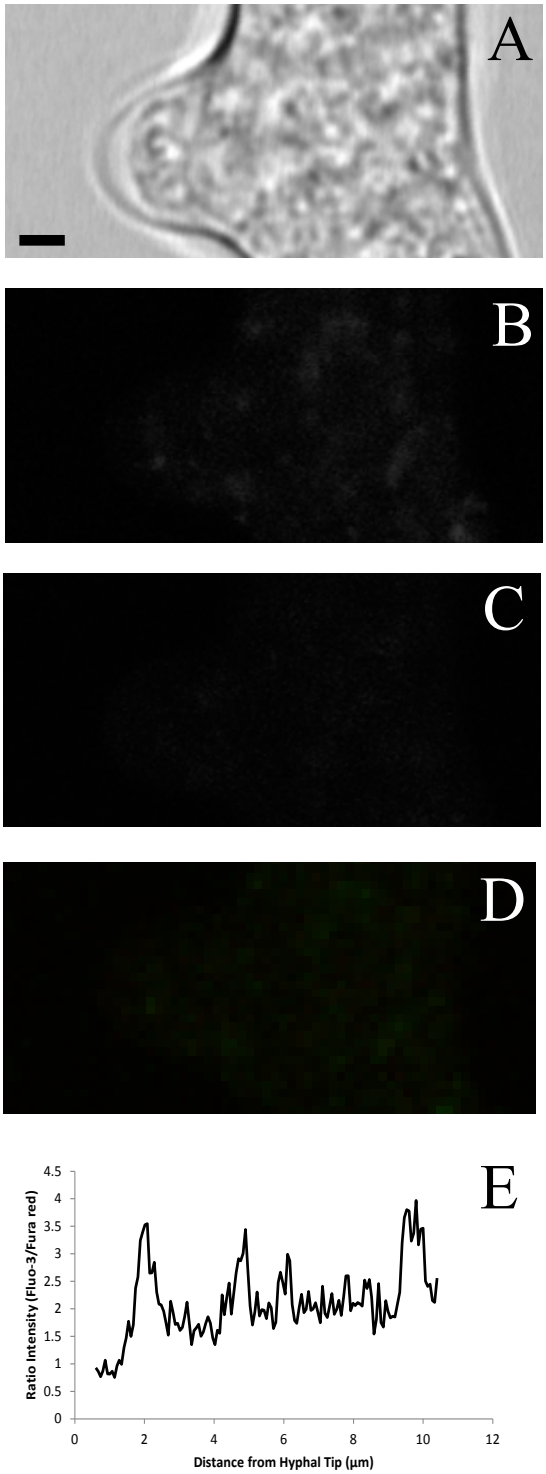

Figure 4.19 - Ca^{2+} levels in a hyphal branch of *N. crassa*. A shows the transmitted light image of the hypha, B shows the fluo-3 fluorescent image of the hypha, C shows the fura red fluorescent image of the hypha, D shows the merged fluorescent image of fluo-3 and fura red, E shows the ratio light intensity of the two dyes showing no tip high Ca^{2+} gradient. Bar = 10 µm.

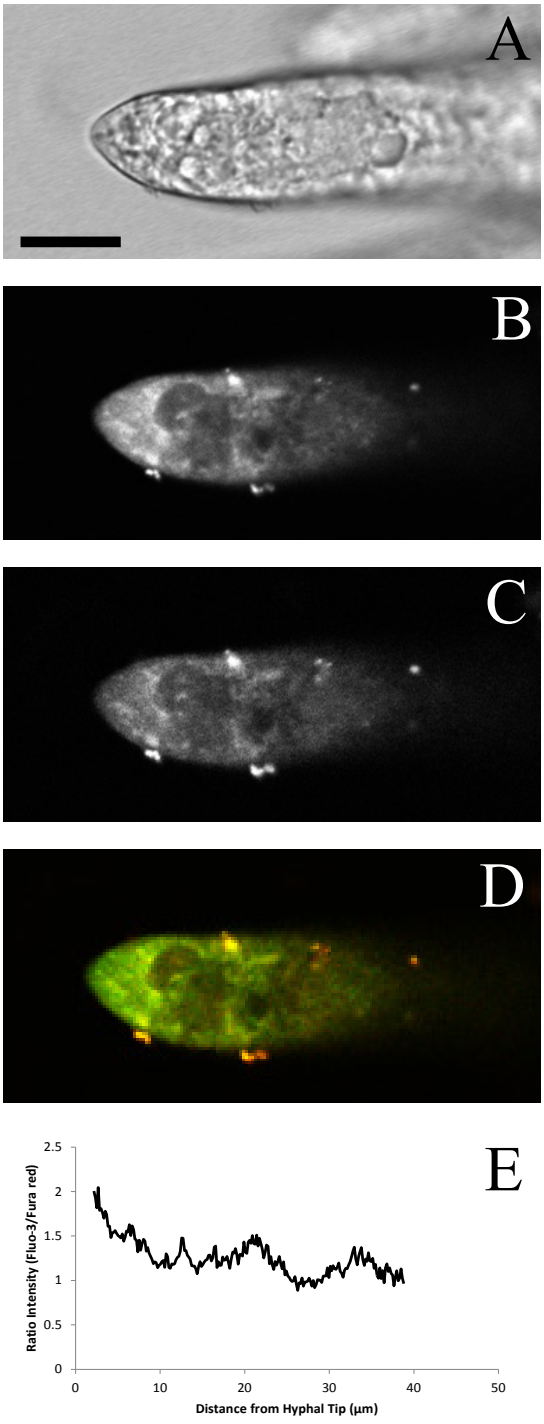

Figure 4.20 - Ca^{2+} levels in a non-growing, streaming hypha of the oomycete *A. bisexualis* exposed to 200 µM verapamil. A shows the transmitted light image of the hypha, B shows the fluo-3 fluorescent image of the hypha, C shows the fura red fluorescent image of the hypha, D shows the merged fluorescent image of fluo-3 and fura red, E shows the ratio light intensity of the two dyes showing a tip-high Ca^{2+} gradient. Bar = 10 µm.

4.4 Discussion

One mechanism that has been proposed to explain the pattern of lateral branching in filamentous microorganisms is that Ca^{2+} is involved in maintaining the dominance of the apical region of the hyphae given that they maintain a tip-high gradient of Ca^{2+}. The inhibition of branch formation would occur where the Ca^{2+} gradient is high (i.e. near the hyphal tip) then when the Ca^{2+} concentration drops below a certain level, branch formation would tend to occur. However, other groups have suggested that Ca^{2+} is involved in the signalling events that may induce branch formation and therefore instead of inhibiting branch development, it would actually promote it. The results from this current investigation support the idea that Ca^{2+} plays a role in apical dominance of hyphal tips by inhibiting the formation of branches in the very apical region of hyphae as disruption to the tip-high Ca^{2+} gradient results in branches forming closer to the hyphal tip.

4.4.1 Mycelial Morphology is Affected by the Addition of Ca^{2+} Channel Inhibitors to Growth Media

The results for the whole plate inhibition of Ca^{2+} channels in this study can be compared with the results from other studies on filamentous microorganisms. Studies on *A. bisexualis* revealed that verapamil concentrations above 10 μM resulted in a significant increase in the number of branches occurring (Morris et al., 2011). This was in a dose-response manner increasing from an average of 1.5 branches per 1000 μm of hypha to an average of 12 branches at 1 mM. When 10 mM $CaCl_2$ was added along with 1 mM verapamil the number of branches was not significantly different to the control. The distance from the tip to the first branch decreased from the control with the addition of 500 μM verapamil. The addition of Gd^{3+} and La^{3+} also resulted in a significant increase in the number of branches at concentrations above 100 μM but when the concentration of La^{3+} and Gd^{3+} increased to 1 mM, branching was inhibited in the former and was not significantly different from the control in the latter (Morris et al., 2011). This investigation revealed a similar response in *N. crassa* with work conducted by Dicker and Turian (1990) where verapamil increases the hyphal branch frequency.

In this study, verapamil increased the primary branch frequency in a dose response manner. The addition of 10 mM $CaCl_2$ to 250 μM verapamil was still significantly higher compared to the addition of no inhibitor. The secondary branch frequency increased in a dose response manner and the addition of 10 mM $CaCl_2$ was still significantly higher than the control. The effects on branch frequency are reflected in a decrease in the radius of the colony in a dose response manner. The addition of 10 mM $CaCl_2$ increased the colony radius which was not significantly different to the control. The ability for an increase in external Ca^{2+} to reverse the effects of verapamil on the colony radius suggests that the inhibitor is having an effect on Ca^{2+} dynamics within hyphae by blocking Ca^{2+} channels. However, since the branch frequency was still significantly higher than in the control and the distance to the first branch was significantly shorter than the control; this suggests that the external Ca^{2+} concentration was not high enough to fully reverse the effects of the inhibitor on internal Ca^{2+} dynamics. Verapamil was the only Ca^{2+} channel inhibitor to have a significant effect on the distance from the tip the first branch. When no inhibitor was added, the distance from the tip to the first branch was 176 μm which significantly decreased to 95 μm with the addition of 250 μm verapamil. The addition of 10 mM $CaCl_2$ to 250 μM verapamil also resulted in a significantly shorter distance to the first branch. This could suggest that the inhibitor is causing a diminished Ca^{2+} gradient and therefore is enabling the development of lateral branches closer to the hyphal tip. Since the addition of 10 mM $CaCl_2$ with the inhibitor had branches forming significantly closer to the hyphal tip than the control, this suggests that the effect verapamil has on the Ca^{2+} dynamics could not be re-established with the presence of that concentration of external Ca^{2+} and that perhaps higher concentrations are required to reverse the effects.

The addition of Gd^{3+} increased the primary and secondary branch frequency compared to the control which is reflected in a decrease in the colony radius. The effect of the inhibitor was reversed to control levels with the addition of external Ca^{2+} which suggests that the inhibitors are blocking Ca^{2+} channels. There was no effect on the distance to the first branch which may be because the channels that Gd^{3+} was blocking do not play an important role in establishing the tip-high Ca^{2+} gradient.

The addition of La^{3+} increased the primary branch frequency but had no effect on the secondary branch frequency compared to the control. A decreased colony radius was observed when the mycelia were exposed to La^{3+}. The addition of external Ca^{2+} reversed the primary branch frequency and colony radius to control levels suggesting that La^{3+} was

affecting Ca^{2+} channels. There was no effect on the distance to the first branch suggesting that these channels may not have such a marked effect on the Ca^{2+} gradient, if indeed the Ca^{2+} gradient is inhibiting branching, and therefore branches are still inhibited close to the hyphal tips.

The addition of 5 mM $CaCl_2$ significantly decreased the distance from the hyphal tip to the first branch but the addition of 10 mM $CaCl_2$ had no significant effect. The reason for this effect is unclear, although this may be a result of a small sample size. The addition of $CaCl_2$ at concentrations of both 5 mM and 10 mM had no significant effect on any other aspect of mycelial morphology measured.

As seen in Figure 4.2, when the concentration of verapamil was increased in the growth media, the colony became more compacted with more branches forming within a smaller area (forming closer to the tip). This suggests that, since verapamil is changing the dynamics of Ca^{2+} within the cell, the tip-high gradient of Ca^{2+} was being disrupted. Therefore it suggests that the Ca^{2+} gradient promotes apical dominance within hyphal tips and promotes the maximal extension rate of the growing tip. The ability for the voltage-gated Ca^{2+} channel inhibitor to have the strongest effect on the morphology of hyphal colonies could be a result of there being a voltage gated channel present that is involved in establishing the tip-high Ca^{2+} gradient or could be a result of verapamil inhibiting other types of channels which are involved in establishing the tip-high Ca^{2+} gradient as verapamil has been shown to inhibit K^+ channels in plant cells (Ketchum and Poole, 1991).

The mechanism underlying the effect that these Ca^{2+} channel inhibitors are having on the branching pattern in *N. crassa* poses an interesting question. This is because tip growth in *N. crassa* does not require a net influx of Ca^{2+} at the tip as mentioned earlier. Instead, Ca^{2+} is released and sequestered from Ca^{2+} storing organelles in order to generate a tip-high gradient of Ca^{2+}. Therefore if this is the case, the inhibitors might be taken up into the hyphae and could be blocking the release of Ca^{2+} from the internal stores and resulting in the lowering of the internal Ca^{2+} concentration. This could then result in the development of more branches that are closer to the hyphal tips because the mechanism of maintaining apical dominance has been disturbed. As the concentration of verapamil was increased, the growth rate of the hyphae slowed, resulting in a smaller colony radius. Ca^{2+} must still be present in the cytoplasm for the hypha to continue growing, however the hyphae are not reaching maximal extension rates as the tip-high gradient is not pronounced.

4.4.2 Branch Development in *N. crassa* is Affected by the Local Application of Verapamil

The local application of Ca^{2+} channel inhibitors on *A. bisexualis* has been investigated previously by Morris et al. (2011). In that study, the local addition of verapamil resulted in bumps formed for 90% of the hypha induced with 67% of these forming branches (n=12) and multiple branches occurring for half of these inductions compared with 5% for the control inductions (n=22). The time between bump formation and branch formation was not significantly different to the control. The chemotropic response was not significantly different to the control. The addition of Gd^{3+} at concentrations up to 10 μM and La^{3+} of concentrations up to 500 μM had no effect on bump and branch frequency. The time taken for a bump to form significantly decreased when Gd^{3+} was added. There was a significant decrease in the time for a bump to form a branch for both Gd^{3+} and La^{3+}. The chemotropic response significantly increased the degree of bending with the addition of Gd^{3+} and La^{3+}. The ability for the local application of verapamil to have different effects on branch formation could possibly be explained by different branching mechanisms, with one mechanism sensitive to the presence of verapamil and the other mechanism not. The time taken when bumps and branches did form was not different to the control inductions. Since verapamil results in the production of more bumps when locally applied it has been suggested that its target may be involved in the early events of branch formation. The role of channels that verapamil blocks may be to determine the site of the new branch or when the branch will form. The time for the new branch site to transition from a bump to a branch was decreased when Gd^{3+} and La^{3+} were applied locally therefore the targets of these inhibitors may have their own role in the process of branch formation. As a result of Gd^{3+} and La^{3+} decreasing the time for bump/branches to form, it has been suggested that their targets are involved in the process of branch development. The results from the local application of Ca^{2+} channel inhibitors suggest that Ca^{2+} influx is not necessary for the formation of branches in *A. bisexualis* and to the contrary, may actually inhibit the formation of branches. This is based on the ability of verapamil to increase the number of bumps and branches produced and the reduction of the time taken for the bumps to form branches when the hypha is exposed to La^{3+} and Gd^{3+}. This supports the apical dominance theory of the role Ca^{2+} plays in hyphal dynamics (Morris et al., 2011).

In this study, an increase in the concentration of verapamil present in the induction solution caused a response where the more rapidly the hyphae took to form a bump, the longer it took for a bud to form. As the verapamil concentration was increased, this effect became stronger. It went from having a slight negative relationship with no inhibitor to having a strong negative correlation with 1000 μM verapamil. As the time to bump increased, the time to bud decreased as the concentration of verapamil increased. The longer it took the hypha to form a bump, the less time it took for the bump to transition into a bud. Also the faster it took for a bud to form, the faster it took for a branch to form with an increase in the concentration of verapamil in the induction solution. It went from having a weak positive relationship with no inhibitor to having a strong positive correlation with 1000 μM verapamil. As the time to bud increased, the time for the bud to transition into a branch increased as the concentration of verapamil increased. The longer it took for a bud to form, the longer it took for the bud to transition into a branch. These results suggest that verapamil was having an effect on the transition between bump and bud stages. The consistency in the aperture of the micropipette and similar distances with the positioning of the micropipette suggests that all the hyphae were exposed to the same concentration of the inhibitor. As the concentration of verapamil increased, the chemotropic response changed from bending towards the micropipette with no verapamil to bending away from the micropipette with 1000 μM verapamil. This response could be the hyphal tip trying to avoid the presence of the inhibitor which could have a detrimental effect to tip growth.

The local application of verapamil enabled comparison between the developments of branches as the concentration increased. When 0 μM verapamil was added, a success rate of 83% with branches forming was observed (n=29 hyphae). Of those hyphae that formed branches 17% (n=24 hyphae) formed multiple branches. When 50 μM verapamil was added to the induction solution, 50% of the hyphae formed branches, with none forming multiple branches (n=6 hyphae). The addition of 500 μM verapamil resulted in a success rate of branches forming in 50% of trials (n=6 hyphae) with none of these forming multiple branches. The addition of 1000 μM verapamil resulted in a success rate of branches forming in 71% of trials (n=7 hyphae) with multiple branches forming in 40% of these trials (n=5 hyphae). From this, it appears that an increase in verapamil in the induction solution resulted in an increase in the number of hyphae that formed multiple branches. However, the small sample size should be noted. When verapamil was added to the induction solution with *A. bisexualis* multiple branches formed for some trials (Morris et al., 2011) which was also

observed in this study with *N. crassa*. In some cases bumps did not form into branches in *A. bisexualis*; this was not seen in *N. crassa*.

The increase in multiple branches forming in response to the local application of 1000 μM verapamil compared with the control corresponded with what was seen with the addition of verapamil in the whole plate experiments increasing the frequency of branches. However, the addition of 50 μM and 500 μM verapamil resulted in no multiple branches forming, unlike in the control. As a result of the small sample sizes of these treatments it is difficult to say how relevant the increase in multiple branch formation with the addition of 1000 μM verapamil may be. The fact that verapamil increased the number of branches formed per hypha and had an effect on the transition between bump and bud stages suggests that it may be having an effect on the early stages of branch formation. It is possible that the target of verapamil may play a role in where or when a branch will form.

4.4.3 Ca^{2+} Imaging in *N. crassa* and *A. bisexualis*

The ability to measure intracellular Ca^{2+} in living hyphal organisms has been difficult and is likely to be part of the reason why the role of Ca^{2+} signalling is not fully understood in hyphal growth and morphology (Nelson et al., 2004). Dye loading and sequestering into organelles have been major hurdles in imaging cytoplasmic Ca^{2+} the past (Nair et al., 2011). There have been many techniques developed for loading dyes inside cells in the past and modifications to the dyes to keep them inside the cells. These methods include microinjection, electroporation, AM dye loading and the transformation of hyphae for Ca^{2+} imaging. The effect that the dyes have inside the cells, in terms of altering internal regulatory mechanisms must also be considered when imaging using dyes that bind ions.

The use of ratio imaging is important for Ca^{2+} imaging in the cytoplasm as it provides accurate spatial definition (Camacho et al., 2000). Ratio imaging has been used previously to image the tip high Ca^{2+} gradient in *N. crassa* (Silverman-Gavrila and Lew, 2000). The ratio imaging used in this study involved one dye that had a single excitation wavelength and increased its emission with the increase of Ca^{2+}, fluo-3 and another dye that is excited by the same wavelength but emits light at a different wavelength. This second dye fluoresces brighter in the absence of Ca^{2+}, fura red (Nair et al., 2011).

In this study, a tip-high gradient of Ca^{2+} was observed in *A. bisexualis*, however these hyphae were not growing but the cytoplasm was streaming. There was no tip-high gradient observed in *N. crassa* however Ca^{2+} could be seen sequestered into vesicles present within the hypha. Ca^{2+} was observed in a branch of *N. crassa* where Ca^{2+} could be seen sequestered into organelles. When hyphae of *A. bisexualis* were exposed to 200 μM verapamil, a tip-high gradient of Ca^{2+} was seen which would be consistent with what was seen in the whole plate experiments where the gradient would not be fully be diminished. Based on the relatively healthy appearance of this hypha, the fact that this gradient was present suggests that the hypha may have temporarily stopped growing and the Ca^{2+} had not dissipated fully or that the hypha was about to start growing again.

Given the transmitted light images, the health of the hyphae in the Ca^{2+} imaging experiments could be questioned. This could be a result of multiple factors. Firstly, there is always the potential in imaging cells that the dye is having a negative effect on the internal dynamics and therefore the status of the cell's health. Another reason could be that the hyphae were not left in an intermediary solution prior to adding the dye and therefore were not able to fully recover normal growth rates. The colony went from growing on agar, to being placed into the dye solution. The solution that the dye was made up in may not have been favoured by the hypha therefore in the future different solutions could be trialled to see if the hyphae look healthier. Also the washing steps used to remove the dye could be having negative effects on the health of the hypha resulting in a stress response or the death of the hyphae.

The lack of dye taken up by hyphae of both species could be a sign that they were not healthy or alive. Another reason could be that the concentration of the dyes was not high enough for imaging purposes. Future research could optimise the imaging process using these dyes. Investigations into alternative solutions that the dyes are made up in would be worthwhile in determining a solution that enables healthier mycelia. As discussed earlier, the development of hyphal organisms expressing aequorin could be used as another non-invasive alternative for investigating Ca^{2+} in hyphal organisms with the possibility of little disruption to normal growth.

This study supports ideas suggested previously of the role of Ca^{2+} in regulating apical dominance of hyphal tips and therefore in regulating tip growth and branching events in hyphal organisms, determining the morphology of the colonies. In Chapter 5, the role of F-

actin was investigated to determine the role it has in hyphal branching. Ca^{2+} is known to affect the dynamics of F-actin.

Chapter 5
The Role of the Cytoskeleton and Signalling Proteins in Hyphal Branch Formation

5.1 Introduction

The aim of this chapter was to investigate the possible role of F-actin in establishing polarity as lateral branches form in the filamentous fungus *N. crassa*. F-actin, a cytoskeletal protein, was imaged in live cells using the genetically modified strain Lifeact. This strain has a fluorescently tagged ABP that binds to F-actin that allows visualisation of actin in its dynamic state inside these cells. Signalling Rho GTPase proteins were also investigated to see if there was a change in the levels of these proteins as the branch frequency increases in response to the Ca^{2+} channel inhibitor verapamil.

5.1.1 Actin Imaging Methods

The distribution of actin imaged in tip-growing cells has shown a lot of variety in the past. One possible reason for this difference may be as a result of the different methods of fixing and labelling actin (Geitmann and Emons, 2000). The patterns observed in fungal cells of actin are dependent on a number of factors including the species being imaged along with the method which is being used for actin preservation and visualisation of the F-actin (Walker and Garrill, 2006). The main methods used to visualise actin in hyphal organisms have been through the use of fluorochrome-labelled phalloidin and anti-actin antibodies (Heath et al., 2000).

Preservation of the actin cytoskeleton prior to fluorescent labelling involves the use of chemical or rapid freeze fixation. This means that an assumption is made that the distribution matches that of living fungi (Yu et al., 2004). Commonly used fixatives are aldehydes as they

have the ability to cross-link proteins. Glutaraldehyde has proven to be the best fixative as it is the best at crosslinking proteins. This is because it has two functioning aldehyde groups meaning that it is capable of rapidly interacting with a number of amino acids. Although this fixative autofluoresces resulting in poor contrast when imaging (Glauert and Lewis, 1998). Formaldehyde is another fixative that has been used to preserve the cellular structure as it is better at entering tissue and does not autofluoresce, unlike glutaraldehyde. However formaldehyde is not as good at crosslinking proteins because it only has one aldehyde group and as a result of this only forms a smaller number of cross-links therefore making it not as stable. Combinations of both these fixatives results in a compromise between good preservation of structure and contrast in the images. This may not provide a full picture of the actual status in the cell, as actin imaging using chemical fixation does not reveal the spatial and temporal dynamics occurring in growing hyphae (Yu et al., 2004).

The use of fluorescent proteins has been used extensively for imaging proteins inside living cells, displaying their localisation, motility and interactions (Merzlyak et al., 2007). Fluorescently tagged ABPs are a recent development in the field of actin imaging in filamentous fungi these enable live cell imaging of actin dynamics in *N. crassa* (Berepiki et al., 2010). Lifeact is a 17-amino acid peptide which is derived from the N-terminus of ABP140, an ABP from *Saccharomyces cerevisiae* (Riedl et al., 2008). ABP140 is a 140 kDa protein that colocalises with actin patches and cables in intact cells. The absence of ABP140 from cells does not negatively affect the cells growth or actin distribution therefore it is not considered a key protein for the growth of cells. However, in budding yeast it could be necessary for reorganisation of the actin cytoskeleton.

There is a direct interaction between ABP140 and F-actin as ABP140 binds on the side of F-actin. The role of ABP140 in cells may be in cross-linking F-actin as it has displayed a weak ability to do so, however it is unlike other members of the cross-linking family as it does not share the same structure (Asakura et al., 1998). Lifeact has been fused with either green fluorescent protein (GFP) or red fluorescent protein (TagRFP). The use of one or other of these proteins will depend on if multiple cellular structures are to be imaged as other structures are commonly tagged with GFP (Berepiki et al., 2010). TagRFP is a monomeric red fluorescent protein which has "high brightness, complete chromophore maturation, prolonged fluorescence lifetime and high pH stability" thus making it a good protein for imaging purposes (Merzlyak et al., 2007).

5.1.2 Actin Patterns in Hyphal Cells

Imaging of F-actin in fungal cells through various imaging techniques has led to the discovery of three main patterns; patches, cables and rings. The patches of actin are linked with the plasma membrane and are a gathering of F-actin found associated with endocytic vesicles (Araujo-Bazán et al., 2008; Huckaba et al., 2004; Upadhyay and Shaw, 2008). Actin patches are thought to be involved in endocytosis and cell wall deposition (Engqvist-Goldstein and Drubin, 2003; Utsugi et al., 2002). Patches of actin are concentrated in apical regions of hyphae and are highly polarised (Araujo-Bazán et al., 2008). Actin patches are dynamic with the ability to assemble, disassemble and reassemble (Walker and Garrill, 2006). Patches have shown two types of behaviour in *N. crassa*, slow/nonlinear movement and fast/linear movement. The patches have been seen to be transported through the cytoplasm in association with other actin cables (Berepiki et al., 2010).

Actin cables are a collection of short F-actin structures that congregate to form bundles. These filaments line up in the same direction, therefore uniform polarity is thought to be achieved. The barbed end is commonly found pointing in the direction of polarity sites as this is the fast-growing end (Moseley and Goode, 2006). These cables in yeast are stabilised through the aid of stabilising ABPs (Moseley and Goode, 2006; Pruyne et al., 1998). They are involved in the movement of organelles within cells as they can act as dynamic tracks (Huckaba et al., 2004). The movement of organelles along actin cables requires the ABP myosin, a motor protein (Moseley and Goode, 2006).

Another pattern of actin found in hyphal organisms is actin rings. This pattern of actin is found at the sites where septa have formed. Actin rings remain associated with the septa after it has fully formed, becoming part of the structure of the septa (Harris et al., 1994; Moseley and Goode, 2006).

Previous attempts to image F-actin at the tip of the oomycete *S. ferax* using formaldehyde as a fixative revealed a fine fibrillar cap, with the densest point at the very tip. This is where the cell wall is thought to have the most plasticity. In the subapical regions, plaques and thick actin cables are present and they are associated with the sides of the hypha. The arrangement of actin around the weakest point of the cell, the hyphal tip, has led to the suggestion that it may play a role in providing structural support, therefore it could have a role in the morphogenesis of the hyphal tip (Heath, 1987; Heath, 1988; Jackson and Heath, 1990). More recent investigations into the organisation of actin at the tips of oomycete

hyphae have suggested two distinct distributions in *A. bisexualis*. This was discovered using fixation with a combination of methylglyoxal and formaldehyde and actin staining with Alexa Phalloidin. This combination of fixatives enabled better resolution of the F-actin within the cells based on the ability of methylglyoxal to cross-link proteins. In half of the hyphae imaged, an F-actin-depleted zone was present at the tip of the hyphae and in the other half a continuous actin cap was present (Yu et al., 2004).

Imaging of actin at the tips of fungal hyphae has revealed two different distributions of actin at hyphal tips in *N. crassa* using chemical fixation with both methylglyoxal and formaldehyde and staining with fluorescently tagged antibodies. Actin depleted zones were found at a majority of the tips of invasively growing hyphae whereas a majority of non-invasively growing hyphae had F-actin present at the hyphal tips. This work has revealed F-actin clouds and plaques present at the tips of the hyphae, yet actin cables have not been seen using this technique. Therefore the dynamics of F-actin in *N. crassa* cannot be fully described using this technique (Suei and Garrill, 2008).

The development of Lifeact has enabled the imaging of actin dynamics in live *N. crassa*. It has allowed the visualisation of actin patches, cables and rings in vivo. However, although it appears to cause little disruption to the actin dynamics in live cells, it only shows a fraction of the F-actin population. This could be a result of the actin populations this protein binds to as well as the fact that this ABP has to compete for actin binding sites with unlabelled ABPs (Berepiki et al., 2010). The ability to image actin dynamics in live cells will enable advances in understanding cellular structural features and functions of hyphal cells. Lifeact will allow visualisation of the underlying mechanisms of the morphological changes associated with hyphal branching.

5.1.3 Actin and Hyphal Branching

Research into the mechanisms behind polarity establishment and maintenance in fungal hyphae is of great interest currently. Research has heavily focused on the role of polarity in hyphal elongation, septation and cellular differentiation, with very few studies on the branching process (Riquelme et al., 2011). F-actin has been observed at the site of branch formation in *N. crassa* using Lifeact. Prior to the emergence of the branch, actin cables were found to gather at the branch site. Cables were seen in the newly developed branch but after

10 minutes these cables disappeared and an F-actin spot along with a collar of F-actin patches appeared as the branch reached a linear rate of extension (Berepiki et al., 2010).

5.1.4 Actin and Septa Formation

A septa band is a contracting band of F-actin that is present during the development of septa (Harris et al., 1994). The process of septation has been visualised in live cells using Lifeact. In these cells, actin cables gather at the sight of future septa sites. These cables gradually pack together to form an actin ring at the site where the new wall material has been deposited. This actin ring remains at the site of the septa, becoming part of the structure (Berepiki et al., 2010).

5.1.5 Actin Dynamics and Ca^{2+}

The possible relationship between the Ca^{2+} gradient and the cytoskeleton is still not fully understood (Silverman-Gavrila and Lew, 2001). The polarity of hyphae is affected when the tip high Ca^{2+} gradient is diminished (Fischer, 2007). When the external Ca^{2+} concentration is changed, the amount of actin and its location is altered in hyphae (Jackson and Heath, 1989). Ca^{2+} can directly influence actin dynamics causing dissociation of actin monomers. It also has the ability to indirectly alter actin dynamics through its interaction with calmodulin-modulated phosphatase systems and Ca^{2+} activated kinases. As well as the ability of Ca^{2+} to alter the configuration of actin, it is also able to alter its transport function. This can be through Ca^{2+} influencing actin dynamics directly or alternatively through calcium-dependent in-/activation of myosin (Geitmann and Emons, 2000).

The role of the tip high Ca^{2+} gradient may be to interact with ABPs that aid in anchoring actin to the plasma membrane and the cell wall. This interaction may be a direct one in which they bind to the ABP or alternatively in which they activate a regulatory protein. Proteins that are similar to spectrin and integrin have been implicated in actin anchoring to the apex of *N. crassa* (Virag and Griffiths, 2004).

Actin may in turn influence the location of Ca^{2+} within the cell. It can influence the location of vesicle secretion which will influence of the location of ion channels inserted into the plasma membrane. The cytoskeleton may influence the maintenance of the polar distribution of ion channels. Another way actin could be determining the Ca^{2+} concentration

inside hyphae is that the cytoskeleton could hold the Ca^{2+} sequestering organelles in place (Geitmann and Emons, 2000). The delivery system of vesicles can be affected when the actin cytoskeleton is altered. This changes the rate of vesicle supply to the hyphal tip. If the release of Ca^{2+} via IP_3 is proportional to the total vesicle supply to the tip, then a decrease in the numbers of vesicles to the tip will result in a lower concentration of Ca^{2+} release therefore a lower Ca^{2+} gradient at the tip (Virag and Griffiths, 2004). Actin and Ca^{2+} may thus be acting in a feedback mechanism in which they influence one another and regulate tip growth (Geitmann and Emons, 2000). When *N. crassa* is exposed to the inhibitor latrunculin B, which binds to G-actin preventing actin polymerisation, the tip stops growing but when the hypha continued growth, the tip bulged. The effect of the latrunculin B on polarity loss is connected with the altered tip-high Ca^{2+} gradient which is dissipated. This shows that actin is involved in the regulation of the tip-high Ca^{2+} gradient (Silverman-Gavrila and Lew, 2001).

5.1.6 Rho-GTPases and Actin Regulation

The polarity of filamentous fungi appears to be heavily influenced by the activity of Cdc42. Cdc42 is a Rho-GTPase that plays a role in activating proteins that influence the dynamics of the actin in cells by regulating it and its organisation. The location of this protein is exclusively in areas where growth is occurring (Momany, 2002). GTPases are involved in the regulation of the cytoskeleton along with the trafficking of vesicles. In filamentous fungi these proteins are conserved in most cases (Harris et al., 2005). Actin polarisation, endocytosis and chemotaxis are some of the roles of Rho-type GTPaes in cells (Rasmussen and Glass, 2005).

The Cdc42p may be a branch morphogen. In *Saccharomyces*, bud initiation and branch formation may be equivalent. Prior to bud formation Cdc42p builds up at the site and results in actin reorganisation. When this protein is not present, the actin cytoskeleton is unable to create the necessary cap and polarised growth fails to occur (Jackson et al., 2001). After the site of polarisation is determined, Rho-GTPases are thought be involved in signal transduction of the location where new growth will occur (Harris et al., 2005). The GTPases are involved in regulating branch formation in the filamentous fungi *A. nidulans*. When there are mutations that affect these proteins the hypha that develop are uncommonly straight without lateral branches. Phenotypes like this have been observed in other filamentous fungi such as *Fusarium oxysporum* and *Alternaria alternate* (Harris, 2008; Virag et al., 2007).

The proteins that Cdc42 and Rac are likely to affect have been described for yeast and other organisms. These include p21-activate (PAK) family of protein kinases, Wiscott Aldrich syndrome protein (WASP) family, formin homology (FH) proteins and IQGAP proteins. The Cdc42/Rac interactive binding (CRIB) domain can be found in most of these proteins. An example of a downstream effect that these proteins have on the cytoskeleton is the Cdc42 or Rac activating PAK. PAK can phoshorylate a protein like cofilin or myosin light chain Cofilin is involved in actin stabilisation and myosin light chain regulates the contraction of actinomyosin systems (Raudaskoski et al., 2001).

5.1.7 Aims of Chapter 5

In this chapter I will use Lifeact *N. crassa* to investigate the roles of F-actin in the process of branch formation from before the branch is visible to when it is a mature growing tip using the induction technique described in Chapter 3. This will be attempted using the induction apparatus in conjunction with a confocal microscope. The expression of Rho-GTPases in *N. crassa* and *A. bisexualis* extracts will be investigated using western blotting to see if they are involved in the branching process. Hyphal colonies will be exposed to verapamil in which they produce more branches as the concentration increases therefore any changes in the expression of these proteins could potentially be attributed to increased production of branches.

5.2 Materials and Methods

See Chapter 2 for full Methods and Materials.

5.3 Results

5.3.1 In Areas where Lifeact Signal was Present there was a Low Signal to Noise Ratio

F-actin fluorescence was present in Lifeact *N. crassa* cultures; however there were difficulties in the imaging process due to the very weak signal present as well as very few areas which were emitting a signal. There was no fluorescence in the hyphae at the growing margin of the colony however further back in the colony there was fluorescence. Images displayed in the figures below show areas in the colony which were back from the growing edge. As a result of this minimal fluorescence in limited areas a decision was made to not use the induction technique described in Chapter 3 on these cells. This was made for a couple of reasons. Firstly, the hyphae that have been induced to branch in Chapter 3 were young cells that were present at the growing edge of the colony. Since there was no fluorescence in this area of the colony, actin dynamics would not have been able to be imaged as the branch emerged, as there would be little or no actin signal. Inducing hyphae further back in the colony where signal was present would have come with its own challenges. Hyphae further back in the colony are typically growing in very close proximity with one another making it hard to find a hypha to induce in a clear area. The second reason for not inducing branches in the Lifeact *N. crassa* colonies was that even though there was signal present in the mature part of the colony, this signal was not universally present in this area. Therefore the signal might not have been present in the area of the colony that been induced to branch.

The decision was thus made to image Lifeact to investigate actin dynamics in areas where a branch was in the process of forming. In order to maximise the weak signal present, the agar that the cultures were grown on for imaging purposes, was poured as a very thin layer enabling as much light as possible to be captured by the microscope. Also the older regions of young colonies, typically 8-10 hours old, were used for imaging. These colonies were healthy and had a better signal than older cultures.

5.3.2 Actin is Present at Branching Sites

F-actin was imaged at branching sites of *N. crassa* using Lifeact and could be seen in both growing and non-growing branches. Unfortunately due to the weak signal in just few locations, F-actin was only seen in one growing branch starting at the bud stage. F-actin could however be seen in this branch transitioning between the early stages where cables were abundant to the later stage of branch formation where plaques were the more abundant form of F-actin. In this growing branch imaging began at the bud stage of growth see (Figure 5.1a). This stage lasted for 2 minutes 32 seconds. In this stage the new branch had a very rounded curvature coming out of the cell wall. At the beginning of the imaging, F-actin cables could be seen at base of the bud on either side. Small F-actin patches were seen moving around the tip and the sides of the bud. As the bud continued to emerge F-actin cables could be seen transiently forming a weak lattice in the growing bud whilst maintaining a strong presence at the base of the bud as thinner cables, until 77 seconds after imaging began. As the bud began to transition into an early branch, the actin cables at the base of the branch became thicker and were associated with the wall at the base of the branch (see Figure 5.1b). F-actin in the actual branch transiently disappeared. After 7 minutes 49 seconds actin patches and cables appear in the branch at the same time as the actin cables disappeared from the base of the branch (see Figure 5.1c). These patches and cables gave a stronger fluorescence at around 12 minutes 42 seconds just back from the growing tip. There was a transition between cables and patches. At 14 minutes 5 seconds patches were seen at the very tip of the growing branch and along the edges just back from the tip which became progressively stronger in fluorescence and in number. At 15 minutes 49 seconds the patches become weaker although were still present around the growing tip until 17 minutes 1 second when the patches began to congregate at the tip and to one side of the tip until observations stopped. Actin was also present in branches that had emerged but were no longer growing. In these branches, the actin plaques were all moving around. These were located around the edges of the branch and were transiently heavily present at the tip of the hypha (see Figures 5.2 and 5.3).

5.3.3 Actin is Involved in the Formation of Septa and Movement of Vesicles

Live imaging of F-actin also revealed its presence in areas of septa formation in *N. crassa.* Actin rings could be seen during the development of the septa. In the early stages of septa formation F-actin cables could be seen. These F-actin cables formed a lattice around the site of the future septa site (Figure 5.4). Over time these F-actin cables begin to condense together to form a single, dense ring at the site of the new internal barrier (Figure 5.5). Actin continued to be present in this ring formation after the septa had formed. In one instance, F-actin was seen surrounding a suspected vesicle in *N. crassa*. This was observed moving through the cytoplasm (Figure 5.6).

5.3.4 Protein was Extracted from *N. crassa* and *A. bisexualis* Cultures

As detailed in Chapter 4, there was an increase in branch frequency as the concentration of the Ca^{2+} channel inhibitor verapamil was increased for both *N. crassa* and *A. bisexualis*. Verapamil treatment thus provides a system for looking for proteins involved in branching as their presence may increase with an increase in verapamil. Good candidate proteins are the Rho-GTPases. In order to see if there are changes in the concentration of Rho-GTPase family members using Western blotting, protein was extracted from both *N. crassa* and *A. bisexualis* exposed to verapamil. Hyphal colonies of both *N. crassa* and *A. bisexualis* were exposed to concentrations of verapamil ranging from 0 µM to 200 µM. These concentrations were chosen as it encompassed the point where the inhibitor began to have an effect on the morphology of the colony. Protein was successfully extracted from both cultures and normalised for Western blotting using total protein concentrations from a BCA assay. The SDS gels showing the presence of protein from both *N. crassa* and *A. bisexualis* can be seen in Figures 5.7 and 5.8 respectively.

5.3.5 Western Blotting Rho-GTPases

Western blotting was conducted on the protein samples extracted from the cultures exposed to verapamil as described in 5.3.4. Unfortunately no bands were seen when antibodies for Rho-GTPases and actin were used on the protein samples for *N. crassa*, *A. bisexualis* or a mammalian protein cancer cell extract positive control.

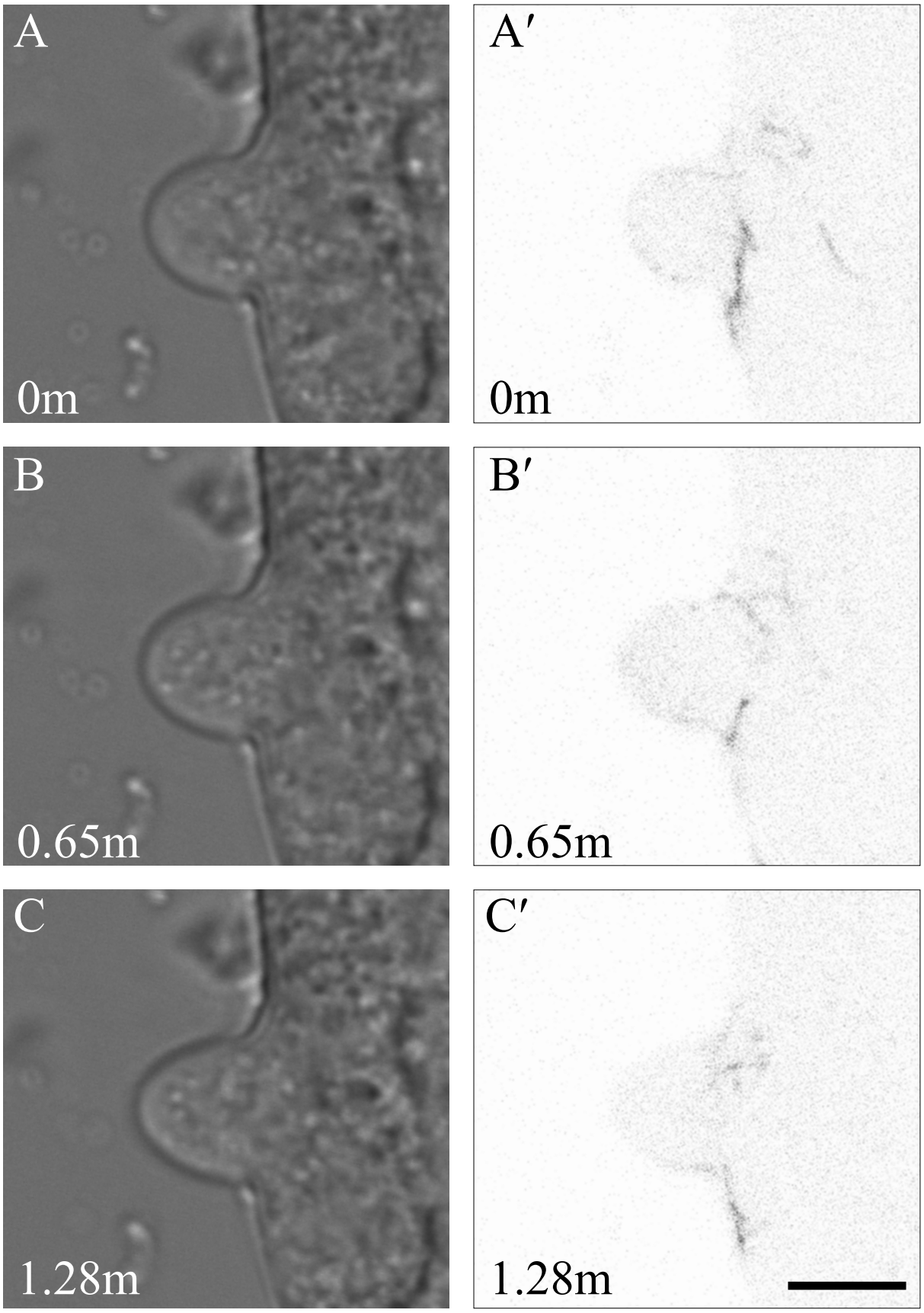

Figure 5.1a - F-actin in an early bud of Lifeact *N. crassa.* This stage is defined by the very rounded tip of the new branch emerging from the cell wall seen in the transmitted light images A-C. F- actin cables can be seen at the base of the bud and small plaques moving around at the tip seen in the fluorescence images A′-C′. Bar = 5 μm. Time measured in minutes (m).

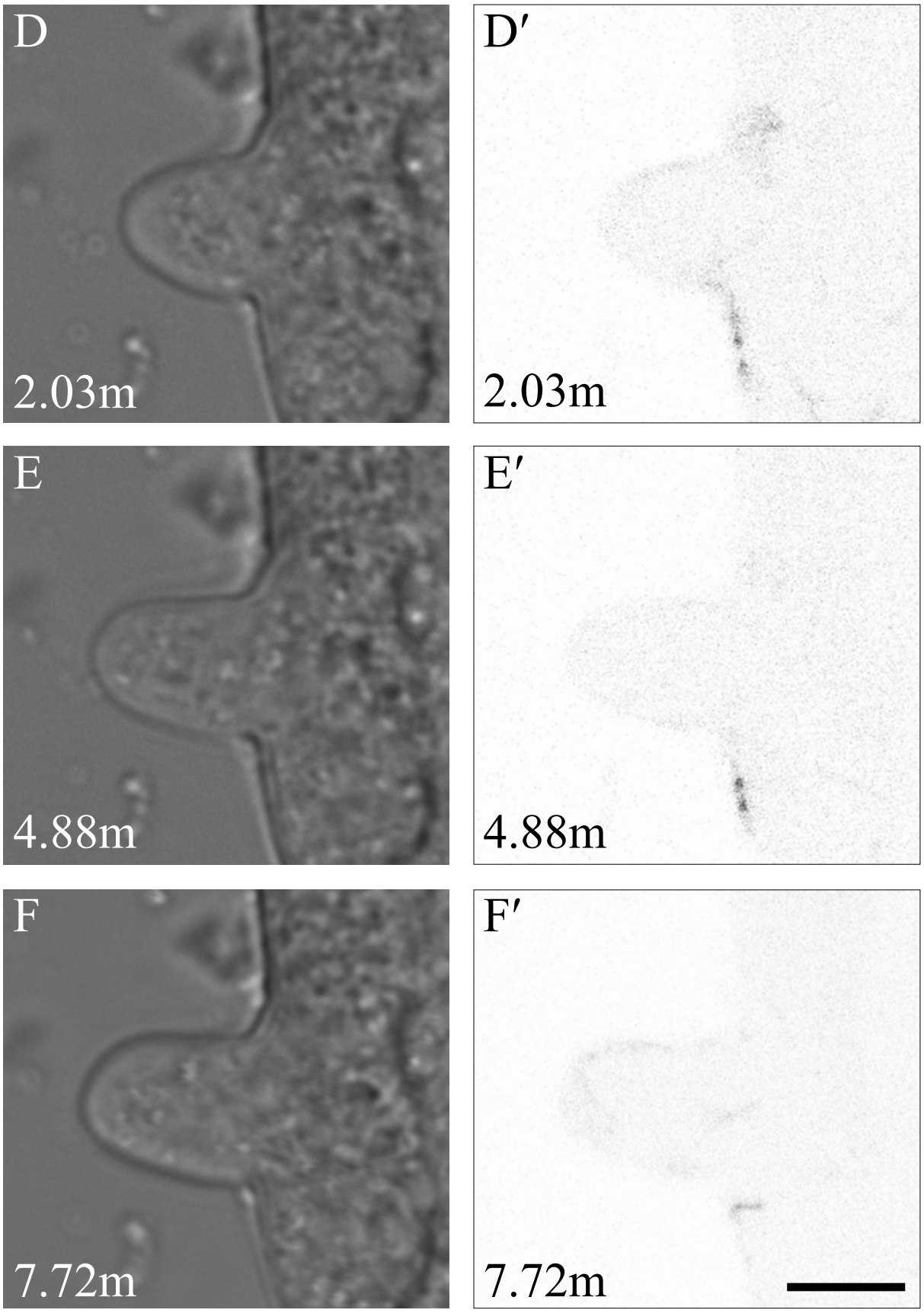

Figure 5.1b - F-actin in an early branch of Lifeact *N. crassa*. This was defined by the generation of a cylindrical hypha with rounded tip seen in the transmitted light images D-F. F-actin cables appear to group together at the base of the new growing tip seen in the fluorescence images D′-F′. Bar = 5 μm. Time measured in minutes (m).

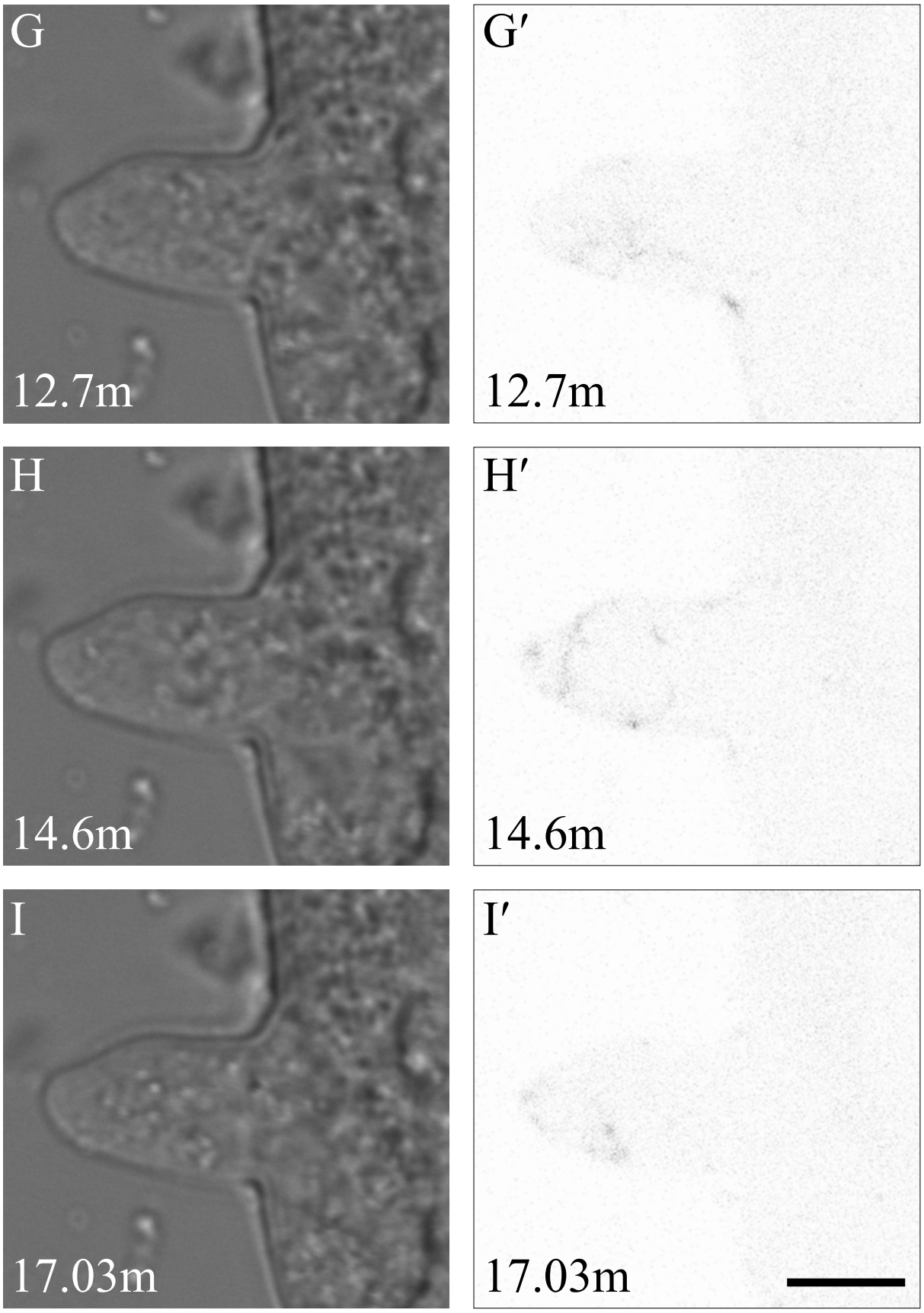

Figure 5.1c - F-actin in maturing branch of Lifeact *N. crassa.* This is defined by the generation of a cylindrical hypha with rounded tip see in the transmitted light images G-I. F-actin patches appear to develop at at the tip and aroung the walls of the growing branch seen in the fluorescence images G′-I′. Bar = 5 μm. Time measured in minutes (m).

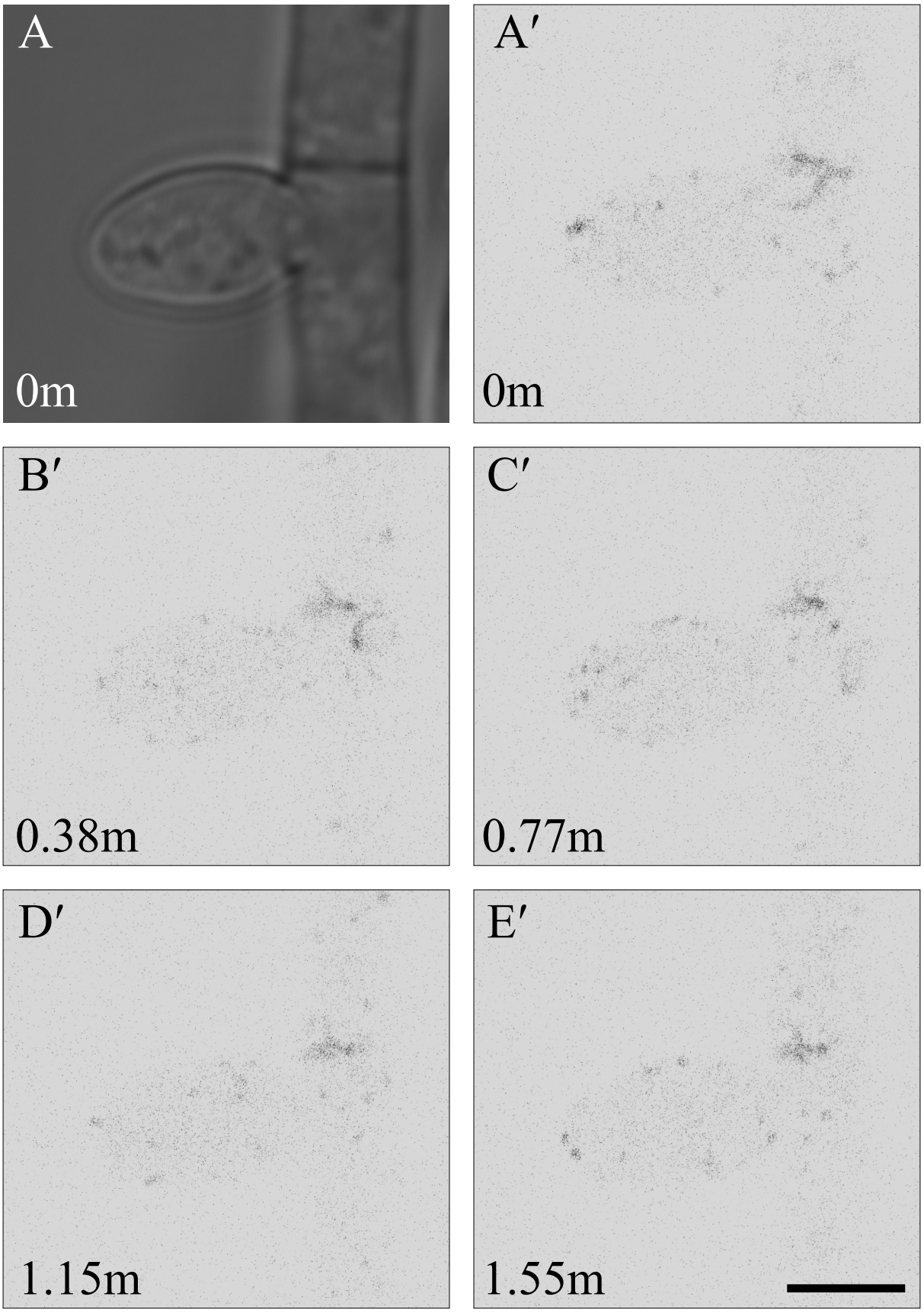

Figure 5.2 - F-actin in a mature branch of Lifeact *N. crassa*. This branch was not growing however actin patches could be seen dynamically moving around the walls. These patches were transiently heavily present at the tip of the hypha. A shows the transmitted light image of the branch at time 0. A′-E′ show the fluorescence images of the branch. Bar = 5 μm. Time in minutes (m).

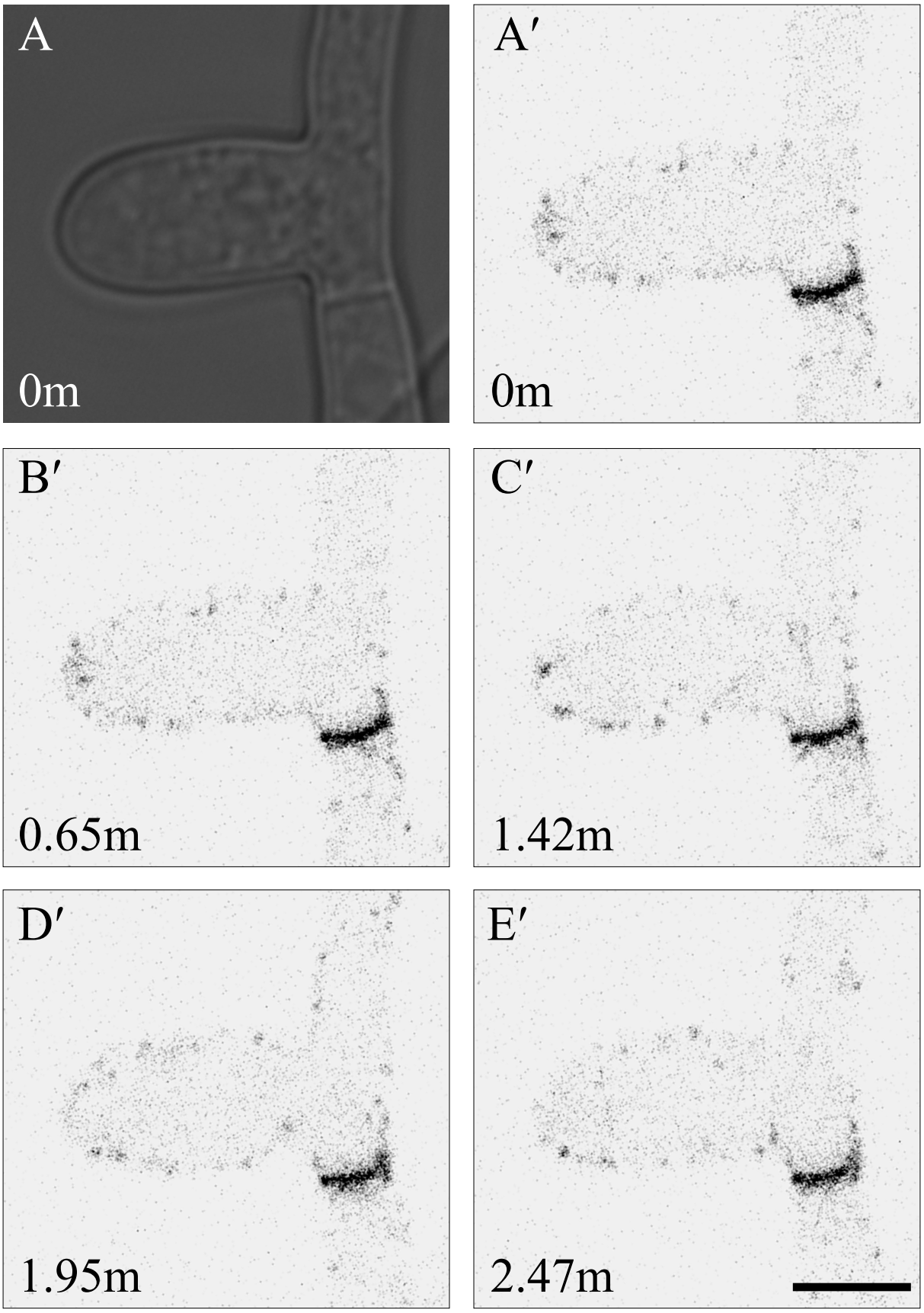

Figure 5.3 - F-actin in a mature branch of Lifeact *N. crassa*. This branch was not growing however actin patches could be seen dynamically moving around the walls. These patches were transiently heavily present at the tip of the hypha. A shows the transmitted light image of the branch at time 0. A′-E′ show the fluorescence images of the branch. Bar = 5 μm. Time in minutes (m).

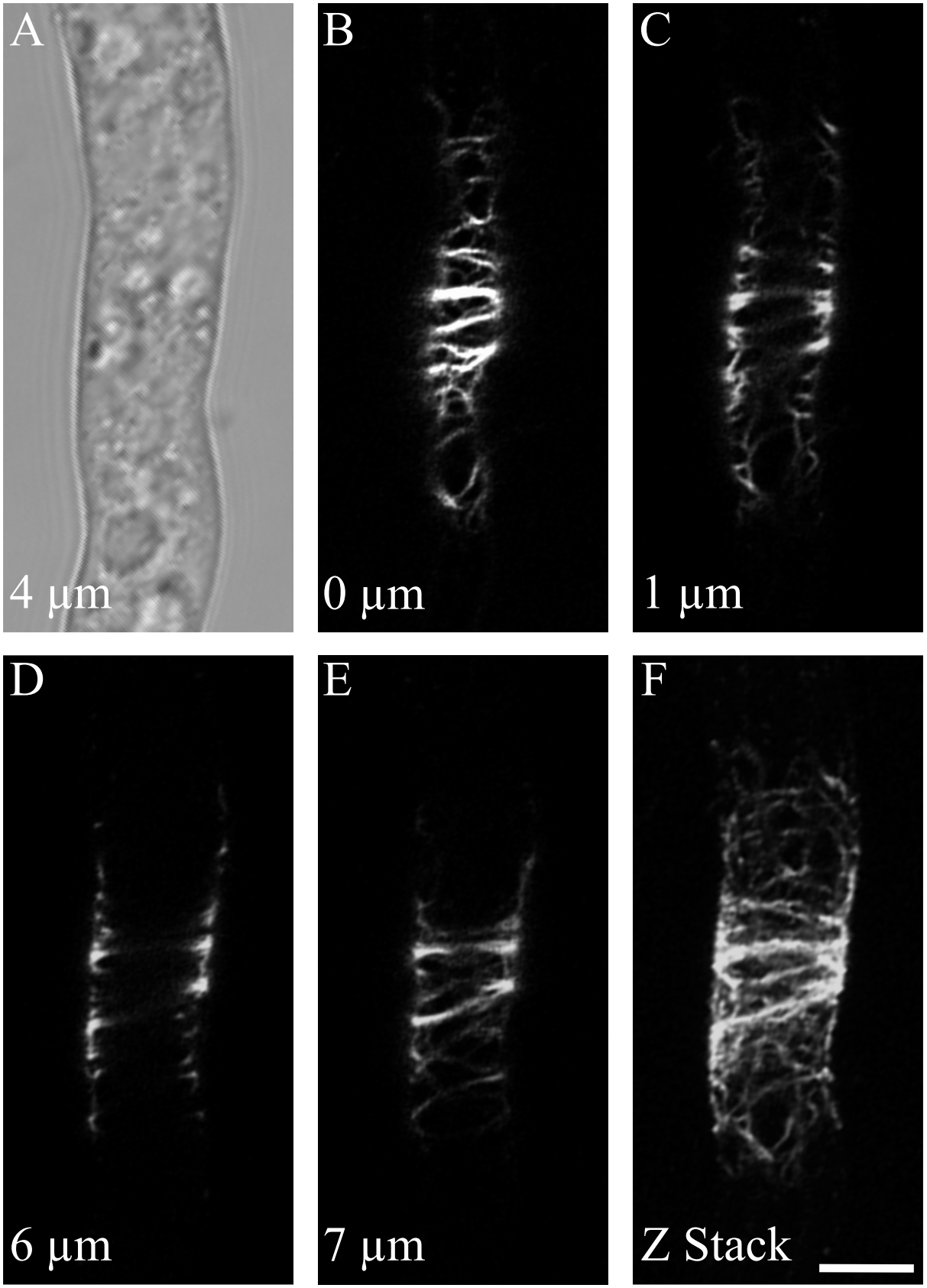

Figure 5.4 - Hypha of Lifeact *N. crassa* showing the presence of F-actin at the sites of septa formation. A shows a transmitted light image of the hypha at a middle plane. B-E show fluorescent images of a z series through a hypha diplaying the network of F-actin rings around the developing septa site. F shows a merged stack of the z series. Bar = 10 µm.

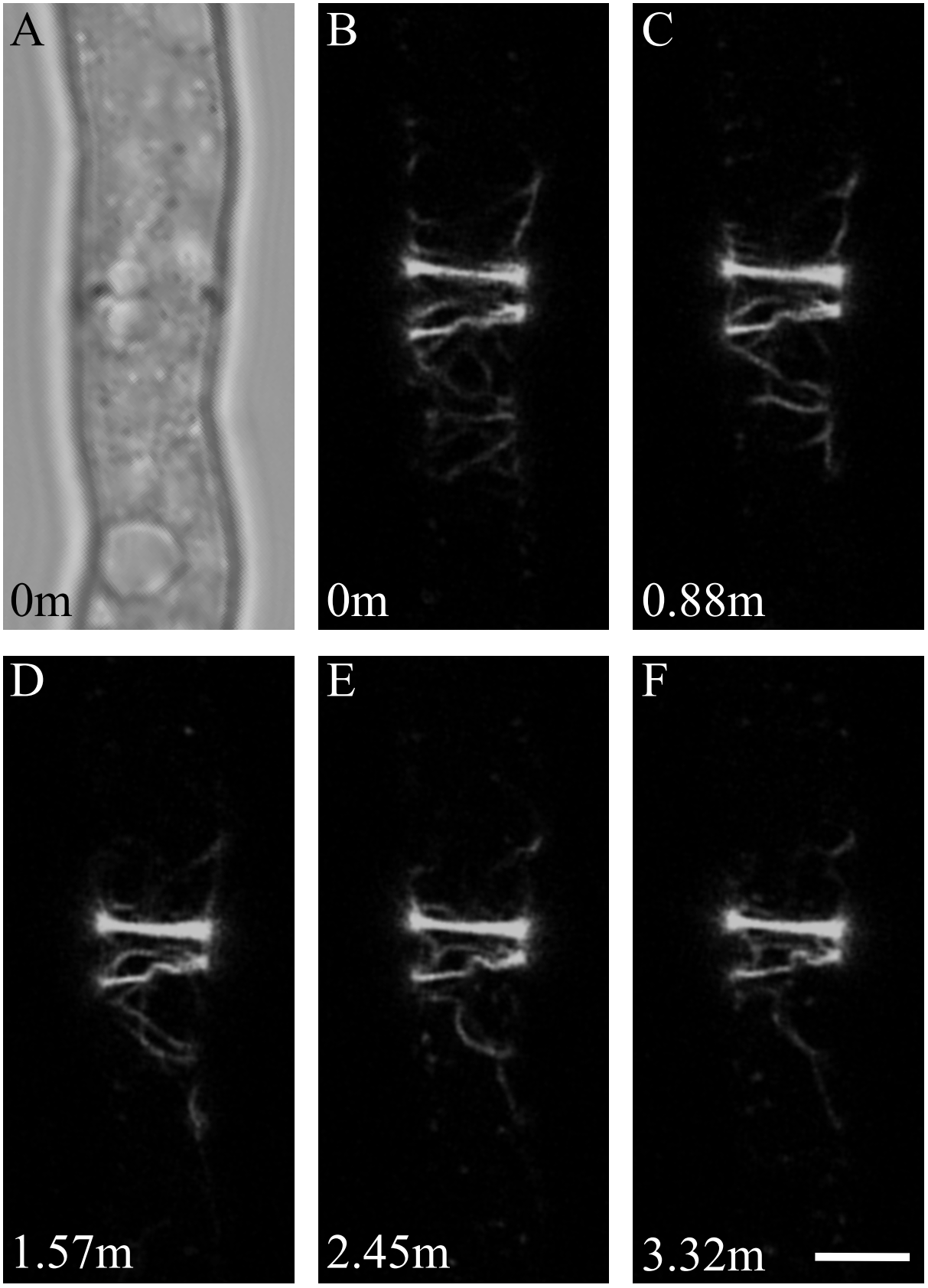

Figure 5.5 - Hypha of Lifeact *N. crassa* showing the presence of F-actin at the site of septa formation. A shows a transmitted light image of the hypha. B-F show a timelapse series of the developing septa. Actin cables form a meshwork aroung the future septa site initially, then condense together forming single actin ring where the new cell wall material is found. Bar= 10 µm. Time in minutes (m).

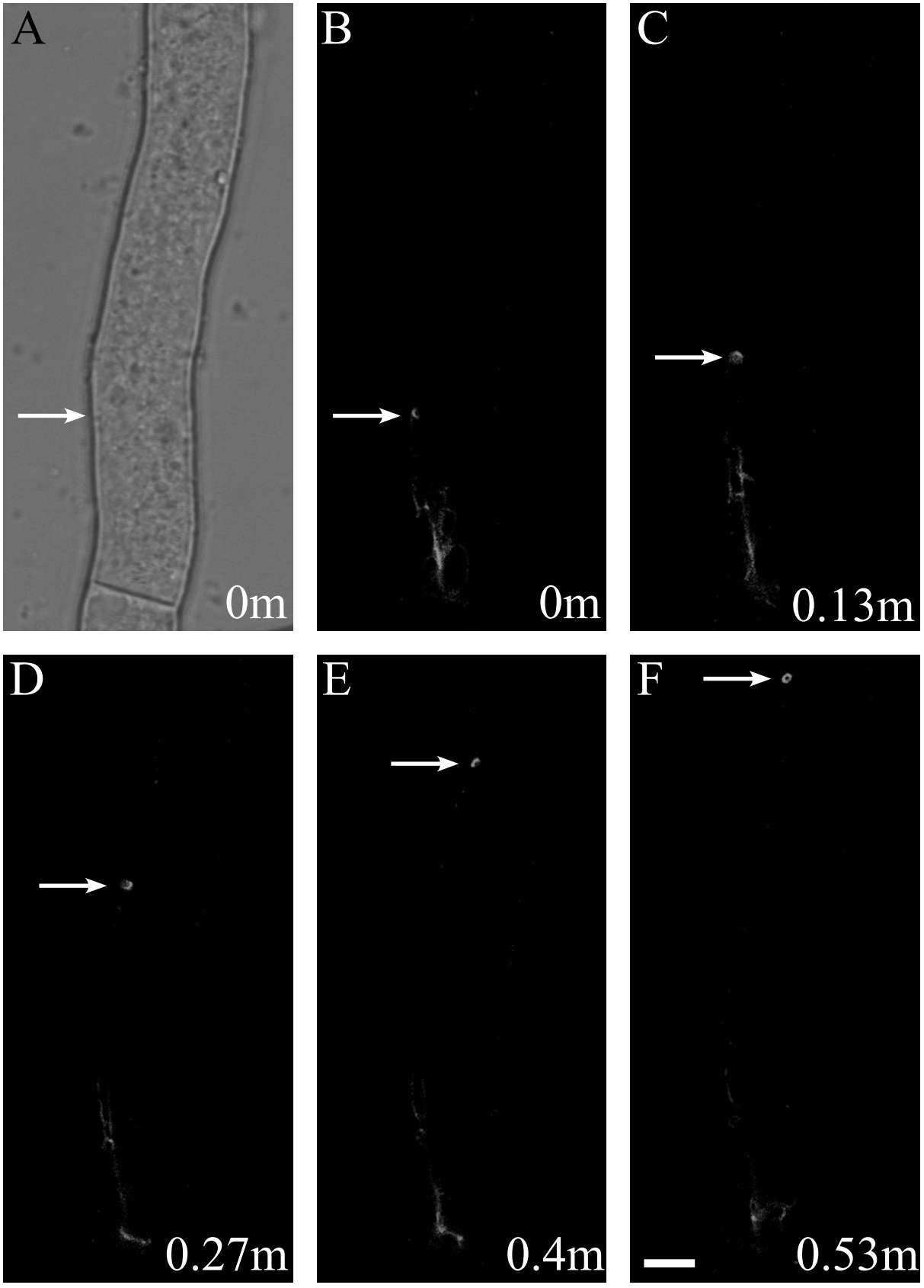

Figure 5.6 - A hypha of Lifeact *N. crassa* showing the association of F-actin around a suspected vesicle moving through the cytoplasm. A shows the transmitted light image of the hypha at time 0. B-F show the fluorescent light images of the F-actin around the suspected vesicle. The white arrow indicates the movement of the vesicle . Bar = 5 µm. Time in minutes (m).

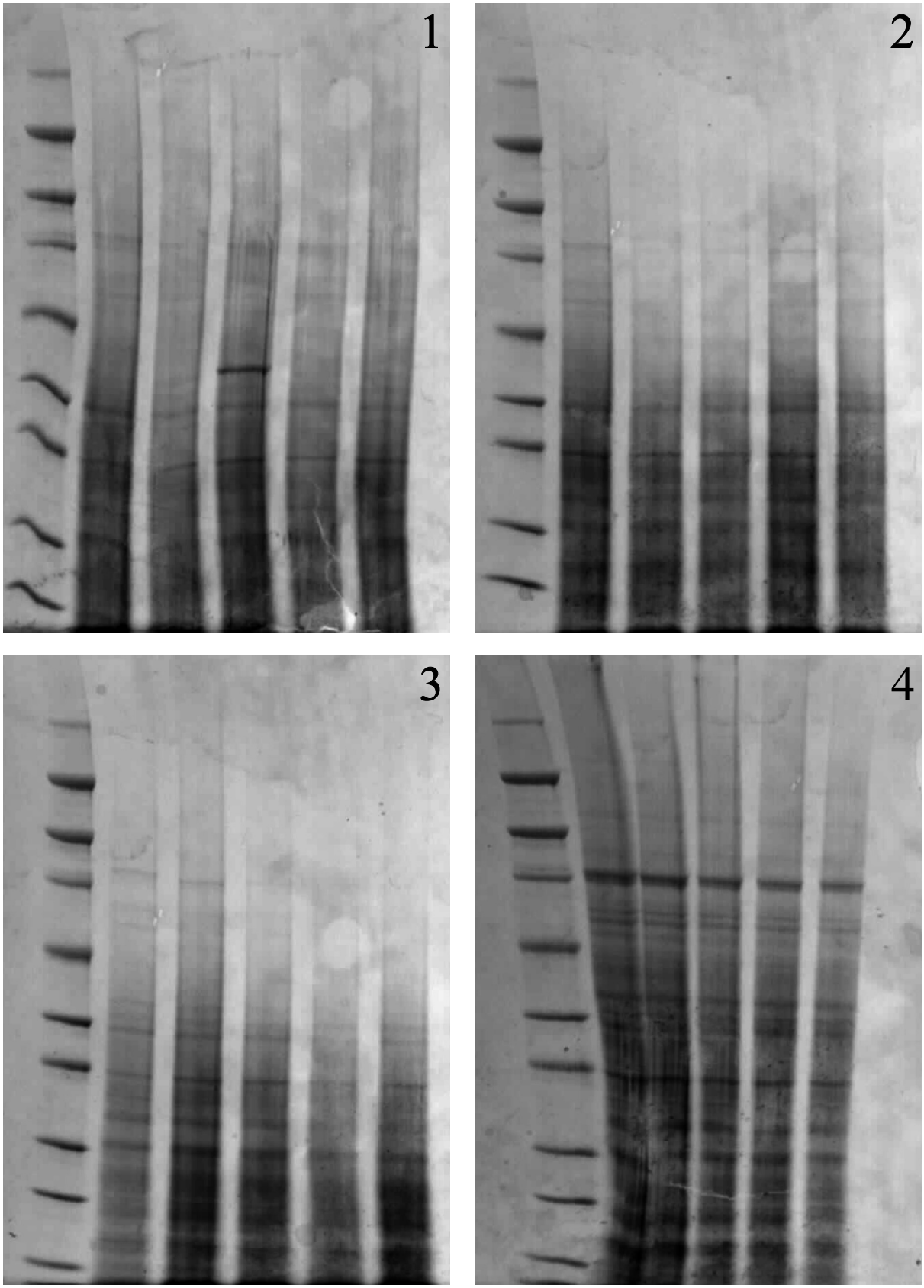

Figure 5.7 - SDS PAGE of *N. crassa* protein extraction. Lane 1, Ladder; Lane 2, 0 μM Verapamil; Lane 3, 5 μM Verapamil; Lane 4, 10 μM Verapamil; Lane 5, 100 μM Verapamil; Lane 6, 200 μM Verapamil. Extraction was repeated 4 times from samples grown on different days (Gels 1-4).

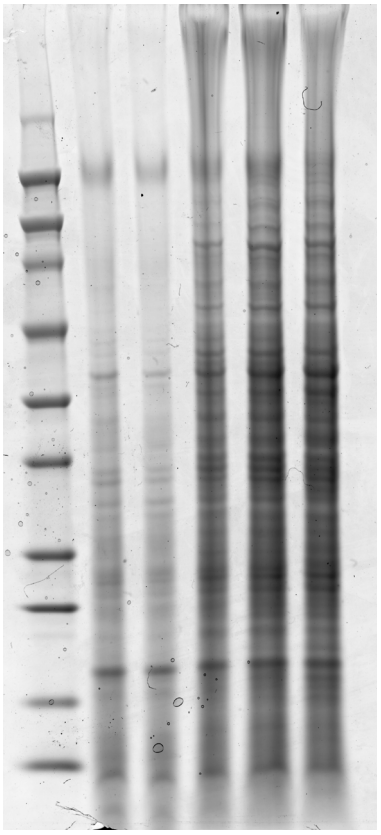

Figure 5.8 - SDS PAGE of *A. bisexualis* protein extraction. Lane 1, Ladder; Lane 2, 0 µM Verapamil; Lane 3, 5 µM Verapamil; Lane 4, 10 µM Verapamil; Lane 5, 100 µM Verapamil; Lane 6, 200 µM Verapamil.

5.4 Discussion

The ability to image actin in live hyphal cells will likely have a huge impact on the understanding of the underlying factors involved in morphological changes, especially in tip growth and branching. This is the most preferable way of imaging actin as other methods can potentially disrupt the actin distribution and also do not permit the visualisation of dynamics within the cells. Live cell imaging has recently become possible with the development of the Lifeact plasmid which *N. crassa* has been transformed with. However, despite the success of visualising actin dynamics in real time using this genetically modified strain, there still appears to be limits to its ability to image actin. This is based on the amount of signal that is emitted and the localisation of the signal. The cause of this weak signal may be a result of where in the hypha the ABP140 binds to actin. This ABP may not be present in the very active growing tips of the colony. As a recent development in live cell imaging, there is clearly still more development needed to be able to visualise the full picture of the actin dynamics in cells. This GM strain of *N. crassa* is still a major advantage for actin visualisation in that it enables the imaging of actin dynamics. Furthermore, as it does not require fixation (killing the cells) it is also less likely to give rise to artifactual distributions of actin.

Fluorescently tagged ABPs have also been used in yeast were they labelled peripheral actin plaques. The absence of actin cables could be a result of the sensitivity of the probe or the ability of the ABP to bind to actin cables (Heath et al., 2000). The β subunit of the ABP capping protein (Cap2p) was tagged with GFP in order to visualise actin in cortical patches of *Saccharomyces* as it is associated with cortical actin patches (Waddle et al., 1996). In *S. cerevisiae* Sac6p and Abplp were tagged with GFP and these localise with actin patches (Doyle and Botstein, 1996).

F-actin was seen at the site of a growing branch of *N. crassa* in this study. The F-actin in this area was very dynamic and changed in form as the branch reached different stages of growth. The actin cables seen at the base of branch in the bud stage could possibly be acting as tracks for the delivery of vesicles containing the required materials for the developing branch. These cables then began to bunch together on either side of the base of the branch where it extended out from the trunk, as the bud transitioned into an early branch and then disappeared as the branch transitioned into a mature branch. Actin cables then reappeared in

the branch, gradually disappearing with F-actin plaques then becoming the main form, these were located around the growing edge of the branch.

In the present study, F-actin was also seen in non-growing branches in the form of patches. These patches were seen to dynamically move around the cell cortex and were sometimes abundant at the tip of the branch. This suggests some activity is occurring within these branches but no growth is occurring. Actin patches are commonly found at sites of polarised growth as described above.

The development of the dynamic F-actin patches around the edge of the branch as it matures is characteristic of what is seen at the growing tips of *N. crassa*. Actin patches have been found previously at sites of polarised growth. These patches are extremely dynamic with a very brief lifetime, around 10 to 20 seconds. These patches are formed at the site of polarised growth and then slowly move around the cell cortex. The movement of F-actin patches may be a result of actin polymerisation (Moseley and Goode, 2006).

Anchoring F-actin cables to the plasma membrane in cells is thought to be a potential role that cortical F-actin patches play. These patches may therefore be very important for determining the site of growth of mature tips and new tips in the form of branches in hyphal organisms. One mechanism through which this could occur is that, by holding F-actin cables in place, which are the tracks in which the vesicles move along, the patches determine the site of vesicle exocytosis. Another mechanism through which F-actin plaques may be involved in polarised cell growth is that their location is where glucan wall microfibrils are synthesized and therefore aid in the determination of the site of cell wall material deposition. Also F-actin patches are thought to be involved in endocytosis of vesicles. The ability of these F-actin patches to do one or all of the above is not certain (Doyle and Botstein, 1996). F-actin plaques observed around the edges of hyphal tips as well as the edges of the hypha just back from the tip are believed to be involved in vesicle exocytosis being localised to the hyphal tips (Heath et al., 2000).

F-actin was abundant around sites of septation during and after the formation of the septa. Initially a network of F-actin cables was seen surrounding the future site of the septa. These cables are likely to be acting as tracks on either side of the septa, moving vesicles in a directional manner towards the site requiring wall deposition. These actin cables begin to contract towards the septa site forming a condensed actin ring associated with the newly formed septa.

With respect to Western blotting of the Rho-GTPases, no bands were seen, even for the positive control. This could be a result of a number of factors that could not be addressed

with the time constraints of this thesis. The reasons may be, firstly that there could be a problem with the antibodies binding to the proteins based on different epitopes in fungal cells to the epitopes the antibodies were raised against. Species that are predicted to react with the Rho-GTPase sampler kit based on 100% sequence homology are human, mouse, rat, monkey, xenopus and bovine cells. However, even though the above may be true, the fact that there was no band for the positive control, a mammalian cancer cell extract, for which this antibody had 100% sequence homology with the protein the antibodies were raised against, suggests that the Western blotting did not work for another reason. The second possible reason it did not work could be that the antibody no longer worked. A third possibility could be that there was a problem with the transfer of the proteins onto the membrane from the gel, however the fluorescent ladder could be seen when imaged suggesting that this was not the reason for the Western blotting not to be working. The fourth reason could be that there is a problem with the blocking solution used which could be affecting the strength of the signal produced.

While the induction technique was not used on the Lifeact strain of *N. crassa*, F-actin was observed at the sites of growing and non-growing branches although only a small sample size was collected. Therefore with further development of the Lifeact strain to increase overall signal within the growing colony it will hopefully enable the induction technique to be used in the future. In regards to changes in protein expression, the SDS gels don't appear to show any major effect on the concentration of protein, suggesting that it isn't having any other effect on the colony other than blocking Ca^{2+} channels although there is one difference between the gels of *N. crassa* protein extract showing a single band in the 10 μM column which is much stronger than in the other columns, although no conclusions can at present be made from this. This is a crude analysis of the effects of verapamil on the protein concentration and it needs to be looked at in more detail.

Chapter 6
Discussion

6.1 Main Conclusions

Hyphal branching in filamentous organisms is one aspect of development that has had little focus in investigations to date, however it is a key developmental process. This investigation aimed to shed light on the involvement of Ca^{2+} and F-actin in branch production in *N. crassa*. The study of branch formation requires the use of a technique that reliably induces branches and this has been achieved through the local application of the amino acid phenylalanine.

It is suggested that amino acids could be activating symporters that facilitate the influx of amino acids with H^{+} to induce branching in *N. crassa*. If this were the case then it would suggest a similar mechanism of branch development to the oomycete *A. bisexualis*. However it is also possible that the mechanism of local branch induction could in past be a result of a mechanical force generated from the micropipette opening SA channels.

Ca^{2+}could be involved in maintaining apical dominance of growing hyphal tips. In this study when Ca^{2+} channel inhibitors were introduced to cultures there was a change in the mycelial morphology with an increase in branch frequency and a decrease in the colony radius. The mechanism through which the Ca^{2+} channel inhibitors have an effect on mycelial morphology may be a result of the tip-high Ca^{2+} gradient being disturbed or the internal concentration slightly diminishing, therefore leading to the development of more branches which form closer to the hyphal tips.

This investigation used the GM *N. crassa*, Lifeact which revealed dynamic F-actin present in a developing branch and also in non-growing branches. F-actin cables were observed in the early stages of branch formation along with F-actin plaques in the latter stages of branch formation, similar to the distribution seen in fixed *N. crassa* tips. It is suggested that F-actin may be involved delivering the required materials for new wall

synthesis to sites of new growth. This investigation also supports the idea that of F-actin cables and F-actin rings play a role in the development of fungal septa.

6.2 Importance of Filamentous Microorganisms

The development of molecular and microscopic tools has enabled the elucidation of many mechanisms of fungal growth to date and continue to be promising for future discoveries. There are still many areas that need to be investigated in fungal growth including the mechanisms that underlie branching as well as the connection between tip growth and branching in filamentous fungi. With greater understanding of how filamentous microorganism colonies develop it will provide greater knowledge of hyphal growth to groups such as fungal biologists and biotechnologists. Filamentous microorganisms such as fungi and oomycetes are of great ecological and economic importance and understanding their growth strategies could enable the manipulation of particular colonies for human benefit (Harris, 2008).

Filamentous microorganisms have the capability of colonising living plant material therefore have the potential to be plant pathogens. This can be severely detrimental to plant growth and can in some cases be fatal, causing great economic loss as well as making human/animal food sources vulnerable to disease. They have the potential to totally inhibit the growth of crop plants as well as infecting growing crops therefore damaging areas or the entire plant. This can result in a decrease of the plant material that can be gathered and consumed (Agrios, 2005). Fungi are also able to colonise and infect living human tissue which can in some cases cause the death of the patient. It is becoming more common for fungal pathogens to cause morbidity and mortality in patients as the number of individuals in the human population that are immunocomprised, therefore an increased understanding of the growth mechanisms is becoming more important. Among the known human fungal pathogens are the following genus; *Fusarium*, *Scedosporium* and *Trichoderma* (Walsh et al., 2004). More research into the growth mechanisms of these pathogens will enable the development of ways to prevent and treat their occurrence.

Filamentous fungi can be used to produce enzymes for industrial purposes, an example this is *Aspergillus orzae*. These fungi are capable of producing large quantities of enzymes which they secrete into the surrounding environment. Enzymes harvested include amylases, proteases, phytases and lipases (Müller et al., 2002). Products produced by fungi

"sustain a billion dollar manufacturing industry" (Harris et al., 2005). Important metabolites can be produced by filamentous fungi and used commercially (Nair et al., 2011)

They also play a key role in fermentation for industrial food and beverage production (Thomas and Paul, 1996). The number of food and beverages that are produced via fermentation using filamentous fungal cultures is increasing (Ferret et al., 1999). Furthermore, in response to food shortages in the world, the filamentous fungi *Fusariam graminearam* A3/5 was used to produce a high protein food called Quorn myco-protein (Trinci, 1994).

6.3 Future research

Future research could involve the use of the induction techniques developed on *N. crassa* and *A. bisexualis* could investigate the various underlying mechanisms of hyphal branching. Further investigation into the role of Ca^{2+} in hyphal branching could involve the use of GM strains expressing the protein aequorin in conjunction with the induction technique could enable imaging of Ca^{2+} during branch dewvelopment. Further work could also involve the addition of Ca^{2+} channel inhibitors to the induction solution coupled with the loading of Ca^{2+} dyes or through aequorin expression to see if there is any effect on the internal Ca^{2+} levels as a branch is developing. Future research into the role of F-actin in hyphal branching could involve further development of Lifeact *N. crassa* to enhance the F-actin signal and the areas in which fluorescence is emitted. This improved strain could then be used to see the role of F-actin in the branching process. The development of GM *A. bisexualis* with the Lifeact plasmid could also enable the visualisation of F-actin and the role it plays in the formation of branches in live hyphae. Furthermore, the imaging of Ca^{2+} and F-actin during the development of branches in both *A. bisexualis* and *N. crassa* could be a future research to see the interaction between the two elements. Western blotting of Rho-GTPases in both *N. crassa* and *A. bisexualis* is still a possibility for future research. This could be investigated using different antibodies to test if there was a problem with the antibodies used in this study, using a different transfer mechanism, other positive controls could also be tested to see if there was a problem with the positive control used in this study and altering the type and strength of the blocking solution.

References

Agrios, G.N. (2005). Plant pathology (Burlington, MA: Elsevier Academic Press).

Araujo-Bazán, L., Peñalva, M.A., and Espeso, E.A. (2008). Preferential localization of the endocytic internalization machinery to hyphal tips underlies polarization of the actin cytoskeleton in *Aspergillus nidulans*. Molecular Microbiology *67*, 891-905.

Asakura, T., Nakanishi, H., Takai, Y., Sasaki, T., Nagano, F., Satoh, A., Obaishi, H., Nishioka, H., Imamura, H., Hotta, K., *et al.* (1998). Isolation and characterization of a novel actin filament-binding protein from *Saccharomyces cerevisiae*. Oncogene *16*, 121-130.

Bartnicki-Garcia, S., Hergert, F., and Gierz, G. (1989). Computer simulation of fungal morphogenesis and the mathematical basis for hyphal (tip) growth. Protoplasma *153*, 46-57.

Bartnicki-Garcia, S., and Lippman, E. (1969). Fungal Morphogenesis: Cell Wall Construction in *Mucor rouxii*. Science *165*, 302-304.

Berepiki, A., Lichius, A., Shoji, J.-Y., Tilsner, J., and Read, N.D. (2010). F-actin dynamics in *Neurospora crassa*. Eukaryotic cell *9*, 547-557.

Bezzi, M., and Ciliberto, A. (2004). Mathematical modeling of filamentous microorganisms.

Bhattacharya, D., Stickel, S.K., and Sogin, M.L. (1991). Molecular phylogenetic analysis of actin genic regions from *Achlya bisexualis* (Oomycota) and *Costaria costata* (Chromophyta). Journal of Molecular Evolution *33*, 525.

Bourne, H.R., Sanders, D.A., and McCormick, F. (1991). The GTPase superfamily: conserved structure and molecular mechanism. Nature *349*, 117-127.

Bowman, B.J., Draskovic, M., Freitag, M., and Bowman, E.J. (2009). Structure and distribution of organelles and cellular location of calcium transporters in *Neurospora crassa*. Eukaryotic cell *8*, 1845-1855.

Brand, A., and Gow, N.A.R. (2009). Mechanisms of hypha orientation of fungi. Current Opinion in Microbiology *12*, 350-357.

Camacho, L., Parton, R., Trewavas, A.J., and Malhó, R. (2000). Imaging cytosolic free-calcium distribution and oscillations in pollen tubes with confocal microscopy: A comparison of different dyes and loading methods. Protoplasma *212*, 162-173.

Castle, E.S. (1958). The topography of tip growth in a plant cell. The Journal of General Physiology *41*, 913-926.

Dicker, J.W., and Turian, G. (1990). Calcium deficiencies and apical hyperbranching in wild-type and the "frost" and "spray" morphological mutants of *Neurospora crassa*. Journal of General Microbiology *136*, 1413.

Doyle, T., and Botstein, D. (1996). Movement of yeast cortical actin cytoskeleton visualized in vivo. Proceedings of the National Academy of Sciences of the United States of America *93*, 3886-3891.

Dynesen, J., and Nielsen, J. (2003). Branching is coordinated with mitosis in growing hyphae of *Aspergillus nidulans*. Fungal Genetics and Biology *40*, 15-24.

Engqvist-Goldstein, Å.E.Y., and Drubin, D.G. (2003). Actin assembly and endocytosis: From Yeast to Mammals. Annual Review of Cell and Developmental Biology *19*, 287-332.

Ferret, E., Siméon, J.H., Molin, P., Jorquera, H., Acuña, G., and Giral, R. (1999). Macroscopic growth of filamentous fungi on solid substrate explained by a microscopic approach. Biotechnology and Bioengineering *65*, 512-522.

Fiddy, C., and Trinci, A.P. (1976). Nuclei, septation, branching and growth of *Geotrichum candidum*. Journal of General Microbiology *97*, 185.

Fischer, R. (2007). The Cytoskeleton and Polarized Growth of Filamentous Fungi

Biology of the Fungal Cell. In, R.J. Howard, and N.A.R. Gow, eds. (Springer Berlin Heidelberg), pp. 121-135.

Garrill, A., Jackson, S.L., Lew, R.R., and Heath, I.B. (1993). Ion channel activity and tip growth: tip-localized stretch-activated channels generate an essential Ca^{2+} gradient in the oomycete *Saprolegnia ferax*. European Journal of Cell Biology *60*, 358-365.

Garrill, A., Lew, R.R., and Heath, I.B. (1992). Stretch-activated Ca^{2+} and Ca^{2+}-activated K^{+} channels in the hyphal tip plasma membrane of the oomycete *Saprolegnia ferax*. Journal of Cell Science *101*, 721-730.

Geitmann, A., and Emons, A.M.C. (2000). The cytoskeleton in plant and fungal cell tip growth. Journal of Microscopy *198*, 218-245.

Glauert, A.M., and Lewis, P.R. (1998). Biological Specimen Preparation for Transmission Electron Microscopy (London, Portland).

Gooday, G.W. (1971). An Autoradiographic Study of Hyphal Growth of Some Fungi. Journal of General Microbiology *67*, 125.

Gow, N.A. (1984). Transhyphal electrical currents in fungi. Journal of General Microbiology *130*, 3313.

Grinberg, A., and Heath, I.B. (1997). Direct Evidence for Ca^{2+}Regulation of Hyphal Branch Induction. Fungal Genetics and Biology *22*, 127-139.

Gustin, M.C., Zhou, X.L., Martinac, B., and Kung, C. (1988). A mechanosensitive ion channel in the yeast plasma membrane. Science (New York, NY) *242*, 762-765.

Harold, F.M. (1997). How hyphae grow: Morphogenesis explained? Protoplasma *197*, 137-147.

Harold, R.L., and Harold, F.M. (1986). Ionophores and cytochalasins modulate branching in *Achlya bisexualis*. Journal of General Microbiology *132*, 213.

Harris, S.D. (2008). Branching of fungal hyphae: regulation, mechanisms and comparison with other branching systems. Mycologia *100*, 823-832.

Harris, S.D., Morrell, J.L., and Hamer, J.E. (1994). Identification and characterization of Aspergillus nidulans mutants defective in cytokinesis. Genetics *136*, 517-532.

Harris, S.D., Read, N.D., Roberson, R.W., Shaw, B., Seiler, S., Plamann, M., and Momany, M. (2005). Polarisome meets spitzenkörper: microscopy, genetics, and genomics converge. Eukaryotic Cell *4*, 225-229.

Heath, I.B. (1987). Preservation of a labile cortical array of actin filaments in growing hyphal tips of the fungus *Saprolegnia ferax*. European Journal of Cell Biology *44*, 10-16.

Heath, I.B. (1988). Evidence against a direct role for cortical actin arrays in saltatory organelle motility in hyphae of the fungus *Saprolegnia ferax*. Journal of Cell Science *91*, 41-47.

Heath, I.B. (1990). The Roles of Actin in Tip Growth of Fungi. International Review of Cytology *123*, 95-127.

Heath, I.B., Gupta, G., and Bai, S. (2000). Plasma Membrane-Adjacent Actin Filaments, but Not Microtubules, Are Essential for both Polarization and Hyphal Tip Morphogenesis in *Saprolegnia ferax* and *Neurospora crassa*. Fungal Genetics and Biology *30*, 45-62.

Heath, I.B., and Kaminskyj, S.G.W. (1989). The organization of tip-growth-related organelles and microtubules revealed by quantitative analysis of freeze-substituted oomycete hyphae. Journal of Cell Science *93*, 41-52.

Hewitt, J.A. (1978). Diffusion gradients, membrane receptors, and the acquisition of orientational information by cells. Journal of Theoretical Biology *74*, 297-306.

Hickey, P.C., Jacobson, D., Read, N.D., and Louise Glass, N.L.G. (2002). Live-cell imaging of vegetative hyphal fusion in *Neurospora crassa*. Fungal Genetics and Biology *37*, 109-109.

Huckaba, T.M., Gay, A.C., Pantalena, L.F., Yang, H.-C., and Pon, L.A. (2004). Live cell imaging of the assembly, disassembly, and actin cable-dependent movement of endosomes and actin patches in the budding yeast, *Saccharomyces cerevisiae*. The Journal of Cell Biology *167*, 519-530.

Hunsley, D., and Gooday, G.W. (1974). The structure and development of septa in *Neurospora crassa*. Protoplasma *82*, 125.

Hyde, G.J., and Heath, I.B. (1997). Ca^{2+}Gradients in Hyphae and Branches of *Saprolegnia ferax*. Fungal Genetics and Biology *21*, 238-247.

Jackson, S., and Heath, I. (1989). Effects of exogenous calcium ions on tip growth, intracellular Ca^{2+} concentration, and actin arrays in hyphae of the fungus *Saprolegnia ferax*. Experimental Mycology *13*, 1-12.

Jackson, S.L. (1995). Microinjection of fungal cells: a powerful experimental technique. Canadian Journal of Botany *73*, 435-443.

Jackson, S.L., and Heath, I.B. (1990). Evidence that actin reinforces the extensible hyphal apex of the oomycete *Saprolegnia ferax*. Protoplasma *157*, 144-153.

Jackson, S.L., and Heath, I.B. (1992). UV microirradiations elict Ca^{2+}-dependent apex-directed cytoplasmic contraction in hyphae. Protoplasma *170*, 46-52.

Jackson, S.L., and Heath, I.B. (1993). Roles of calcium ions in hyphal tip growth. Microbiological Reviews *57*, 367-382.

Jackson, S.L., Morris, E.J.S., and Garrill, A. (2001). Hyphal Branching and the Induction of Cell Polarity. Cell Biology of Plant and Fungal Tip Growth *328*, 69-79.

Jaffe, L.F. (1981). The role of ionic currents in establishing developmental pattern. Philosophical transactions of the Royal Society of London Series B, Biological sciences *295*, 553-566.

Jaffe, L.F., and Nuccitelli, R. (1977). Electrical Controls of Development. Annual Review of Biophysics and Bioengineering *6*, 445-476.

Katz, D., Goldstein, D., and Rosenberger, R.F. (1972). Model for Branch Initiation in *Aspergillus nidulans* Based on Measurements of Growth Parameters. The Journal of Bacteriology *109*, 1097-1100.

Ketchum, K.A., and Poole, R.J. (1991). Cytosolic calcium regulates a potassium current in corn (*Zea mays*) protoplasts. The Journal of Membrane Biology *119*, 277-288.

Knechtle, P., Wendland, J., and Philippsen, P. (2006). The SH3/PH domain protein AgBoi1/2 collaborates with the Rho-type GTPase AgRho3 to prevent nonpolar growth at hyphal tips of *Ashbya gossypii*. Eukaryotic Cell *5*, 1635-1647.

Knight, H., Trewavas, A.J., and Read, N.D. (1993). Confocal microscopy of living fungal hyphae microinjected with Ca^{2+}-sensitive fluorescent dyes. Mycological Research *97*, 1505-1515.

Kropf, D.L. (1986). Electrophysiological properties of *Achlya* hyphae: ionic currents studied by intracellular potential recording. The Journal of Cell Biology *102*, 1209-1216.

Kropf, D.L., Caldwell, J.H., and Harold, F.M. (1984). Transcellular Ion Currents in the Water Mold *Achlya*. Amino Acid Proton Symport as a Mechanism of Current Entry. The Journal of Cell Biology *99*, 486-496.

Kropf, D.L., Lupa, M.D., Caldwell, J.H., and Harold, F.M. (1983). Cell polarity: endogenous ion currents precede and predict branching in the water mold *Achyla*. Science *220*, 1385-1387.

Levina, N.N., Lew, R.R., and Heath, I.B. (1994). Cytoskeletal regulation of ion channel distribution in the tip-growing organism *Saprolegnia ferax*. Journal of Cell Science *107 (Pt 1)*, 127.

Levina, N.N., Lew, R.R., Hyde, G.J., and Heath, I.B. (1995). The roles of Ca^{2+} and plasma membrane ion channels in hyphal tip growth of *Neurospora crassa*. Journal of Cell Science *108 (Pt 11)*, 3405.

Lew, R.R. (1998). Mapping Fungal Ion Channel Locations. Fungal Genetics and Biology *24*, 69-76.

Lew, R.R. (1999). Comparative analysis of Ca^{2+} and H^{+} flux magnitude and location along growing hyphae of *Saprolegnia ferax* and *Neurospora crassa*. European Journal of Cell Biology *78*, 892.

Lew, R.R., Levina, N.N., Walker, S.K., and Garrill, A. (2004). Turgor regulation in hyphal organisms. Fungal Genetics and Biology *41*, 1007-1015.

Lew, R.R., Serlin, B.S., Schauf, C.L., and Stockton, M.E. (1990). Red light regulates calcium-activated potassium channels in mougeotia plasma membrane. Plant Physiology *92*, 822-830.

Li, R., Zheng, Y., and Drubin, D.G. (1995). Regulation of cortical actin cytoskeleton assembly during polarized cell growth in budding yeast. The Journal of Cell Biology *128*, 599-615.

McKerracher, L.J., and Heath, I.B. (1986). Polarized cytoplasmic movement and inhibition of saltations induced by calcium-mediated effects of microbeams in fungal hyphae. Cell Motility and the Cytoskeleton *6*, 136-145.

Merzlyak, E.M., Gadella, T.W.J., Goedhart, J., Shcherbo, D., Bulina, M.E., Shcheglov, A.S., Fradkov, A.F., Gaintzeva, A., Lukyanov, K.A., and Lukyanov, S. (2007). Bright monomeric red fluorescent protein with an extended fluorescence lifetime. Nature Methods *4*, 555-557.

Momany, M. (2002). Polarity in filamentous fungi: establishment, maintenance and new axes. Current opinion in microbiology *5*, 580-585.

Morris, E.J.S., Jackson, S.L., and Garrill, A. (2011). An investigation of the effects of Ca^{2+} channel inhibitors on branching and chemotropism in the oomycete *Achlya bisexualis*: Support for a role for Ca^{2+} in apical dominance. Fungal Genetics and Biology *48*, 512-518.

Moseley, J.B., and Goode, B.L. (2006). The yeast actin cytoskeleton: from cellular function to biochemical mechanism. Microbiology and Molecular Biology Reviews *70*, 605-645.

Mouriño-Pérez, R.R., Roberson, R.W., and Bartnicki-García, S. (2006). Microtubule dynamics and organization during hyphal growth and branching in *Neurospora crassa*. Fungal Genetics and Biology *43*, 389-400.

Müller, C., McIntyre, M., Hansen, K., and Nielsen, J. (2002). Metabolic engineering of the morphology of *Aspergillus oryzae* by altering chitin synthesis. Applied and Environmental Microbiology *68*, 1827-1836.

Nair, R., Raina, S., Keshavarz, T., and Kerrigan, M.J.P. (2011). Application of fluorescent indicators to analyse intracellular calcium and morphology in filamentous fungi. Fungal Biology *115*, 326-334.

Nelson, G., Kozlova-Zwinderman, O., Collis, A.J., Knight, M.R., Fincham, J.R.S., Stanger, C.P., Renwick, A., Hessing, J.G.M., Punt, P.J., Van Den Hondel, C.A.M.J.J., *et al.* (2004). Calcium measurement in living filamentous fungi expressing codon-optimized aequorin. Molecular Microbiology *52*, 1437-1450.

Picton, J.M., and Steer, M.W. (1982). A model for the mechanism of tip extension in pollen tubes. Journal of Theoretical Biology *98*, 15-20.

Pollard, T.D., and Cooper, J.A. (1986). Actin and Actin-Binding Proteins. A Critical Evaluation of Mechanisms and Functions. Annual Review of Biochemistry *55*, 987-1035.

Prosser, J.I., and Trinci, A.P. (1979). A model for hyphal growth and branching. Journal of General Microbiology *111*, 153.

Pruyne, D.W., Schott, D.H., and Bretscher, A. (1998). Tropomyosin-containing actin cables direct the Myo2p-dependent polarized delivery of secretory vesicles in budding yeast. The Journal of Cell Biology *143*, 1931-1945.

Rasmussen, C.G., and Glass, N.L. (2005). A Rho-type GTPase, rho-4, is required for septation in *Neurospora crassa*. Eukaryotic Cell *4*, 1913-1925.

Raudaskoski, M., Pardo, A.G., Tarkka, M.T., Gorfer, M., Hanif, M., and Laitiainen, E. (2001). Small GTPases, Cytoskeleton and Signal Transduction in Filamentous Homobasidiomycetes. Cell Biology of Plant and Fungal Tip Growth *328*, 123-136.

Rayner, A.D.M. (1991). The Challenge of the Individualistic Mycelium. Mycologia *83*, 48-71.

Reissig, J.L., and Kinney, S.G. (1983). Calcium as a branching signal in Neurospora crassa. Journal of bacteriology *154*, 1397-1402.

Riedl, J., Werb, Z., Crevenna, A.H., Kessenbrock, K., Yu, J.H., Neukirchen, D., Bista, M., Bradke, F., Jenne, D., and Holak, T.A. (2008). Lifeact: a versatile marker to visualize F-actin. Nature Methods *5*, 605-607.

Riquelme, M., and Bartnicki-Garcia, S. (2004). Key differences between lateral and apical branching in hyphae of *Neurospora crassa*. Fungal Genetics and Biology *41*, 842-851.

Riquelme, M., Mouriño-Pérez, R., Plamann, M., Rasmussen, C., Richthammer, C., Roberson, R.W., Sanchez-Leon, E., Seiler, S., Watters, M.K., Yarden, O., *et al.* (2011). Architecture and development of the *Neurospora crassa* hypha – a model cell for polarized growth. Fungal Biology *115*, 446-474.

Robson, G.D., Wiebe, M.G., and Trinci, A.P.J. (1991a). Involvement of Ca^{2+} in the regulation of hyphal extension and branching in *Fusarium graminearum* A 3/5. Experimental Mycology *15*, 263-272.

Robson, G.D., Wiebe, M.G., and Trinci, A.P.J. (1991b). Low calcium concentrations induce increased branching in *Fusarium graminearum*. Mycological Research *95*, 561-565.

Schmid, J., and Harold, F.M. (1988). Dual Roles for Calcium Ions in Apical Growth of *Neurospora crassa*. Journal of General Microbiology *134*, 2623.

Schreurs, W.J., and Harold, F.M. (1988). Transcellular Proton Current in *Achlya bisexualis* Hyphae: Relationship to Polarized Growth. Proceedings of the National Academy of Sciences of the United States of America *85*, 1534-1538.

Schreurs, W.J., Harold, R.L., and Harold, F.M. (1989). Chemotropism and branching as alternative responses of *Achlya bisexualis* to amino acids. Journal of General Microbiology *135*, 2519.

Seiler, S., and Plamann, M. (2003). The genetic basis of cellular morphogenesis in the filamentous fungus *Neurospora crassa*. Molecular Biology of the Cell *14*, 4352-4364.

Semighini, C.P., and Harris, S.D. (2008). Regulation of Apical Dominance in *Aspergillus nidulans* Hyphae by Reactive Oxygen Species. Genetics *179*, 1919-1932.

Shear, and Dodge, B.O. (1927). Journal of Agricultural Research.

Sietsma, J.H., and Wessels, J.G.H. (2006). Apical Wall Biogenesis. In (Berlin, Heidelberg: Springer Berlin Heidelberg), pp. 53-72.

Silverman-Gavrila, L.B., and Lew, R.R. (2000). Calcium and tip growth in *Neurospora crassa*. Protoplasma *213*, 203-217.

Silverman-Gavrila, L.B., and Lew, R.R. (2001). Regulation of the tip-high [Ca^{2+}] gradient in growing hyphae of the fungus *Neurospora crassa*. European Journal of Cell Biology *80*, 379-390.

Silverman-Gavrila, L.B., and Lew, R.R. (2002). An IP_3-activated Ca^{2+} channel regulates fungal tip growth. Journal of Cell Science *115*, 5013-5025.

Silverman-Gavrila, L.B., and Lew, R.R. (2003). Calcium gradient dependence of *Neurospora crassa* hyphal growth. Microbiology *149*, 2475-2485.

Steele, G.C., and Trinci, A.P.J. (1975). The Extension Zone of Mycelial Hyphae. New Phytologist *75*, 583-587.

Steinberg, G. (2007). Hyphal growth: a tale of motors, lipids, and the Spitzenkörper. Eukaryotic Cell *6*, 351-360.

Suei, S., and Garrill, A. (2008). An F-actin-depleted zone is present at the hyphal tip of invasive hyphae of *Neurospora crassa*. Protoplasma *232*, 165-172.

Takaishi, K., Sasaki, T., Kotani, H., Nishioka, H., and Takai, Y. (1997). Regulation of cell-cell adhesion by rac and rho small G proteins in MDCK cells. The Journal of Cell Biology *139*, 1047-1059.

Takeuchi, Y., Schmid, J., Caldwell, J.H., and Harold, F.M. (1988). Transcellular ion currents and extension of *Neurospora crassa* hyphae. The Journal of Membrane Biology *101*, 33.

Thomas, C.R., and Paul, G.C. (1996). Applications of image analysis in cell technology. Current Opinion in Biotechnology *7*, 35-45.

Torralba, S., and Heath, I.B. (2001). Cytoskeleton and Ca^{2+} regulation of hyphal tip growth and initiation. Current Topics in Developmental Biology *53*, 135-187.

Torralba, S., Raudaskoski, M., Pedregosa, A.M., and Laborda, F. (1998). Effect of cytochalasin A on apical growth, actin cytoskeleton organization and enzyme secretion in *Aspergillus nidulans*. Microbiology *144*, 45.

Trinci, A.P. (1994). Evolution of the Quorn myco-protein fungus, *Fusarium graminearum* A3/5. Microbiology *140*, 2181-2188.

Trinci, A.P.J. (1973). The hyphal growth unit of wild type and spreading colonial mutants of *Neurospora crassa*. Archiv f r Mikrobiologie *91*, 127-136.

Trinci, A.P.J. (1974). A Study of the Kinetics of Hyphal Extension and Branch Initiation of Fungal Mycelia. Journal of General Microbiology *81*, 225.

Turner, B.C., Perkins, D.D., and Fairfield, A. (2001). *Neurospora* from natural populations: a global study. Fungal Genetics and Biology *32*, 67-92.

Upadhyay, S., and Shaw, B.D. (2008). The role of actin, fimbrin and endocytosis in growth of hyphae in *Aspergillus nidulans*. Molecular Microbiology *68*, 690-705.

Utsugi, T., Minemura, M., Hirata, A., Abe, M., Watanabe, D., and Ohya, Y. (2002). Movement of yeast 1,3-beta-glucan synthase is essential for uniform cell wall synthesis. Genes to Cells : Devoted to Molecular & Cellular Mechanisms *7*, 1.

Virag, A., and Griffiths, A.J.F. (2004). A mutation in the *Neurospora crassa* actin gene results in multiple defects in tip growth and branching. Fungal Genetics and Biology *41*, 213-225.

Virag, A., Lee, M.P., Si, H., and Harris, S.D. (2007). Regulation of hyphal morphogenesis by cdc42 and rac1 homologues in *Aspergillus nidulans*. Molecular Microbiology *66*, 1579-1596.

Waddle, J.A., Karpova, T.S., Waterston, R.H., and Cooper, J.A. (1996). Movement of cortical actin patches in yeast. The Journal of Cell Biology *132*, 861-870.

Walker, S.K., and Garrill, A. (2006). Actin microfilaments in fungi. Mycologist *20*, 26-31.

Walsh, T.J., Groll, A., Hiemenz, J., Fleming, R., Roilides, E., and Anaissie, E. (2004). Infections due to emerging and uncommon medically important fungal pathogens. Clinical microbiology and infection : the official publication of the European Society of Clinical Microbiology and Infectious Diseases *10*, 48-66.

Watters, M.K. (2013). Control of Branching in *Neurospora crassa*. Neurospora Genomics and Molecular Biology.

Watters, M.K., Virag, A., Haynes, J., and Griffiths, A.J.F. (2000). Branch initiation in *Neurospora* is influenced by events at the previous branch. Mycological Research *104*, 805-809.

Yu, Y.P., Jackson, S.L., and Garrill, A. (2004). Two distinct distributions of F-actin are present in the hyphal apex of the oomycete *Achlya bisexualis*. Plant & Cell Physiology *45*, 275-280.

Zalokar, M. (1959). Growth and Differentiation of *Neurospora* hyphae. American Journal of Botany *46*, 602-610.

Zhou, X.-L., Stumpf, M.A., Hoch, H.C., and Kung, C. (1991). A Mechanosensitive Channel in Whole Cells and in Membrane Patches of the Fungus *Uromyces*. Science *253*, 1415-1417.

Zhou, X.L., and Kung, C. (1992). A mechanosensitive ion channel in *Schizosaccharomyces pombe*. The European Molecular Biology Organization Journal *11*, 2869-2875.

Appendix 1

Statistical Analysis for Branch Inductions and Whole Plate Ca^{2+} Channel Inhibition

t-test no inhibitor – Hyphal growth rate before vs 1 minute after induction began

Unpaired t test	
P value	0.0294
P value summary	*
Significantly different? (P < 0.05)	Yes
One- or two-tailed P value?	Two-tailed
t, df	t=2.236 df=56
How big is the difference?	
Mean ± SEM of hyphal growth rate before	13.38 ± 1.282 N=29
Mean ± SEM of hyphal growth rate 1 minute after	9.690 ± 1.037 N=29
Difference between means	-3.686 ± 1.649
95% confidence interval	-6.989 to -0.3830
R square	0.08193
F test to compare variances	
F,DFn, Dfd	1.526, 28, 28
P value	0.2695
P value summary	ns
Significantly different? (P < 0.05)	No

t-test 50 µM verapamil – Hyphal growth rate before vs 1 minute after induction began

Unpaired t test	
P value	0.7643
P value summary	ns
Significantly different? (P < 0.05)	No

One- or two-tailed P value?	Two-tailed
t, df	t=0.3081 df=10
How big is the difference?	
Mean ± SEM of hyphal growth rate before	26.80 ± 3.610 N=6
Mean ± SEM of hyphal growth rate 1 minute after	24.53 ± 6.441 N=6
Difference between means	-2.275 ± 7.384
95% confidence interval	-18.73 to 14.18
R square	0.009404
F test to compare variances	
F,DFn, Dfd	3.182, 5, 5
P value	0.2297
P value summary	ns
Significantly different? (P < 0.05)	No

Mann Whitney test 500 µM verapamil – Hyphal growth rate before vs 1 minute after induction began

Mann Whitney test	
P value	0.7771
Exact or approximate P value?	Exact
P value summary	ns
Significantly different? (P < 0.05)	No
One- or two-tailed P value?	Two-tailed
Sum of ranks	41.00 , 37.00
Mann-Whitney U	16

t-test 1000 µM verapamil – Hyphal growth rate before vs 1 minute after induction began

Unpaired t test	
P value	0.4479
P value summary	ns
Significantly different? (P < 0.05)	No
One- or two-tailed P value?	Two-tailed
t, df	t=0.7845 df=12

How big is the difference?	
Mean ± SEM of hyphal growth rate before	20.64 ± 4.248 N=7
Mean ± SEM of hyphal growth rate 1 minute after	15.63 ± 4.775 N=7
Difference between means	-5.014 ± 6.391
95% confidence interval	-18.94 to 8.912
R square	0.04879
F test to compare variances	
F,DFn, Dfd	1.264, 6, 6
P value	0.7835
P value summary	ns
Significantly different? (P < 0.05)	No

Kruskal-Wallis test verapamil primary branch frequency

Ho: There is no difference in mean primary branch frequency between treatments of verapamil

Ha: There is a difference in mean primary branch frequency between treatments of verapamil

Kruskal-Wallis test	
P value	< 0.0001
Exact or approximate P value?	Approximate
P value summary	****
Do the medians vary significantly. (P < 0.05)	Yes
Number of groups	8
Kruskal-Wallis statistic	119.2
Data summary	
Number of treatments (columns)	8
Number of values (total)	762

Conclusion: p < 0.0001 therefore reject null hypothesis. There is sufficient evidence that there is a difference in mean primary branch frequencies between treatments of verapamil at α=0.05

Dunn's multiple comparisons test verapamil primary branch frequency

Dunn's multiple comparisons test	**Mean rank diff.**	**Significant?**	**Summary**	**Adjusted P Value**
0 vs. 5	-5.777	No	ns	> 0.9999
0 vs. 10	13.67	No	ns	> 0.9999
0 vs. 50	-102.6	Yes	*	0.013
0 vs. 100	-170	Yes	****	< 0.0001

0 vs. 200	-123.9	Yes	**	0.003
0 vs. 250	-246.8	Yes	****	< 0.0001
0 vs. 250 + 10 mM $CaCl_2$	-164.1	Yes	****	< 0.0001
5 vs. 10	19.45	No	ns	> 0.9999
5 vs. 50	-96.87	Yes	*	0.0268
5 vs. 100	-164.2	Yes	****	< 0.0001
5 vs. 200	-118.2	Yes	**	0.0061
5 vs. 250	-241	Yes	****	< 0.0001
5 vs. 250 + 10 mM $CaCl_2$	-158.3	Yes	****	< 0.0001
10 vs. 50	-116.3	Yes	**	0.0021
10 vs. 100	-183.7	Yes	****	< 0.0001
10 vs. 200	-137.6	Yes	***	0.0005
10 vs. 250	-260.5	Yes	****	< 0.0001
10 vs. 250 + 10 mM $CaCl_2$	-177.8	Yes	****	< 0.0001
50 vs. 100	-67.37	No	ns	0.7426
50 vs. 200	-21.3	No	ns	> 0.9999
50 vs. 250	-144.2	Yes	***	0.0006
50 vs. 250 + 10 mM $CaCl_2$	-61.47	No	ns	> 0.9999
100 vs. 200	46.07	No	ns	> 0.9999
100 vs. 250	-76.8	No	ns	0.7607
100 vs. 250 + 10 mM $CaCl_2$	5.903	No	ns	> 0.9999
200 vs. 250	-122.9	Yes	*	0.0191
200 vs. 250 + 10 mM $CaCl_2$	-40.16	No	ns	> 0.9999
250 vs. 250 + 10 mM $CaCl_2$	82.7	No	ns	0.6207

Sample Sizes:

0	**5**	**10**	**50**	**100**	**200**	**250**	**250 + 10 mM $CaCl_2$**
110	110	110	110	96	80	66	80

Kruskal-Wallis test verapamil secondary branch frequency

Ho: There is no difference in mean secondary branch frequency between treatments of verapamil

Ha: There is a difference in mean secondary branch frequency between treatments of verapamil

Kruskal-Wallis test	
P value	< 0.0001
Exact or approximate P value?	Approximate
P value summary	****
Do the medians vary signif. (P < 0.05)	Yes
Number of groups	8

Kruskal-Wallis statistic	182
Data summary	
Number of treatments (columns)	8
Number of values (total)	762

Conclusion: $p < 0.0001$ therefore reject null hypothesis. There is sufficient evidence that there is a difference in mean secondary branch frequencies between treatments of verapamil at $\alpha=0.05$

Dunn's multiple comparisons test verapamil secondary branch frequency

Dunn's multiple comparisons test	Mean rank diff.	Significant?	Summary	Adjusted P Value
0 vs. 5	-34.9	No	ns	> 0.9999
0 vs. 10	-26.8	No	ns	> 0.9999
0 vs. 50	-150.5	Yes	****	< 0.0001
0 vs. 100	-190.4	Yes	****	< 0.0001
0 vs. 200	-249.3	Yes	****	< 0.0001
0 vs. 250	-351.1	Yes	****	< 0.0001
0 vs. 250 + 10 mM $CaCl_2$	-104.3	Yes	*	0.0348
5 vs. 10	8.1	No	ns	> 0.9999
5 vs. 50	-115.6	Yes	**	0.0027
5 vs. 100	-155.5	Yes	****	< 0.0001
5 vs. 200	-214.4	Yes	****	< 0.0001
5 vs. 250	-316.2	Yes	****	< 0.0001
5 vs. 250 + 10 mM $CaCl_2$	-69.43	No	ns	0.8857
10 vs. 50	-123.7	Yes	***	0.0009
10 vs. 100	-163.6	Yes	****	< 0.0001
10 vs. 200	-222.5	Yes	****	< 0.0001
10 vs. 250	-324.3	Yes	****	< 0.0001
10 vs. 250 + 10 mM $CaCl_2$	-77.53	No	ns	0.4595
50 vs. 100	-39.89	No	ns	> 0.9999
50 vs. 200	-98.73	No	ns	0.0629
50 vs. 250	-200.5	Yes	****	< 0.0001
50 vs. 250 + 10 mM $CaCl_2$	46.2	No	ns	> 0.9999
100 vs. 200	-58.84	No	ns	> 0.9999
100 vs. 250	-160.6	Yes	***	0.0001
100 vs. 250 + 10 mM $CaCl_2$	86.09	No	ns	0.2717
200 vs. 250	-101.8	No	ns	0.1504
200 vs. 250 + 10 mM $CaCl_2$	144.9	Yes	***	0.0009
250 vs. 250 + 10 mM $CaCl_2$	246.7	Yes	****	< 0.0001

Sample Sizes:

0	5	10	50	100	200	250	250 + 10 mM $CaCl_2$
110	110	110	110	96	80	66	80

Kruskal-Wallis test verapamil distance between the hyphal tip and the first branch

Ho: There is no difference in mean distance between the hyphal tip and the first branch between treatments of verapamil

Ha: There is a difference in mean distance between the hyphal tip and the first branch between treatments of verapamil

Kruskal-Wallis test	
P value	0.0043
Exact or approximate P value?	Approximate
P value summary	**
Do the medians vary signif. (P < 0.05)	Yes
Number of groups	8
Kruskal-Wallis statistic	20.65
Data summary	
Number of treatments (columns)	8
Number of values (total)	362

Conclusion: $p < 0.0001$ therefore reject null hypothesis. There is sufficient evidence that there is a difference in the mean distance between the hyphal tip and the first branch between treatments of verapamil at $\alpha=0.05$

Dunn's multiple comparisons test verapamil distance between the hyphal tip and the first branch

Dunn's multiple comparisons test	Mean rank diff.	Significant?	Summary	Adjusted P Value
0 vs. 5	24.44	No	ns	> 0.9999
0 vs. 10	27.4	No	ns	> 0.9999
0 vs. 50	42.37	No	ns	0.727
0 vs. 100	41.61	No	ns	> 0.9999
0 vs. 200	60.73	No	ns	0.2567
0 vs. 250	98.81	Yes	*	0.0211
0 vs. 250 + 10 mM $CaCl_2$	76.29	Yes	*	0.0298
5 vs. 10	2.958	No	ns	> 0.9999

5 vs. 50	17.93	No	ns	> 0.9999
5 vs. 100	17.17	No	ns	> 0.9999
5 vs. 200	36.28	No	ns	> 0.9999
5 vs. 250	74.37	No	ns	0.3138
5 vs. 250 + 10 mM $CaCl_2$	51.85	No	ns	0.7301
10 vs. 50	14.97	No	ns	> 0.9999
10 vs. 100	14.21	No	ns	> 0.9999
10 vs. 200	33.33	No	ns	> 0.9999
10 vs. 250	71.41	No	ns	0.4165
10 vs. 250 + 10 mM $CaCl_2$	48.89	No	ns	> 0.9999
50 vs. 100	-0.7525	No	ns	> 0.9999
50 vs. 200	18.36	No	ns	> 0.9999
50 vs. 250	56.45	No	ns	> 0.9999
50 vs. 250 + 10 mM $CaCl_2$	33.93	No	ns	> 0.9999
100 vs. 200	19.11	No	ns	> 0.9999
100 vs. 250	57.2	No	ns	> 0.9999
100 vs. 250 + 10 mM $CaCl_2$	34.68	No	ns	> 0.9999
200 vs. 250	38.09	No	ns	> 0.9999
200 vs. 250 + 10 mM $CaCl_2$	15.57	No	ns	> 0.9999
250 vs. 250 + 10 mM $CaCl_2$	-22.52	No	ns	> 0.9999

Sample Sizes:

0	**5**	**10**	**50**	**100**	**200**	**250**	**250 + 10 mM $CaCl_2$**
60	60	60	60	46	30	16	30

One-way ANOVA test verapamil distance between the first branch and the second branch

Ho: There is no difference in mean distance between the hyphal tip and the first branch between treatments of verapamil

Ha: There is a difference in mean distance between the hyphal tip and the first branch between treatments of verapamil

	SS	**DF**	**MS**	**F (DFn, DFd)**	**P value**
Treatment (between columns)	201058	7	28723	F (7, 354) = 3.324	P = 0.0019
Residual (within columns)	3059000	354	8641		
Total	3260000	361			

Conclusion: p = 0.0019 therefore reject null hypothesis. There is sufficient evidence that there is a difference in the mean distance between the first branch and the second branch between treatments of verapamil at α=0.05

Tukey's multiple comparisons test verapamil distance between the first branch and the second branch

Tukey's multiple comparisons test	Mean Diff.	95% CI of diff.	Significant?	Summary	Adjusted P Value
0 vs. 5	-32.85	-84.60 to 18.90	No	ns	0.5273
0 vs. 10	-3.375	-55.13 to 48.38	No	ns	> 0.9999
0 vs. 50	22.95	-28.80 to 74.70	No	ns	0.8779
0 vs. 100	35.77	-19.78 to 91.31	No	ns	0.5084
0 vs. 200	9.9	-53.48 to 73.28	No	ns	0.9998
0 vs. 250	51.36	-28.40 to 131.1	No	ns	0.5082
0 vs. 250 + 10 mM $CaCl_2$	26.55	-36.83 to 89.93	No	ns	0.9068
5 vs. 10	29.48	-22.28 to 81.23	No	ns	0.6632
5 vs. 50	55.8	4.050 to 107.6	Yes	*	0.0244
5 vs. 100	68.62	13.07 to 124.2	Yes	**	0.0047
5 vs. 200	42.75	-20.63 to 106.1	No	ns	0.4453
5 vs. 250	84.21	4.454 to 164.0	Yes	*	0.0301
5 vs. 250 + 10 mM $CaCl_2$	59.4	-3.981 to 122.8	No	ns	0.0846
10 vs. 50	26.33	-25.43 to 78.08	No	ns	0.7789
10 vs. 100	39.14	-16.41 to 94.69	No	ns	0.386
10 vs. 200	13.28	-50.11 to 76.66	No	ns	0.9983
10 vs. 250	54.73	-25.02 to 134.5	No	ns	0.4218
10 vs. 250 + 10 mM $CaCl_2$	29.93	-33.46 to 93.31	No	ns	0.8382
50 vs. 100	12.82	-42.73 to 68.36	No	ns	0.9969
50 vs. 200	-13.05	-76.43 to 50.33	No	ns	0.9985
50 vs. 250	28.41	-51.35 to 108.2	No	ns	0.9594
50 vs. 250 + 10 mM $CaCl_2$	3.6	-59.78 to 66.98	No	ns	> 0.9999
100 vs. 200	-25.87	-92.38 to 40.65	No	ns	0.9357
100 vs. 250	15.59	-66.68 to 97.86	No	ns	0.9991
100 vs. 250 + 10 mM $CaCl_2$	-9.215	-75.73 to 57.30	No	ns	0.9999
200 vs. 250	41.46	-46.29 to 129.2	No	ns	0.8377
200 vs. 250 + 10 mM $CaCl_2$	16.65	-56.54 to 89.84	No	ns	0.9971
250 vs. 250 + 10 mM $CaCl_2$	-24.81	-112.6 to 62.94	No	ns	0.9891

Sample Sizes:

0	5	10	50	100	200	250	250 + 10 mM $CaCl_2$
60	60	60	60	46	30	16	30

Kruskal-Wallis test Gd^{3+} primary branch frequency

Ho: There is no difference in mean primary branch frequency between treatments of Gd^{3+}

Ha: There is a difference in mean primary branch frequency between treatments of Gd^{3+}

Kruskal-Wallis test	
P value	< 0.0001
Exact or approximate P value?	Approximate
P value summary	****
Do the medians vary signif. (P < 0.05)	Yes
Number of groups	13
Kruskal-Wallis statistic	93.43
Data summary	
Number of treatments (columns)	13
Number of values (total)	819

Conclusion: $p < 0.0001$ therefore reject null hypothesis. There is sufficient evidence that there is a difference in mean primary branch frequencies between treatments of Gd^{3+} at $\alpha=0.05$

Kruskal-Wallis test verapamil colony radius

Ho: There is no difference in the mean colony radius between treatments of verapamil

Ha: There is a difference in the mean colony radius between treatments of verapamil

Kruskal-Wallis test	
P value	< 0.0001
Exact or approximate P value?	Approximate
P value summary	****
Do the medians vary signif. (P < 0.05)	Yes
Number of groups	14
Kruskal-Wallis statistic	361.9
Data summary	
Number of treatments (columns)	14
Number of values (total)	436

Conclusion: $p < 0.0001$ therefore reject null hypothesis. There is sufficient evidence that there is a difference in mean colony radius between treatments of verapamil at $\alpha=0.05$

Dunn's multiple comparisons test verapamil colony radius

Dunn's multiple comparisons test	Mean rank diff.	Significant?	Summary	Adjusted P Value
0 vs. 5	22.64	No	ns	> 0.9999
0 vs. 10	5.154	No	ns	> 0.9999
0 vs. 50	71.87	No	ns	> 0.9999
0 vs. 100	73.64	No	ns	0.8455
0 vs. 200	173.3	Yes	****	< 0.0001
0 vs. 250	211.2	Yes	****	< 0.0001
0 vs. 300	219.1	Yes	****	< 0.0001
0 vs. 400	231.1	Yes	****	< 0.0001
0 vs. 500	266.5	Yes	****	< 0.0001
0 vs. 750	310.7	Yes	****	< 0.0001
0 vs. 1000	332.7	Yes	****	< 0.0001
0 vs. 250 + 10 mM $CaCl_2$	13.25	No	ns	> 0.9999
0 vs. 1000 + 10 mM $CaCl_2$	88.15	No	ns	0.7133
5 vs. 10	-17.48	No	ns	> 0.9999
5 vs. 50	49.23	No	ns	> 0.9999
5 vs. 100	51	No	ns	> 0.9999
5 vs. 200	150.6	Yes	***	0.0002
5 vs. 250	188.5	Yes	****	< 0.0001
5 vs. 300	196.5	Yes	****	< 0.0001
5 vs. 400	208.4	Yes	****	< 0.0001
5 vs. 500	243.8	Yes	****	< 0.0001
5 vs. 750	288.1	Yes	****	< 0.0001
5 vs. 1000	310	Yes	****	< 0.0001
5 vs. 250 + 10 mM $CaCl_2$	-9.387	No	ns	> 0.9999
5 vs. 1000 + 10 mM $CaCl_2$	65.52	No	ns	> 0.9999
10 vs. 50	66.72	No	ns	> 0.9999
10 vs. 100	68.48	No	ns	> 0.9999
10 vs. 200	168.1	Yes	****	< 0.0001
10 vs. 250	206	Yes	****	< 0.0001
10 vs. 300	214	Yes	****	< 0.0001
10 vs. 400	225.9	Yes	****	< 0.0001
10 vs. 500	261.3	Yes	****	< 0.0001
10 vs. 750	305.6	Yes	****	< 0.0001
10 vs. 1000	327.5	Yes	****	< 0.0001
10 vs. 250 + 10 mM $CaCl_2$	8.097	No	ns	> 0.9999
10 vs. 1000 + 10 mM $CaCl_2$	83	No	ns	> 0.9999
50 vs. 100	1.766	No	ns	> 0.9999
50 vs. 200	101.4	No	ns	0.1172

50 vs. 250	139.3	Yes	***	0.0009
50 vs. 300	147.2	Yes	***	0.0003
50 vs. 400	159.2	Yes	***	0.0009
50 vs. 500	194.6	Yes	****	< 0.0001
50 vs. 750	238.9	Yes	****	< 0.0001
50 vs. 1000	260.8	Yes	****	< 0.0001
50 vs. 250 + 10 mM $CaCl_2$	-58.62	No	ns	> 0.9999
50 vs. 1000 + 10mM $CaCl_2$	16.28	No	ns	> 0.9999
100 vs. 200	99.64	No	ns	0.1423
100 vs. 250	137.5	Yes	**	0.0012
100 vs. 300	145.5	Yes	***	0.0004
100 vs. 400	157.4	Yes	**	0.0011
100 vs. 500	192.8	Yes	****	< 0.0001
100 vs. 750	237.1	Yes	****	< 0.0001
100 vs. 1000	259	Yes	****	< 0.0001
100 vs. 250 + 10 mM $CaCl_2$	-60.39	No	ns	> 0.9999
100 vs. 1000 + 10 mM $CaCl_2$	14.52	No	ns	> 0.9999
200 vs. 250	37.88	No	ns	> 0.9999
200 vs. 300	45.83	No	ns	> 0.9999
200 vs. 400	57.8	No	ns	> 0.9999
200 vs. 500	93.19	No	ns	0.2818
200 vs. 750	137.5	Yes	**	0.0049
200 vs. 1000	159.4	Yes	****	< 0.0001
200 vs. 250 + 10 mM $CaCl_2$	-160	Yes	****	< 0.0001
200 vs. 1000 + 10 mM $CaCl_2$	-85.13	No	ns	> 0.9999
250 vs. 300	7.953	No	ns	> 0.9999
250 vs. 400	19.93	No	ns	> 0.9999
250 vs. 500	55.31	No	ns	> 0.9999
250 vs. 750	99.58	No	ns	0.3119
250 vs. 1000	121.5	Yes	*	0.0178
250 vs. 250 + 10 mM $CaCl_2$	-197.9	Yes	****	< 0.0001
250 vs. 1000 + 10 mM $CaCl_2$	-123	No	ns	0.0562
300 vs. 400	11.97	No	ns	> 0.9999
300 vs. 500	47.36	No	ns	> 0.9999
300 vs. 750	91.63	No	ns	0.6444
300 vs. 1000	113.5	Yes	*	0.0454
300 vs. 250 + 10 mM $CaCl_2$	-205.9	Yes	****	< 0.0001
300 vs. 1000 + 10 mM $CaCl_2$	-131	Yes	*	0.0243
400 vs. 500	35.39	No	ns	> 0.9999
400 vs. 750	79.66	No	ns	> 0.9999
400 vs. 1000	101.6	No	ns	0.5367
400 vs. 250 + 10 mM $CaCl_2$	-217.8	Yes	****	< 0.0001
400 vs. 1000 + 10 mM $CaCl_2$	-142.9	Yes	*	0.0306
500 vs. 750	44.27	No	ns	> 0.9999

500 vs. 1000	66.19	No	ns	> 0.9999
500 vs. 250 + 10 mM $CaCl_2$	-253.2	Yes	****	< 0.0001
500 vs. 1000 + 10 mM $CaCl_2$	-178.3	Yes	****	< 0.0001
750 vs. 1000	21.92	No	ns	> 0.9999
750 vs. 250 + 10 mM $CaCl_2$	-297.5	Yes	****	< 0.0001
750 vs. 1000 + 10 mM $CaCl_2$	-222.6	Yes	****	< 0.0001
1000 vs. 250 + 10 mM $CaCl_2$	-319.4	Yes	****	< 0.0001
1000 vs. 1000 + 10 mM $CaCl_2$	-244.5	Yes	****	< 0.0001
250 + 10 mM $CaCl_2$ vs. 1000 + 10 mM $CaCl_2$	74.9	No	ns	> 0.9999

Sample Sizes:

0	**5**	**10**	**50**	**100**	**200**	**250**	**300**	**400**	**500**	**750**	**1000**	**250 + 10 mM $CaCl_2$**	**1000 + 10 mM $CaCl_2$**
52	32	32	32	32	32	32	32	20	32	24	28	36	20

Dunn's multiple comparisons test Gd^{3+} primary branch frequency

Dunn's multiple comparisons test	**Mean rank diff.**	**Significant?**	**Summary**	**Adjusted P Value**
0 vs. 5	-79.56	No	ns	> 0.9999
0 vs. 10	-45.18	No	ns	> 0.9999
0 vs. 50	-77.9	No	ns	> 0.9999
0 vs. 100	-144.3	Yes	*	0.0242
0 vs. 200	-228.1	Yes	****	< 0.0001
0 vs. 250	-75.83	No	ns	> 0.9999
0 vs. 300	-136.9	Yes	*	0.0486
0 vs. 400	-247.2	Yes	****	< 0.0001
0 vs. 500	-109.1	No	ns	0.1213
0 vs. 750	-201.6	Yes	****	< 0.0001
0 vs. 1000	-217.3	Yes	****	< 0.0001
0 vs. 1000 + 10 mM $CaCl_2$	-41.57	No	ns	> 0.9999
5 vs. 10	34.38	No	ns	> 0.9999
5 vs. 50	1.66	No	ns	> 0.9999
5 vs. 100	-64.76	No	ns	> 0.9999
5 vs. 200	-148.6	No	ns	0.1202
5 vs. 250	3.73	No	ns	> 0.9999
5 vs. 300	-57.35	No	ns	> 0.9999
5 vs. 400	-167.7	Yes	*	0.0275
5 vs. 500	-29.51	No	ns	> 0.9999
5 vs. 750	-122.1	No	ns	0.7223
5 vs. 1000	-137.8	No	ns	0.0875

5 vs. 1000 + 10 mM $CaCl_2$	37.99	No	ns	> 0.9999
10 vs. 50	-32.72	No	ns	> 0.9999
10 vs. 100	-99.14	No	ns	> 0.9999
10 vs. 200	-183	Yes	**	0.0075
10 vs. 250	-30.65	No	ns	> 0.9999
10 vs. 300	-91.73	No	ns	> 0.9999
10 vs. 400	-202.1	Yes	**	0.0013
10 vs. 500	-63.89	No	ns	> 0.9999
10 vs. 750	-156.5	No	ns	0.0667
10 vs. 1000	-172.2	Yes	**	0.0037
10 vs. 1000 + 10 mM $CaCl_2$	3.606	No	ns	> 0.9999
50 vs. 100	-66.42	No	ns	> 0.9999
50 vs. 200	-150.2	Yes	*	0.0353
50 vs. 250	2.07	No	ns	> 0.9999
50 vs. 300	-59.01	No	ns	> 0.9999
50 vs. 400	-169.3	Yes	**	0.006
50 vs. 500	-31.17	No	ns	> 0.9999
50 vs. 750	-123.7	No	ns	0.3013
50 vs. 1000	-139.5	Yes	*	0.017
50 vs. 1000 + 10 mM $CaCl_2$	36.33	No	ns	> 0.9999
100 vs. 200	-83.82	No	ns	> 0.9999
100 vs. 250	68.49	No	ns	> 0.9999
100 vs. 300	7.41	No	ns	> 0.9999
100 vs. 400	-102.9	No	ns	> 0.9999
100 vs. 500	35.25	No	ns	> 0.9999
100 vs. 750	-57.31	No	ns	> 0.9999
100 vs. 1000	-73.03	No	ns	> 0.9999
100 vs. 1000 + 10 mM $CaCl_2$	102.7	No	ns	> 0.9999
200 vs. 250	152.3	No	ns	0.0912
200 vs. 300	91.23	No	ns	> 0.9999
200 vs. 400	-19.09	No	ns	> 0.9999
200 vs. 500	119.1	No	ns	0.3795
200 vs. 750	26.51	No	ns	> 0.9999
200 vs. 1000	10.79	No	ns	> 0.9999
200 vs. 1000 + 10 mM $CaCl_2$	186.6	Yes	**	0.0011
250 vs. 300	-61.08	No	ns	> 0.9999
250 vs. 400	-171.4	Yes	*	0.0202
250 vs. 500	-33.24	No	ns	> 0.9999
250 vs. 750	-125.8	No	ns	0.5713
250 vs. 1000	-141.5	No	ns	0.0639
250 vs. 1000 + 10 mM $CaCl_2$	34.26	No	ns	> 0.9999
300 vs. 400	-110.3	No	ns	> 0.9999
300 vs. 500	27.84	No	ns	> 0.9999
300 vs. 750	-64.72	No	ns	> 0.9999

300 vs. 1000	-80.44	No	ns	> 0.9999
300 vs. 1000 + 10 mM $CaCl_2$	95.34	No	ns	> 0.9999
400 vs. 500	138.2	No	ns	0.0848
400 vs. 750	45.6	No	ns	> 0.9999
400 vs. 1000	29.88	No	ns	> 0.9999
400 vs. 1000 + 10 mM $CaCl_2$	205.7	Yes	***	0.0001
500 vs. 750	-92.56	No	ns	> 0.9999
500 vs. 1000	-108.3	No	ns	0.2734
500 vs. 1000 + 10 mM $CaCl_2$	67.5	No	ns	> 0.9999
750 vs. 1000	-15.72	No	ns	> 0.9999
750 vs. 1000 + 10 mM $CaCl_2$	160.1	Yes	*	0.0152
1000 vs. 1000 + 10 mM $CaCl_2$	175.8	Yes	***	0.0003

Sample Sizes:

0	**5**	**10**	**50**	**100**	**200**	**250**	**300**	**400**	**500**	**750**	**1000**	**1000 + 10 mM $CaCl_2$**
110	50	50	75	50	50	50	50	50	80	50	80	74

Kruskal-Wallis test Gd^{3+} secondary branch frequency

Ho: There is no difference in mean secondary branch frequency between treatments of Gd^{3+}

Ha: There is a difference in mean secondary branch frequency between treatments of Gd^{3+}

Kruskal-Wallis test	
P value	< 0.0001
Exact or approximate P value?	Approximate
P value summary	****
Do the medians vary signif. (P < 0.05)	Yes
Number of groups	13
Kruskal-Wallis statistic	111.8
Data summary	
Number of treatments (columns)	13
Number of values (total)	819

Conclusion: $p < 0.0001$ therefore reject null hypothesis. There is sufficient evidence that there is a difference in mean secondary branch frequencies between treatments of Gd^{3+} at $\alpha=0.05$

Dunn's multiple comparisons test Gd^{3+} secondary branch frequency

Dunn's multiple comparisons test	Mean rank diff.	Significant?	Summary	Adjusted P Value
0 vs. 5	-67.55	No	ns	> 0.9999
0 vs. 10	-47.96	No	ns	> 0.9999
0 vs. 50	-93.72	No	ns	0.6287
0 vs. 100	-43.62	No	ns	> 0.9999
0 vs. 200	-94.85	No	ns	> 0.9999
0 vs. 250	-155.7	Yes	**	0.0087
0 vs. 300	-102.4	No	ns	0.8577
0 vs. 400	-254.6	Yes	****	< 0.0001
0 vs. 500	-96.89	No	ns	0.4094
0 vs. 750	-190.8	Yes	***	0.0002
0 vs. 1000	-258	Yes	****	< 0.0001
0 vs. 1000 + 10 mM $CaCl_2$	17.57	No	ns	> 0.9999
5 vs. 10	19.59	No	ns	> 0.9999
5 vs. 50	-26.18	No	ns	> 0.9999
5 vs. 100	23.93	No	ns	> 0.9999
5 vs. 200	-27.3	No	ns	> 0.9999
5 vs. 250	-88.18	No	ns	> 0.9999
5 vs. 300	-34.9	No	ns	> 0.9999
5 vs. 400	-187.1	Yes	**	0.0059
5 vs. 500	-29.35	No	ns	> 0.9999
5 vs. 750	-123.2	No	ns	0.7096
5 vs. 1000	-190.4	Yes	***	0.0006
5 vs. 1000 + 10 mM $CaCl_2$	85.12	No	ns	> 0.9999
10 vs. 50	-45.77	No	ns	> 0.9999
10 vs. 100	4.34	No	ns	> 0.9999
10 vs. 200	-46.89	No	ns	> 0.9999
10 vs. 250	-107.8	No	ns	> 0.9999
10 vs. 300	-54.49	No	ns	> 0.9999
10 vs. 400	-206.7	Yes	***	0.001
10 vs. 500	-48.94	No	ns	> 0.9999
10 vs. 750	-142.8	No	ns	0.1954
10 vs. 1000	-210	Yes	****	< 0.0001
10 vs. 1000 + 10 mM $CaCl_2$	65.53	No	ns	> 0.9999
50 vs. 100	50.11	No	ns	> 0.9999
50 vs. 200	-1.123	No	ns	> 0.9999
50 vs. 250	-62	No	ns	> 0.9999
50 vs. 300	-8.723	No	ns	> 0.9999
50 vs. 400	-160.9	Yes	*	0.0149
50 vs. 500	-3.168	No	ns	> 0.9999
50 vs. 750	-97.05	No	ns	> 0.9999

50 vs. 1000	-164.2	Yes	**	0.0012
50 vs. 1000 + 10 mM $CaCl_2$	111.3	No	ns	0.3148
100 vs. 200	-51.23	No	ns	> 0.9999
100 vs. 250	-112.1	No	ns	> 0.9999
100 vs. 300	-58.83	No	ns	> 0.9999
100 vs. 400	-211	Yes	***	0.0006
100 vs. 500	-53.28	No	ns	> 0.9999
100 vs. 750	-147.2	No	ns	0.1438
100 vs. 1000	-214.4	Yes	****	< 0.0001
100 vs. 1000 + 10 mM $CaCl_2$	61.19	No	ns	> 0.9999
200 vs. 250	-60.88	No	ns	> 0.9999
200 vs. 300	-7.6	No	ns	> 0.9999
200 vs. 400	-159.8	No	ns	0.0562
200 vs. 500	-2.045	No	ns	> 0.9999
200 vs. 750	-95.93	No	ns	> 0.9999
200 vs. 1000	-163.1	Yes	*	0.01
200 vs. 1000 + 10 mM $CaCl_2$	112.4	No	ns	0.7279
250 vs. 300	53.28	No	ns	> 0.9999
250 vs. 400	-98.92	No	ns	> 0.9999
250 vs. 500	58.84	No	ns	> 0.9999
250 vs. 750	-35.05	No	ns	> 0.9999
250 vs. 1000	-102.2	No	ns	> 0.9999
250 vs. 1000 + 10 mM $CaCl_2$	173.3	Yes	**	0.0048
300 vs. 400	-152.2	No	ns	0.0996
300 vs. 500	5.555	No	ns	> 0.9999
300 vs. 750	-88.33	No	ns	> 0.9999
300 vs. 1000	-155.5	Yes	*	0.0204
300 vs. 1000 + 10 mM $CaCl_2$	120	No	ns	0.4302
400 vs. 500	157.8	Yes	*	0.0166
400 vs. 750	63.87	No	ns	> 0.9999
400 vs. 1000	-3.32	No	ns	> 0.9999
400 vs. 1000 + 10 mM $CaCl_2$	272.2	Yes	****	< 0.0001
500 vs. 750	-93.89	No	ns	> 0.9999
500 vs. 1000	-161.1	Yes	**	0.0013
500 vs. 1000 + 10 mM CaCl2	114.5	No	ns	0.2078
750 vs. 1000	-67.19	No	ns	> 0.9999
750 vs. 1000 + 10 mM $CaCl_2$	208.3	Yes	***	0.0001
1000 vs. 1000 + 10 mM $CaCl_2$	275.5	Yes	****	< 0.0001

Sample Sizes:

0	**5**	**10**	**50**	**100**	**200**	**250**	**300**	**400**	**500**	**750**	**1000**	**1000 + 10 mM $CaCl_2$**
110	50	50	75	50	50	50	50	50	80	50	80	74

Kruskal-Wallis test Gd^{3+} distance between the hyphal tip and the first branch

Ho: There is no difference in mean distance between the hyphal tip and the first branch between treatments of Gd^{3+}

Ha: There is a difference in mean distance between the hyphal tip and the first branch between treatments of Gd^{3+}

Kruskal-Wallis test	
P value	0.1203
Exact or approximate P value?	Approximate
P value summary	ns
Do the medians vary signif. (P < 0.05)	No
Number of groups	5
Kruskal-Wallis statistic	7.311
Data summary	
Number of treatments (columns)	5
Number of values (total)	169

Conclusion: p = 0.1203 therefore accept the null hypothesis. There is sufficient evidence that there is not a difference in the mean distance between the hyphal tip and the first branch between treatments of Gd^{3+} at α=0.05

Sample Sizes:

0	**50**	**500**	**1000**	**1000 + 10 mM $CaCl_2$**
60	25	30	30	24

One-way ANOVA test Gd^{3+} distance between the first branch and the second branch

Ho: There is no difference in mean distance between the hyphal tip and the first branch between treatments of Gd^{3+}

Ha: There is a difference in mean distance between the hyphal tip and the first branch between treatments of Gd^{3+}

ANOVA table	**SS**	**DF**	**MS**	**F (DFn, DFd)**	**P value**
Treatment (between columns)	53092	4	13273	F (4, 164) = 1.713	P = 0.1495
Residual (within columns)	1271000	164	7748		
Total	1324000	168			

Conclusion: p = 0.1495 therefore accept the null hypothesis. There is sufficient evidence that there is not a difference in the mean distance between the first branch and the second branch between treatments of Gd^{3+} at α=0.05

Sample Sizes:

0	50	500	1000	1000 + 10 mM $CaCl_2$
60	25	30	30	24

Kruskal-Wallis test Gd^{3+} colony radius

Ho: There is no difference in the mean colony radius between treatments of Gd^{3+}

Ha: There is a difference in the mean colony radius between treatments of Gd^{3+}

Kruskal-Wallis test	
P value	< 0.0001
Exact or approximate P value?	Approximate
P value summary	****
Do the medians vary signif. (P < 0.05)	Yes
Number of groups	13
Kruskal-Wallis statistic	146.9
Data summary	
Number of treatments (columns)	13
Number of values (total)	388

Conclusion: p < 0.0001 therefore reject null hypothesis. There is sufficient evidence that there is a difference in mean colony radius between treatments of Gd^{3+} at α=0.05

Dunn's multiple comparisons test Gd^{3+} colony radius

Dunn's multiple comparisons test	Mean rank diff.	Significant?	Summary	Adjusted P Value
0 vs. 5	66.78	No	ns	> 0.9999
0 vs. 10	-19.55	No	ns	> 0.9999
0 vs. 50	74.57	No	ns	0.1684
0 vs. 100	84.61	No	ns	0.1738
0 vs. 200	30.13	No	ns	> 0.9999
0 vs. 250	183.4	Yes	****	< 0.0001

0 vs. 300	-2.638	No	ns	> 0.9999
0 vs. 400	55.17	No	ns	> 0.9999
0 vs. 500	142	Yes	****	< 0.0001
0 vs. 750	44.53	No	ns	> 0.9999
0 vs. 1000	187.3	Yes	****	< 0.0001
0 vs. 1000 + 10 mM $CaCl_2$	-10.05	No	ns	> 0.9999
5 vs. 10	-86.33	No	ns	0.5959
5 vs. 50	7.792	No	ns	> 0.9999
5 vs. 100	17.83	No	ns	> 0.9999
5 vs. 200	-36.65	No	ns	> 0.9999
5 vs. 250	116.6	Yes	*	0.0247
5 vs. 300	-69.42	No	ns	> 0.9999
5 vs. 400	-11.6	No	ns	> 0.9999
5 vs. 500	75.26	No	ns	0.8461
5 vs. 750	-22.25	No	ns	> 0.9999
5 vs. 1000	120.5	Yes	**	0.0036
5 vs. 1000 + 10 mM $CaCl_2$	-76.83	No	ns	0.7257
10 vs. 50	94.13	No	ns	0.1127
10 vs. 100	104.2	No	ns	0.1007
10 vs. 200	49.69	No	ns	> 0.9999
10 vs. 250	202.9	Yes	****	< 0.0001
10 vs. 300	16.92	No	ns	> 0.9999
10 vs. 400	74.73	No	ns	> 0.9999
10 vs. 500	161.6	Yes	****	< 0.0001
10 vs. 750	64.08	No	ns	> 0.9999
10 vs. 1000	206.8	Yes	****	< 0.0001
10 vs. 1000 + 10 mM $CaCl_2$	9.5	No	ns	> 0.9999
50 vs. 100	10.04	No	ns	> 0.9999
50 vs. 200	-44.44	No	ns	> 0.9999
50 vs. 250	108.8	Yes	*	0.0181
50 vs. 300	-77.21	No	ns	0.6993
50 vs. 400	-19.4	No	ns	> 0.9999
50 vs. 500	67.47	No	ns	0.832
50 vs. 750	-30.04	No	ns	> 0.9999
50 vs. 1000	112.7	Yes	**	0.0016
50 vs. 1000 + 10 mM $CaCl_2$	-84.63	No	ns	0.1065
100 vs. 200	-54.48	No	ns	> 0.9999
100 vs. 250	98.75	No	ns	0.178
100 vs. 300	-87.25	No	ns	0.5476
100 vs. 400	-29.44	No	ns	> 0.9999
100 vs. 500	57.43	No	ns	> 0.9999
100 vs. 750	-40.08	No	ns	> 0.9999
100 vs. 1000	102.6	Yes	*	0.0401
100 vs. 1000 + 10 mM $CaCl_2$	-94.67	No	ns	0.1058

200 vs. 250	153.2	Yes	***	0.0002
200 vs. 300	-32.77	No	ns	> 0.9999
200 vs. 400	25.04	No	ns	> 0.9999
200 vs. 500	111.9	Yes	*	0.0119
200 vs. 750	14.4	No	ns	> 0.9999
200 vs. 1000	157.1	Yes	****	< 0.0001
200 vs. 1000 + 10 mM $CaCl_2$	-40.19	No	ns	> 0.9999
250 vs. 300	-186	Yes	****	< 0.0001
250 vs. 400	-128.2	Yes	**	0.0059
250 vs. 500	-41.32	No	ns	> 0.9999
250 vs. 750	-138.8	Yes	**	0.0014
250 vs. 1000	3.889	No	ns	> 0.9999
250 vs. 1000 + 10 mM $CaCl_2$	-193.4	Yes	****	< 0.0001
300 vs. 400	57.81	No	ns	> 0.9999
300 vs. 500	144.7	Yes	****	< 0.0001
300 vs. 750	47.17	No	ns	> 0.9999
300 vs. 1000	189.9	Yes	****	< 0.0001
300 vs. 1000 + 10 mM $CaCl_2$	-7.417	No	ns	> 0.9999
400 vs. 500	86.87	No	ns	0.256
400 vs. 750	-10.65	No	ns	> 0.9999
400 vs. 1000	132.1	Yes	***	0.0006
400 vs. 1000 + 10 mM $CaCl_2$	-65.23	No	ns	> 0.9999
500 vs. 750	-97.51	No	ns	0.0754
500 vs. 1000	45.21	No	ns	> 0.9999
500 vs. 1000 + 10 mM $CaCl_2$	-152.1	Yes	****	< 0.0001
750 vs. 1000	142.7	Yes	***	0.0001
750 vs. 1000 + 10 mM $CaCl_2$	-54.58	No	ns	> 0.9999
1000 vs. 1000 + 10 mM $CaCl_2$	-197.3	Yes	****	< 0.0001

Sample Sizes:

0	**5**	**10**	**50**	**100**	**200**	**250**	**300**	**400**	**500**	**750**	**1000**	**1000 + 10 mM $CaCl_2$**
52	24	24	36	24	24	24	24	24	36	24	36	36

Kruskal-Wallis test La^{3+} primary branch frequency

Ho: There is no difference in mean primary branch frequency between treatments of La^{3+}

Ha: There is a difference in mean primary branch frequency between treatments of La^{3+}

Kruskal-Wallis test	
P value	< 0.0001
Exact or approximate P value?	Approximate

P value summary	****
Do the medians vary signif. (P < 0.05)	Yes
Number of groups	13
Kruskal-Wallis statistic	46.16
Data summary	
Number of treatments (columns)	13
Number of values (total)	828

Conclusion: $p < 0.0001$ therefore reject null hypothesis. There is sufficient evidence that there is a difference in mean primary branch frequencies between treatments of La^{3+} at $\alpha=0.05$

Dunn's multiple comparisons test La^{3+} primary branch frequency

Dunn's multiple comparisons test	Mean rank diff.	Significant?	Summary	Adjusted P Value
0 vs. 5	-34.42	No	ns	> 0.9999
0 vs. 10	-53.87	No	ns	> 0.9999
0 vs. 50	-23.28	No	ns	> 0.9999
0 vs. 100	-123.5	No	ns	0.173
0 vs. 200	-8.725	No	ns	> 0.9999
0 vs. 250	-107	No	ns	0.626
0 vs. 300	-63.89	No	ns	> 0.9999
0 vs. 400	-163.2	Yes	**	0.0041
0 vs. 500	-64.86	No	ns	> 0.9999
0 vs. 750	-157.4	Yes	**	0.0075
0 vs. 1000	-132.8	Yes	*	0.0105
0 vs. 1000 + 10 mM $CaCl_2$	-130.8	Yes	*	0.014
5 vs. 10	-19.45	No	ns	> 0.9999
5 vs. 50	11.14	No	ns	> 0.9999
5 vs. 100	-89.08	No	ns	> 0.9999
5 vs. 200	25.69	No	ns	> 0.9999
5 vs. 250	-72.58	No	ns	> 0.9999
5 vs. 300	-29.47	No	ns	> 0.9999
5 vs. 400	-128.8	No	ns	0.5067
5 vs. 500	-30.45	No	ns	> 0.9999
5 vs. 750	-123	No	ns	0.7289
5 vs. 1000	-98.39	No	ns	> 0.9999
5 vs. 1000 + 10 mM $CaCl_2$	-96.39	No	ns	> 0.9999
10 vs. 50	30.59	No	ns	> 0.9999
10 vs. 100	-69.63	No	ns	> 0.9999
10 vs. 200	45.14	No	ns	> 0.9999
10 vs. 250	-53.13	No	ns	> 0.9999

10 vs. 300	-10.02	No	ns	> 0.9999
10 vs. 400	-109.4	No	ns	> 0.9999
10 vs. 500	-11	No	ns	> 0.9999
10 vs. 750	-103.6	No	ns	> 0.9999
10 vs. 1000	-78.94	No	ns	> 0.9999
10 vs. 1000 + 10 mM $CaCl_2$	-76.94	No	ns	> 0.9999
50 vs. 100	-100.2	No	ns	> 0.9999
50 vs. 200	14.55	No	ns	> 0.9999
50 vs. 250	-83.72	No	ns	> 0.9999
50 vs. 300	-40.61	No	ns	> 0.9999
50 vs. 400	-139.9	No	ns	0.0788
50 vs. 500	-41.59	No	ns	> 0.9999
50 vs. 750	-134.1	No	ns	0.1266
50 vs. 1000	-109.5	No	ns	0.2592
50 vs. 1000 + 10 mM $CaCl_2$	-107.5	No	ns	0.3167
100 vs. 200	114.8	No	ns	> 0.9999
100 vs. 250	16.5	No	ns	> 0.9999
100 vs. 300	59.61	No	ns	> 0.9999
100 vs. 400	-39.73	No	ns	> 0.9999
100 vs. 500	58.63	No	ns	> 0.9999
100 vs. 750	-33.93	No	ns	> 0.9999
100 vs. 1000	-9.306	No	ns	> 0.9999
100 vs. 1000 + 10 mM $CaCl_2$	-7.308	No	ns	> 0.9999
200 vs. 250	-98.27	No	ns	> 0.9999
200 vs. 300	-55.16	No	ns	> 0.9999
200 vs. 400	-154.5	No	ns	0.0857
200 vs. 500	-56.14	No	ns	> 0.9999
200 vs. 750	-148.7	No	ns	0.1311
200 vs. 1000	-124.1	No	ns	0.2835
200 vs. 1000 + 10 mM $CaCl_2$	-122.1	No	ns	0.3362
250 vs. 300	43.11	No	ns	> 0.9999
250 vs. 400	-56.23	No	ns	> 0.9999
250 vs. 500	42.13	No	ns	> 0.9999
250 vs. 750	-50.43	No	ns	> 0.9999
250 vs. 1000	-25.81	No	ns	> 0.9999
250 vs. 1000 + 10 mM $CaCl_2$	-23.81	No	ns	> 0.9999
300 vs. 400	-99.34	No	ns	> 0.9999
300 vs. 500	-0.9767	No	ns	> 0.9999
300 vs. 750	-93.54	No	ns	> 0.9999
300 vs. 1000	-68.92	No	ns	> 0.9999
300 vs. 1000 + 10 mM $CaCl_2$	-66.92	No	ns	> 0.9999
400 vs. 500	98.36	No	ns	> 0.9999
400 vs. 750	5.8	No	ns	> 0.9999
400 vs. 1000	30.42	No	ns	> 0.9999

400 vs. 1000 + 10 mM $CaCl_2$	32.42	No	ns	> 0.9999
500 vs. 750	-92.56	No	ns	> 0.9999
500 vs. 1000	-67.94	No	ns	> 0.9999
500 vs. 1000 + 10 mM $CaCl_2$	-65.94	No	ns	> 0.9999
750 vs. 1000	24.62	No	ns	> 0.9999
750 vs. 1000 + 10 mM $CaCl_2$	26.62	No	ns	> 0.9999
1000 vs. 1000 + 10 mM $CaCl_2$	1.999	No	ns	> 0.9999

Sample Sizes:

0	**5**	**10**	**50**	**100**	**200**	**250**	**300**	**400**	**500**	**750**	**1000**	**1000 + 10 mM $CaCl_2$**
110	50	50	81	50	50	50	50	50	78	50	80	79

Kruskal-Wallis test La^{3+} secondary branch frequency

Ho: There is no difference in mean secondary branch frequency between treatments of La^{3+}

Ha: There is a difference in mean secondary branch frequency between treatments of La^{3+}

Kruskal-Wallis test	
P value	0.0008
Exact or approximate P value?	Approximate
P value summary	***
Do the medians vary signif. (P < 0.05)	Yes
Number of groups	13
Kruskal-Wallis statistic	33.61
Data summary	
Number of treatments (columns)	13
Number of values (total)	828

Conclusion: p = 0.0008 therefore reject null hypothesis. There is sufficient evidence that there is a difference in mean secondary branch frequencies between treatments of La^{3+} at α=0.05

Dunn's multiple comparisons test La^{3+} secondary branch frequency

Dunn's multiple comparisons test	**Mean rank diff.**	**Significant?**	**Summary**	**Adjusted P Value**
0 vs. 5	-90.65	No	ns	> 0.9999
0 vs. 10	12.89	No	ns	> 0.9999
0 vs. 50	-13.11	No	ns	> 0.9999
0 vs. 100	-104.8	No	ns	0.778

0 vs. 200	-30.44	No	ns	> 0.9999
0 vs. 250	35.12	No	ns	> 0.9999
0 vs. 300	-29.72	No	ns	> 0.9999
0 vs. 400	-148.5	Yes	*	0.0203
0 vs. 500	-4.936	No	ns	> 0.9999
0 vs. 750	-3.638	No	ns	> 0.9999
0 vs. 1000	-78.93	No	ns	> 0.9999
0 vs. 1000 + 10 mM $CaCl_2$	-6.509	No	ns	> 0.9999
5 vs. 10	103.5	No	ns	> 0.9999
5 vs. 50	77.54	No	ns	> 0.9999
5 vs. 100	-14.13	No	ns	> 0.9999
5 vs. 200	60.21	No	ns	> 0.9999
5 vs. 250	125.8	No	ns	0.6512
5 vs. 300	60.93	No	ns	> 0.9999
5 vs. 400	-57.89	No	ns	> 0.9999
5 vs. 500	85.71	No	ns	> 0.9999
5 vs. 750	87.01	No	ns	> 0.9999
5 vs. 1000	11.72	No	ns	> 0.9999
5 vs. 1000 + 10 mM $CaCl_2$	84.14	No	ns	> 0.9999
10 vs. 50	-26	No	ns	> 0.9999
10 vs. 100	-117.7	No	ns	> 0.9999
10 vs. 200	-43.33	No	ns	> 0.9999
10 vs. 250	22.23	No	ns	> 0.9999
10 vs. 300	-42.61	No	ns	> 0.9999
10 vs. 400	-161.4	No	ns	0.0556
10 vs. 500	-17.83	No	ns	> 0.9999
10 vs. 750	-16.53	No	ns	> 0.9999
10 vs. 1000	-91.82	No	ns	> 0.9999
10 vs. 1000 + 10 mM $CaCl_2$	-19.4	No	ns	> 0.9999
50 vs. 100	-91.67	No	ns	> 0.9999
50 vs. 200	-17.33	No	ns	> 0.9999
50 vs. 250	48.23	No	ns	> 0.9999
50 vs. 300	-16.61	No	ns	> 0.9999
50 vs. 400	-135.4	No	ns	0.1239
50 vs. 500	8.171	No	ns	> 0.9999
50 vs. 750	9.469	No	ns	> 0.9999
50 vs. 1000	-65.82	No	ns	> 0.9999
50 vs. 1000 + 10 mM $CaCl_2$	6.598	No	ns	> 0.9999
100 vs. 200	74.34	No	ns	> 0.9999
100 vs. 250	139.9	No	ns	0.2612
100 vs. 300	75.06	No	ns	> 0.9999
100 vs. 400	-43.76	No	ns	> 0.9999
100 vs. 500	99.84	No	ns	> 0.9999
100 vs. 750	101.1	No	ns	> 0.9999

100 vs. 1000	25.85	No	ns	> 0.9999
100 vs. 1000 + 10 mM $CaCl_2$	98.27	No	ns	> 0.9999
200 vs. 250	65.56	No	ns	> 0.9999
200 vs. 300	0.72	No	ns	> 0.9999
200 vs. 400	-118.1	No	ns	> 0.9999
200 vs. 500	25.5	No	ns	> 0.9999
200 vs. 750	26.8	No	ns	> 0.9999
200 vs. 1000	-48.49	No	ns	> 0.9999
200 vs. 1000 + 10 mM $CaCl_2$	23.93	No	ns	> 0.9999
250 vs. 300	-64.84	No	ns	> 0.9999
250 vs. 400	-183.7	Yes	**	0.0092
250 vs. 500	-40.06	No	ns	> 0.9999
250 vs. 750	-38.76	No	ns	> 0.9999
250 vs. 1000	-114.1	No	ns	0.6213
250 vs. 1000 + 10 mM $CaCl_2$	-41.63	No	ns	> 0.9999
300 vs. 400	-118.8	No	ns	0.9909
300 vs. 500	24.78	No	ns	> 0.9999
300 vs. 750	26.08	No	ns	> 0.9999
300 vs. 1000	-49.21	No	ns	> 0.9999
300 vs. 1000 + 10 mM $CaCl_2$	23.21	No	ns	> 0.9999
400 vs. 500	143.6	No	ns	0.0692
400 vs. 750	144.9	No	ns	0.1855
400 vs. 1000	69.61	No	ns	> 0.9999
400 vs. 1000 + 10 mM $CaCl_2$	142	No	ns	0.0765
500 vs. 750	1.298	No	ns	> 0.9999
500 vs. 1000	-73.99	No	ns	> 0.9999
500 vs. 1000 + 10 mM $CaCl_2$	-1.573	No	ns	> 0.9999
750 vs. 1000	-75.29	No	ns	> 0.9999
750 vs. 1000 + 10 mM $CaCl_2$	-2.871	No	ns	> 0.9999
1000 vs. 1000 + 10 mM $CaCl_2$	72.42	No	ns	> 0.9999

Sample Sizes:

0	**5**	**10**	**50**	**100**	**200**	**250**	**300**	**400**	**500**	**750**	**1000**	**1000 + 10 mM $CaCl_2$**
110	50	50	81	50	50	50	50	50	78	50	80	79

Kruskal-Wallis test La^{3+} distance between the hyphal tip and the first branch

Ho: There is no difference in mean distance between the hyphal tip and the first branch between treatments of La^{3+}

Ha: There is a difference in mean distance between the hyphal tip and the first branch between treatments of La^{3+}

Kruskal-Wallis test	
P value	0.1093
Exact or approximate P value?	Approximate
P value summary	ns
Do the medians vary signif. (P < 0.05)	No
Number of groups	5
Kruskal-Wallis statistic	7.555
Data summary	
Number of treatments (columns)	5
Number of values (total)	178

Conclusion: p = 0.1093 therefore accept the null hypothesis. There is sufficient evidence that there is not a difference in the mean distance between the hyphal tip and the first branch between treatments of La^{3+} at α=0.05

Sample Sizes:

0	**50**	**500**	**1000**	**1000 + 10 mM $CaCl_2$**
60	31	28	30	29

One-way ANOVA test La^{3+} distance between the first branch and the second branch

Ho: There is no difference in mean distance between the hyphal tip and the first branch between treatments of La^{3+}

Ha: There is a difference in mean distance between the hyphal tip and the first branch between treatments of La^{3+}

ANOVA table	**SS**	**DF**	**MS**	**F (DFn, DFd)**	**P value**
Treatment (between columns)	40137	4	10034	F (4, 173) = 1.258	P = 0.2883
Residual (within columns)	1380000	173	7974		
Total	1420000	177			

Conclusion: p = 0.2883 therefore accept the null hypothesis. There is sufficient evidence that there is not a difference in the mean distance between the first branch and the second branch between treatments of La^{3+} at α=0.05

Sample Sizes:

0	50	500	1000	1000 + 10 mM $CaCl_2$
60	31	28	30	29

Kruskal-Wallis test La^{3+} colony radius

Ho: There is no difference in the mean colony radius between treatments of La^{3+}

Ha: There is a difference in the mean colony radius between treatments of La^{3+}

Kruskal-Wallis test	
P value	< 0.0001
Exact or approximate P value?	Approximate
P value summary	****
Do the medians vary signif. (P < 0.05)	Yes
Number of groups	13
Kruskal-Wallis statistic	139.7
Data summary	
Number of treatments (columns)	13
Number of values (total)	384

Conclusion: $p < 0.0001$ therefore reject null hypothesis. There is sufficient evidence that there is a difference in mean colony radius between treatments of La^{3+} at $\alpha=0.05$

Dunn's multiple comparisons test La^{3+} colony radius

Dunn's multiple comparisons test	Mean rank diff.	Significant?	Summary	Adjusted P Value
0 vs. 5	200.1	Yes	****	< 0.0001
0 vs. 10	134.9	Yes	***	0.0003
0 vs. 50	99.49	Yes	**	0.0028
0 vs. 100	77.07	No	ns	0.3793
0 vs. 200	146.2	Yes	****	< 0.0001
0 vs. 250	66.59	No	ns	> 0.9999
0 vs. 300	53.55	No	ns	> 0.9999
0 vs. 400	50.01	No	ns	> 0.9999
0 vs. 500	138.3	Yes	****	< 0.0001
0 vs. 750	49.37	No	ns	> 0.9999
0 vs. 1000	144.4	Yes	****	< 0.0001
0 vs. 1000 + 10 mM $CaCl_2$	-40.45	No	ns	> 0.9999

5 vs. 10	-65.25	No	ns	> 0.9999
5 vs. 50	-100.6	Yes	*	0.0449
5 vs. 100	-123.1	Yes	**	0.0095
5 vs. 200	-53.98	No	ns	> 0.9999
5 vs. 250	-133.5	Yes	**	0.0024
5 vs. 300	-146.6	Yes	***	0.0004
5 vs. 400	-150.1	Yes	***	0.0002
5 vs. 500	-61.83	No	ns	> 0.9999
5 vs. 750	-150.8	Yes	***	0.0002
5 vs. 1000	-55.78	No	ns	> 0.9999
5 vs. 1000 + 10 mM $CaCl_2$	-240.6	Yes	****	< 0.0001
10 vs. 50	-35.4	No	ns	> 0.9999
10 vs. 100	-57.82	No	ns	> 0.9999
10 vs. 200	11.27	No	ns	> 0.9999
10 vs. 250	-68.3	No	ns	> 0.9999
10 vs. 300	-81.34	No	ns	> 0.9999
10 vs. 400	-84.88	No	ns	0.8951
10 vs. 500	3.419	No	ns	> 0.9999
10 vs. 750	-85.53	No	ns	0.8472
10 vs. 1000	9.461	No	ns	> 0.9999
10 vs. 1000 + 10 mM $CaCl_2$	-175.3	Yes	****	< 0.0001
50 vs. 100	-22.42	No	ns	> 0.9999
50 vs. 200	46.67	No	ns	> 0.9999
50 vs. 250	-32.9	No	ns	> 0.9999
50 vs. 300	-45.94	No	ns	> 0.9999
50 vs. 400	-49.48	No	ns	> 0.9999
50 vs. 500	38.82	No	ns	> 0.9999
50 vs. 750	-50.13	No	ns	> 0.9999
50 vs. 1000	44.86	No	ns	> 0.9999
50 vs. 1000 + 10 mM $CaCl_2$	-139.9	Yes	****	< 0.0001
100 vs. 200	69.08	No	ns	> 0.9999
100 vs. 250	-10.48	No	ns	> 0.9999
100 vs. 300	-23.52	No	ns	> 0.9999
100 vs. 400	-27.06	No	ns	> 0.9999
100 vs. 500	61.24	No	ns	> 0.9999
100 vs. 750	-27.71	No	ns	> 0.9999
100 vs. 1000	67.28	No	ns	> 0.9999
100 vs. 1000 + 10 mM $CaCl_2$	-117.5	Yes	**	0.0045
200 vs. 250	-79.56	No	ns	> 0.9999
200 vs. 300	-92.6	No	ns	0.2983
200 vs. 400	-96.15	No	ns	0.2087
200 vs. 500	-7.847	No	ns	> 0.9999
200 vs. 750	-96.79	No	ns	0.1953
200 vs. 1000	-1.806	No	ns	> 0.9999

200 vs. 1000 + 10 mM $CaCl_2$	-186.6	Yes	****	< 0.0001
250 vs. 300	-13.04	No	ns	> 0.9999
250 vs. 400	-16.58	No	ns	> 0.9999
250 vs. 500	71.72	No	ns	> 0.9999
250 vs. 750	-17.23	No	ns	> 0.9999
250 vs. 1000	77.76	No	ns	0.6085
250 vs. 1000 + 10 mM $CaCl_2$	-107	Yes	*	0.0195
300 vs. 400	-3.542	No	ns	> 0.9999
300 vs. 500	84.76	No	ns	0.2912
300 vs. 750	-4.188	No	ns	> 0.9999
300 vs. 1000	90.8	No	ns	0.1477
300 vs. 1000 + 10 mM $CaCl_2$	-94.01	No	ns	0.1014
400 vs. 500	88.3	No	ns	0.1966
400 vs. 750	-0.6458	No	ns	> 0.9999
400 vs. 1000	94.34	No	ns	0.0974
400 vs. 1000 + 10 mM $CaCl_2$	-90.47	No	ns	0.1535
500 vs. 750	-88.94	No	ns	0.1827
500 vs. 1000	6.042	No	ns	> 0.9999
500 vs. 1000 + 10 mM $CaCl_2$	-178.8	Yes	****	< 0.0001
750 vs. 1000	94.99	No	ns	0.0902
750 vs. 1000 + 10 mM $CaCl_2$	-89.82	No	ns	0.1654
1000 vs. 1000 + 10 mM $CaCl_2$	-184.8	Yes	****	< 0.0001

Sample Sizes:

0	**5**	**10**	**50**	**100**	**200**	**250**	**300**	**400**	**500**	**750**	**1000**	**1000 + 10 mM $CaCl_2$**
52	24	20	36	24	24	24	24	24	36	24	36	36

One-way ANOVA test $CaCl_2$ primary branch frequency

Ho: There is no difference in mean primary branch frequency between treatments of

Ha: There is a difference in mean primary branch frequency between treatments of

ANOVA table	SS	DF	MS	F (DFn, DFd)	P value
Treatment (between columns)	34.12	2	17.06	F (2, 253) = 2.905	P = 0.0566
Residual (within columns)	1486	253	5.873		
Total	1520	255			

Conclusion: p = 0.0566 therefore accept the null hypothesis. There is sufficient evidence that there is not a difference in mean secondary branch frequencies between treatments of at α=0.05

Sample Sizes:

0	5 mM $CaCl_2$	10 mM $CaCl_2$
110	79	67

Kruskal-Wallis test $CaCl_2$ secondary branch frequency

Ho: There is no difference in mean secondary branch frequency between treatments of

Ha: There is a difference in mean secondary branch frequency between treatments of

Kruskal-Wallis test	
P value	0.0554
Exact or approximate P value?	Approximate
P value summary	ns
Do the medians vary signif. (P < 0.05)	No
Number of groups	3
Kruskal-Wallis statistic	5.785
Data summary	
Number of treatments (columns)	3
Number of values (total)	256

Sample Sizes:

0	5 mM $CaCl_2$	10 mM $CaCl_2$
110	79	67

Kruskal-Wallis test $CaCl_2$ distance between the hyphal tip and the first branch

Ho: There is no difference in mean distance between the hyphal tip and the first branch between treatments of

Ha: There is a difference in mean distance between the hyphal tip and the first branch between treatments of

Kruskal-Wallis test	
P value	0.0119
Exact or approximate P value?	Approximate
P value summary	*
Do the medians vary signif. (P < 0.05)	Yes
Number of groups	3
Kruskal-Wallis statistic	8.864

Data summary	
Number of treatments (columns)	3
Number of values (total)	106

Conclusion: p = 0.0119 therefore reject null hypothesis. There is sufficient evidence that there is a difference in mean distance between the hyphal tip and the first branch between treatments of at α=0.05

Dunn's multiple comparisons test $CaCl_2$ distance between the hyphal tip and the first branch

Dunn's multiple comparisons test	Mean rank diff.	Significant?	Summary	Adjusted P Value
0 vs. 5 mM $CaCl_2$	19.77	Yes	*	0.0129
0 vs. 10 mM $CaCl_2$	-0.3181	No	ns	> 0.9999
5 mM $CaCl_2$ vs. 10 mM $CaCl_2$	-20.09	No	ns	0.0948

Sample Sizes:

0	5 mM $CaCl_2$	10 mM $CaCl_2$
60	29	17

Kruskal-Wallis test $CaCl_2$ distance between the first branch and the second branch

Ho: There is no difference in mean distance between the first branch and the second between treatments of

Ha: There is a difference in mean distance between the first branch and the second branch between treatments of

ANOVA table	SS	DF	MS	F (DFn, DFd)	P value
Treatment (between columns)	457.1	2	228.5	F (2, 103) = 0.02631	P = 0.9740
Residual (within columns)	894693	103	8686		
Total	895150	105			

Conclusion: p = 0.9740 therefore accept the null hypothesis. There is sufficient evidence that there is not a difference in mean distance between the first branch and the second branch between treatments of at α=0.05

Sample Sizes:

0	5 mM $CaCl_2$	10 mM $CaCl_2$
60	29	17

Kruskal-Wallis test $CaCl_2$ colony radius

Ho: There is no difference in the mean colony radius between treatments of

Ha: There is a difference in the mean colony radius between treatments of

Kruskal-Wallis test	
P value	0.4952
Exact or approximate P value?	Approximate
P value summary	ns
Do the medians vary signif. (P < 0.05)	No
Number of groups	3
Kruskal-Wallis statistic	1.406
Data summary	
Number of treatments (columns)	3
Number of values (total)	116

Mann Whitney test DMSO primary branch frequency

Ho: There is no difference in mean primary branch frequency between treatments of

Ha: There is a difference in mean primary branch frequency between treatments of

Mann Whitney test	
P value	0.0087
Exact or approximate P value?	Exact
P value summary	**
Significantly different? (P < 0.05)	Yes
One- or two-tailed P value?	Two-tailed
Sum of ranks in No inhhibitor,DMSO	10007 , 10094
Mann-Whitney U	3902

Conclusion: p = 0.0087 therefore reject the null hypothesis. There is sufficient evidence that there is a difference in mean primary branch frequencies between treatments α=0.05

Sample Sizes:

0 Inhibitor	**DMSO**
110	90

Mann Whitney test DMSO secondary branch frequency

Ho: There is no difference in mean secondary branch frequency between treatments of

Ha: There is a difference in mean secondary branch frequency between treatments of

Mann Whitney test	
P value	0.0544
Exact or approximate P value?	Exact
P value summary	ns
Significantly different? (P < 0.05)	No
One- or two-tailed P value?	Two-tailed
Sum of ranks in No inhhibitor,DMSO	10275 , 9825
Mann-Whitney U	4170

Conclusion: p = 0.0544 therefore accept the null hypothesis. There is sufficient evidence that there is not a difference in mean secondary branch frequencies between treatments α=0.05

Sample Sizes:

0 Inhibitor	**DMSO**
110	90

Mann Whitney test DMSO distance between the hyphal tip and the first branch

Ho: There is no difference in mean distance between the hyphal tip and the first branch between treatments of

Ha: There is a difference in mean distance between the hyphal tip and the first branch between treatments of

Mann Whitney test	
P value	0.0801
Exact or approximate P value?	Exact
P value summary	ns
Significantly different? (P < 0.05)	No
One- or two-tailed P value?	Two-tailed
Sum of ranks in No inhhibitor,DMSO	3278 , 1773
Mann-Whitney U	952.5

Conclusion: p = 0.0801 therefore accept the null hypothesis. There is sufficient evidence that there is not a difference in mean distance between the hyphal tip and the first branch between treatments of at α=0.05

Sample Sizes:

0 Inhibitor	DMSO
60	40

Unpaired t test DMSO distance between the first branch and the second branch

Ho: There is no difference in mean distance between the first branch and the second between treatments of

Ha: There is a difference in mean distance between the first branch and the second branch between treatments DMSO

Unpaired t test	
P value	0.4999
P value summary	ns
Significantly different? (P < 0.05)	No
One- or two-tailed P value?	Two-tailed
t, df	t=0.6772 df=98
How big is the difference?	
Mean ± SEM of No inhibitor	133.2 ± 12.85 N=60
Mean ± SEM of column DMSO	120.2 ± 13.62 N=40
Difference between means	-13.05 ± 19.27
95% confidence interval	-51.29 to 25.19
R square	0.004658
F test to compare variances	
F,DFn, Dfd	1.334, 59, 39
P value	0.3409
P value summary	ns
Significantly different? (P < 0.05)	No

Conclusion: p = 0.4999 therefore accept the null hypothesis. There is sufficient evidence that there is not a difference in mean distance between the first branch and the second branch between treatments of at α=0.05

Sample Sizes:

0 Inhibitor	DMSO
60	40

Mann Whitney test DMSO colony radius

Ho: There is no difference in the mean colony radius between treatments of

Ha: There is a difference in the mean colony radius between treatments of

Mann Whitney test	
P value	0.1788
Exact or approximate P value?	Exact
P value summary	ns
Significantly different? (P < 0.05)	No
One- or two-tailed P value?	Two-tailed
Sum of ranks in No inhibitor,DMSO	2356 , 1214
Mann-Whitney U	686

Conclusion: p =0.1788 therefore accept the null hypothesis. There is sufficient evidence that there is not a difference in mean colony radius between treatments α=0.05

Sample Sizes:

0 Inhibitor	**DMSO**
52	32